Environmental Impact and Environmental Sourcing Risks in Humanitarian Supply Chains

A Decision Support Tool for World Food Programme in Sub-Saharan Africa

Authors
Ebba Evers & Ebba Häggström

Supervisors
Andreas Norrman, Lund University
Nicholas Finney, World Food Programme

Examiner
Joakim Kembro

Division of Engineering Logistics
Faculty of Engineering

Lund, Sweden 2026

Acknowledgment

This master's thesis was written during the spring of 2026 in collaboration with the United Nations World Food Programme, as the final part of our studies at the Faculty of Engineering (LTH), Lund University.

We would like to thank our supervisor at the World Food Programme, Nicholas Finney, for giving us the opportunity to work on a meaningful problem within a humanitarian supply chain context, and for his continuous support and valuable insights into the realities of procurement at WFP. We are equally grateful to our supervisor at Lund University, Professor Andreas Norrman, whose thorough feedback and guidance have been invaluable and have raised the quality of this thesis.

Finally, we would like to thank our families for their endless love and support. We are deeply grateful to them, including for their shared decision to give both of us the great name Ebba. A choice that, somewhat unexpectedly, made things a little easier.

Lund, June 2026
Ebba Evers and Ebba Häggström

Abstract

Background

Climate change has become one of the leading drivers of global food insecurity, and its effects are felt most strongly in regions such as Sub-Saharan Africa. As environmental degradation and climate-related stresses increasingly affect agricultural production, large buyers of food commodities become exposed to growing environmental sourcing risks. The United Nations World Food Programme (WFP) is the world's largest humanitarian organisation and relies heavily on the procurement of agricultural commodities to deliver food assistance. These procurement decisions are currently guided primarily by price and availability. WFP has begun to integrate environmental considerations into its operations through ECODASH, a tool that monitors carbon emissions and waste, but the scope of this work remains limited to those two dimensions. Other environmental impacts and environmental sourcing risks are not yet considered in a structured way within procurement, which limits WFP's ability to make fully risk-informed sourcing decisions.

Problem Definition and Purpose

The central problem addressed in this thesis is the absence of a practical decision support tool that combines environmental impact and environmental sourcing risk in a way that allows WFP to systematically assess, compare and prioritise country-crop sourcing options. The purpose of the thesis is therefore to develop, in collaboration with WFP, a decision support tool that informs sourcing decisions by presenting environmental impact and environmental sourcing risk indicators for country-crop combinations in Sub-Saharan Africa. Three research questions guide the work. The first concerns which environmental impact and environmental sourcing risk dimensions are relevant for agricultural sourcing decisions in the region. The second concerns how these dimensions can be quantified and compared across country-crop combinations. The third concerns how the resulting indicators can be structured into a decision support framework that informs WFP's sourcing decisions.

Method

The thesis adopts a pragmatic research philosophy and an abductive approach, combined with a multi-method design. A Design Science Research strategy was applied and structured according to the Design Science Research Methodology, with elements of Action Design Research incorporated in the design and development phase to support iterative artifact development together with WFP. The work combined a literature search, analysis of secondary quantitative geospatial data and iterative qualitative input from WFP stakeholders. All spatial analysis was carried out in Google Earth Engine, using the Spatial Production Allocation Model (SPAM 2020) as a common crop-specific spatial reference. The tool was demonstrated by applying it to maize sourced from Benin and Tanzania, two of WFP's largest current sourcing origins for maize in Sub-Saharan Africa.

Conclusions

The study identifies two analytically distinct but complementary dimensions of environmental concern in agricultural sourcing. Environmental sourcing risk is structured around abiotic crop stressors related to temperature, water, soil, and biotic stressors such as pests, diseases and weeds. Environmental impact is structured around five ecological consequences of crop production, greenhouse gas emissions, deforestation and land use change, biodiversity loss, water use and quality, and pesticide use. All dimensions are shown to be crop-specific and country-specific. Quantification is achieved through a shared methodological architecture anchored to SPAM 2020 and to a documented two-tier dataset selection process. Environmental sourcing risk indicators are calculated as production-weighted means across the crop production footprint in the sourcing country, while environmental impact indicators are expressed as a per-tonne intensity that can be scaled by procurement volume. Each indicator is reported both as an absolute value and as a ratio to a crop-specific African production-weighted reference mean. The final tool is structured as an integrated but non-aggregated framework that presents a hazard-specific risk profile and a dimension-specific impact profile side by side, making environmental trade-offs visible without reducing them to a single score. The two profiles are presented as paired radar charts in which each indicator is plotted relative to a reference ring set at the African production-weighted mean, so that worse- and better-than-average conditions can be read directly for each sourcing option. The demonstration confirmed that the framework produces coherent, interpretable and directly comparable outputs across sourcing origins. An indicator-level plausibility check further indicated that the computed values are consistent with independent sources and documented regional patterns. Academically, the thesis connects the previously separate research streams of humanitarian logistics and sustainable supply chain risk management, and provides an operational, indicator-based layer for assessing environmental sourcing risk and environmental impact together. In practice, the framework and its accompanying documentation give WFP a transparent and extendable basis for more risk-informed and climate-smart sourcing decisions.

Key words: Humanitarian supply chain, Sustainable procurement, Environmental sourcing risk, Environmental impact, Decision support tool, Supply chain risk management, Design Science Research, Country-crop combination, Sub-Saharan Africa, World Food Programme

Contribution: This thesis has been a complete collaboration between the two authors. Each author has been involved in every part of the process and contributed equally.

Table of Abbreviations

ADR Action Design Research
AWARE Available WAter REmaining
BIE Build, Intervention, and Evaluation
BII Biodiversity Intactness Index
BWF Blue Water Footprint
CGIAR Consultative Group on International Agricultural Research
CHIRPS Climate Hazards Group InfraRed Precipitation with Station Data
CV Coefficient of Variation
DSR Design Science Research
DSRM Design Science Research Methodology
DSS Decision Support System
ECODASH Environmental and Carbon Operations Dashboard
FAO Food and Agriculture Organization of the United Nations
FAOSTAT Food and Agriculture Organization Corporate Statistical Database
GEE Google Earth Engine
GFC Global Forest Change
GHG Greenhouse Gas
GSHTD Global Seamless High-resolution Temperature Dataset
GWP Global Warming Potential
IFAD International Fund for Agricultural Development
IFPRI International Food Policy Research Institute
IPCC Intergovernmental Panel on Climate Change
ISO International Organization for Standardization
JRC Joint Research Centre
LCA Life Cycle Assessment
OECD Organisation for Economic Co-operation and Development
PCR-GLOBWB PCRaster Global Water Balance Model
SCR Supply Chain Risk
SCRM Supply Chain Risk Management
SOC Soil Organic Carbon
SPAM Spatial Production Allocation Model
SPEI Standardised Precipitation Evapotranspiration Index
SPI Standardised Precipitation Index
SSCRM Sustainable Supply Chain Risk Management
TROPOMI TROPOspheric Monitoring Instrument
UN United Nations
UNISDR United Nations International Strategy for Disaster Reduction
WFP World Food Programme
WMO World Meteorological Organization
WRI World Resources Institute

Contents

1 Introduction **1**

1.1 Background . . . 1

1.1.1 United Nations World Food Programme . . . 2

1.1.2 World Food Programme's System Context . . . 2

1.2 Problem Formulation . . . 5

1.3 Tool Requirements . . . 5

1.4 Purpose of Thesis . . . 6

1.5 Research Questions . . . 6

1.6 Delimitation of Scope . . . 6

1.7 Structure of Thesis . . . 7

2 Theoretical Background **9**

2.1 Humanitarian Logistics . . . 9

2.1.1 Definitions and Conceptual Foundations . . . 9

2.1.2 Structural Characteristics . . . 10

2.1.3 Procurement in Humanitarian Logistics . . . 11

2.2 Supply Chain Risk Management . . . 13

2.2.1 Supply Chain Risk . . . 13

2.2.2 Supply Chain Risk Management Process . . . 13

2.2.2.1 Risk Identification . . . 14

2.2.2.2 Risk Assessment . . . 15

2.2.2.3 Risk Mitigation . . . 16

2.2.2.4 Risk Monitoring . . . 17

2.2.3 Sustainable Supply Chain Risk Management . . . 17

2.3 Decision Support Systems . . . 18

2.3.1 The Data Subsystem . . . 19

2.3.2 The Model Subsystem . . . 20

2.3.3 The User Interface Subsystem . . . 21

2.3.4 Synthesis of Design Attributes . . . 22

2.4 Risk Assessment Tools . . . 23

2.4.1 Approaches of Risk Assessment Tools . . . 23

2.4.1.1 Qualitative Tools . . . 24

2.4.1.2 Hybrid Tools . . . 26
2.4.1.3 Quantitative Tools . . . 27
2.4.2 Risk Model Structures . . . 27
2.4.2.1 Probabilistic Risk Models . . . 28
2.4.2.2 Disaster Risk Frameworks . . . 28
2.4.3 Indicator Construction . . . 29
2.4.3.1 Variable Selection . . . 30
2.4.3.2 Normalisation of Variables . . . 31
2.4.3.3 Aggregation and Representation of Risk . . . 32
2.4.3.4 Limitations of Indicators . . . 33
2.5 Crop Growth . . . 36
2.5.1 Crop Growth Requirements . . . 36
2.5.2 Growth Stages . . . 37
2.5.3 Stress Factors Affecting Crop Growth . . . 37
2.5.3.1 Abiotic Stress . . . 38
2.5.3.2 Biotic Stress . . . 41
2.5.3.3 Interactions Between Crop Stress Factors . . . 42
2.5.4 Environmental Impact from Crop Production . . . 43
2.5.4.1 Greenhouse Gas Emission . . . 43
2.5.4.2 Deforestation and Land Use Change . . . 44
2.5.4.3 Biodiversity Loss . . . 44
2.5.4.4 Water Use and Quality . . . 45
2.5.4.5 Pesticide Use . . . 45
2.5.5 Environmental Impact as a Driver and Amplifier of Crop Stressors . . . 46
2.6 Conceptual Framework . . . 46

3 Methodology **48**
3.1 Research Philosophy . . . 49
3.2 Research Approach . . . 49
3.3 Methodological Choice . . . 49
3.4 Research Strategy . . . 50
3.5 Research Design . . . 50
3.5.1 Problem Identification and Motivation . . . 51
3.5.2 Define Objectives for a Solution . . . 51
3.5.3 Design and Development . . . 52
3.5.4 Demonstration . . . 53
3.5.5 Evaluation . . . 53
3.5.6 Communication . . . 54
3.6 Time Horizon . . . 54
3.7 Data Collection . . . 54
3.7.1 Primary Data . . . 54

3.7.2 Secondary Data . . . 55
3.8 Research Quality . . . 56
3.8.1 Validity . . . 56
3.8.2 Reliability . . . 57
3.8.3 Artifact Utility . . . 57
3.8.4 Traceability . . . 58

4 Conceptual Decision Support Tool **59**
4.1 Applying the Disaster Risk Framework to Agricultural Sourcing . . . 60
4.1.1 Hazard . . . 61
4.1.2 Exposure . . . 62
4.1.3 Vulnerability . . . 62
4.1.4 Yield Loss as Sourcing Risk . . . 62
4.1.5 Hazard-Specific Risk Profile . . . 64
4.2 Environmental Impact Assessment of Agricultural Sourcing . . . 65
4.2.1 Procurement Volume as the Basis for Impact Assessment . . . 66
4.2.2 Dimension-Specific Impact Profile . . . 66
4.3 Integrated Risk and Impact Framework . . . 67
4.4 Integrated Output Visualisation . . . 69

5 Development of the Decision Support Tool **71**
5.1 Analytical Foundations . . . 72
5.1.1 Google Earth Engine . . . 72
5.1.2 Spatial Production Allocation Model . . . 72
5.1.3 Climatological Reference Period . . . 74
5.1.4 Calculating African Reference Mean . . . 74
5.2 Development of the Environmental Risk Assessment . . . 75
5.2.1 Dataset Selection Criteria . . . 76
5.2.2 Environmental Risk Dimensions . . . 77
5.2.2.1 Temperature . . . 80
5.2.2.2 Water . . . 81
5.2.2.3 Soil . . . 89
5.2.2.4 Air and Light . . . 92
5.2.2.5 Biotic Stressors . . . 92
5.2.2.6 Synthesis of Limitations and Future Refinements . . . 93
5.3 Development of the Environmental Impact Assessment . . . 96
5.3.1 Dataset Selection Criteria . . . 96
5.3.2 Environmental Impact Dimensions . . . 98
5.3.2.1 Greenhouse Gas Emissions . . . 101
5.3.2.2 Deforestation and Land-use Change . . . 102
5.3.2.3 Biodiversity Loss . . . 104

5.3.2.4 Water Use and Quality 105
5.3.2.5 Pesticide Use 109
5.3.2.6 Synthesis of Limitations and Future Refinements 109

6 Final Decision Support Tool 113

6.1 Overview of the Final Framework 114
6.2 General Formulas and Supporting Variables 116
6.3 Environmental Risk Assessment Component 116
6.4 Environmental Impact Assessment Component 119
6.5 Demonstration 121
6.5.1 Environmental Risk Profile 121
6.5.2 Environmental Impact Profile 124
6.5.3 Combined Interpretation 126
6.6 Evaluation 127
6.6.1 Verification of Results 127
6.6.2 Evaluation Against the Design Objectives and DSS Design Attributes . . 129
6.6.3 Reflections on Methodological Trade-offs 131

7 Conclusion and Discussion 134

7.1 Answering the Research Questions 134
7.1.1 Conclusions for RQ1 134
7.1.2 Conclusions for RQ2 135
7.1.3 Conclusions for RQ3 136
7.2 Contributions 138
7.2.1 Academic Contribution 138
7.2.2 Practical Contribution 140
7.3 Limitations and Future Research 141
7.3.1 Limitations 141
7.3.2 Future Refinements of the Tool 141
7.3.3 Future Research 142
References 144

A SPAM 2020 Crop Coverage 160

B Google Earth Engine Scripts 161

C Dataset Licenses 169

List of Figures

1.1 The operational procurement loop in WFP's supply chain. 4
1.2 Illustration of the scope of the thesis as the intersection of agricultural production, environmental impact and environmental sourcing risk. 7

2.1 Overview of the theoretical background chapter, summarising what is included in each section of the theoretical background. 9
2.2 The components of a decision support system. 19
2.3 A general risk matrix with two dimensions, likelihood and impact. 24
2.4 The Kraljic Purchasing Portfolio Matrix with two dimensions, profit impact and supply risk. 25
2.5 The Sustainable Purchasing Portfolio Matrix with two dimensions, threat to triple bottom line and supply risk (Pagell et al., 2010, p. 68). 26
2.6 Sequential steps in the construction of indicators, from theoretical framework to final risk representation. 30
2.7 The conceptual framework of the thesis, derived from findings of the review of existing literature. 47

3.1 The Research Onion illustrating the methodological structure of this thesis, adapted from Saunders et al. (2019), p. 108. 48
3.2 Illustration of the DSRM process (Peffers et al., 2007) and how ADR is applied within the Design and Development phase. 51
3.3 Research design based on DSRM (Peffers et al., 2007), with the Design and Development phase structured into four building components following the BIE logic of ADR (Sein et al., 2011). 52
3.4 Examples of keywords used in this thesis. 55

4.1 Position of *Chapter 4* within the Design and Development phase of the research design as the first building component, Conceptual Framework Design. 59
4.2 High level conceptual architecture of the decision support system, structured around a database subsystem, a model base subsystem and a user interface subsystem (Sprague & Carlson, 1982). 60
4.3 Detailed conceptual architecture of the decision support system, structured around a database subsystem, a model base subsystem and a user interface subsystem. . 69
4.4 Conceptual illustration of the integrated radar visualisation, with equal sectoral allocation across dimensions, a proportional rainfed and irrigated split within the water hazard sector, and a reference ring marking the regional benchmark. 70

5.1 Position of Chapter 5 within the Design and Development phase of the research design as the second and third building components, Analytical Infrastructure Development and Indicator Development. 71
5.2 SPAM 2020 maize production estimates for Tanzania, expressed in metric tonnes per grid cell at approximately ten kilometre resolution (IFPRI, 2026). 73

6.1 Position of *Chapter 6* within the Design and Development phase of the research design as the fourth building component, Output Formalisation. 113
6.2 Environmental sourcing risk profile for maize sourced from Benin and Tanzania, normalised to the African production-weighted mean. Values outside the reference ring at 1.0 indicate worse-than-average conditions. 123
6.3 Environmental impact profile for maize sourced from Benin and Tanzania, normalised to the African production-weighted mean. Values outside the reference ring at 1.0 indicate worse-than-average impact intensity per tonne of crop produced. . 125
6.4 Integrated environmental sourcing risk profile (left) and environmental impact profile (right) for maize sourced from Benin and Tanzania, normalised to the African production-weighted mean. 126

7.1 Integrated environmental sourcing risk profile (left) and environmental impact profile (right) for maize sourced from Benin and Tanzania, normalised to the African production-weighted mean. 137
7.2 Detailed conceptual architecture of the decision support system, structured around a database subsystem, a model base subsystem and a user interface subsystem. . 138

List of Tables

2.1 Design attributes of the data subsystem. 20
2.2 Design attributes of the model subsystem. 21
2.3 Design attributes of the user interface subsystem. 22
2.4 Synthesis of DSS design attributes by subsystem. 22
2.5 Comparison between probabilistic risk models and disaster risk frameworks. . . . 29
2.6 Summary of challenges and limitations in indicator development. 35
2.7 A general plant's principal growth stages, adapted from Meier (2001, p. 2). 37
2.8 Crop growth requirements and corresponding abiotic stress factors. 41

4.1 Overview of abiotic and biotic stressors that act as hazards in the framework. . . 61

5.1 Dataset selection criteria for the environmental risk assessment. 77
5.2 Dataset selection summary for the environmental risk assessment. 78
5.3 Limitations and future refinements of the environmental sourcing risk dimensions. 94
5.4 Dataset selection criteria for the environmental impact assessment. 98
5.5 Dataset selection summary for the environmental impact assessment. 99
5.6 Limitations and future refinements of the environmental impact indicators. 111

6.1 Complete indicator set of the final decision support tool. 115
6.2 General formulas and supporting variables. 116
6.3 Risk indicator overview, including dataset references. 117
6.4 Environmental impact indicator overview, including dataset references. 120
6.5 Environmental sourcing risk profile for maize sourced from Benin and Tanzania, with the African production-weighted mean and normalisation ratios. 122
6.6 Environmental impact profile for maize sourced from Benin and Tanzania. 124

A.1 All 46 crops included in SPAM 2020 Version 2.0, with their internal crop codes. . 160

C.1 Datasets used in Chapter 5 and their licences. 169

1 Introduction

This chapter introduces the study by establishing its background and context, formulating the problem, and defining the tool requirements and purpose of the thesis. It further presents the research questions guiding the study and clarifies the scope and delimitations.

1.1 Background

Food security is defined as a situation that exists when all people, at all times, have physical and economic access to sufficient, safe and nutritious food that meets their dietary needs and food preferences for an active and healthy life (FAO, 1996). Today, more than 340 million people are facing acute levels of food insecurity worldwide. Although hunger is one of the biggest problems in the world, it is also one of the most solvable (WFP, 2026b).

Historically, improvements in global food security have been closely linked to poverty reduction, as reflected in international development strategies such as those of the World Bank (Binswanger & Landell-Mills, 1995). However, in recent years a change in this relationship has been observed at a global level, where the number of people living in poverty has continued to decline while both the proportion and absolute number of people experiencing food insecurity have increased (Dasgupta & Robinson, 2022). This reverse trend has been driven by a combination of conflict, climate change, economic shocks and displacement. These drivers are often overlapping and reinforcing, making food insecurity a complex and persistent global challenge (FAO et al., 2020).

Climate change is one of the leading drivers of the recent escalation in global hunger. Climate-related hazards increasingly undermine agricultural production, livelihoods and food systems, particularly in vulnerable regions such as Sub-Saharan Africa, where the most negative impact has been observed (Dasgupta & Robinson, 2022). In 2024, 307 million people, representing 20 % of the continent's population, were affected by hunger (FAO et al., 2025). In addition, agricultural supply chains are increasingly exposed to environmental degradation and climate-related stresses. Issues such as water scarcity, soil degradation, deforestation, biodiversity loss and rising temperatures are already affecting agricultural productivity in many regions (WFP, 2026b). These environmental pressures translate directly into sourcing risks for large buyers of food commodities.

Without immediate climate action, climate change is likely to accelerate existing trends of increasing food insecurity. As a consequence, humanitarian supply chains face not only rising demand for relief supplies but also growing sourcing risks (WFP, 2024).

1.1.1 United Nations World Food Programme

The United Nations World Food Programme (WFP) is the world's largest humanitarian organisation, working towards the ultimate goal of a world where no one is left without enough food. WFP delivers life-saving food assistance in emergencies where people suffer from conflict, disasters and the impact of climate change (WFP, 2026b).

Within procurement, sourcing decisions can be understood as combinations of a specific crop sourced from a specific country, for example maize from Tanzania. In this thesis, such combinations are referred to as country-crop combinations. To deliver food assistance, WFP relies on two main sourcing approaches. The first is in-kind contributions, where donors provide food commodities directly. The food often originates from surplus production in donor countries such as the United States or South Korea. As these contributions are donations, they offer limited flexibility in terms of commodity choice and country of origin. The second approach is procurement, whereby WFP purchases food commodities directly from markets. Unlike in-kind contributions, procurement allows WFP to actively choose which crops to buy, where to source them and from which suppliers. Currently, procurement decisions are primarily guided by price and availability, ensuring that sufficient quantities of food can be delivered efficiently. However, procurement also takes other factors into account, such as ethical and local sourcing, suitability of the food basket for beneficiary preferences and nutritional value.[1]

One of WFP's guiding principles is the use of risk-based decision-making (WFP, 2021). This means identifying, assessing and managing multiple threats and complex risks related to WFP's ability to achieve its goals.

In recent years, WFP has strengthened its focus on sustainability within its supply chain operations through the development of ECODASH, a tool designed to measure, monitor and analyse carbon emissions and waste across supply chain activities. ECODASH is primarily used to establish emissions baselines, support reporting and evaluate different operational scenarios (WFP, 2026a). While this represents an important step towards integrating environmental considerations into operational decision-making, its current scope is limited to carbon emissions and waste monitoring. Other dimensions of environmental impact and environmental sourcing risk are not yet integrated into ECODASH. As a result, the tool does not currently provide a comprehensive basis for fully risk-informed sourcing decisions. This limitation raises the question of how broader environmental dimensions can be systematically integrated into procurement decision-making.

1.1.2 World Food Programme's System Context

Humanitarian supply chains play a critical role in saving lives. At the same time, the agricultural production systems they rely on for food procurement generate environmental impact and greenhouse gas emissions. Within the food systems WFP sources from, they act as one of many

[1] Nicholas Finney, Supply Chain Sustainability Officer, World Food Programme. Internal online meeting, 22 January 2026.

buyers and typically account for only a small share of regional production and demand. Applying risk-based decision-making to sourcing and procurement nonetheless allows WFP to anticipate environmental risks to its own operations and to account for the share of environmental impact associated with its sourcing. This supports the long-term resilience of the production systems on which WFP depends and is consistent with extending the humanitarian principle of "do no harm" to protect smallholder production systems and strengthen the health and resilience of food systems.

Environmental impact refers to the ecological effects associated with the production and sourcing of agricultural commodities, such as greenhouse gas emissions, water use and biodiversity loss (Gallardo, 2024). Environmental sourcing risk refers to the probability and severity of procurement instability arising from environmental conditions affecting agricultural production systems (Giannakis & Papadopoulos, 2016). Although analytically distinct, these dimensions are interrelated. Production systems with high environmental impact may contribute to long-term ecosystem degradation, which in turn increases exposure to environmental sourcing risks (Oliveira et al., 2019). These environmental risks may ultimately affect procurement outcomes by reducing yields, which in turn lowers availability and increases price volatility.

At a broader system level, climate change is a key driver of food insecurity, as it alters the environmental conditions on which agricultural production depends. Rising food insecurity increases the need for humanitarian response, which organisations such as WFP meet in part by sourcing agricultural commodities. These commodities are produced within conventional agricultural food systems whose cumulative practices can generate environmental impact, and over time, contribute to ecosystem degradation. The broader context in which WFP procures is therefore one where climate change, food insecurity, and the environmental impacts of agricultural production interact in ways that can affect smallholder resilience and long-term food system health.

At an operational level, WFP's procurement decisions determine which crops are purchased and from which regions, and therefore which production systems its sourcing supports. The agricultural practices used in these systems may contribute to environmental impact, a share of which can be attributed to WFP's procurement volume. Over time, these impacts can contribute to the degradation of the natural resource base, with implications primarily for smallholder producers in sourcing areas. While these producers are not necessarily the same population as WFP's beneficiaries, they are still part of the food systems affected by WFP's procurement footprint. In this sense, the "do no harm" principle in humanitarian sourcing means considering how procurement decisions may affect the productive capacity and resilience of smallholder producers over time. Additionally, declining land productivity also reduces and destabilises yields, lowering availability and contributing to price volatility. These conditions feed back into WFP's own procurement as environmental sourcing risk, which WFP may respond to by adjusting suppliers or regions, closing the operational loop shown in *Figure 1.1.* The environmental impact of agricultural sourcing therefore represents a largely indirect externality that affects both the producers WFP relies on and WFP's own continuity of supply.

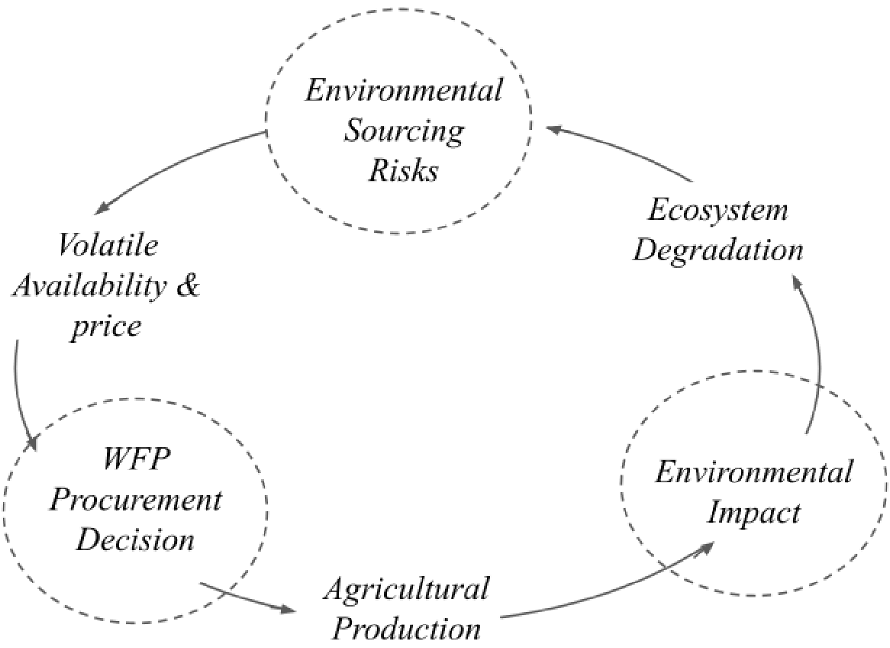

Figure 1.1: The operational procurement loop in WFP's supply chain.

WFP's procurement decisions therefore sit within two connected systems. At the broader level, they are embedded in the climate–food security context to which WFP responds. At the operational level, they shape and respond to environmental sourcing risk and supply stability. Through its wider programming, WFP is already deeply engaged in strengthening these systems by improving the resilience, livelihoods and market access of the producers and communities it works with. The environmental impacts described here are largely indirect. However, greater consideration of smallholder production and food-system resilience can help WFP address environmental risk both to their own operations and to the producers they source from. WFP's current procurement risk assessment does not yet take these dynamics into account, which is the gap this thesis addresses.

While WFP's procurement decisions are embedded in complex and interrelated systems, existing research provides relevant perspectives on how such decisions can be supported. Research on supply chain risk management has led to the development of various tools and frameworks to identify, assess and manage risks in sourcing decisions (Ho et al., 2015; Tang, 2006). Over time, traditional procurement tools have also been adapted to incorporate environmental considerations in sourcing decisions (Pagell et al., 2010). In parallel, environmental sustainability has gained increasing attention in the literature on humanitarian procurement (Tay et al., 2025; Thakur-Weigold et al., 2025). This growing focus on sustainability extends beyond procurement to the broader humanitarian supply chain, where environmental considerations such as emissions, resource use and life cycle impacts are gaining increasing attention (Van Wassenhove, 2006; Kembro et al., 2024; Besiou & Van Wassenhove, 2020; Corbett et al., 2022). However, these research streams have largely developed separately, with limited integration of environmental impact and environmental sourcing risk in decision support tools for humanitarian procurement.

1.2 Problem Formulation

While WFP has successfully developed ECODASH to monitor greenhouse gas emissions and waste across its supply chains, its current scope is limited to these dimensions. Other critical environmental impacts and environmental sourcing risks are not yet systematically integrated within its procurement risk assessment. This limits WFP's ability to make fully informed risk-based decisions when procuring in Sub-Saharan Africa.

The central problem addressed in this thesis is therefore the absence of a practical decision support tool that combines environmental impact and environmental sourcing risk in a way that WFP could use to support the systematic assessment, comparison and prioritisation of country-crop sourcing options.

1.3 Tool Requirements

Building on the problem formulation in *Section 1.2*, a set of requirements has been defined that a solution must fulfil to address WFP's identified need. These requirements were clarified through iterative discussions with the WFP supervisor and reflect the operational realities of procurement decision-making at WFP.

The primary users of the tool are procurement personnel responsible for sourcing decisions and supplier selection. Secondary users include supply chain planning teams, programme design personnel and sustainability teams involved in sourcing strategy development, sustainability reporting and food basket planning.

The tool must support two distinct use cases. The first is comparative assessment, where multiple sourcing options are being evaluated and the tool enables structured environmental comparison across them. The second is risk profiling, where a sourcing country has already been selected and the tool should provide a detailed environmental profile for monitoring and reporting purposes. The tool must be usable in both situations.

In terms of inputs, the tool should accept the crop, sourcing country and intended procurement volume in metric tonnes as the primary parameters describing a sourcing decision. In terms of outputs, the tool must provide indicator-level results for each environmental dimension, expressed both as absolute values and in relation to a regional reference. This enables procurement personnel to interpret whether a result is high or low compared to alternative sourcing options. The tool does not aim to model price or yield outcomes directly, but to make the environmental drivers of sourcing risk and impact visible and comparable.

To be useful in practice, the tool must be usable without technical expertise, transparent in its reasoning, and scalable so that additional dimensions can be incorporated as data availability improves.

1.4 Purpose of Thesis

The purpose of this master's thesis is to develop, in collaboration with WFP, a decision support tool that informs sourcing decisions by presenting environmental impact and environmental sourcing risk indicators for country-crop combinations in Sub-Saharan Africa.

1.5 Research Questions

The following questions form the foundation of the thesis, and answering them should help in achieving the purpose stated in *Section 1.4*.

RQ1 Which environmental impact and environmental sourcing risk dimensions are relevant for agricultural sourcing decisions in Sub-Saharan Africa?

RQ2 How can these dimensions be quantified and compared across country-crop combinations?

RQ3 How can these indicators be structured into a decision support framework that informs WFP's sourcing decisions?

1.6 Delimitation of Scope

The scope of this thesis is limited to environmental impact and environmental sourcing risks at a country-crop level in Sub-Saharan Africa. The country-crop combination is the primary unit of analysis, reflecting sourcing decisions defined by both commodity type and country of origin. The decision support tool is developed for WFP's procurement and sourcing functions, aimed at supporting more informed and risk-based sourcing decisions. The selection and initial prioritisation of specific crops and countries are determined in consultation with WFP.

While many different factors may influence procurement decisions, the analysis is restricted to impacts and risks that originate in the production stage of the crop and that can translate into sourcing risks. This delimitation is based on the scope defined in collaboration with WFP, where the primary focus is on environmental conditions affecting agricultural production and their implications for sourcing. Activities occurring after production, such as processing, transportation, storage or handling, are therefore excluded from the analysis. Furthermore, the study is limited to environmental dimensions of both impact and sourcing risk. Other categories of impact and risk that may influence sourcing decisions, such as social, economic, political or governance-related factors, are not considered. This means that aspects such as labour conditions, supplier ethics, corruption and broader market or policy risks are excluded. The conceptual scope of this thesis is illustrated in *Figure 1.2*.

While the decision support tool incorporates multiple environmental impact and environmental sourcing risk dimensions, the scope is restricted to developing a useful framework rather than exhaustive quantitative models for every possible dimension. The tool is intended to support decision-making by identifying potential areas of concern that may require further analysis or mitigating actions. It is not intended to serve as the sole basis for decision-making.

While the long-term goal for WFP is to integrate the decision support tool as a standalone module within ECODASH, the development of a fully integrated technical application is beyond the scope of this thesis due to time and resource constraints. This project therefore focuses on designing and demonstrating the underlying framework and methodology, providing a foundation for future integration and expansion into ECODASH.

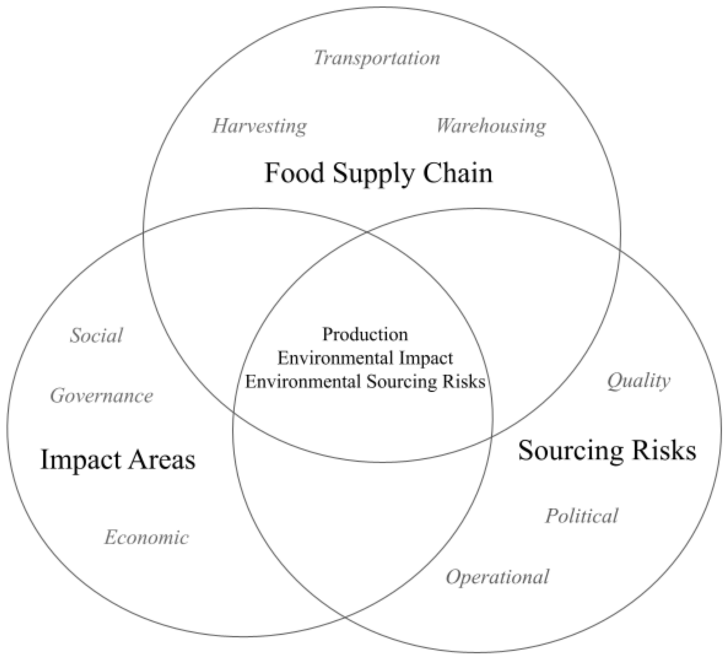

Figure 1.2: Illustration of the scope of the thesis as the intersection of agricultural production, environmental impact and environmental sourcing risk.

1.7 Structure of Thesis

This section presents an overview of each chapter in this thesis.

***Chapter 2*: Theoretical Background**
The second chapter establishes the theoretical foundation by reviewing literature on humanitarian logistics, supply chain risk management, and decision support systems. It then examines risk assessment tools and the environmental factors influencing crop production, covering both crop stressors and the ecological impacts of production. The chapter concludes by synthesising these streams into the conceptual framework that guides the thesis.

***Chapter 3*: Methodology**

The third chapter outlines the research methodology, structured according to the Research Onion. It describes the research philosophy, approach and design, including the Design Science Research strategy and its building components, followed by the data collection methods and analysis procedures. Finally, the quality of the research is discussed in terms of validity, reliability, artifact utility and traceability.

***Chapter 4*: Conceptual Decision Support Tool**

The fourth chapter develops the conceptual design of the tool, translating the theoretical relationships into concrete design choices. It defines the two analytical components, environmental sourcing risk and environmental impact, and the integrated framework structure they produce, presenting the ideal design before practical constraints are considered.

***Chapter 5*: Development of the Decision Support Tool**

The fifth chapter translates the conceptual framework into a functional tool through concrete choices about indicators, datasets and calculations. It first introduces the shared analytical foundations and then documents the development of the environmental risk assessment and the environmental impact assessment separately, including the dataset selection process and the limitations of each dimension together with possible future refinements.

***Chapter 6*: Final Decision Support Tool**

The sixth chapter presents the final structure of the tool, describing the overall framework and the two assessment components together with their complete indicator set. The outputs are then illustrated and interpreted through an applied example using maize sourced from Benin and Tanzania. The chapter concludes by verifying the plausibility of the computed results, evaluating the tool against the design objectives and decision support attributes and reflecting on the methodological trade-offs that shaped it.

***Chapter 7*: Conclusion and Discussion**

The seventh and final chapter brings the thesis to a close by returning to the three research questions and presenting the answers to each. It then positions the academic and practical contributions of the study, and finally discusses its limitations and outlines a prioritised agenda for future research.

2 Theoretical Background

This chapter establishes the theoretical foundation of the study by reviewing existing literature structured as in Figure 2.1. The chapter covers key concepts and frameworks within humanitarian logistics, supply chain risk management, and decision support systems. It further examines risk assessment tools and environmental factors influencing crop production, leading to the development of a conceptual framework.

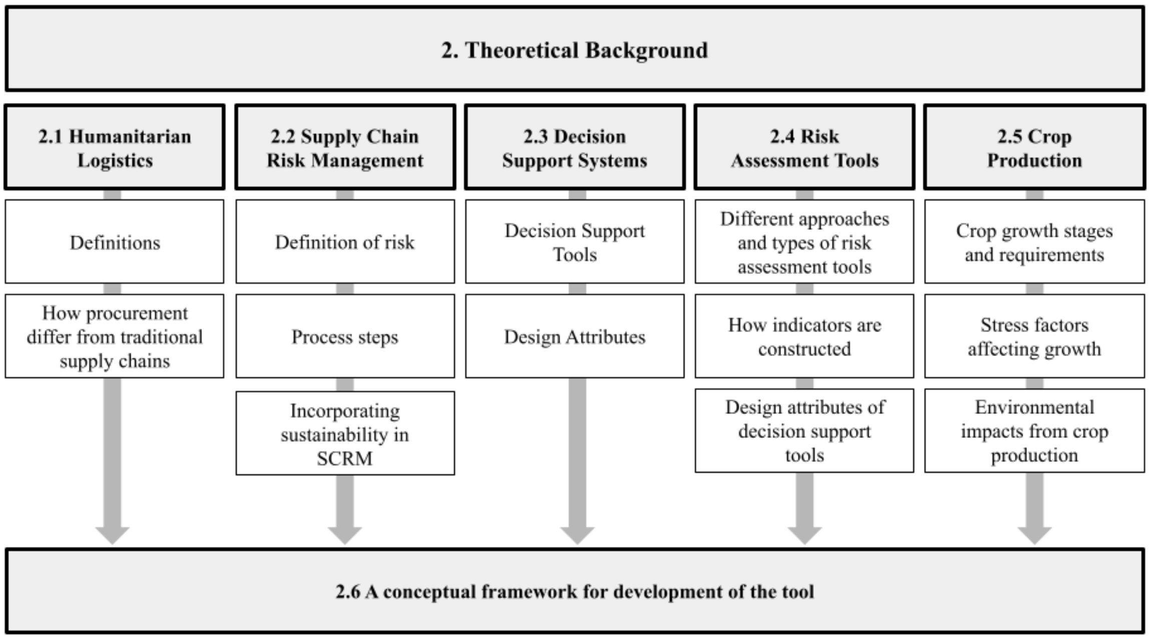

Figure 2.1: Overview of the theoretical background chapter, summarising what is included in each section of the theoretical background.

2.1 Humanitarian Logistics

2.1.1 Definitions and Conceptual Foundations

Humanitarian logistics is a relatively new research area, and the definition of the concept has evolved over the past two decades. Early dominating definitions were first formulated around 2005 and primarily framed humanitarian logistics in operational terms, focusing on the movement and storage of relief goods under emergency conditions (Van Wassenhove, 2006). Since then, both the scope of activities and objectives have expanded (Kembro et al., 2024), reflecting a shift toward a more comprehensive supply chain perspective. This development includes a growing recognition of environmental sustainability and the application of life cycle assessment approaches, addressing issues such as waste management, energy use and CO_2 emissions within humanitarian operations

(Besiou & Van Wassenhove, 2020; Corbett et al., 2022). More recently, Kembro et al. (2024) revisited and refined the definition to better reflect the maturity of the field. They propose defining humanitarian logistics as:

> "The logistics and supply chain management focusing on the preparation for, response to and recovery from a humanitarian crisis, with the aim of saving lives and alleviating the suffering of affected populations."

While evolving definitions clarify what humanitarian logistics covers, it is also important to understand the context in which it operates. Humanitarian and commercial supply chains share similar activities, such as procurement, transportation and warehousing. However, they operate in fundamentally different institutional and operational environments (Faruquee et al., 2026). Humanitarian supply chains cannot be managed according to commercial logics, as their goals, funding mechanisms, demand patterns and operating conditions are different.

The purpose of the supply chains is central in distinguishing humanitarian logistics from commercial logistics (Tomasini & Van Wassenhove, 2009). Humanitarian logistics is fundamentally mission driven. Whereas commercial supply chains typically prioritise profitability and customer value, the primary purpose of humanitarian supply chains is to save lives and alleviate the suffering of vulnerable people affected by disasters and crises (Kembro et al., 2024). This shapes how performance is defined, how priorities are set and which trade-offs are considered acceptable. Decisions that may be considered inefficient or suboptimal in a commercial perspective may be justified in a humanitarian context if they contribute to saving lives.

2.1.2 Structural Characteristics

While the mission of humanitarian logistics provides its normative foundation, understanding the structural conditions under which it operates is essential for contextualising the decision-making environment. Humanitarian supply chains function in settings characterised by high uncertainty, urgency, funding constraints, limited data and complex multi-stakeholder environments (Faruquee et al., 2026).

Humanitarian operations are characterised by profound uncertainty. Disasters and crises are difficult to predict in terms of timing, scale, location and duration (Kovács & Spens, 2007). In the early stages of response, needs assessments are often incomplete, and reliable information regarding affected populations, infrastructure status and available local resources may be limited. As situations evolve, demand can change rapidly both in scale and in the type of required relief items (Tomasini & Van Wassenhove, 2009). In addition to uncertainty, disaster response is often marked by extreme urgency and time pressure. This puts high pressure on lead times and rapid decision-making. Delays in delivery of critical aid can directly affect survival rates and exacerbate suffering (Van Wassenhove, 2006).

A third structural characteristic distinguishing humanitarian supply chains from commercial systems is resource and funding constraints. Humanitarian operations are heavily shaped by external donor funding, which is frequently earmarked, short-term and volatile, leading to funding gaps and constrained budgets (Jahre & Heigh, 2008). Consequently, humanitarian organisations must align operational decisions with donor requirements and available funding. Moreover, humanitarian supply chains operate in a complex multi-stakeholder environment involving NGOs, UN agencies, donors, governments, military actors, local authorities and private suppliers (Jahre & Jensen, 2010). These actors often operate under differing mandates, accountability structures and performance priorities, which can create conflicting objectives and coordination challenges. Furthermore, limited data availability, inconsistent data quality and underdeveloped IT infrastructure reduce supply chain visibility and add to the difficulties of effective coordination and overall management (Jahre et al., 2016). Lastly, poor infrastructure, political instability and security risks add substantial complexity to the environment in which humanitarian supply chains work (Van Wassenhove, 2006).

Taken together, these structural characteristics generate a constant balancing of trade-offs in humanitarian supply chains. Unlike commercial supply chains, where performance is often measured through efficiency and financial outcomes, humanitarian supply chains are primarily evaluated in terms of speed, responsiveness and life-saving performance (Kovács & Spens, 2007; Van Wassenhove, 2006). As a result, decision-making is shaped by trade-offs where immediate life-saving necessities and operational feasibility may take precedence over longer-term objectives (Corbett et al., 2022). These conditions show the constrained flexibility under which strategic choices are made in humanitarian contexts. Understanding this structure is essential for analysing how sustainability considerations can be integrated into humanitarian logistics.

2.1.3 Procurement in Humanitarian Logistics

Procurement is a critical and challenging process in humanitarian logistics. Purchasing of goods and services accounts for 65% of total operational expenditure in humanitarian organisations (Falasca & Zobel, 2011). Procurement typically covers food commodities, medical supplies, shelter materials, logistics services and other relief items. In food assistance organisations such as WFP, procurement mainly concerns large volumes of staple commodities. Humanitarian procurement can broadly be divided into prepositioning and emergency procurement. Prepositioning refers to purchasing and positioning goods in advance of a crisis in order to reduce response time and improve preparedness (Van Wassenhove, 2006; Falasca & Zobel, 2011). Emergency procurement takes place after a crisis has occurred and is driven by urgent operational needs. Humanitarian organisations must constantly balance investments in prepositioned stock with post-disaster purchasing under high uncertainty (Thakur-Weigold et al., 2025).

Procurement decisions are guided by price and availability, but these are not the only criteria. Supplier reliability, delivery capacity, quality standards and compliance with formal procedures are central considerations (Moshtari et al., 2021). Humanitarian organisations must follow strict ethical and governance principles, including transparency, equality and accountability. The involvement of multiple stakeholders further increases the complexity of procurement, as they may have different and sometimes conflicting objectives (Moshtari et al., 2021). Additionally, donor funding is often earmarked for specific projects, countries or purposes, which can further restrict sourcing flexibility (Moshtari et al., 2021). Procurement is therefore not only a technical sourcing activity but also a regulated function shaped by donor requirements and public scrutiny, meaning that decisions may reflect political and institutional priorities alongside operational needs.

Risk mitigation is embedded in procurement decisions. Supplier selection and sourcing strategies are key tools for reducing exposure to supply disruption, quality failures and contextual instability (Pontré et al., 2011). Unlike commercial procurement, which may accept certain risks in pursuit of competitive advantage, humanitarian procurement prioritises continuity of supply. Stockouts cannot be valued in purely financial terms, as failure to deliver may directly affect lives and cause death (Thakur-Weigold et al., 2025).

Sourcing decisions also shape longer-term outcomes. Large-scale procurement may influence production systems and market dynamics in the areas from which food is purchased (Tay et al., 2025). Prioritising local, national, or regional sourcing can support domestic markets, create income opportunities, and contribute to recovery and resilience in sourcing areas, even when procurement does not take place in the same sub-national areas where assistance is distributed. In less developed or fragile agricultural regions, such procurement may still support livelihoods, strengthen market access, and contribute to local economic development among producer communities. At the same time, local markets may have limited capacity, higher price volatility or be exposed to climate-related risks. In such cases, global sourcing can provide access to larger supplier bases and potentially more stable volumes. However, global sourcing increases dependency on international trade flows, transport infrastructure and currency conditions (Thakur-Weigold et al., 2025). These choices illustrate recurring trade-offs. Local sourcing may support resilience and reduce transport distances but may be more costly or risky in the short term. Global sourcing may enhance short-term supply security but weaken local market development and increase environmental impact.

Sustainability has gained increasing attention in humanitarian procurement (Thakur-Weigold et al., 2025; Tay et al., 2025). Relief operations often generate significant environmental impact, for example through temporary shelters, packaging and transport. Procurement practices such as framework agreements, supplier selection and group purchasing influence both cost and environmental outcomes. Incorporating sustainability criteria adds further complexity, as organisations must balance environmental impact with speed, cost and availability. This highlights the importance of processes that clearly identify and assess trade-offs, rather than allowing them to remain unexamined.

2.2 Supply Chain Risk Management

2.2.1 Supply Chain Risk

Supply chains have become increasingly complex due to globalisation, outsourcing, and the growing interdependence between firms and their suppliers (Ho et al., 2015). As a result, organisations are exposed to a wide range of uncertainties and potential disruptions that can negatively affect supply chain performance and business continuity.

In engineering and safety contexts, risk is commonly presented as a combination of the probability of an event and the severity of its consequences (Aven, 2010). The standard ISO 31000, issued by the International Organization for Standardization (ISO) defines risk as "the effect of uncertainty on objectives" (ISO, 2018). This definition highlights that risk is always related to organisational goals and that uncertainty is a central component.

Supply chain risk is often described as the likelihood and impact of unexpected events or conditions that disrupt the flow of materials, information, or financial resources within a supply chain, thereby negatively affecting operational or strategic performance (Ho et al., 2015). These disruptions can occur at different stages of the supply chain. Upstream risks originate from suppliers and production systems, while downstream risks occur in distribution and delivery activities. More specifically, supply chain risks represent the potential for negative deviations from expected performance outcomes such as delivery reliability, product quality, or financial results (Hofmann et al., 2014).

Given the complexity and interdependencies within modern supply chains, understanding potential sources of risk is therefore essential for organisations seeking to maintain stable operations and improve supply chain resilience (Ho et al., 2015; Wang et al., 2022).

2.2.2 Supply Chain Risk Management Process

In response to the various risks and challenges that supply chains are exposed to, the concept of supply chain risk management (SCRM) has gained increasing attention (Ho et al., 2015). SCRM refers to the identification and evaluation of risks within supply chains and the implementation of coordinated strategies to mitigate their potential impact across supply chain actors (Bandaly et al., 2012). The objective of SCRM is to reduce supply chain vulnerability and improve the ability of organisations to anticipate, respond to, and recover from disruptions.

In SCRM, risks across the broader supply chain network are considered and coordinated efforts among multiple actors are therefore emphasised (Bandaly et al., 2012). This broader perspective reflects the interdependent nature of modern supply chains, where disruptions affecting one actor may propagate across the entire network. Supply chain risk management can involve both proactive and reactive approaches (Ho et al., 2015). Proactive strategies aim to identify and prevent potential disruptions before they occur, whereas reactive strategies focus on responding to and recovering from disruptions once they have materialised.

In the literature, SCRM is a structured process consisting of several stages. Although the terminology may vary across studies, the process typically includes (1) risk identification, (2) risk assessment, (3) risk mitigation and (4) continuous monitoring of risks (Bandaly et al., 2012; Ho et al., 2015). These stages provide a systematic framework for analysing potential supply chain risks and developing strategies to manage them effectively. The following sections describe the main stages of the process in more detail.

2.2.2.1 Risk Identification

Risk identification represents the first step in the supply chain risk management process and focuses on detecting potential threats that may disrupt supply chain operations. The purpose of this stage is to identify all relevant risks that could affect the flow of materials, information, or financial resources within the supply chain before they materialise into actual disruptions (Fan & Stevenson, 2018). Identifying risks at an early stage is essential, as risks that remain undetected cannot be assessed or managed effectively. Consequently, risk identification provides the foundation for all subsequent risk management activities (Kern et al., 2012; Fan & Stevenson, 2018).

Supply chain risks are categorised in different ways in the literature, and no single classification scheme appears to dominate across all studies (Ho et al., 2015; Fan & Stevenson, 2018). Ho et al. (2015) show that previous research has classified supply chain risks as internal and external risks, as operational and disruption risks, or as organisational, network-related, and environmental risks. They further note that supply chain risks may also be understood in terms of micro-risks and macro-risks, depending on the degree and scope of their impact. Additionally, risk identification should adopt a holistic perspective, since supply chains consist of interconnected actors and activities and disruptions in one part of the network may propagate to other parts of the chain (Kern et al., 2012; Fan & Stevenson, 2018). Procurement decisions play an important role in this context, as they determine which suppliers and sourcing regions become part of the supply chain and thereby shape the conditions under which downstream activities operate (Kern et al., 2012). Risk identification therefore needs to consider not only isolated risk sources, but also how vulnerabilities are linked across the broader supply chain structure.

Adopting a systematic and structured risk identification approach enables organisations to identify risks in a more comprehensive and resource-efficient manner (Fan & Stevenson, 2018). One way to structure this process is by analysing underlying risk drivers, defined as factors that increase the likelihood or potential impact of disruptions. Kern et al. (2012) suggest that organisations can improve the efficiency of risk identification by defining observation fields that represent known sources of risk or vulnerable areas within the supply chain. Such observation fields are often closely related to the structural characteristics and strategic choices of the supply chain (Kern et al., 2012). In many cases, the way a supply chain is designed or managed may itself create conditions that increase exposure to risk. For example, humanitarian organisations may adopt local sourcing strategies in order to support local markets, reduce transportation distances and contribute to economic recovery in affected regions. At the same time, local markets may also have limited capacity or be exposed to environmental conditions such as droughts or climate-related disruptions. In such situations, supply chains relying heavily on local suppliers may become vulnerable if environmental events affect local production or market availability. Consequently, managers must consider how supply chain strategies may act as drivers of potential supply chain risks.

In addition to analysing structural characteristics and strategic choices, organisations can apply other practical approaches. One commonly suggested method is supply chain mapping, which visualises the structure of the supply chain network and highlights critical suppliers, processes and nodes where disruptions may occur (Polyviou et al., 2022). Another approach involves the use of operational data or check-sheets that track past supply chain events (Tummala & Schoenherr, 2011). Organisations may also use tools such as brainstorming sessions and fault tree analysis (Polyviou et al., 2022).

2.2.2.2 Risk Assessment

Following the identification of potential supply chain risks, the next step in the supply chain risk management process is risk assessment (Bandaly et al., 2012; Ho et al., 2015). The purpose of risk assessment is to evaluate the significance of identified risks by analysing their likelihood of occurrence and the potential consequences they may have for supply chain performance (Kern et al., 2012).

The assessment stage typically aims to develop a thorough understanding of each identified risk (Kern et al., 2012). This involves gathering information about the type of risk, its possible sources, and the stage of the supply chain where the disruption may occur. The assessment also considers the potential consequences of the disruption and how it may affect supply chain performance. Such information may be derived from historical data, quantitative analyses, or more qualitative approaches such as expert judgement (Polyviou et al., 2022).

Through this evaluation, organisations are able to compare different risks and prioritise those that require the most urgent attention (Fan & Stevenson, 2018). Risk prioritisation is necessary because organisations rarely have sufficient resources to mitigate all identified risks simultaneously. In practice, this prioritisation is often supported by analytical tools that facilitate the comparison of risks based on their likelihood and impact. Further discussion of such risk assessment tools is provided in *Section 2.4*.

However, the probability-based interpretation of risk has been critically examined in the risk literature. Aven (2016) argues that defining risk solely through probabilities and consequences may be too narrow, particularly in situations characterised by limited knowledge or high uncertainty. In practice, probability estimates are influenced by assumptions, data limitations and expert judgement. This means that probabilities in risk assessments should not be understood as exact representations of reality. Instead, they reflect a judgement about uncertainty based on the knowledge available at the time of the assessment (Aven, 2010, 2016).

Aven (2016) further emphasises that risk assessments therefore should not only present numerical estimates, but also reflect the strength and limitations of the knowledge supporting those estimates. Two assessments may produce identical probability values while being based on very different levels of data quality, modelling assumptions or expert consensus. Ignoring this distinction can lead to misleading interpretations. Risk is therefore closely linked to uncertainty and to the quality of the underlying knowledge, rather than being an objective quantity that can be measured independently of context.

Together, these perspectives illustrate that risk assessment is not only a technical calculation of probabilities. It is a structured process for analysing uncertain consequences in relation to objectives while also explicitly stating the assumptions and knowledge on which the assessment is based. By enabling organisations to compare and prioritise risks, risk assessment provides the foundation for selecting appropriate risk mitigation strategies.

2.2.2.3 Risk Mitigation

In the risk mitigation stage, organisations identify and implement appropriate strategies for managing the risks that have been prioritised during the assessment phase (Fan & Stevenson, 2018). Through mitigation efforts, organisations aim to reduce supply chain vulnerability and improve their ability to maintain operational performance despite disruption (Polyviou et al., 2022).

After risks have been assessed and prioritised, organisations may choose between several response options depending on the nature and severity of the risk (Fan & Stevenson, 2018; Ho et al., 2015). One option is risk avoidance, which involves eliminating the source of risk entirely, for example by discontinuing activities or avoiding certain suppliers or markets associated with high levels of uncertainty (Polyviou et al., 2022). Another approach is risk reduction, where organisations implement measures aimed at lowering either the likelihood of disruptions or their potential consequence (Tang, 2006). This may involve strategies such as increasing flexibility, building redundancy or improving coordination between supply chain actors. In some cases, organisations may choose risk transfer, where responsibility for certain risks is shifted to other actors through mechanisms such as insurance or contractual agreements (Polyviou et al., 2022). Finally, organisations may also accept certain risks when the cost of mitigation exceeds the expected impact of the disruption (Fan & Stevenson, 2018). These response options illustrate that mitigation does not necessarily imply eliminating risks entirely, but rather selecting appropriate strategies for managing them within the broader supply chain context.

However, mitigation strategies may involve trade-offs, as actions taken to reduce one type of supply chain risk may simultaneously increase exposure to other risks (Fan & Stevenson, 2018).

For instance, strategies such as increasing inventory or adding capacity can reduce the impact of supply disruptions but may also increase costs or reduce operational efficiency (Tang, 2006). In addition, organisations must often prioritise mitigation actions within limited financial and organisational resources (Fan & Stevenson, 2018). This highlights the importance of adopting a system-wide perspective when selecting mitigation strategies, as supply chains consist of interconnected processes and decisions.

2.2.2.4 Risk Monitoring

The final stage in the supply chain risk management process is risk monitoring. This stage focuses on continuously tracking identified risks and observing changes that may affect their likelihood or potential consequences over time (Fan & Stevenson, 2018). Risk monitoring is necessary because supply chains operate in dynamic environments where new risks may emerge and previously assessed risks may change as conditions evolve (Ho et al., 2015). As a result, earlier risk assessments may quickly become outdated if risks are not continuously monitored.

The purpose of risk monitoring is therefore not only to track existing risks, but also to evaluate whether implemented mitigation strategies remain effective and if additional actions are required (Fan & Stevenson, 2018). To support the process, organisations may rely on performance indicators, monitoring systems or early warning signals that allow deviations in supply chain performance to be detected at an early stage (Tummala & Schoenherr, 2011). Overall, risk monitoring ensures that the supply chain risk management process remains adaptive and responsive to changing conditions. By continuously observing risk developments and evaluating mitigation measures, organisations can update their risk assessments and refine their risk management strategies over time.

2.2.3 Sustainable Supply Chain Risk Management

Sustainability considerations have increasingly been integrated into supply chain management as environmental and social issues are gaining greater importance in both research and practice (Wang et al., 2022). As a result, the scope of supply chain risk management has expanded to include risks related to economic, environmental and social objectives, often referred to as the triple bottom line (Xu et al., 2019). Traditional SCRM has mainly focused on risks that disrupt and affect the flow and performance of the supply chain (Ho et al., 2015). However, sustainability challenges can both generate new risks and intensify existing operational risks (Giannakis & Papadopoulos, 2016; Wang et al., 2022). Consequently, the concept of Sustainable Supply Chain Risk Management (SSCRM) has developed as an extension of traditional SCRM, incorporating sustainability-related risks that may arise from supply chain activities (Hofmann et al., 2014).

Rather than replacing the established SCRM process, sustainability considerations are typically integrated into existing risk management structures and decision-making processes (Wang et al., 2022). This means that organisations apply the same general risk management logic while expanding the scope of risks that are considered relevant within supply chains. Environmental risks may arise, for example, from climate variability, use of pesticides and ecosystem degradation that influence production systems and resource availability (Oliveira et al., 2019). These risks are often linked to broader environmental systems and may therefore develop gradually over time rather than appearing as sudden disruptions (Wang et al., 2022). Social risks are typically linked to issues with labour conditions, human rights violations or other social responsibility concerns in supplier operations (Giannakis & Papadopoulos, 2016). Finally, economic risks can arise from increased production costs due to environmental regulation or resource scarcity. The consequences of these sustainability risks may extend beyond operational disruptions and include environmental impacts, stakeholder reactions, reputational damage and regulatory consequences (Giannakis & Papadopoulos, 2016).

Sustainability-related risks often originate in upstream supply chain activities where focal organisations have limited direct control (Oliveira et al., 2019). This makes them more difficult to detect and manage compared to internal operational risks. In addition, sustainability risks are often interconnected with environmental, economic and social systems that extend beyond the boundaries of individual supply chains (Wang et al., 2022).

Sustainability-related risks may also develop over longer time horizons than many traditional supply chain risks (Oliveira et al., 2019). Environmental degradation, for example, may gradually influence production conditions, resource availability and supplier reliability over time (Wang et al., 2022). This increases the importance of continuous monitoring. These risks are often more difficult to measure and assess than traditional operational risks, as their impacts may be uncertain, complex and difficult to quantify.

Furthermore, sustainability objectives may sometimes conflict with traditional supply chain priorities such as cost efficiency or delivery reliability, which can create trade-offs that organisations must consider when managing risks (Giannakis & Papadopoulos, 2016).

2.3 Decision Support Systems

A decision support system (DSS) is defined as an interactive computer-based system designed to help decision-makers use data, documents, knowledge and models to solve problems (Power, 2002). In environments characterised by uncertainty and complexity, the purpose of such a tool is to enhance the effectiveness of the decision process rather than replacing human judgement (Mir & Quadri, 2009). Successful implementation depends on a design approach that aligns technical functionality with cognitive requirements, ensuring the tool supports rather than disrupts human intuition (Little, 1970).

Structurally, a modern DSS can be conceptualised through three fundamental components: the data subsystem, the model subsystem and the user interface subsystem as illustrated in *Figure 2.2*. While more complex frameworks exist, this specific structure is often cited in DSS books and articles as the standard architecture for decision support systems (Sprague & Carlson, 1982; Holsapple, 2008).

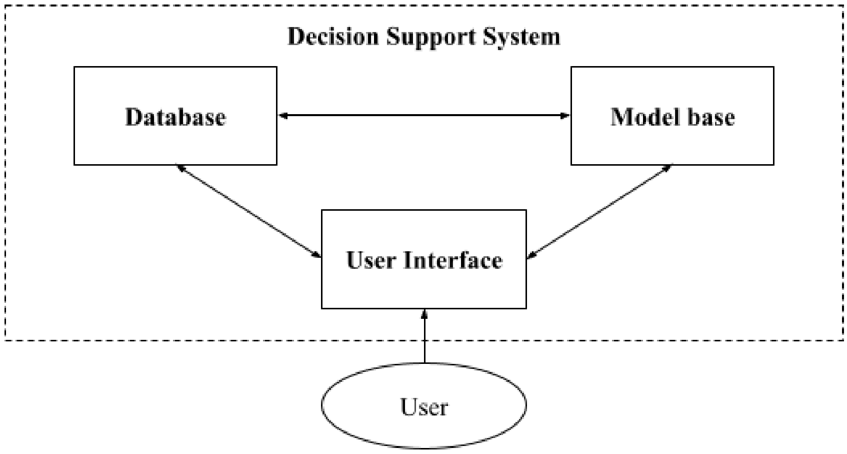

Figure 2.2: The components of a decision support system.

The data subsystem serves as the foundational component that manages the collection and organisation of internal and external information, often taking the form of a data warehouse (Sprague & Carlson, 1982). Built upon this foundation is the model subsystem, which transforms the raw data into results through mathematical or logical procedures. Finally, the user interface subsystem provides the communication link, allowing the user to interact with the system, input specific requests and interpret the resulting visual outputs. For a DSS to be successfully adopted and utilised, these pillars must be supported by specific design attributes that ensure both technical reliability and user comprehension.

2.3.1 The Data Subsystem

The primary requirement for the data subsystem is scientific validity, which ensures the information is a verifiable and sound representation of the decision domain (Holsapple, 2008). To achieve this, the repository must accurately reflect the physical conditions and governing laws of the environment (Mir & Quadri, 2009). This is accomplished through rigorous data selection, where variables are chosen based on their proven relevance to the problem (Little, 1970). By prioritising this accuracy over user convenience, the designer ensures the tool produces outcomes applicable to real-world constraints (Mir & Quadri, 2009). The system will fail to provide a trustworthy representation of reality without such rigour, causing the user to ultimately lose confidence in the model's outputs (Little, 1970).

However, the pursuit of validity must be balanced with parsimony. This refers to maintaining system simplicity by using the minimum amount of data necessary to solve the problem (Little, 1970). High maintenance requirements, such as constant manual data entry, risk the tool becoming a burden rather than a decision support. When the effort required to maintain the data repository outweighs the perceived benefit of the resulting insights, decision-makers are likely to reject the system (Little, 1970).

Finally, the system must establish technical legitimacy through traceability. Users often resist tools that operate as “black boxes” where the origin of information is hidden from view (Mir & Quadri, 2009). To mitigate this risk, the system should include metadata and audit trails that allow the decision-maker to verify the source and any transformations performed on the data. This transparency provides a clear record of how data was sourced and transformed which supports confidence and encourages long-term adoption (Holsapple, 2008).

The three design attributes of the data subsystem are summarised in Table 2.1.

Table 2.1: Design attributes of the data subsystem.

DSS Component	Design Attribute	Functional Description
Database	Scientific Validity	Verifiable representation of empirical reality
	Traceability	Verifiable audit trail of data origins
	Parsimony	Minimum data required to prevent overload

2.3.2 The Model Subsystem

While the data subsystem provides the input data, the model subsystem performs the analytical functions of the tool by utilising mathematical and statistical solvers to discover patterns and transform raw data into results (Sprague & Carlson, 1982). The operational cycle of this subsystem typically involves three distinct stages which are the model formulation, algorithmic solution and the subsequent analysis of results (Shim et al., 2002). A primary design attribute is robustness, such that the model structure remains resilient and reliable even when subjected to extreme or outlier input data (Little, 1970). By making the model resistant to erratic results from extreme inputs, the developer ensures that the system maintains technical credibility.

Furthermore, the model subsystem must support user understanding through intellectual accessibility (Little, 1970). Similar to the data subsystem’s need for parsimony, the model should be simple to understand so the user can understand and internalise the logic behind its suggestions. If the mathematical transformations are too complex, the system risks becoming an analytical “black box”, which creates a barrier for the user and prevents the application of necessary human judgement to the results (Mir & Quadri, 2009). To prevent this, the model must be designed to preserve the user’s authority and understanding of why the model behaves in a certain way (Little, 1970).

To sustain this authority over time, the model must also possess evolutionary capability. This means the backend logic is designed for easy modification as the user’s understanding of the risk environment matures (Er, 1988). By allowing the underlying algorithms to evolve alongside organisational knowledge, the logic embedded within the system remains a direct extension of the user’s own thought process (Holsapple, 2008; Little, 1970). This continuous alignment between the system’s logic and the user’s growing expertise ultimately sustains its utility within a changing organisational context.

The three design attributes of the model subsystem are summarised in Table 2.2.

Table 2.2: Design attributes of the model subsystem.

DSS Component	Design Attribute	Description
Model base	Robustness	Stability under extreme or outlier inputs
	Intellectual accessibility	Logic that can be internalised by the user
	Evolutionary capability	Structural growth as user expertise matures

2.3.3 The User Interface Subsystem

The user interface subsystem provides the communication link that enables the decision-maker to interact with both the data and model subsystems (Sprague & Carlson, 1982). According to Slovic et al. (2004), human cognition functions through two systems, the analytic and the experiential. In the context of risk management, the analytic system represents risk as analysis while the experiential system represents risk as feelings. While the model subsystem performs formal risk analysis using logic and algorithms, the user primarily processes information through the experiential system, which is fast and intuitive (Slovic et al., 2004).

The user interface must be designed to bridge the gap between these two systems. If the interface is too complex, it might cause the user to reject a technically valid tool based on the difficulty of the interaction rather than the quality of the results. The design therefore determines the practical utility of the system by serving as the deciding factor in whether the system's output is converted into useful results or dismissed due to a lack of intuitive clarity.

One requirement for this to be achieved is that the interface must prioritise simplicity and ease of communication. This can be achieved by utilising terminology and visual layouts that are familiar to the specific professional context of the decision maker (Little, 1970). Systems that rely on non-intuitive workflows create extra mental effort where the user must spend more energy on navigating the tool than evaluating the information itself. This often leads to systemic resistance and the rejection of the artifact during implementation (Mir & Quadri, 2009). Therefore, a successful interface must be designed to use language the user is familiar with, using operational terms rather than abstract mathematical coefficients (Little, 1970).

The interface must also establish transparency by making the underlying logic easy to verify. Slovic et al. (2004) argue that analytic reasoning is most effective when it is supported by clear visual cues, so the interface must translate raw data into formats that support meaningful interpretation. This is achieved through visual attributes such as dashboards or charts which allow the user to immediately perceive the status of a task while still being able to verify the calculations behind it (Holsapple, 2008). Multi-dimensional visualisation tools, such as radar charts, support this by letting decision-makers compare several dimensions at once without reducing the information to a single value. This preserves the transparency that analytical decision support requires (Holsapple, 2008). This visual transparency mitigates the risk of the system operating as a “black box”, ensuring the user trusts the system’s logic enough to act on its suggestions.

Finally, the interface requires flexibility to support the changing needs of the user. This attribute allows the interface to adapt to different scenarios, providing multiple ways to view and manipulate the same data (Er, 1988). A flexible design supports different modes of reasoning by allowing users to switch between high-level summaries and detailed analytical views (Slovic et al., 2004). This ensures that as the expertise of the user grows, the tool remains a relevant extension of their own thought process rather than a static constraint (Mir & Quadri, 2009).

The three design attributes of the user interface subsystem are summarised in Table 2.3.

Table 2.3: Design attributes of the user interface subsystem.

DSS Component	Design Attribute	Description
User Interface	Ease of Communication	Use of familiar professional terminology
	Transparency	Visual proof of the system’s reasoning markers
	Flexibility	User control over analytical perspectives

2.3.4 Synthesis of Design Attributes

The ultimate value of a DSS lies in its ability to transform technical complexity into actionable human insight while sustaining user trust. As shown in Table 2.4, the design attributes required to achieve this are distributed across the data, model and interface subsystems, each contributing a distinct set of properties that must be aligned to convert complex data into decision support (Holsapple, 2008)

Table 2.4: Synthesis of DSS design attributes by subsystem.

DSS Component	Design Attribute	Functional Description
Database	Scientific Validity	Verifiable representation of empirical reality
	Traceability	Verifiable audit trail of data origins
	Parsimony	Minimum data required to prevent overload
Model base	Robustness	Stability under extreme or outlier inputs
	Intellectual accessibility	Logic that can be internalised by the user
	Evolutionary capability	Structural growth as user expertise matures
User Interface	Ease of Communication	Use of familiar professional terminology
	Transparency	Visual proof of the system’s reasoning markers
	Flexibility	User control over analytical perspectives

Technical reliability of the system is established by combining scientific validity in the data with robustness in the model base. While validity ensures the data accurately represents the empirical conditions, robustness ensures the system remains stable even when faced with extreme or outlier scenarios (Mir & Quadri, 2009; Little, 1970). Together, these ensure the system’s foundation is technically reliable before it reaches the user interface.

Establishing trust and proving the system's logic to the user prevents the tool from being perceived as an unreadable black box (Mir & Quadri, 2009). This is achieved by linking backend traceability in the data with frontend transparency in the interface (Holsapple, 2008). Traceability provides a verifiable audit trail of data origins and transformations, while transparency uses visual markers to show how that data resulted in a specific insight. These attributes work together to make the system's logic and reasoning verifiable and clear.

Reducing mental effort and ensuring the system is conceptually clear requires alignment between the attributes parsimony, intellectual accessibility and ease of communication. Maintaining simplicity in the data and logic through parsimony prevents information overload, while intellectual accessibility ensures the user can internalise how the model reaches its conclusions (Little, 1970). When these are matched with an interface that uses the terminology and layouts familiar to the user, the decision-maker can focus on evaluating information rather than navigating the tool.

Ensuring the system remains relevant over time requires both structural and operational growth. Evolutionary capability allows the backend logic to be restructured as the user's knowledge of the environment matures, while flexibility allows the interface to offer different analytical views (Er, 1988). While the ability to evolve focuses on the long-term growth of the engine, flexibility focuses on the user's immediate control over the dashboard, such as toggling between high-level summaries and detailed analysis. This ensures the tool adapts alongside the user's growing expertise and changing situational needs.

2.4 Risk Assessment Tools

2.4.1 Approaches of Risk Assessment Tools

Risk assessment methodologies differ significantly in terms of complexity, data requirements and the type of output they generate. A common classification in the literature distinguishes between qualitative, hybrid and quantitative approaches (Marhavilas et al., 2011). The classification is grounded in different assumptions regarding uncertainty, measurability and decision support.

The boundaries between the approaches are not always clear in practice. Many assessments combine descriptive judgement with numerical scoring, and the level of quantification often depends on available data, time constraints and the purpose of the analysis (Altenbach, 1995; Vinnem, 2014). The three levels can therefore be understood as different degrees of quantification rather than strictly separate methods.

2.4.1.1 Qualitative Tools

Qualitative risk assessment represents the lowest level of analytical complexity. Data requirements for qualitative tools are limited, and assessments are largely based on expert judgement and contextual knowledge rather than statistical datasets (Vinnem, 2014). Risks are typically assessed in relative terms using verbal scales such as low, medium and high (Marhavilas et al., 2011).

A common method within qualitative risk assessment is the two-dimensional risk matrix, where likelihood and impact are represented on separate axes, which is illustrated in *Figure 2.3* (Altenbach, 1995; Marhavilas et al., 2011). By categorising risks in this way, organisations can prioritise attention and resources toward risks that are both more probable and more severe, while lower-priority risks may be monitored or accepted (Duijm, 2015). Both axes are ordinal in such matrices, meaning that the categories indicate order but do not define measurable distances along the axes (Altenbach, 1995). As a result, risks can only be ranked within the matrix and no measurable risk values can be derived.

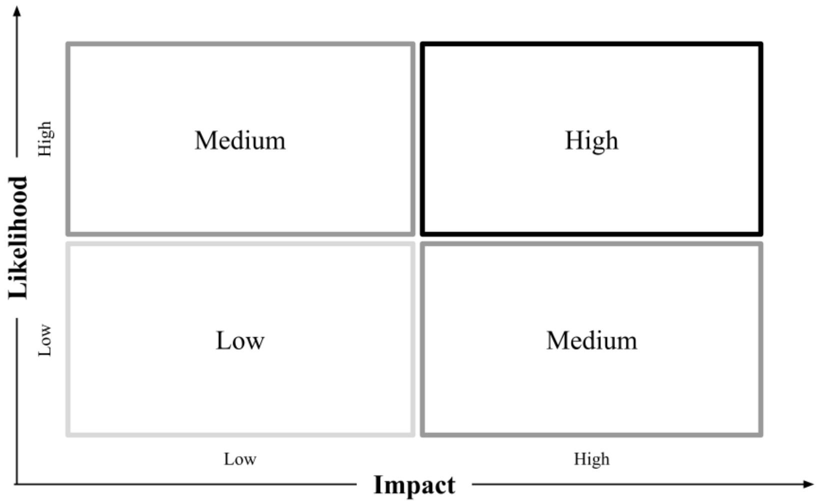

Figure 2.3: A general risk matrix with two dimensions, likelihood and impact.

In terms of decision support, qualitative tools are primarily used for screening, initial prioritisation and structured discussion of risks. Marhavilas et al. (2011) note that this approach is widely applied in practice because it is relatively easy to implement. The strength lies in supporting systematic identification and comparison of risks in situations where fast assessment and transparency are more important than numerical precision. However, because qualitative matrices are based on ordinal categories, they do not allow for consistent quantitative comparison or calculation across risk levels (Altenbach, 1995). Risk matrices have therefore been criticised for oversimplification and having limited sensitivity to underlying assumptions (Cox, 2008).

More structured qualitative matrix tools also exist, one example within procurement being the Kraljic Purchasing Portfolio Matrix, which is illustrated in *Figure 2.4*. This matrix categorises sourcing items along the two dimensions supply risk and profit impact (Kraljic, 1983). Profit impact reflects the financial significance of a category, for example through purchasing volume or share of total costs. Supply risk captures the vulnerability of supply and is commonly assessed using factors such as the number of available suppliers, switching costs and availability of substitutes. These dimensions create four categories: strategic, leverage, bottleneck and routine items. Each category is associated with different sourcing and risk management strategies. Although originally designed for profit-oriented companies, the Kraljic matrix can also be applied in non-profit and humanitarian organisations, where operational or budgetary impact replaces profit (Weele & Rozemeijer, 2022).

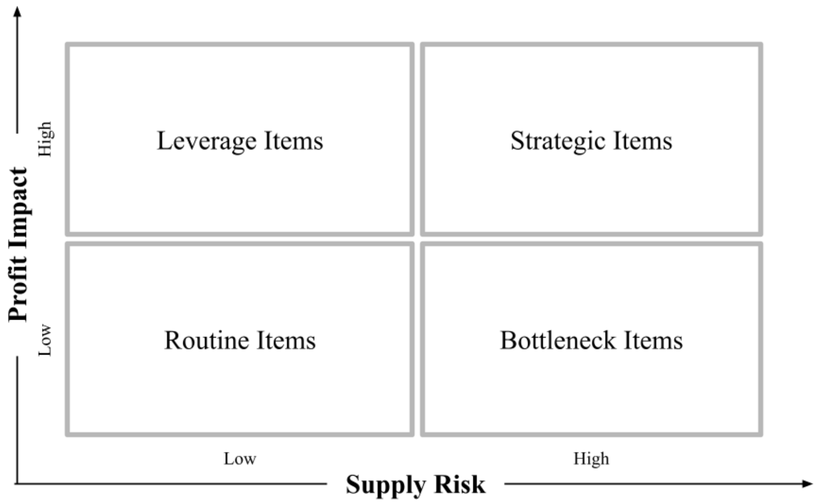

Figure 2.4: The Kraljic Purchasing Portfolio Matrix with two dimensions, profit impact and supply risk.

The Kraljic matrix has also been adapted to address modern supply chain challenges, including sustainability considerations. For example, Pagell et al. (2010) proposed a Sustainable Purchasing Portfolio Model, which incorporates environmental impact into the matrix, illustrated in *Figure 2.5.* In their study of leading organisations working with sustainable sourcing, the authors observed that firms did not always manage purchasing categories according to the traditional Kraljic logic. Some items that would typically be classified as leverage items were instead managed as strategic suppliers due to their environmental or social implications. This occurs when products or raw materials are associated with significant sustainability risks, such as high greenhouse gas emissions, critical resource use, biodiversity impacts or reputational risks linked to supplier practices. In such cases, the environmental or social consequences of sourcing decisions increase the strategic importance of the purchasing category. By incorporating sustainability considerations into the purchasing portfolio, it allows organisations to prioritise suppliers and sourcing decisions based not only on cost and supply risk but also on environmental sustainability.

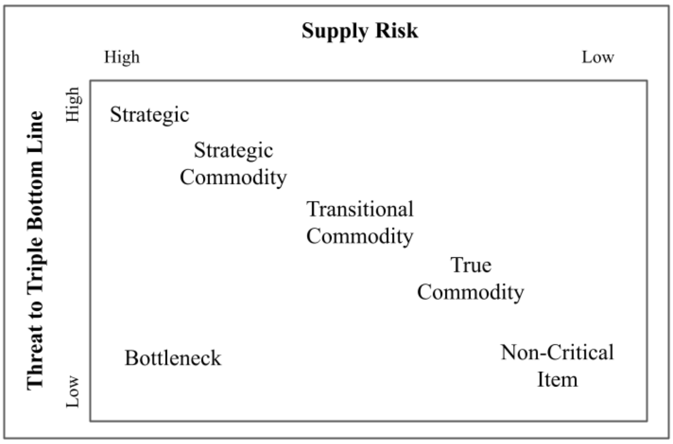

Figure 2.5: The Sustainable Purchasing Portfolio Matrix with two dimensions, threat to triple bottom line and supply risk (Pagell et al., 2010, p. 68).

2.4.1.2 Hybrid Tools

Hybrid, or semi-quantitative, approaches represent an intermediate level of analytical complexity and introduce numerical elements into an otherwise categorical structure (Marhavilas et al., 2011). This may involve assigning numerical scores to qualitative categories or expressing one dimension numerically while retaining ordinal scales for the rest (Altenbach, 1995).

Data requirements are moderate, as hybrid approaches require some numerical estimation but do not depend on extensive statistical datasets. Formal scoring rules are often introduced to enable calculation, but expert judgement remains central in defining scales and assigning values (Vinnem, 2014).

Hybrid tools provide enhanced decision support compared to qualitative approaches, since they can provide structured comparison across a larger set of risks (Marhavilas et al., 2011). However, the resulting scores remain dependent on how categories and scales are defined. The numerical output should therefore be interpreted as a structured prioritisation rather than a validated measure of risk. As emphasised in the broader risk literature, such scores may create an impression of precision that exceeds the strength of the underlying knowledge base (Aven, 2016). Hybrid methods are particularly common in contexts such as industrial safety, environmental screening and supply chain risk management where a balance between analytical structure and practical feasibility is required (Marhavilas et al., 2011).

Although the Kraljic matrix, described in the previous section, is conceptually a qualitative tool, organisations often operationalise the two dimensions using weighted scoring models which makes the tool semi-quantitative in practice.

2.4.1.3 Quantitative Tools

Quantitative risk assessment represents the highest level of analytical complexity, and risk is calculated using probabilistic or statistical models (Marhavilas et al., 2011). These methods rely on formally defined mathematical structures rather than categorical classifications.

Data requirements are substantial. Quantitative approaches require statistical input data, clearly defined system boundaries and explicit modelling assumptions (Vinnem, 2014). Probability distributions, frequency data or consequence models are typically used to estimate risk values. Quantitative methods generally involve more extensive data collection and specialised analytical expertise compared to qualitative and hybrid approaches, which can make them more resource-intensive to implement (Marhavilas et al., 2011; Vinnem, 2014).

In terms of decision support, quantitative tools enable consistent comparison, aggregation and evaluation of risks across different scenarios. Because risk is expressed in numerical units, these methods allow sensitivity analysis and assessment against predefined risk criteria (Marhavilas et al., 2011). This supports more detailed analytical evaluation compared to qualitative or hybrid approaches.

However, the validity of quantitative results depends strongly on data quality, modelling assumptions and system definition. Quantitative methods are therefore most commonly applied in fields such as nuclear engineering and large-scale industrial systems, where sufficient data and clearly defined technical boundaries are available (Vinnem, 2014).

2.4.2 Risk Model Structures

Risk assessment tools commonly rely on structured models that decompose risk into separate dimensions. This approach reflects the fact that risk outcomes are shaped by several interacting factors that cannot be captured well by a single variable or metric (Cardona et al., 2012). By structuring risk into dimensions, these models translate abstract risk concepts into operational elements that can be analysed and compared (Aven, 2016). Such structuring also clarifies which aspects of risk are included in the assessment and how they are separated before aggregation, which supports a more transparent interpretation of results (Birkmann, 2006; Aven, 2012).

Risk is therefore often described in the literature as a multidimensional structure, where different dimensions represent distinct drivers and outcomes of risk (Cardona et al., 2012). The literature uses slightly different terminology, but these analytical parts are most commonly referred to as risk components or dimensions, depending on the framework and research field (Cardona et al., 2012; Cutter, 1996).

Risk models organise these dimensions in different ways depending on the context of analysis. Two perspectives that are particularly relevant for analytical risk assessment tools are probabilistic risk models and disaster risk frameworks. Probabilistic risk models represent risk through events that describe what can happen, how likely it is through probability, and what the consequence would be (Kaplan & Garrick, 1981; Aven, 2012). Disaster risk frameworks, in contrast, conceptualise risk as the interaction between hazards, exposure and vulnerability that together shape risk outcomes (Cardona et al., 2012).

2.4.2.1 Probabilistic Risk Models

In probabilistic risk models, risk is analysed through the relationship between what can happen, how likely it is and the consequences from it (Kaplan & Garrick, 1981; Aven, 2012). ISO 31000 reflects this logic by describing risk in terms of risk sources, events, consequences and likelihood (ISO, 2018). In this structure, risk sources represent underlying drivers that may give rise to events, events describe what may occur, and consequences represent the impacts that follow. Considering likelihood together with consequences allows different risk situations to be compared by analysing both how plausible events are and how severe their impacts may be (Kaplan & Garrick, 1981; ISO, 2018).

Kaplan & Garrick (1981) formalised this perspective by representing risk as a set of scenario triplets:

$$(s_i,\, p_i,\, x_i) \tag{2.1}$$

where each triplet represents a scenario s_i, its probability p_i and its consequence x_i. In this representation, risk is described as a collection of possible scenarios rather than a single expected outcome, each contributing differently to the overall risk depending on both how likely it is and how severe its consequences may be (Kaplan & Garrick, 1981).

2.4.2.2 Disaster Risk Frameworks

Disaster risk frameworks extend this logic by introducing the concepts of hazard, exposure and vulnerability to explain why similar events can produce different outcomes depending on the conditions in which they occur (Cardona et al., 2012). In this perspective, hazards are treated as one component of risk rather than the risk itself, representing a shift from focusing on the results of an event to focusing on the drivers that cause those results (Aven, 2012; Cardona et al., 2012). This relationship is often expressed as:

$$R = f(H,\, E,\, V) \tag{2.2}$$

where R represents risk, H hazard, E exposure and V vulnerability (Cardona et al., 2012).

A hazard is a process, phenomenon or human activity that may cause loss of life, injury, property damage or other disruption (United Nations Office for Disaster Risk Reduction, 2016). This definition separates the potentially damaging process from the actual risk outcomes, such that risk depends on what is exposed and how those exposed elements are affected, not only on the hazard itself (Cardona et al., 2012).

Exposure refers to the presence of people, property or systems in hazard zones that are subject to potential losses, describing what may be affected rather than how strongly (United Nations Office for Disaster Risk Reduction, 2016). Exposure alone does not explain adverse outcomes, since exposed elements may differ in their vulnerability to harm (Cardona et al., 2012). Vulnerability refers to the characteristics and circumstances that make an exposed element susceptible to the damaging effects of a hazard, effectively determining the magnitude and severity of the resulting consequence (United Nations Office for Disaster Risk Reduction, 2016; Cardona et al., 2012). While probabilistic models focus on the probability of a specific consequence level, disaster frameworks focus on the sensitivity of the system to explain why that level of damage occurs (Aven, 2012; Cardona et al., 2012).

The framework also highlights that changes in risk are not driven only by changes in hazards, but also by changes in exposure and vulnerability, including broader social and development processes (Cardona et al., 2012). This clarifies which determinants of risk are being assessed and where risk reduction efforts may be directed.

As illustrated in Table 2.5, these two perspectives are functionally aligned. A hazard acts as the triggering scenario, while exposure and vulnerability are the determinants that shape the resulting consequence. Regardless of the specific framework, these dimensions are operationalised through measurable indicators that function as proxies for the underlying drivers of risk.

Table 2.5: Comparison between probabilistic risk models and disaster risk frameworks.

Risk Component	**Probabilistic Risk Model**	**Disaster Risk Framework**
The Triggering Event	Scenario (s_i): Answers the question “What can go wrong?”	Hazard (H): A potentially damaging physical event or phenomenon
The Measure of Uncertainty	Probability (p_i): Quantifies how likely a scenario is to occur	Likelihood / Frequency: Often treated as a characteristic of the hazard
The Resulting Impact	Consequence (x_i): The measure of damage or impact on objectives	Exposure (E) and Vulnerability (V): Interaction between what is at stake and its susceptibility

2.4.3 Indicator Construction

Once risk has been structured into dimensions, they need to be made measurable. This is not straightforward, since many relevant aspects are not directly observable in a single variable. In such cases, indicators provide a way of representing those aspects through variables that can be observed, measured and compared (Cardona et al., 2005). An indicator is defined as a quantitative or qualitative measure derived from observed facts that can reveal a relative position in a given area and, when evaluated over time, point out the direction of change (Freudenberg, 2003).

The transition from a dimension to an indicator is a structured process consisting of several steps. It begins with a theoretical framework that clarifies what is to be measured and how the broader phenomenon is structured (European Commission et al., 2008; Freudenberg, 2003). The literature identifies a structured sequence for constructing these measures, which Freudenberg (2003) categorises into three primary technical pillars: the selection, standardisation and weighting of variables. These pillars function as sequential stages, where the output of one step forms the analytical foundation for the next. This framework is further detailed by the OECD Handbook on Constructing Composite Indicators, which expands the methodology into a sequence of ten steps to ensure the final output is transparent, robust and fit for purpose (European Commission et al., 2008).

This approach allows theoretical concepts to be transformed into a functional decision support tool that reduces complex reality into a manageable form (European Commission et al., 2008). However, as highlighted in the concluding section of this chapter, each of these technical steps is subject to methodological limitations and trade-offs (European Commission et al., 2008). These choices must be documented transparently so that final scores are understood as indicative approximations rather than exact representations of absolute risk (European Commission et al., 2008).

Figure 2.6 illustrates the broader sequence of steps involved in indicator construction. The following sections focus on the three main technical pillars within this process. First, variable selection concerns the choice of variables that provide a meaningful representation of a dimension. Second, normalisation transforms heterogeneous data onto a common scale to ensure comparability. Finally, aggregation and risk representation combine indicators and weights into a single representation of risk (European Commission et al., 2008).

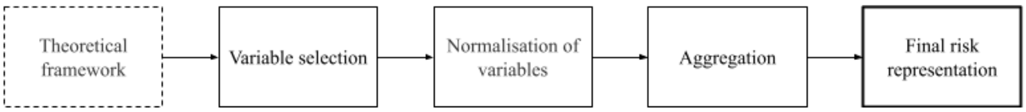

Figure 2.6: Sequential steps in the construction of indicators, from theoretical framework to final risk representation.

2.4.3.1 Variable Selection

Once a dimension has been translated into possible variables, the next step is to select which to use. This choice depends on three main considerations (Freudenberg, 2003; European Commission et al., 2008).

The first consideration is relevance to the phenomenon being measured. Variable selection should be guided by a theoretical framework that defines the phenomenon, its sub-groups and the criteria for inclusion (European Commission et al., 2008). This ensures that variables are chosen for their relevance rather than for the availability of data (Freudenberg, 2003).

The second consideration concerns the quality and usability of the underlying information. Variables should rely on data that can be identified, collected and interpreted consistently (Cardona et al., 2005). This may include figures, indices, rates or proportions from reliable sources. Qualitative assessments may also be used when based on clearly defined criteria. Since the quality of the underlying data strongly affects the quality of the final model, factors such as timeliness, accessibility and comparability are also important (European Commission et al., 2008). In practice, however, variable selection is often constrained by data availability. Relevant data may be unavailable, outdated, difficult to compare across cases or only loosely connected to the concept being measured (Freudenberg, 2003; European Commission et al., 2008). When this is the case, proxy measures can be used as indirect substitutes, though they should be treated as approximations (European Commission et al., 2008).

The third consideration is how variables relate to one another. Since variables are selected as part of a wider set, their value depends on whether they contribute distinct information (Freudenberg, 2003). Overlapping variables can lead to double counting, giving certain aspects greater influence within the model (Cardona et al., 2005). This becomes especially problematic across different contexts and scales, where variables that appear distinct in one setting may reflect the same underlying condition in another (Birkmann, 2007).

Taken together, these considerations show that variable selection involves more than identifying available data. It requires deciding which variables best represent the dimension, which can be supported by usable data, and which contribute distinct information within the wider set. Variables should therefore be understood as selected representations of a dimension rather than direct or complete measures of it. In practice, these criteria often need to be balanced against each other, since conceptually strong variables may be difficult to measure consistently, while easily available ones may only capture part of the intended concept (Birkmann & UNU-EHS Expert Working Group on Measuring Vulnerability, 2013).

2.4.3.2 Normalisation of Variables

Once variables have been selected, they need to be made comparable before they can be interpreted jointly or combined (Freudenberg, 2003). Variables often differ in scale, unit and distribution, and cannot be combined in raw form (Freudenberg, 2003; European Commission et al., 2008). When data are strongly skewed, logarithmic transformation may first be applied to reduce skewness and compress extreme values, and outliers may be trimmed if they are likely to distort the results (Freudenberg, 2003; European Commission et al., 2008). These adjustments can improve comparability but affect the meaning of the resulting variable and should therefore be applied with care.

Several normalisation methods exist, and the choice between them affects how values should be interpreted and how variables can later be aggregated (European Commission et al., 2008). Ranking orders observations from lowest to highest and assigns a rank, making it less sensitive to outliers but removing information about the size of differences between cases (European Commission et al., 2008). Z-score standardisation transforms each value in relation to the mean and standard deviation, preserving information about distance from the mean, though it is sensitive to extreme values (Freudenberg, 2003; European Commission et al., 2008). Min-max normalisation rescales each variable onto a fixed range, often from 0 to 1, which supports transparency and ease of interpretation, but is sensitive to outliers since the full scale is defined by the observed minimum and maximum (Freudenberg, 2003; European Commission et al., 2008).

A fourth approach is distance-to-reference normalisation, where values are transformed in relation to a specific benchmark rather than to the observed range or distribution (European Commission et al., 2008). The reference point may be a target value, the best performing case or the group mean, and results depend strongly on how it is defined (Freudenberg, 2003; European Commission et al., 2008). A specific variant used in this study is comparison to the group mean, where each value is expressed as a ratio to the arithmetic mean of all observations, such that values above 1.0 indicate above-average exposure or risk and values below 1.0 indicate below-average. European Commission et al. (2008) identifies this as particularly suited to assessments where the purpose is to understand performance relative to prevailing conditions in a defined peer group, rather than against an external standard or extreme case.

An alternative to continuous normalisation is scoring and categorisation, where values are converted into classes or assigned scores (Freudenberg, 2003; European Commission et al., 2008). Classes are often ordinal, such as low, medium and high, with thresholds based on percentile bands or defined criteria. This simplifies interpretation and communication, but reduces the information retained from the original data and introduces an element of judgement in how thresholds are defined (Freudenberg, 2003; European Commission et al., 2008).

Different methods preserve different properties of the data and support different forms of interpretation. Ranking emphasises position, z-scores emphasise distance from the mean, min-max normalisation emphasises relative position within an observed range, and distance-to-reference methods emphasise deviation from a chosen benchmark. Scoring and categorisation prioritise communication and interpretability over numerical precision. The choice between them should therefore be guided by the properties of the data and the purpose of the model (Freudenberg, 2003; European Commission et al., 2008).

2.4.3.3 Aggregation and Representation of Risk

After indicators have been selected and normalised, they need to be combined into a form that supports interpretation and comparison (European Commission et al., 2008). This step is referred to as aggregation, and its result is a composite indicator that combines several individual indicators into a single overall measure. While such a score simplifies comparison across cases, the process of combining separate indicators creates a new risk characterisation rather than acting as a neutral summary. Its validity therefore depends entirely on the assumptions built into the aggregation (Aven, 2019; European Commission et al., 2008).

Those assumptions concern three interrelated principles. The first is weighting, which determines how strongly each indicator contributes to the final result. Even equal weighting is an assumption, since it implies that all included dimensions are equally important. The second principle concerns model structure. When several indicators are grouped under the same broader dimension, dimensions represented by more indicators will carry greater overall influence even when individual weights are equal (European Commission et al., 2008; Birkmann, 2007). The third principle concerns compensability, meaning whether strong performance on one indicator can offset weak performance on another. High compensability allows serious weaknesses in specific dimensions to disappear in the final score, which can mislead interpretation and prevent identification of appropriate actions (European Commission et al., 2008).

These three principles mean that a composite score is more useful when its aggregation rules can be defended clearly. When defensible rules cannot be established, for example because the included dimensions are measured in categorically different units or because the relationships between them are not sufficiently understood, the aggregated result risks conveying a false sense of precision (Aven, 2019; Saltelli, 2007). In such cases, a disaggregated representation that presents separate results for each dimension preserves the distinctions needed to understand what drives a result and to identify possible courses of action. The drawback is that direct comparison becomes less immediate (Birkmann, 2007; Saisana & Tarantola, 2016).

One methodological family developed specifically to address the challenge of weighting heterogeneous criteria is Multi-Criteria Decision-Making (MCDM). MCDM approaches structure complex decisions involving multiple, incommensurable criteria into a form that allows systematic comparison and prioritisation (European Commission et al., 2008). Within this family, the Analytic Hierarchy Process (AHP), developed by Saaty (1990), elicits expert judgements through pairwise comparison of criteria, asking which is more important and by how much. Because weights are derived from expert judgement rather than from the data themselves, AHP can accommodate criteria that are qualitative, quantitative or measured on entirely different scales, making it particularly relevant where incommensurable dimensions need to be balanced (Handfield et al., 2002). The method has been applied in both procurement contexts, where Handfield et al. (2002) use it to weight environmental supplier performance criteria, and in supply chain risk management, where Salehi Heidari et al. (2018) apply fuzzy AHP to weight qualitatively different risk dimensions across a product life cycle. When expert judgements are consistent and sufficiently informed, AHP provides a transparent and replicable basis for producing defensible composite scores from disaggregated indicator sets (Handfield et al., 2002; Saltelli, 2007).

2.4.3.4 Limitations of Indicators

While indicator-based models are essential for making multidimensional phenomena measurable, they are fundamentally indicative approximations rather than precise or exhaustive measures. They support relative assessment and help identify patterns, but they do not replace more detailed analysis of the underlying conditions they represent (Cardona et al., 2005). Developing indicators requires conceptual judgement before technical measurement begins. This means that the final model acts as a new characterisation of risk shaped by the designer's choices, rather than a neutral summary of existing information (Aven, 2019; Freudenberg, 2003).

As shown in Table 2.6, the transition from raw data to a final risk representation involves several methodological trade-offs where simplicity and communication value are often gained at the expense of granular detail. To mitigate the risks of oversimplification and the masking of critical vulnerabilities during aggregation, the literature emphasises the importance of maintaining high levels of transparency in how the model is constructed and weighted (European Commission et al., 2008; Saisana & Tarantola, 2016). Furthermore, while a single composite score is useful for broad comparison, maintaining access to disaggregated values and sub-indices remains essential for a robust interpretation (Birkmann, 2007). By presenting results in a decomposed form, the model ensures that specific weaknesses remain visible, allowing decision-makers to identify appropriate courses of action based on the specific drivers of risk rather than relying on a potentially misleading summary value (Saisana & Tarantola, 2016; Saltelli, 2007).

Table 2.6: Summary of challenges and limitations in indicator development.

Process Step	Limitation	Description	Key Sources
Selection	Partial Representation	Indicators represent only selected aspects of a dimension. A single variable is rarely sufficient to capture the full concept.	Cardona et al. (2005); European Commission et al. (2008)
	Data Constraints	Relevant data is often unavailable, outdated, or lacks comparability, forcing a reliance on "most visible" data.	Freudenberg (2003); European Commission et al. (2008)
	Proxy Approximation	Indirect measures (proxies) used when ideal data is missing provide only an approximation of the phenomenon.	European Commission et al. (2008)
	Redundancy	Overlapping indicators can lead to double counting, distorting the influence of certain aspects within the model.	Cardona et al. (2005); Birkmann (2007)
Normalisation	Sensitivity to Outliers	Methods like min-max and z-score are sensitive to extreme values, which can compress differences between other cases.	European Commission et al. (2008); Freudenberg (2003)
	Information Loss	Scoring and categorisation simplify data but hide internal variation and small differences between cases.	European Commission et al. (2008); Freudenberg (2003)
	Subjective Thresholds	The definition of percentile bands or risk levels is often based on judgement and influences the final interpretation.	Freudenberg (2003); European Commission et al. (2008)
Aggregation	Compensability	Additive aggregation allows high scores in one area to cancel out serious weaknesses in another, masking critical risks.	European Commission et al. (2008); Aven (2019)
	Structural Influence	Dimensions with more indicators may have greater influence on the result, even when equal weights are applied.	European Commission et al. (2008)
	Oversimplification	Highly simplified composite indices can invite stronger policy conclusions than the underlying data justify.	Saltelli (2007)
	Loss of Distinction	Highly aggregated results can cause critical distinctions between dimensions to disappear.	Aven (2019); European Commission et al. (2008)

2.5 Crop Growth

Crop growth refers to the irreversible biological process through which a crop increases in size and accumulates biomass (Sadras et al., 2016). Crop development is the continuous change in plant form and function through a sequence of characteristic growth stages. Yield is the final harvested output and reflects how crop growth and development have been supported or constrained by interactions between the plant and its surrounding environment throughout the growing season (Hatfield et al., 2011). Crop production depends on the alignment between crop-specific requirements and the timing of fundamental environmental conditions throughout the growing season.

2.5.1 Crop Growth Requirements

At a general level, crops require light, temperature, water, air in the form of carbon dioxide and a suitable growing medium that provides both nutrients and physical support (Hatfield et al., 2011). Together, these factors support essential physiological processes that enable plant development from germination to harvest.

Light provides the energy required for photosynthesis, through which plants convert carbon dioxide and water into carbohydrates that drive biomass accumulation. The amount and duration of solar radiation influence the rate of photosynthesis and thereby the overall productivity of the crop (Pan et al., 2020). Temperature regulates the rate of key physiological processes, including photosynthesis, respiration and plant development (Hatfield et al., 2011). Water is essential for maintaining cell structure, enabling nutrient transport and supporting biochemical reactions (Samani, 2014). It also plays a central role in photosynthesis and transpiration. Water availability is typically determined by precipitation or irrigation and is closely linked to soil moisture conditions. Air, specifically carbon dioxide, is required for photosynthesis and is an input for biomass production (Pan et al., 2020). The growing medium, typically soil, provides both physical support for root development and access to essential nutrients (Yali & Begna, 2022). Soil properties such as structure, moisture retention and drainage capacity determine the plant's root development and the plant's ability to access water and essential elements.

Different crops have varying sensitivities and requirements (Hatfield et al., 2011). Each crop is characterised by specific ranges of these key environmental factors that define minimum, optimal, and maximum thresholds for growth, beyond which development is reduced or ceased. This means that the same environmental conditions may support the growth of one crop while limiting another.

2.5.2 Growth Stages

While these inputs define the core requirements for crop growth, their importance is not static over time. Crop development can be divided into ten distinct and relatively long-lasting growth stages, typically described using standardised classification systems such as the BBCH scale (Biologische Bundesanstalt, Bundessortenamt and CHemical industry). The different stages are presented in Table 2.7 and include phases such as germination, vegetative growth and reproductive development (Meier, 2001). Each stage is associated with different physiological processes and therefore different resource requirements. As a result, the quantity and timing of required inputs vary throughout the growth cycle.

Table 2.7: A general plant's principal growth stages, adapted from Meier (2001, p. 2).

Stage	Description
0	Germination / sprouting / bud development
1	Leaf development (main shoot)
2	Formation of side shoots / tillering
3	Stem elongation or rosette growth / shoot development (main shoot)
4	Development of harvestable vegetative plant parts or vegetatively propagated organs / booting (main shoot)
5	Inflorescence emergence (main shoot) / heading
6	Flowering (main shoot)
7	Development of fruit
8	Ripening or maturity of fruit and seed
9	Senescence, beginning of dormancy

In general, crops are most sensitive to environmental changes during key growth stages such as germination, flowering and grain filling (Bedeke, 2023). Early in the growth cycle, inadequate soil moisture or drought can shorten germination and reduce leaf development, limiting the plant's ability to establish properly. Later, during the flowering and grain filling stages, crops become particularly vulnerable to extreme heat and water stress. For example, high temperatures at these stages can reduce pollination success (Hatfield et al., 2011). Additionally, variability in rainfall and increased frequency of droughts or floods can disrupt the overall growing period and shorten the crop life cycle (Bedeke, 2023).

2.5.3 Stress Factors Affecting Crop Growth

When environmental conditions deviate from the ranges required for normal crop growth and development, they can act as stress factors that constrain physiological processes and reduce yield formation. Abiotic and biotic stresses are commonly used to categorise the environmental factors that influence crop production (Ngoune Tandzi & Mutengwa, 2020). The distinction is based on the origin of the stress. Abiotic stress refers to non-living environmental factors such as temperature extremes, water availability, soil conditions and other climatic variables that affect plant growth and yield. In contrast, biotic stress originates from living organisms, including pests, pathogens, weeds and other biological interactions within the ecosystem.

2.5.3.1 Abiotic Stress

Light

Solar radiation influences the rate of photosynthesis and thereby crop growth (Pan et al., 2020). Light becomes an abiotic stressor when levels deviate from the optimal range, which occurs under conditions of excessive irradiance, shading or ultraviolet (UV) radiation (Khan et al., 2025; Cramer et al., 2011).

The relevance of light stress varies by geographic context. In Sub-Saharan Africa, solar radiation levels are among the highest in the world, meaning that light deficit is rarely a limiting factor for crop production (FAO & WMO, 2026). Excessive light, on the other hand, tends to cause damage mainly when it coincides with other stressors. Under drought or cold conditions, plants are less able to use incoming radiation for photosynthesis, and the excess energy instead drives the formation of reactive oxygen species that damage plant cells (Mittler, 2006). Light stress in this region therefore acts primarily as a secondary effect that amplifies the damage caused by other concurrent environmental stresses rather than as an independent hazard.

Temperature

Temperature-related stress occurs at both ends of the thermal spectrum, where extreme heat and cold disrupt normal plant functioning (Ngoune Tandzi & Mutengwa, 2020).

Heat stress develops both gradually, through rising average temperatures linked to climate change, and abruptly through extreme heat events such as heatwaves (FAO & WMO, 2026). When temperatures exceed optimal levels, key physiological processes including photosynthesis, reproductive development and pollen viability are disrupted, reducing crop yields. This is particularly critical in Sub-Saharan Africa, where many agricultural systems already operate close to thermal limits (Omokpariola et al., 2025). Studies show that staple crop yields may decline by 4–10% for every 1°C increase in temperature (FAO & WMO, 2026). Unlike gradual warming, extreme heat events can cause immediate and irreversible damage within a single growing season. These include heatwaves and other conditions where temperatures exceed critical thresholds and induce severe physiological stress (FAO & WMO, 2026). Such events may also act as risk multipliers by intensifying hazards such as drought and pest outbreaks.

Cold stress represents the opposite end of the spectrum. Chilling temperatures between 0 and 15°C can cause substantial crop losses, particularly in crops originating from tropical and subtropical regions. Common effects include poor germination, stunted growth, chlorosis and reduced development.

Water

Both insufficient and excessive water availability represent major sources of stress for crop production (Ngoune Tandzi & Mutengwa, 2020). These stressors can develop gradually, through prolonged droughts or shifts in rainfall patterns, or occur suddenly, as in floods and flash droughts. The relevance of different water-related hazards also differs between rainfed and irrigated systems, which is especially important in Sub-Saharan Africa where most crop production is rainfed (IFPRI, 2026).

Drought is a slow-developing phenomenon caused by prolonged precipitation deficits that progressively reduce soil moisture below levels that can sustain plant growth, leading to lower yields or complete crop failure (Bedeke, 2023; FAO & WMO, 2026). On a global scale, droughts have been shown to reduce cereal production by around 10%, with larger impacts at regional and local levels (Lesk et al., 2016). Higher temperatures further intensify drought conditions by accelerating soil moisture depletion (FAO & WMO, 2026). Excess water leads to waterlogging and flooding, which damages crops and disrupts farm-level production, even if impacts are less visible at national scales (Lesk et al., 2016).

Beyond absolute water availability, changes in precipitation patterns alter the timing, intensity and distribution of water inputs to crop systems (Bedeke, 2023; Omokpariola et al., 2025). In Sub-Saharan Africa, where production is predominantly rainfed, precipitation variability is one of the dominant threats to crop production (Intergovernmental Panel On Climate Change, 2022). Shifts in rainfall onset and intensity can create mismatches between crop development stages and water availability, while increased variability raises uncertainty in production outcomes. Where total seasonal precipitation remains unchanged, altered distribution can still result in alternating periods of deficit and excess within the same growing season. Reductions in wet season precipitation are associated with substantial yield losses, while moderate increases can have positive effects (Omokpariola et al., 2025).

Air

Like the other abiotic stressors discussed above, atmospheric composition supports crop growth within a certain range but becomes a source of stress when it shifts beyond normal conditions. The two primary drivers are rising CO_2 concentrations and air pollutants, particularly tropospheric ozone (O_3) and nitrogen oxides (NO_x) (Swann et al., 2016; Felzer et al., 2007). While elevated CO_2 can initially stimulate growth, it can also dilute mineral nutrient concentrations in plant tissues, constraining development and limiting yield quality (Pan et al., 2020).

Tropospheric ozone, formed through photochemical reactions between NO_x and volatile organic compounds, accounts for over 90% of atmospheric-related vegetation damage (Felzer et al., 2007). Field-level yield losses of approximately 10 to 12% have been recorded for soybean, cotton and wheat (Felzer et al., 2007). The effects of ozone are not, however, uniformly negative. Ozone exposure can activate some of the same defence responses that plants use against UV-B radiation and pathogens, which may increase resistance to other environmental stresses under certain conditions (Mittler, 2006). Tropospheric ozone concentrations are highest in South and East Asia, Europe and parts of North America, while levels in Sub-Saharan Africa remain comparatively low (Felzer et al., 2007).

Soil

Soil degradation is an abiotic stressor that directly affects crop growth and productivity (Ngoune Tandzi & Mutengwa, 2020). Soil provides nutrients, water and physical support for plant growth, with the nutrient-rich topsoil layer being particularly important (Weil & Brady, 2017). Soil degradation refers to processes that reduce the productive capacity of soils. Although generally gradual, these processes can be intensified by acute events such as heavy rainfall and drought (Olsson et al., 2019). Degradation is commonly expressed through physical, chemical and biological changes in soil properties (Weil & Brady, 2017).

Physical degradation includes soil erosion and structural decline. Erosion removes fertile topsoil, reducing nutrient availability and water retention, while floods may further accelerate erosion and nutrient leaching (Bedeke, 2023). Structural degradation, including compaction, restricts root penetration and water infiltration, increasing vulnerability to both drought and excessive rainfall (Olsson et al., 2019). Tolerability thresholds for erosion have been formalised through soil-loss tolerance values, or T-values, which define the rate of soil loss below which long-term productivity can be maintained. The United States Department of Agriculture established T-values in the 1950s, with soil conservation programmes generally applying a range of approximately 5 to 12 Mg/ha/yr as the upper bound of acceptable loss (Montgomery, 2007). Erosion rates below 5 Mg/ha/yr are considered fully tolerable, rates between 5 and 12 Mg/ha/yr are tolerable for productivity but exceed ecologically sustainable levels, and rates above 12 Mg/ha/yr place long-term productivity at clear risk. Historical soil erosion has been estimated to reduce yields by approximately 8.2% across Africa and 6.2% in Sub-Saharan Africa (Omokpariola et al., 2025).

Chemical degradation involves changes in soil composition that reduce suitability for plant growth. This includes nutrient depletion and salinity. Nutrient depletion, often driven by continuous cultivation without replenishment, limits plant growth and reduces yield potential (Weil & Brady, 2017). Salinity, particularly in irrigated and coastal areas, impairs plant water uptake by increasing soil salt concentrations (Ngoune Tandzi & Mutengwa, 2020).

Biological degradation refers to the decline in soil organic matter and biological activity. Loss of soil organic carbon weakens soil structure, reduces fertility and lowers water-holding capacity (Weil & Brady, 2017). Reduced biological activity also limits nutrient cycling and increases crop sensitivity to drought and rainfall variability. Although these processes develop slowly, their cumulative effects can substantially reduce agricultural resilience and long-term productivity. The relationship between SOC content and crop productivity is not linear across all soil types, but a widely applied critical threshold has been established at 20 g/kg (Loveland, 2003; Lal, 2004). This is the level below which soil quality deterioration begins, with the soil considered to be functioning adequately above this threshold and in a risk zone below it (Loveland, 2003). This threshold was developed for temperate soils, and tropical soils naturally have lower baseline SOC concentrations, meaning the 20 g/kg level may be conservative when applied in Sub-Saharan African contexts (Lal, 2004).

Taken together, abiotic stress factors affect crop production by disrupting the environmental conditions required for plant growth. As summarised in Table 2.8, these stressors relate to the main resource requirements of crops, including light, temperature, water, air and soil. While individual stressors may act independently, they frequently interact and reinforce one another. The combined effects of interacting stress factors are examined further in *Section 2.5.3.3*.

Table 2.8: Crop growth requirements and corresponding abiotic stress factors.

Crop Requirement	Abiotic Stress Factor
Light	High irradiance Shading UV radiation
Temperature	Heat stress Cold stress
Water	Flooding Drought Change in precipitation patterns
Air	Elevated CO_2 Pollution (NO_x, O_3)
Soil	Physical degradation (erosion, structural decline) Chemical degradation (nutrient depletion, salinity) Biological degradation (SOC decline)

2.5.3.2 Biotic Stress

Biotic stress refers to the negative effects on crops caused by living organisms. The main categories of biotic stress in agricultural systems are insects and pests, diseases and pathogens, and weeds (Singh, 2023). Unlike abiotic stressors, biotic stress originates from biological interactions within the crop environment. However, biotic and abiotic stress are closely connected, as drought, high temperatures and poor soil conditions can weaken crops and increase their susceptibility to pests and diseases.

Insects and Pests

Insects and pests are a major source of biotic stress in crop production. Sap-sucking insects can cause wilting, stunted growth and, under severe infestation, plant death (Singh, 2023). Other pests consume plant tissues and thereby reduce leaf area and productivity. Insects may also transmit diseases between plants, which can intensify their overall effect on crop health and yield. Changes in temperature and precipitation can alter the distribution, lifecycle and reproduction rates of pests. As a result, global yield losses for major crops such as maize, rice and wheat are projected to increase by 10 to 25% per degree of warming because of insect pests (Deutsch et al., 2018). Warmer conditions often accelerate pest development and increase the number of generations per season, while also enabling the spread of species into new regions. At the same time, stressed crops become more vulnerable to infestation and infection (Omokpariola et al., 2025).

Diseases and Pathogens

Plant diseases and pathogens are a major source of biotic stress in agriculture (Singh, 2023). They are caused by microorganisms such as fungi, bacteria and viruses that infect plants through roots, leaves or stems and disrupt normal plant functioning. Their effects range from mild symptoms to severe yield losses or complete crop failure. The occurrence and spread of plant diseases are influenced by environmental conditions (Ngoune Tandzi & Mutengwa, 2020). Climatic variation can favour pathogen multiplication and enable climate-driven migration, exposing locally adapted crop varieties to new biotic stress factors. Climate variability and change may also lead to the emergence of new diseases or increased occurrence of existing ones.

Weeds

Weeds are unwanted plants that compete with crops for essential resources such as water, nutrients, light and space (Singh, 2023). Through this competition, they can reduce crop growth, yield and quality. Some weeds can also harbour pests and diseases, thereby facilitating their spread within agricultural systems. Weeds are particularly difficult to manage because of their high reproductive capacity, diverse propagation mechanisms and, in some cases, resistance to herbicides.

2.5.3.3 Interactions Between Crop Stress Factors

Environmental stress factors affecting crop growth rarely occur in isolation. Crops are typically exposed to multiple simultaneous or sequential stressors that interact in complex ways (Mittler, 2006; Zhang et al., 2022). Importantly, environmental risks are highly interconnected and often occur simultaneously. Such combinations can produce impacts that are greater than the sum of individual risks (Mittler, 2006; Omokpariola et al., 2025).

A central finding in stress combination research is that the response of plants to two different stresses applied simultaneously is unique and cannot be directly extrapolated from the response of plants to each stress applied individually (Mittler, 2006). This is because plant acclimation to any given stress condition requires a physiological, molecular and biochemical response tailored to that specific set of environmental conditions. When stresses are combined, these individual responses can interact in synergistic or antagonistic ways that produce outcomes distinct from either response in isolation (Mittler, 2006).

On this basis, Mittler (2006) argues that stress combination should be regarded as a distinct state of abiotic stress in plants, requiring its own acclimation response, rather than treated as the simple sum of two individual stressors. Farmers and breeders have long recognised that it is often the co-occurrence of multiple stresses, rather than any single stress condition, that is most lethal to crops (Mittler, 2006).

Not all stress combinations increase damage. Some combinations interact antagonistically to reduce overall damage through a process called cross-protection (Mittler, 2006). The direction of an interaction, whether it amplifies or reduces stress damage, therefore depends on the specific combination of stressors, the timing and intensity of each, and the physiological state of the crop (Mittler, 2006). In Sub-Saharan Africa, where crops frequently face concurrent water deficit, heat and variable radiation, understanding both the synergistic and antagonistic dimensions of stress interaction is relevant to accurately interpreting observed patterns of crop loss.

2.5.4 Environmental Impact from Crop Production

Environmental impact, as used in this study, refers to the ecological consequences generated by crop production (Gallardo, 2024). Although crop production is often discussed as a general activity, its environmental impact is not uniform. The type and magnitude of impact differ between crops, production systems and locations (Reynolds et al., 2015; Jwaideh & Dalin, 2025). In a comprehensive review, Gallardo (2024) structures the environmental impacts of agriculture into five main areas: greenhouse gas emissions, land use and land-use change, biodiversity, water quantity and quality, and pesticide-related environmental effects. These five areas are used to structure the following section.

2.5.4.1 Greenhouse Gas Emission

Crop production contributes to greenhouse gas emissions through several mechanisms. Agriculture alters the composition of the atmosphere through emissions of carbon dioxide (CO_2), methane (CH_4) and nitrous oxide (N_2O). The contribution comes from several processes. Carbon dioxide emissions arise from processes such as land conversion and soil disturbance, nitrous oxide emissions are closely linked to nitrogen fertiliser application, and methane emissions are particularly associated with flooded rice cultivation (Gallardo, 2024; Reynolds et al., 2015).

Taken together, agricultural activities, including both crop and livestock production, are estimated to contribute around 18 to 20% of global anthropogenic greenhouse gas (GHG) emissions (Gallardo, 2024). Land use change for agricultural purposes further amplifies this contribution, as the conversion of forests or grasslands releases the carbon stored in vegetation and soils.

GHG emissions from crop production therefore contribute to climate change by increasing the atmospheric concentration of heat-trapping gases (Gallardo, 2024).

2.5.4.2 Deforestation and Land Use Change

Crop production affects the environment through land occupation and land-use change. This conversion, most notably from forests to cropland, is a leading driver of global deforestation (Gallardo, 2024). It reduces carbon storage, weakens watershed protection, removes habitats and diminishes the regulatory functions that forests provide to surrounding agricultural systems (Gallardo, 2024).

The environmental effects of crop production depend partly on whether additional production is achieved through expansion into new land or intensification on land already under cultivation. Agricultural expansion is a common response where land remains relatively available, particularly in parts of Sub-Saharan Africa, and the conversion of forests, grasslands and other non-agricultural land to cropland changes land cover, soil structure, soil nutrients and biodiversity (Reynolds et al., 2015). Intensification on existing cropland may reduce the need for further land conversion, but can also increase environmental pressure through repeated cultivation and greater input use (Reynolds et al., 2015). Land-use impact is therefore shaped by both the crop being produced and the production system in which it is cultivated.

2.5.4.3 Biodiversity Loss

Biodiversity loss can manifest in several ways, such as reductions in the number of species present, declines in the abundance of species populations, the disappearance of threatened or geographically rare species, and the degradation of ecosystem functioning. Importantly, biodiversity decline does not necessarily imply species extinction, but can also occur through reductions in the abundance and distribution of originally present species, weakening ecosystem resilience and ecological interactions (United Nations Office for Disaster Risk Reduction, 2016).

While biodiversity loss is driven by multiple pressures, such as climate change, invasive species and pollution, agricultural production is the primary driver of global biodiversity loss (Gallardo, 2024). Monocultures, repeated plantings, habitat removal and agrochemical use reduce the diversity of species within and around agricultural systems, leading to biodiversity loss (Reynolds et al., 2015; Pereira et al., 2025). Habitat destruction through land conversion is the most direct pathway, as converting natural ecosystems into cropland eliminates the species that depended on those habitats (Gallardo, 2024). The intensification of crop production further reduces biodiversity through the use of pesticides and herbicides, which harm non-target species including pollinators and natural pest predators, as well as through the simplification of landscapes into monocultures that offer limited ecological structure. As biodiversity declines, ecosystem functions and nutrient cycling are weakened, reducing the ecological functions that support agricultural systems (Reynolds et al., 2015; Pereira et al., 2025).

2.5.4.4 Water Use and Quality

Crop production affects both water quantity and water quality in the area where the crop is being cultivated. Irrigation is the dominant human activity leading to water stress globally (Pfister & Bayer, 2025). Agriculture is responsible for approximately 85% of total global water consumption and around 70% of global water withdrawal. This can contribute to the depletion of surface water and groundwater resources, particularly where water extraction exceeds natural replenishment, leading to water stress (Gallardo, 2024; Reynolds et al., 2015).

To understand the environmental implications of crop water use, it is useful to distinguish between three categories of water (Mekonnen & Hoekstra, 2011; Hoekstra et al., 2011). Blue water refers to surface water and groundwater, the water found in rivers, lakes and aquifers, that is withdrawn and consumed through irrigation. Green water refers to precipitation that is stored in the soil and consumed by crops through evapotranspiration during the growing season. Because green water is sourced from rainfall and does not represent a direct withdrawal from surface or groundwater bodies, it does not carry the same risk of depriving other users or ecosystems of water. Grey water refers to the volume of freshwater required to dilute pollutants, such as nutrients and pesticides from agricultural runoff, to the point where water quality standards are met.

The environmental impact of blue water use depends strongly on where the water is withdrawn. The same amount of irrigation water can have a limited effect in a region where water is abundant but place significant pressure on rivers, aquifers and downstream users in a water-scarce region (Jwaideh & Dalin, 2025). In these regions, additional withdrawals may reduce the water available for other farms, households and ecosystems, and in severe cases affect drinking water supply and ecosystem functioning.

Crop production also affects water quality through runoff and leaching of agricultural inputs (Gallardo, 2024; Jwaideh & Dalin, 2025). Nutrients such as nitrogen and phosphorus from fertilisers and organic waste can enter waterways, causing eutrophication. This could lead to excessive nutrient enrichment, which promotes algal growth, reduces oxygen levels and degrades aquatic ecosystems. Pesticide residues can also reach water bodies through runoff and harm aquatic organisms. Overall, the severity of these impacts depends on the crop type, production intensity and local vulnerability of water resources (Jwaideh & Dalin, 2025).

2.5.4.5 Pesticide Use

Pesticides are used in crop production to control weeds, insects and diseases, but their use can also create environmental harm beyond the target organisms (Gallardo, 2024). Pesticides can enter the wider environment through processes such as adsorption, leaching, volatilisation, spray drift and runoff. Once released, they may contaminate soil and groundwater and affect non-target organisms.

The environmental effects of pesticides include impacts on non-target organisms and ecosystem functions. Herbicide drift can damage nearby vegetation, broad-spectrum insecticides can reduce beneficial insect populations such as bees and beetles, and fungicides may indirectly affect birds and mammals by reducing earthworm populations that serve as food sources. Pesticides can also disrupt soil microorganisms that support nutrient cycling and plant health. In addition, pesticide overuse can contribute to the evolution of resistant pests, which may in turn encourage the application of larger pesticide quantities (Gallardo, 2024; Reynolds et al., 2015).

Agrochemical use is one of the mechanisms through which agricultural intensification contributes to biodiversity loss (Pereira et al., 2025). However, pesticide-related impacts vary across crops and production systems because pest pressure and pesticide use differ between agricultural contexts. Intensive production systems are generally associated with greater pesticide contamination than lower-input systems, while crop-specific pest and disease challenges can also lead to different patterns of pesticide use and resistance development (Reynolds et al., 2015).

2.5.5 Environmental Impact as a Driver and Amplifier of Crop Stressors

While *Section 2.5.3* treated environmental stressors as external conditions acting upon crop production systems, the relationship is not unidirectional. Crop production does not only respond to its environment, it also modifies it. While some environmental stressors occur naturally as part of climatic variability, climate change acts as a key driver that amplifies many of these stressors. It increases the frequency and intensity of extreme events while also driving long-term changes in environmental conditions (Tchonkouang et al., 2024). In this way, the environmental impacts generated by crop production can become drivers of environmental stress factors. In addition, environmental impact from crop production can also affect the capacity of ecosystems to withstand these stressors (Pereira et al., 2025). Degraded ecosystems provide weaker regulation and support functions, which limits the ability of agricultural systems to cope with environmental variability and disturbances. Consequently, environmental impact not only contributes to the intensification of stressors, but also amplifies their effects by weakening the underlying systems on which crop production depends.

2.6 Conceptual Framework

The theoretical review across *Section 2.1* to 2.5 informs the conceptual framework presented in *Figure 2.7*. Humanitarian logistics establishes the decision context in which WFP operates, shaped by overarching external pressures of climate change, food insecurity and humanitarian response. Within this context, procurement decisions are determined by the environmental sourcing risks facing each sourcing region and the environmental impact those decisions generate. Crop growth theory explains that these sourcing risks arise as deviations from biophysical growth requirements. Risk assessment theory provides the basis for making both environmental sourcing risks and environmental impacts measurable and comparable. Risk frameworks translate theory into actual risk for a given sourcing context. They can be operationalised through indicators, which represent the underlying dimensions of risk and impact across different countries and crops. Once indicators are selected, normalised and aggregated into composite scores, crop growth requirements serve as scientifically grounded thresholds that give these scores meaning in relation to actual production conditions. The resulting output can then be structured and designed in accordance with decision support theory, ensuring it is transparent, accessible and actionable for procurement decision-makers. In this way, the framework connects environmental and agricultural theory to a decision support output that directly informs WFP's country-crop procurement decisions.

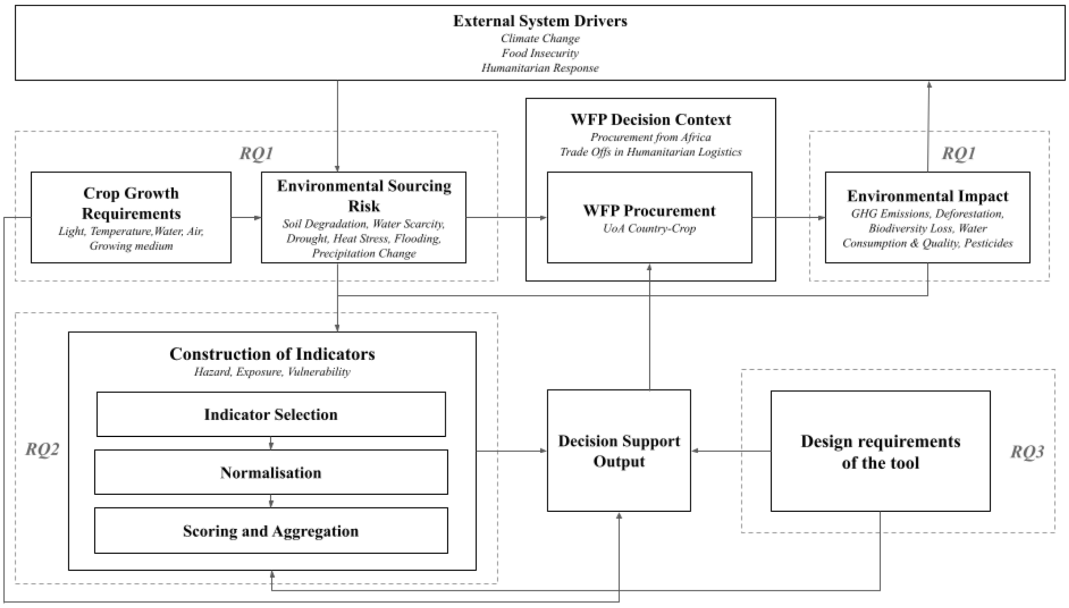

Figure 2.7: The conceptual framework of the thesis, derived from findings of the review of existing literature.

3 Methodology

This chapter outlines the research methodology applied in the study. It describes the research philosophy, approach, and design, followed by the data collection methods and analysis procedures. Finally, the quality of the research is discussed.

A structured methodology helps ensure that the research is conducted in a systematic and transparent way. By describing the methodological approach, the reader can understand how the research questions are addressed, how methods are chosen and how conclusions are reached. Such transparency is essential for assessing the credibility and quality of academic research (Saunders et al., 2019).

In this thesis, the Research Onion is used as the overarching framework to structure and present the methodology. The Research Onion presents research design as a series of layers that build on each other, ranging from overarching philosophical assumptions to specific techniques for data collection and analysis (Saunders et al., 2019). Each layer builds on the previous one, illustrating how fundamental assumptions influence methodological choices at later stages. Using the Research Onion as a base therefore supports internal consistency and provides a logical structure for explaining the overall research approach. The following sections of this chapter are organised according to the main layers of the Research Onion, which can be seen in *Figure 3.1.*

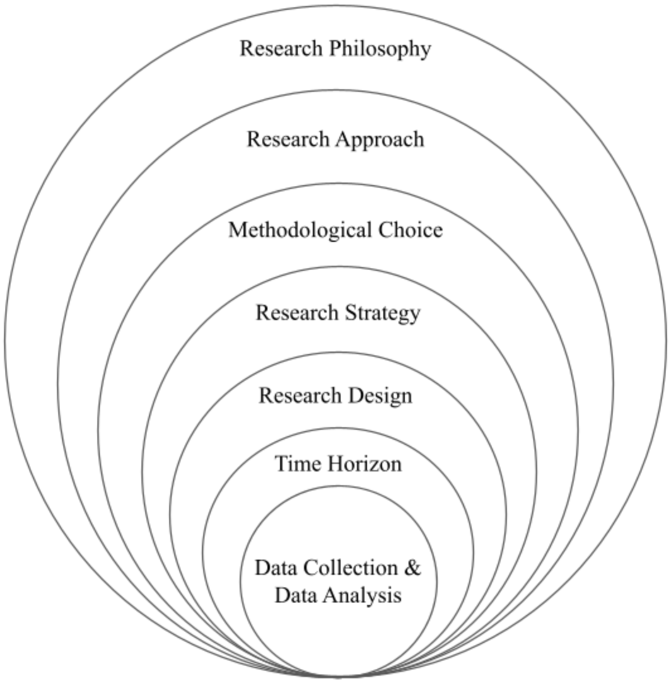

Figure 3.1: The Research Onion illustrating the methodological structure of this thesis, adapted from Saunders et al. (2019), p. 108.

3.1 Research Philosophy

Research philosophy reflects the assumptions about the nature of reality (ontology) and how knowledge is acquired (epistemology). These philosophical assumptions influence subsequent methodological choices. Commonly discussed philosophical positions include positivism, interpretivism, realism and pragmatism (Saunders et al., 2019). Positivism typically emphasises objective measurement and hypothesis testing, interpretivism focuses on understanding social phenomena through subjective meanings, while realism combines elements of both perspectives by acknowledging an objective reality that is interpreted through human experience.

This thesis adopts a pragmatic research philosophy. From a pragmatic perspective, reality is viewed as complex and context dependent and knowledge is evaluated based on its practical consequences. Pragmatism is appropriate when the primary aim of research is to address a practical problem and to produce knowledge that is useful in a specific context, rather than to test universal laws (Saunders et al., 2019). As the objective of this thesis is to develop a decision support tool for WFP's procurement operations, the focus lies on producing knowledge that is useful and applicable within a specific organisational setting. A pragmatic stance therefore allows methodological choices to be guided by their suitability for achieving the research purpose rather than by adherence to a single epistemological tradition.

3.2 Research Approach

The approach to theory development may be deductive, inductive or abductive (Saunders et al., 2019). The deductive approach begins with existing theory and is tested through empirical observations, while an inductive approach focuses on building theory from empirical observations. Abduction combines these approaches through an iterative process in which theory and empirical insights inform and refine each other.

An abductive approach to knowledge development is adopted in this thesis, integrating elements of both deductive and inductive reasoning. The process was initiated with existing theory, which was applied to the specific case. Empirical findings from WFP were then used to evaluate, refine and further develop the theoretical framework. Through this iterative movement between theory and empirical material, knowledge was generated.

3.3 Methodological Choice

The third layer is the methodological choice, referring to whether the study adopts a mono-method, multi-method or mixed-method design (Saunders et al., 2019). This thesis adopts a multi-method approach, combining a literature search, analysis of secondary quantitative data and iterative qualitative input from organisational stakeholders. The integration of these different methods supports the development and refinement of the artifact while maintaining alignment with the research objectives.

3.4 Research Strategy

The research strategy refers to the overall plan for answering the research questions (Saunders et al., 2019). A Design Science Research (DSR) strategy was used in this thesis. DSR is a well-established research paradigm that focuses on the creation of artifacts designed to solve identified problems within a specific context (Hevner et al., 2004). In DSR, artifacts are categorised as constructs, models, methods or instantiations. DSR aims to generate solutions that are both practically applicable and theoretically informed. By developing artifacts such as frameworks and tools, DSR can contribute to organisational practice while also offering insights that may be transferable to similar contexts (Peffers et al., 2007).

The research addressed in this thesis is practical and decision-oriented, as it concerns how WFP can systematically assess and compare environmental impact and environmental sourcing risks in procurement decisions. There is currently no structured and integrated tool within WFP that enables risk assessments at a country-crop level. This type of problem, where the challenge lies not in identifying the issue but in designing a solution, is particularly well suited to a Design Science Research strategy (Hevner et al., 2004).

3.5 Research Design

According to Saunders et al. (2019), research design refers to the general plan of how the research questions will be answered and how methodological decisions are implemented in practice. While the research strategy outlines the overall approach, the research design explains how the study was carried out in practice. It describes the main steps of the study, the methods used for data collection and analysis and how the research objectives are implemented in order to fulfil the purpose of the thesis. This is particularly important in design-oriented research, as Design Science Research provides a general research logic but does not prescribe a single, standardised methodology (Blessing & Chakrabarti, 2009).

The research design for this thesis was structured in line with the Design Science Research methodology (DSRM) proposed by Peffers et al. (2007). It comprises six interrelated activities: (1) Problem Identification and Motivation, (2) Definition of Objectives for a Solution, (3) Design and Development, (4) Demonstration, (5) Evaluation and (6) Communication.

While DSRM provides the overarching research structure for the study, elements of Action Design Research (ADR) (Sein et al., 2011) were incorporated within the Design and Development phase. ADR was particularly relevant in this step due to its emphasis on iterative artifact development in close collaboration with the practitioners. In this study, ADR principles were applied to ensure that the risk assessment tool evolved through iterative refinement in interaction with WFP stakeholders.

The overall DSRM process proposed by Peffers et al. (2007), including the integration of ADR within the Design and Development phase, is illustrated in Figure 3.2.

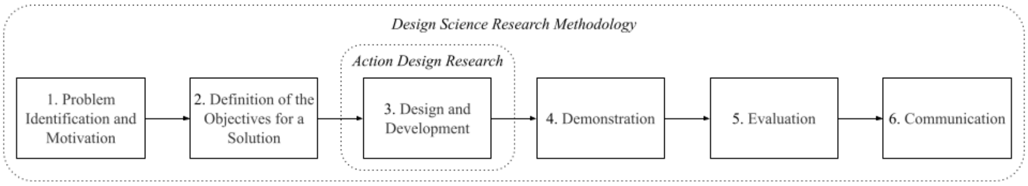

Figure 3.2: Illustration of the DSRM process (Peffers et al., 2007) and how ADR is applied within the Design and Development phase.

The following sections describe how this research design was implemented across the different phases of the study.

3.5.1 Problem Identification and Motivation

Problem identification is the first step of DSRM and aims to define the research problem and justify the need for a solution (Peffers et al., 2007). This step should ensure that the artifact development is grounded in a clearly defined practical problem.

The research process was initiated by a problem-centered entry point, as described by Peffers et al. (2007), since the initial problem was presented by WFP as an identified need within its procurement operations. Specifically, the organisation expressed an ambition to expand environmental considerations in their procurement operations beyond greenhouse gas emissions currently addressed through the ECODASH system.

Following this initial problem articulation, a series of structured meetings were conducted with the WFP supervisor to clarify and delimit the scope of the problem. The initially broad organisational need was refined into a more specific and researchable problem formulation through iterative discussions. The resulting problem formulation provided the motivation and foundation for the subsequent artifact development.

3.5.2 Define Objectives for a Solution

The second activity of DSRM involved defining the objectives for the proposed solution (Peffers et al., 2007) and aimed to translate the problem formulation into explicit objectives that would guide the development of the artifact.

The objectives were derived through a combination of theoretical insights and empirical input from WFP stakeholders. The DSS design attributes established in *Section 2.3.4* guided the structural and functional requirements of the solution. In parallel, discussions with WFP stakeholders clarified the intended purpose, scope and application context of the tool, as outlined in *Section 1.3*. By explicitly defining the objectives before the design and development phase, alignment was ensured between the identified organisational need and the intended functionality of the artifact.

3.5.3 Design and Development

In line with the third step of DSRM, the design and development phase focused on creating the artifact itself and specifying its components and structure (Peffers et al., 2007). Throughout this phase, principles from Action Design Research (ADR) were applied (Sein et al., 2011). In particular, the Building-Intervention-Evaluation (BIE) logic structured development as an iterative rather than sequential process.

Building, intervention and evaluation were conducted throughout the development process. Building activities focused on developing and refining the artifact based on the defined objectives and the theoretical foundation. Intervention took place through weekly online meetings with the supervisor at WFP, where draft versions of the framework were presented and discussed in relation to its intended use. Evaluation was ongoing, as feedback from these discussions informed subsequent revisions of the artifact. Evaluation was therefore integrated into the development process rather than solely treated as a separate final step, in line with ADR (Sein et al., 2011).

Within the building activities of ADR, the development of the artifact was organised into four methodological components (*Figure 3.3*): (1) Conceptual Framework Design, (2) Analytical Infrastructure Development, (3) Indicator Development, and (4) Output Formalisation.

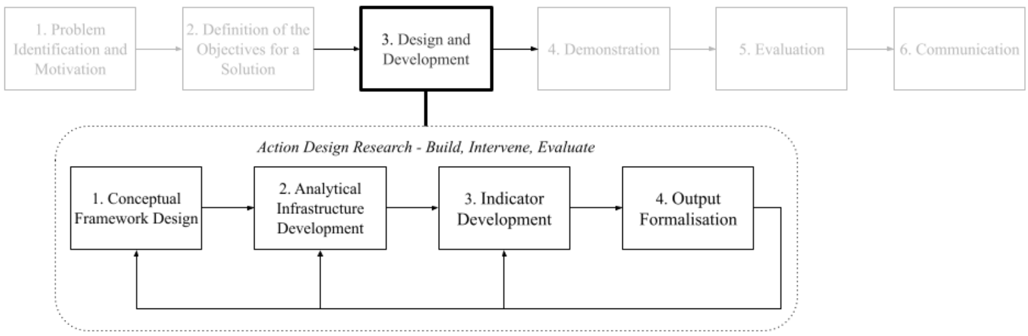

Figure 3.3: Research design based on DSRM (Peffers et al., 2007), with the Design and Development phase structured into four building components following the BIE logic of ADR (Sein et al., 2011).

The first component, Conceptual Framework Design, involved translating the theoretical foundations established in the literature search into a conceptual architecture for the tool. This included selecting an appropriate risk model structure (Disaster Risk Framework) and determining the output format of the assessment. The second component, Analytical Infrastructure Development, involved establishing the spatial, computational and temporal foundations applied consistently across all subsequent indicator development. The third component, Indicator Development, addressed each environmental dimension through a structured design process. This process covered metric selection, the identification and evaluation of candidate datasets against predefined criteria, and the derivation of indicator formulas. The fourth component, Output Formalisation, involved consolidating the developed indicators into a coherent final structure and defining how results would be expressed and presented.

These components were initially approached in this order, as the conceptual architecture informed the infrastructure requirements, which in turn constrained the indicator development, which shaped the final output structure. However, in line with the iterative logic of ADR, the process was not strictly linear (Sein et al., 2011). Insights from later stages led to adjustments to earlier design decisions throughout the process.

3.5.4 Demonstration

Demonstration constitutes the fourth activity of DSRM and involves using the artifact to solve one or more instances of the identified problem (Peffers et al., 2007). The purpose of this step is to show how the artifact can be used in a relevant context.

In this study, demonstration was conducted by applying the developed framework to maize sourced from Benin and Tanzania (see *Section 6.5*), chosen to represent realistic procurement situations within WFP operations. The combination was chosen to illustrate the full indicator set across two contrasting country contexts, verifying that the framework generates structured, interpretable and comparable outputs under realistic procurement conditions.

3.5.5 Evaluation

According to Peffers et al. (2007), evaluation involves assessing how well the artifact fulfils the objectives defined earlier in the research process. The purpose is to determine whether the artifact supports a solution to the identified problem and to identify potential areas for refinement.

In this study, evaluation was conducted at two levels. At the process level, iterative assessment was integrated throughout the Design and Development phase in accordance with the ADR-inspired building-intervention-evaluation logic. Feedback from the WFP supervisor continuously informed revisions to the artifact.

At the artifact level, evaluation was conducted in three steps, all presented in *Section 6.6.* First, the indicator values computed during the demonstration are assessed for plausibility in *Section 6.6.1* through cross-checks against independent sources and regional literature, verifying that the results are consistent with known environmental conditions in the respective production regions. Second, the consolidated framework is evaluated against the organisational objectives established in *Section 1.3*, examining the extent to which the tool meets the practical requirements defined in collaboration with WFP. Third, the framework is evaluated against the decision support system design attributes synthesised in *Section 2.3.4*, assessing whether the tool fulfils the theoretical criteria for a well-designed decision support system.

3.5.6 Communication

The final activity in DSRM involves communicating the problem, the artifact, the design process and its relevance to appropriate audiences (Peffers et al., 2007). In this study, communication was conducted at both an academic and an organisational level. At the academic level, the thesis documents the full research process. At the organisational level, the developed framework and the reasoning behind key design decisions were presented to WFP representatives. The aim was to make the methodology accessible and actionable for potential further development and implementation within WFP operations. The thesis therefore serves both as an academic contribution and as a technical specification that provides a direct foundation for future integration into WFP's procurement systems.

3.6 Time Horizon

The time horizon layer of the Research Onion distinguishes between cross-sectional and longitudinal studies (Saunders et al., 2019). Cross-sectional studies capture data at a single point in time, while longitudinal studies involve data collection over an extended period. This thesis follows a cross-sectional time horizon, as data collection and artifact development are conducted within a limited timeframe corresponding to the master's thesis period of 20 weeks.

3.7 Data Collection

At the core of the Research Onion are the techniques and procedures used for data collection and analysis (Saunders et al., 2019). In line with the previously described multi-method choice, this study combined qualitative primary data and secondary data to support the development and refinement of the artifact. This combination is consistent with DSRM. The study integrates existing knowledge with contextual insights in order to design a practically relevant artifact (Peffers et al., 2007).

3.7.1 Primary Data

Primary data collection in this study was limited and served an orienting and evaluative function rather than a generative one. It consisted of two sources.

The main source was iterative engagement with the WFP supervisor, Nicholas Finney, through weekly online meetings and email correspondence conducted throughout the study. These interactions were ad hoc in nature and followed the needs of each development stage rather than a formal data collection protocol. They provided insights into current decision-making practices, helped define the scope and objectives of the artifact and supported continuous refinement of the framework through feedback on draft versions. Meetings were documented through notes used to guide revisions during the Design and Development phase. Within the ADR framework, these interactions are best understood as practitioner collaboration rather than structured data collection (Sein et al., 2011).

The second source was two informal consultations with academic staff at Lund University from the Division of Technical Water Resources Engineering. Kenneth M. Persson and Erik Nilsson, both with expertise in water resources and agricultural systems, reviewed early drafts and provided input on the framework. Their feedback focused primarily on the structure of environmental dimensions and the selection and placement of indicators. The consultations took place sequentially in the early stages of the study. As these interactions were informal and exploratory rather than structured, and the resulting input is not directly cited in the thesis, they are documented here for transparency.

3.7.2 Secondary Data

Secondary data refers to data that were originally collected for other purposes but can still be used and analysed within the specific context of the thesis (Saunders et al., 2019). In this research, secondary data constituted the primary basis for both the theoretical foundation and the construction of the framework. It consisted of three categories: academic literature, publicly available datasets and internal WFP documents. Of these, the publicly available datasets were the main source of data used to construct the framework.

The first category consisted of academic literature, collected through a literature search across five main areas: humanitarian logistics, supply chain risk management, decision support systems, risk assessment tools and indicator construction, and crop growth and environmental stress. The search process began with identifying keywords related to each area, combined using Boolean operators to broaden or refine results. An example of the keywords used for literature search on Humanitarian Logistics (*Section 2.1*) is illustrated in *Figure 3.4*.

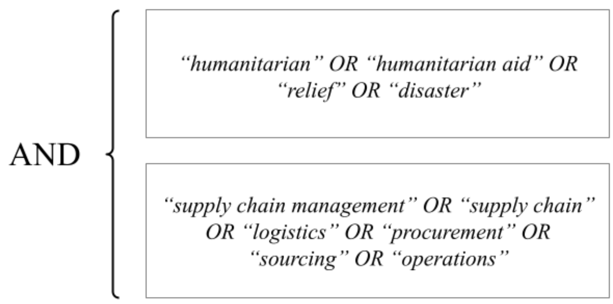

Figure 3.4: Examples of keywords used in this thesis.

In addition to traditional keyword searches, the Scopus AI tool was used as a complementary method for identifying relevant literature. The tool allows users to input descriptive prompts, which are then translated into structured search queries across the Scopus database. The generated results are based on peer-reviewed literature and include references to relevant academic publications. This tool was used to complement the manual search process and to identify additional relevant articles that may not have appeared through the initial keyword searches. After the initial search, the results were screened based on relevance to the research topic. Titles and abstracts were reviewed to identify studies addressing the research themes of the thesis, while articles focusing on unrelated topics were excluded. In addition to relevance, citation frequency was considered when selecting sources, as highly cited articles were assumed to be more relevant.

The second category of secondary data consisted of publicly available datasets used to operationalise the indicators developed in *Chapter 5*. Candidate datasets were identified through open searches of Google Earth Engine's native catalogue, academic literature and technical documentation from international organisations and research institutions. Selection was guided by predefined two-tier criteria. Tier one established minimum requirements that all datasets had to satisfy to be considered, while tier two provided comparative criteria for evaluating and ranking candidates that met the minimum threshold. Separate criteria were established for the risk and impact assessments, documented in *Section 5.2.1* and *Section 5.3.1* respectively.

The third category of secondary data consisted of internal documents from WFP. These included data from the procurement division on sourcing countries and purchased commodities. According to Blessing & Chakrabarti (2009), using internal documents supports efficient data collection. Additionally, it helps to reach a better understanding of the context of the problem at hand (Peffers et al., 2007).

3.8 Research Quality

Ensuring research quality is essential to establish the credibility, transparency and robustness of the study. Ensuring research quality is particularly emphasised within design science research (Peffers et al., 2007), as well as in research designs involving close collaboration with organisations (Näslund et al., 2010). Quality is commonly assessed through criteria such as validity and reliability (Yin, 2014). However, in design-oriented research, additional considerations such as artifact utility and traceability of design decisions are also important (Hevner et al., 2004).

3.8.1 Validity

The purpose of validity is to ensure that the study measures what it is intended to measure and that the collected data are capable of addressing the research questions.

Construct validity refers to whether appropriate concepts are identified and correctly operationalised (Yin, 2014). In this study, key concepts such as environmental impact and environmental sourcing risks are established from literature and clearly defined before being translated into measurable indicators within the decision support tool. Where possible, indicators are based on recognised datasets. Potential shortcomings in data availability, indicator comparability and scoring assumptions are explicitly addressed to reduce the risk of bias. The plausibility of the computed indicator values is further assessed in *Section 6.6.1*, where each indicator is cross-checked against independent sources and known regional patterns.

External validity means to what extent findings can be generalised beyond the specific study context (Yin, 2014). In this thesis, generalisation is analytical rather than statistical. While the artifact is developed in collaboration with a single organisation, the underlying design logic and structured development process may be transferable to similar procurement contexts. The formulation of design principles increases the potential for adaptation beyond the immediate study.

Validity is further strengthened through triangulation by ensuring that the same conclusions are supported from more than one direction (Denscombe, 2010). In this thesis, the choice of environmental dimensions converges across the theoretical literature in *Section 2.5.3*, the academic consultations described in *Section 3.7.1*, and initial discussions with WFP stakeholders. Investigator triangulation is ensured as two researchers are involved in data collection, analysis and interpretation, allowing discussion and cross-validation of findings.

3.8.2 Reliability

Reliability addresses whether the research process is transparent, consistent and sufficiently documented to allow replication of the procedures (Saunders et al., 2019). In design-oriented research, exact replication of outcomes is rarely achievable since artifacts are embedded in specific organisational contexts (Hevner et al., 2004), but the methodological approach itself should be replicable.

Reliability is strengthened in this thesis through systematic documentation of each phase of the DSRM process. The two-tier dataset selection criteria in *Section 5.2.1* and *Section 5.3.1* provide an explicit and replicable basis for all indicator development decisions. The indicator formulas in *Section 6.2* and the Google Earth Engine scripts in Appendix B allow the full computational pipeline to be independently reproduced. Where design decisions involve judgement, for example in the exclusion of dimensions such as air quality and chemical soil degradation, the reasoning is documented in the relevant sections.

3.8.3 Artifact Utility

In design science research, the quality of a study depends not only on methodological consistency but also on the demonstrated utility of the produced artifact (Hevner et al., 2004). Utility refers to the extent to which the artifact addresses the identified problem and supports its intended users in the relevant decision setting. Hevner et al. (2004) emphasise that this must be demonstrated through appropriate evaluation methods rather than asserted.

In this thesis, artifact utility is addressed at three stages. First, the tool requirements established in *Section 1.3* in consultation with WFP define the intended utility before the artifact is developed, grounding it in operational procurement needs. Second, the artifact is formally evaluated in *Section 6.6* against both these requirements and the DSS design attributes synthesised in *Section 2.3.4*, enabling assessment against both practical and theoretical criteria. Third, the demonstration using maize sourced from Benin and Tanzania in *Section 6.5* illustrates how the artifact performs under realistic procurement conditions and provides a basis for assessing whether the intended utility is achieved.

The iterative Build, Intervention and Evaluation cycle of Action Design Research, embedded within the Design and Development phase, additionally supports utility by exposing the artifact to repeated feedback from WFP throughout its development rather than only at completion.

3.8.4 Traceability

Traceability refers to the extent to which the components of the developed artifact can be linked back to the reasoning, datasets and design choices that produced them. In design science research, this supports the guideline of Hevner et al. (2004), which requires that artifacts be constructed and evaluated using existing foundations from the knowledge base in a documented and verifiable manner.

In this thesis, traceability is established at three levels. At the conceptual level, each indicator is grounded in the theoretical dimensions identified in *Chapter 2* and structured through the conceptual framework presented in *Chapter 4*. At the methodological level, indicator selection follows the two-tier dataset selection criteria documented in *Section 5.2.1* and *Section 5.3.1*, which provides an explicit and replicable basis for including or excluding candidate datasets. At the computational level, each indicator can be traced from its formula in *Section 6.2* through its dataset reference in *Section 6.3* or *Section 6.4* to the underlying raster operations encoded in the Google Earth Engine script in Appendix B. The reliance on open datasets with documented methodologies further supports traceability, as external observers can independently verify the source of each measurement.

This layered documentation allows the design choices behind the artifact to be examined and revised by external parties. Decisions to exclude dimensions are documented together with the reasoning behind them, supporting transparency over the boundaries of the final artifact.

4 Conceptual Decision Support Tool

This chapter develops the conceptual design of the decision support tool, defining the two analytical components of the model base and the integrated framework structure they produce.

Within the research design presented in *Section 3.5*, this chapter represents the first of the four building components of the Design and Development phase, the *Conceptual Framework Design* (compare with *Figure 3.3*). The position of the chapter within the overall design and development phase is illustrated in *Figure 4.1*.

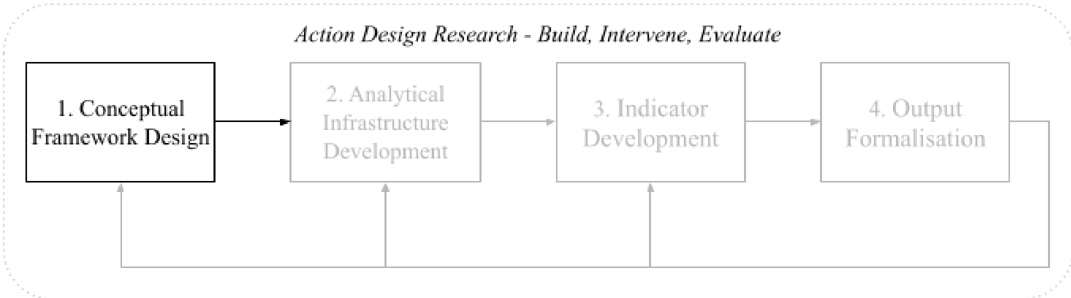

Figure 4.1: Position of *Chapter 4* within the Design and Development phase of the research design as the first building component, Conceptual Framework Design.

While *Section 2.6* outlined how the theoretical streams relate to one another, this chapter translates those relationships into the design choices that define the artifact. Drawing on the theoretical background established in *Chapter 2*, the tool is structured around the three subsystems of a decision support system: a database subsystem, a model base subsystem and a user interface subsystem (Sprague & Carlson, 1982). The overall architecture is illustrated in *Figure 4.2*. The model base consists of two parallel analytical components, each developed in turn below. The operationalisation of the user interface falls outside the scope of this thesis. The chapter presents the ideal design from a theoretical and analytical perspective, before practical constraints such as data availability and implementation feasibility are considered. *Chapter 5* describes how this ideal framework was subsequently translated into the operational tool.

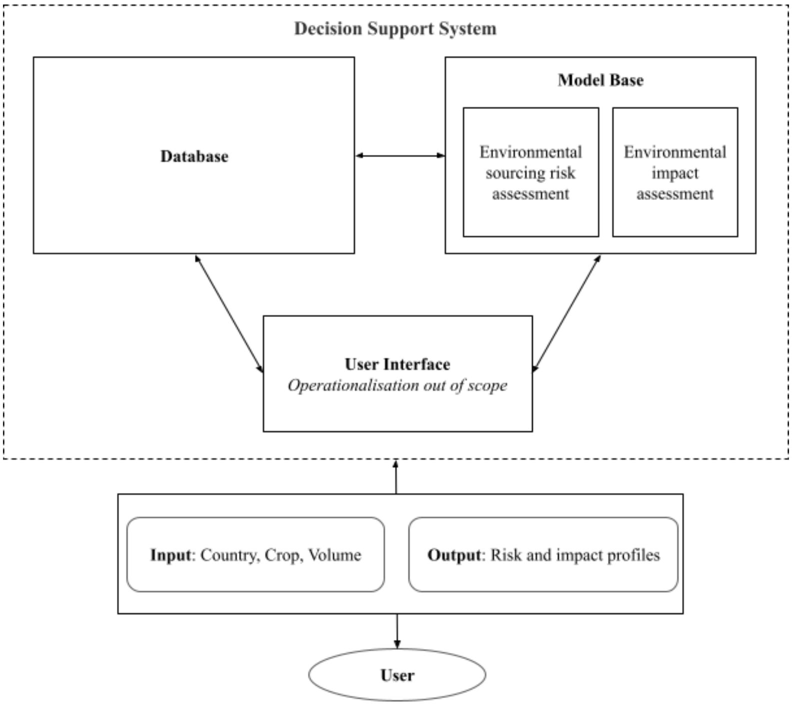

Figure 4.2: High level conceptual architecture of the decision support system, structured around a database subsystem, a model base subsystem and a user interface subsystem (Sprague & Carlson, 1982).

4.1 Applying the Disaster Risk Framework to Agricultural Sourcing

The theoretical background identified two principal risk model structures. The probabilistic risk models structure risk around scenarios, probabilities and consequences, and disaster risk frameworks structure risk around hazards, exposure and vulnerability (Cardona et al., 2012; Kaplan & Garrick, 1981). Both approaches are conceptually valid, but they are suited to different analytical contexts. The choice of framework has direct implications for what can be measured, how indicators are constructed and what kind of outputs the tool can generate. For WFP's procurement context, the disaster risk framework is the more appropriate structure for two reasons.

First, as established in *Section 2.2.3*, procurement risk in agricultural supply chains is fundamentally place-bound. The risk of sourcing crops from a particular country is shaped by the environmental conditions in the growing regions and by how strongly those conditions affect the crop being sourced, rather than how often supply disruptions have occurred in the past. This spatial logic aligns with the disaster risk framework's emphasis on the geographic distribution of hazards and their intersection with exposed elements (Cardona et al., 2012). A probabilistic model requires event frequency data, which for agricultural sourcing decisions is rarely available at sufficient resolution or consistency (Lesk et al., 2016). A disaster risk framework, by contrast, can be operationalised through spatial environmental data which is increasingly available through remote sensing and global datasets.

Second, if risk is understood as the risk of harvest or yield loss, the stress factors identified in *Section 2.5.3* can be understood as hazards rather than risk in themselves. Whether these hazards translate into production disruption depends on what is exposed, meaning where and to what extent a crop is cultivated, and how vulnerable the crop is to those conditions. Crop characteristics therefore shape how strongly environmental stress affects production outcomes. In this sense, risk emerges from the interaction between hazards, exposure and vulnerability rather than from hazards alone (Cardona et al., 2012).

Thus, the disaster risk framework provides the conceptual architecture for the tool. Rather than estimating the probability of discrete disruption events, the tool assesses the conditions under which environmental stress may translate into reduced agricultural production and sourcing constraints.

4.1.1 Hazard

In the disaster risk framework, a hazard is defined as a potentially damaging physical event or phenomenon (United Nations Office for Disaster Risk Reduction, 2016). For the context of WFP, hazards refer to the environmental conditions and processes that can disrupt crop production and the intensity of those. Drawing on the stress factors reviewed in *Section 2.5.3*, hazards in this framework are understood as the abiotic and biotic stressors that push environmental conditions outside the ranges within which crops can grow and develop successfully (Zhang et al., 2022; Mittler, 2006). An overview of these stressors is provided in Table 4.1, derived by combining the abiotic stress factors summarised in Table 2.8 and the biotic stressors identified in *Section 2.5.3.2*.

Table 4.1: Overview of abiotic and biotic stressors that act as hazards in the framework.

Type of Stressor	**Stressor**
Abiotic Stress	High irradiance Shading UV radiation Heat stress Cold stress Flooding Drought Precipitation change Elevated CO_2 Pollution (NO_x, O_3) Physical degradation (erosion, structural decline) Chemical degradation (nutrient depletion, salinity) Biological degradation (SOC decline)
Biotic Stress	Insects and Pests Diseases and Pathogens Weeds

4.1.2 Exposure

Exposure refers to the presence of elements within areas affected by a given hazard (United Nations Office for Disaster Risk Reduction, 2016). Within WFP's procurement context, exposure can therefore be understood as the extent to which a specific crop is produced in regions where a given hazard occurs. A country may experience severe drought conditions, but if the crop in question is grown primarily in well-irrigated highland regions unaffected by that drought, the actual risk of yield loss is lower than the country-level hazard intensity would suggest. Exposure must therefore be assessed at the level of the crop's geographical distribution rather than aggregated country-level conditions (Cardona et al., 2012). Operationally, exposure should therefore be determined by the spatial intersection between the hazard and the crop's growing area. For water-related hazards, the distinction between rainfed and irrigated production area is particularly relevant, as discussed in *Section 4.4*.

4.1.3 Vulnerability

Vulnerability refers to the susceptibility of exposed elements to the damaging effects of a hazard (United Nations Office for Disaster Risk Reduction, 2016; Cutter, 1996). Vulnerability should therefore capture how severely a crop's growth and yield are affected when it is exposed to a given hazard. It is therefore treated as crop-specific, since the same level of exposure may result in severe yield losses for one crop but have limited effects on another with higher physiological tolerance (Cutter, 1996). The crop growth requirements reviewed in *Section 2.5.1* and the stage-specific sensitivities discussed in *Section 2.5.2* provide the theoretical basis for assessing crop vulnerability. For most stressors, vulnerability is defined in relation to crop-specific minimum, optimal and maximum thresholds for growth requirements. When hazards push conditions beyond these thresholds, particularly during sensitive growth stages, the likelihood of reduced growth or yield loss increases (Hatfield et al., 2011). Vulnerability is therefore understood as a function of both the distance between ambient conditions and the crop's tolerance thresholds, and the growth stage at which exposure occurs.

4.1.4 Yield Loss as Sourcing Risk

The preceding sections have defined the three components of the risk framework independently. This section addresses how they are theoretically combined to produce an assessment of environmental sourcing risk, and what that risk ultimately represents in WFP's procurement context.

The connection between the framework and environmental sourcing risk runs through yield. When hazard conditions exceed the tolerances of an exposed crop, growth is disrupted and yield is reduced (Hatfield et al., 2011). It is this yield loss that constitutes the focused procurement risk, because reduced or failed harvests in a sourcing country translate into reduced supply availability (Lesk et al., 2016). The framework therefore positions yield loss as the critical intermediary between environmental hazard and sourcing disruption.

Only when hazard conditions are present in the areas where a crop is grown, and when that crop is sensitive to those conditions, does risk materialise. The three components are therefore not additive but jointly necessary, as first expressed in *Equation (2.2)*:

$$R = f(H, E, V) \tag{2.2}$$

where H is the intensity and frequency of the hazard in the areas where the crop is grown, E is the spatial extent to which the crop's harvested area overlaps with those hazard conditions, and V is the degree to which the crop's physiological tolerances are exceeded under those conditions. The ideal assessment of sourcing risk for a given country-crop-hazard combination would therefore proceed through three steps.

First, identifying the hazard zone. For each hazard, the geographic areas where conditions exceed or fall short of the thresholds relevant to agricultural production are identified (Cardona et al., 2012). The relevant threshold is not a universal value but a crop-specific optimal range, within which growth proceeds without significant stress (Hatfield et al., 2011). Areas where conditions deviate from this optimal range constitute the hazard zone for that crop-hazard combination. The severity of the hazard is dependent on the magnitude of the deviation and its duration or frequency during the growing season.

Second, intersecting the hazard zone with the crop's spatial distribution. The crop's harvested area, distributed across sub-national spatial units, is overlaid with the identified hazard zone. This intersection produces an exposure estimate, capturing the share of the crop's production that is located in areas affected by hazard conditions during the growing season (Cardona et al., 2012). A crop concentrated in the most severely affected zones will show high exposure. Restricting the assessment to the growing season ensures that only those periods during which the crop is physiologically active and therefore sensitive to environmental conditions are considered.

Third, adjusting for crop vulnerability. Not all crops respond equally to the same hazard conditions. For any stressor, a crop's vulnerability is characterised by two properties. The first is its tolerance threshold, meaning the range of conditions within which growth proceeds without significant disruption (Hatfield et al., 2011). The second is its yield response beyond that threshold, meaning the rate at which yield declines as conditions move further from the optimal range (Wheeler & Von Braun, 2013). Together these define a crop-specific yield response function, and both vary across crops and stressors. Two crops exposed to identical conditions may therefore experience very different yield outcomes. A further dimension of vulnerability is growth stage sensitivity, as the same stressor may cause limited damage during some phases of development while producing severe and irreversible losses during others (Hatfield et al., 2011).

The vulnerability adjustment uses these properties to transform the hazard-exposure signal into a crop-differentiated yield impact estimate. Where tolerance thresholds are high and yield response gradual, the same exposure produces a lower risk estimate. Where thresholds are lower and the response steeper, the same conditions translate into substantially higher risk. The result is a risk signal that varies across crops even when environmental conditions and spatial exposure are identical, reflecting real differences in biological sensitivity (Cutter, 1996; Hatfield et al., 2011). Taken together, this logic produces a risk estimate for each country-crop-hazard combination that reflects three things. First, it reflects how severe and frequent the hazard conditions are in the areas where the crop is grown. Second, it reflects what proportion of the crop's production is exposed to those conditions during the growing season. Lastly, it reflects how sensitive the specific crop is to that level of stress given its physiological characteristics. A high-risk profile for a given hazard therefore indicates that the crop is substantially exposed to conditions that exceed its tolerance thresholds across a significant portion of its growing area, conditions under which yield loss is a plausible and potentially severe outcome (Lesk et al., 2016; Cardona et al., 2012).

4.1.5 Hazard-Specific Risk Profile

Normalisation is applied to support the interpretation of individual indicator results. Absolute indicator values are expressed in different units and scales, and even two values for the same indicator may be difficult to interpret without a contextual reference point. As discussed in *Section 2.4.3.2*, normalisation provides a way of transforming indicator results into a more interpretable form by relating them to a defined reference, with the choice of method depending on the purpose of the assessment and the properties of the data (European Commission et al., 2008).

This tool applies mean-referenced normalisation, where each indicator value is expressed in relation to the African mean for the same crop and indicator. The purpose of the tool is to support comparison between country-crop sourcing options within Sub-Saharan Africa, which makes a mean-referenced normalisation approach appropriate (European Commission et al., 2008). The operational definition of the reference mean and its formula are established in *Section 5.1.4*. For indicators where established absolute thresholds exist in the literature, those thresholds are used as a complementary interpretive layer alongside the relative comparison, providing an absolute anchor independent of how other countries in the dataset happen to perform.

The most direct output of an environmental sourcing risk framework would be a single composite score for each country-crop combination. Such a score would enable straightforward comparison across sourcing countries and support procurement decision-making in the most direct way. It would allow WFP to rank potential sourcing origins by overall environmental risk without having to interpret multiple separate assessments.

However, producing such a score within this framework raises two challenges. Together, these make aggregation a boundary of the thesis scope rather than a theoretical impossibility. The first challenge concerns how the different dimensions should be combined. As discussed in *Section 2.5.3.3*, crops do not necessarily respond to combined stresses in the same way as they respond to each stress separately. Compound events can also lead to impacts that are larger than those predicted by single-hazard assessments (Mittler, 2006; Omokpariola et al., 2025). A simple additive score would therefore risk misrepresenting the relationships between hazard dimensions and could give a false impression of precision (Saltelli, 2007).

The second challenge concerns weighting. Aggregating across hazard dimensions requires assigning relative importance to each, which in turn requires knowledge about how much one type of environmental stress matters relative to another for WFP's procurement priorities. As discussed in *Section 2.4.3.3*, Multi-Criteria Decision-Making approaches such as the Analytic Hierarchy Process (AHP) have been developed precisely for this type of problem, where criteria are incommensurable and weights must be derived from expert judgement rather than from analytical relationships between dimensions (Handfield et al., 2002). AHP structures the weighting process through pairwise comparison, allowing domain experts to express relative importance judgements in a systematic and replicable way. Applying AHP to the hazard dimensions in this framework would require a dedicated expert elicitation session with crop scientists and WFP procurement staff to establish crop-specific and context-specific weights. This process falls outside the scope of this thesis, but is proposed as a direct next step in *Section 7.3.2*.

The output of the framework is therefore a hazard-specific risk profile for each country-crop combination, rather than a single composite risk score. For each hazard dimension, the profile shows both the absolute indicator value and the normalised value relative to the African mean. The absolute value preserves the original meaning and unit of the indicator, while the normalised value places the result in a regional context and indicates whether conditions are relatively high or low compared with other sourcing origins. While less immediately comparable than a single score, this structure preserves the distinctions between hazard dimensions that are needed to understand what drives a given risk profile and to identify possible courses of action (Birkmann, 2007; Saisana & Tarantola, 2016). The translation of this structure into the operational indicator set is documented in *Chapter 5*.

4.2 Environmental Impact Assessment of Agricultural Sourcing

As reviewed in *Section 2.5.4*, the environmental impacts of crop production can be structured into five main areas: greenhouse gas emissions, deforestation and land use change, biodiversity loss, water use and quality, and pesticide use (Gallardo, 2024). Each of these dimensions represents an impact pathway through which crop production generates ecological harm. The type and magnitude of impact varies across crops, production systems and geographic contexts (Reynolds et al., 2015; Jwaideh & Dalin, 2025). Together, these five dimensions define the environmental impact scope of the conceptual decision support tool. Including them enables the tool to capture the main ecological consequences associated with crop sourcing and provides a structured basis for assessing the share of environmental pressure attributable to a sourcing decision.

4.2.1 Procurement Volume as the Basis for Impact Assessment

The preceding section identified the five environmental impact dimensions that the framework should incorporate. This section describes how those dimensions should be operationalised in a way that is directly connected to and useful for WFP's procurement decisions.

The first step in the environmental impact assessment is to set the environmental impact intensity of a country-crop combination. This means assessing, in a relevant metric, how much impact is generated per unit of crop produced in a given country. Conceptually, this can be done by estimating the total environmental impact associated with the national production of a crop and relating this to the total quantity of that crop produced in the same country. The result is an impact intensity, expressing how much environmental pressure is generated per tonne of crop produced.

Once an impact intensity has been estimated for each dimension, the procurement volume becomes the basis for translating this into a sourcing-specific impact profile. If WFP intends to procure a given quantity of a crop from a specific country, the impact intensity for that country-crop combination can be multiplied by the intended procurement volume. This produces an estimate of the environmental impact associated with that particular sourcing decision. The result is an impact profile that is directly tied to procurement volume. This makes the assessment more relevant for WFP's operational context, since environmental consequences depend not only on which crop is sourced from which country, but also on how much is sourced. This volume-based operationalisation was identified in discussions with WFP procurement staff as the analytically relevant framing, since procurement quantities vary substantially across sourcing decisions and affect the scale of environmental consequences (see *Section 3.7.1*).

4.2.2 Dimension-Specific Impact Profile

The environmental impact indicators are normalised using the same mean-referenced approach as the risk indicators described in *Section 4.1.5*. This is done for the same purpose, to support interpretation by placing each indicator value in relation to the African mean (European Commission et al., 2008). Each impact indicator is expressed as a ratio to the African mean for that crop and indicator, communicating whether a sourcing country generates above or below average impact per tonne of crop produced relative to the regional norm.

As with the risk framework in *Section 4.1.5*, the most direct output of an environmental impact assessment would be a single composite score per procurement decision. Such a score would allow WFP to rank sourcing options by aggregated environmental harm without interpreting five separate estimates. However, producing such a score presents the same type of scope boundary as in the risk component. The five impact dimensions are measured in categorically different units, such as tonnes of CO_2 equivalent, hectares converted, biodiversity pressure, water use and pesticide use. Although normalisation places the indicators in a more comparable form, it does not resolve the question of how different forms of ecological harm should be weighted against one another. As noted in *Section 2.4.3.3*, this is precisely the type of problem that structured MCDM approaches such as AHP have been developed to address. AHP could in principle enable WFP procurement staff and sustainability specialists to express relative importance judgements across the five dimensions through a pairwise comparison process, producing an organisationally grounded and replicable set of weights (Handfield et al., 2002). In a supply chain risk management and procurement context, this kind of expert-elicited weighting has been shown to support more informed and transparent decision-making than either equal weighting or ad hoc judgement (Handfield et al., 2002). Carrying out such an elicitation process was not part of this thesis. In addition, the impact dimensions are not fully independent. Some impacts can contribute to, or partly manifest through, other dimensions. For example, deforestation and land use change may lead to biodiversity loss, even though both are assessed as separate impact dimensions (Gallardo, 2024; Reynolds et al., 2015). A single additive score could therefore risk double-counting related effects, which is a limitation that a future AHP implementation should account for when structuring the comparison hierarchy. For both reasons, the indicators are retained as separate outputs in the current version of the tool. The use of an MCDM layer for weight elicitation is proposed as a future development in *Section 7.3.2*.

The environmental impact framework therefore takes the form of a dimension-specific impact profile rather than one aggregated impact score. The profile presents the different environmental impact dimensions separately, with each indicator reported both as an absolute value and as a normalised value relative to the African mean. The absolute value preserves the original meaning and unit of the indicator, while the normalised value places the result in a regional context and indicates whether it is relatively high or low compared with other sourcing origins. This allows decision-makers to see which dimensions are driving the environmental concern for each country-crop combination. The translation of this structure into the operational indicator set is documented in *Chapter 5*.

4.3 Integrated Risk and Impact Framework

The preceding sections have established the two components of the final framework. *Section 4.1* structures environmental sourcing risk around hazard, exposure and vulnerability, producing a risk profile for each country-crop combination. *Section 4.2* structures environmental impact around the five ecological consequences of crop production, producing an impact profile tied to procurement volume. This section describes how the two components are presented in the final framework structure.

Since the two components each take the form of a disaggregated profile, for the reasons established in *Section 4.1.5* and *Section 4.2.2*, combining them into a single integrated composite score is not pursued within the scope of this framework. Doing so would require not only the expert-elicited weights discussed in those sections for each component separately, but also a set of weights expressing the relative importance of environmental risk versus environmental impact in WFP's procurement priorities. As noted in *Section 2.4.3.3*, an MCDM approach such as

AHP could in principle provide a structured process for this kind of cross-component weighting, and *Section 7.3.2* identifies this as a future development direction. In the current tool, the two components are instead presented in parallel, allowing procurement staff to consider both types of information together without the framework pre-specifying how they should be traded off.

A relationship that should be recognised in the combined framework is the connection between environmental impact and environmental sourcing risk. As discussed in *Section 2.5.5*, the environmental impacts of crop production are not only consequences of sourcing decisions, but may also become drivers or amplifiers of future crop stressors, which feed back into environmental sourcing risk. The framework presents environmental risk and environmental impact as parallel but separate analytical outputs, which means that the tool does not model this causal connection but makes both visible simultaneously for the same country-crop combination. The theoretical background establishes that such feedback exists without specifying how a given amount of environmental impact translates into a change in risk for each dimension, crop or geographic context (Tchonkouang et al., 2024; Pereira et al., 2025). Presenting both outputs simultaneously allows users to observe, for instance, that a given sourcing option carries both high water stress risk and high water use, and draw the connection without the model implying a quantified causal link that the theory cannot support (Birkmann, 2007).

The ideal tool is therefore an integrated but non-aggregated framework. It presents environmental sourcing risk and environmental impact side by side, with separate dimension-specific profiles under each component. This structure preserves the analytical distinction between environmental risk and environmental impact while still allowing them to be considered together in procurement decision-making (European Commission et al., 2008; Saisana & Tarantola, 2016).

Together, the environmental sourcing risk assessment and the environmental impact assessment constitute the model base subsystem, which transforms database inputs into decision-relevant outputs (Sprague & Carlson, 1982). The model base draws on a database subsystem holding five categories of data: spatially explicit stressor conditions, crop-specific production area data, crop physiological tolerance thresholds, environmental impact intensities per unit of crop produced and crop production data on a national level. The outputs of the model base, an environmental sourcing risk profile and an environmental impact profile, are then communicated to the decision-maker through the user interface subsystem. The structural relationship between these three subsystems, the two model components and the user is illustrated in *Figure 4.3*.

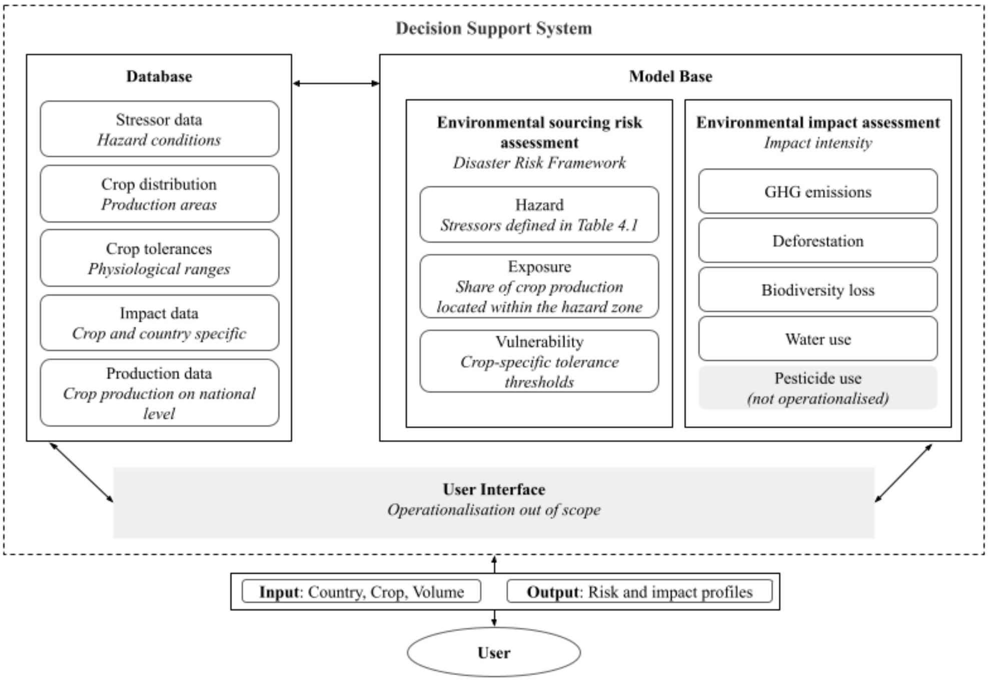

Figure 4.3: Detailed conceptual architecture of the decision support system, structured around a database subsystem, a model base subsystem and a user interface subsystem.

4.4 Integrated Output Visualisation

Although the dimension-specific profiles established in sections 4.1.5 and 4.2.2 preserve the integrity of individual indicators, comparing values across dimensions and country-crop combinations simultaneously can be cognitively demanding. The framework therefore proposes two side-by-side radar charts, illustrated in *Figure 4.4*, to support interpretation without aggregating into a composite score.

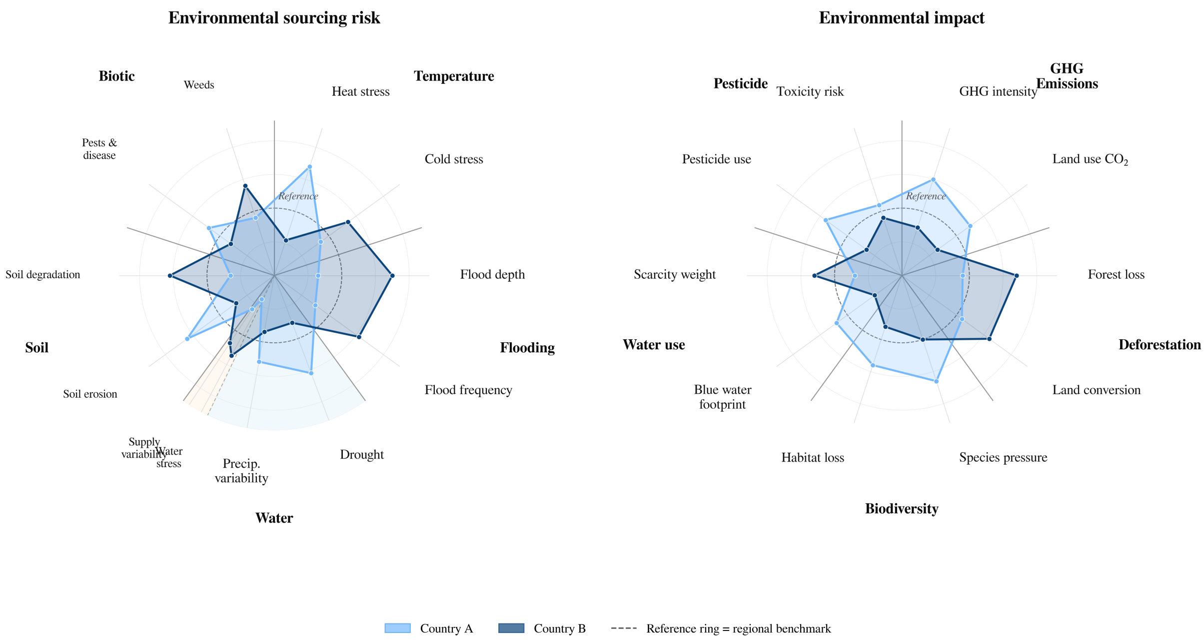

Figure 4.4: Conceptual illustration of the integrated radar visualisation, with equal sectoral allocation across dimensions, a proportional rainfed and irrigated split within the water hazard sector, and a reference ring marking the regional benchmark.

Each chart divides the full circle equally among the major analytical dimensions, with indicators receiving equal angular space within each dimension. The exception is the water hazard sector in the risk profile, which is divided proportionally between a rainfed and an irrigated sub-sector based on the crop's harvested area share under each production system. Within each sub-sector, the indicators are spaced equally. Sector width therefore encodes exposure while indicator radius encodes hazard intensity, directly expressing the $R = f(H, E, V)$ structure without numerical aggregation. When a single country-crop combination is profiled, the actual production system shares determine the split. When two combinations are overlaid, the African production-weighted mean is used as a neutral reference.

Each indicator is expressed relative to a regional reference value. The specific normalisation method is established in *Chapter 5*. At the conceptual level, the reference ring marks the regional benchmark. Values outside indicate worse-than-average conditions, with all indicators oriented consistently in this direction. Multiple country-crop combinations can be overlaid as transparent polygons, making trade-offs directly visible without aggregation.

Equal sector widths are the neutral default, but as established in *Section 2.4.3.3*, equal weighting is itself an assumption (European Commission et al., 2008). The same challenge that made a composite score unfeasible in sections 4.1.5 and 4.2.2 applies here. Sector widths can therefore be adjusted to reflect institutional priorities without altering the model or producing a composite score. A structured approach to weight elicitation is identified as future work in *Section 7.3.2*. The visualisation is applied to real data in *Figure 6.4*.

5 Development of the Decision Support Tool

This chapter translates the conceptual framework from Chapter 4 into a functional tool by making concrete methodological choices about indicators, datasets and calculations. It first introduces the shared analytical foundations before documenting the development of the environmental risk assessment and the environmental impact assessment separately.

Within the research design presented in *Section 3.5*, this chapter covers the second and third building components of the Design and Development phase, *Analytical Infrastructure Development* and *Indicator Development* (compare with *Figure 3.3*). Together, these two components translate the conceptual framework from *Chapter 4* into a functional tool by first establishing the shared analytical foundations and then developing the individual indicators on top of them. The position of the chapter within the design and development phase is illustrated in *Figure 5.1.*

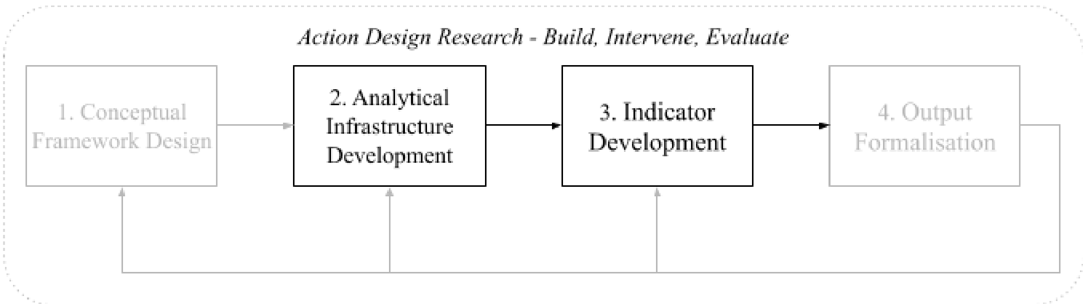

Figure 5.1: Position of Chapter 5 within the Design and Development phase of the research design as the second and third building components, Analytical Infrastructure Development and Indicator Development.

Chapter 4 established the conceptual structure of the tool by combining an environmental risk assessment based on abiotic and biotic crop stressors with an environmental impact assessment focused on the ecological consequences of crop production. Translating this structure into a functional tool requires making concrete methodological choices about how each dimension is measured, how each indicator is defined and which datasets are used. As established in *Section 2.4.3*, this process is complex and each step involves methodological trade-offs that must be documented transparently so that results are understood as indicative approximations rather than exact representations (European Commission et al., 2008). In line with the DSS design attributes outlined in *Section 2.3.4*, scientific validity and traceability require that each indicator is grounded in published and independently validated data sources (Little, 1970; Holsapple, 2008).

The approach throughout this chapter is therefore to identify and integrate existing and established datasets rather than constructing new indicators for each environmental dimension. Across both the environmental risk assessment and the environmental impact assessment, a central objective is crop specificity, meaning that each indicator is designed to produce a result for a specific crop within a specific country. This enables comparison between sourcing options rather than relying on national averages. The Spatial Production Allocation Model (SPAM 2020) is the common spatial reference that enables this, and the dataset selection process for both assessments was guided by the objective of identifying indicators already compatible with its spatial logic. The following sections first introduce the shared technical infrastructure before documenting the development of the environmental risk assessment and the environmental impact assessment separately.

5.1 Analytical Foundations

5.1.1 Google Earth Engine

All spatial analysis in this study was conducted using Google Earth Engine, a cloud-based geospatial analysis platform developed by Google that provides access to large collections of satellite imagery and geospatial datasets together with extensive computational resources (Gorelick et al., 2017). Instead of requiring users to download and process data locally, Google Earth Engine allows analysis to run directly on Google's servers, where the data is already stored. This is practically significant for a study of this scope, as the indicator calculations involve global raster datasets at resolutions of ten kilometres or finer, applied across more than forty country-crop combinations and multiple time periods. In addition, many of the climate and environmental datasets used in this study are already available on the platform as native assets, meaning they can be accessed directly without additional preprocessing. This reduces the risk of data handling errors and improves reproducibility by ensuring that all indicator calculations are based on shared and version-controlled datasets.

5.1.2 Spatial Production Allocation Model

A central ambition in developing both the environmental risk and environmental impact assessments was to find datasets that are already crop-specific, meaning that the indicator value is attributed to a particular crop rather than to a country or region as a whole. The Spatial Production Allocation Model (SPAM 2020, Version 2.0) provides the spatial foundation by disaggregating national crop production statistics into gridded, crop-specific estimates of four crop variables: harvested area, physical area, production and yield (IFPRI, 2026). For the environmental impact assessment, most underlying datasets already incorporated crop-specific spatial attribution built on SPAM's crop distribution logic and were used directly. For the environmental risk assessment, no equivalent pre-built crop-specific indicators were available for the dimensions covered. Environmental risk indicator values were therefore constructed by overlaying stressor datasets with SPAM crop masks directly in Google Earth Engine. Both assessments are described further in *Section 5.2* and *Section 5.3* respectively. The SPAM data was provided by the International Food Policy Research Institute (IFPRI). IFPRI bears no responsibility for the analyses or interpretations of the data presented here.

SPAM 2020 provides gridded estimates for 46 crops at a spatial resolution of five arc minutes, corresponding to approximately ten kilometres at the equator. The model is built on a cross-entropy optimisation framework that distributes nationally and sub-nationally reported crop production statistics across grid cells by combining multiple conditioning datasets, including satellite-derived land cover maps, biophysical crop suitability assessments, irrigation extent, market accessibility indices and rural population density (You et al., 2014). The result is a globally consistent, crop-specific map of where production actually occurs, validated in collaboration with CGIAR research centres, an international partnership of agricultural research organisations. SPAM datasets have been released for the reference years 2000, 2005, 2010, 2017 and 2020, following an irregular schedule with intervals ranging from three to seven years between versions (IFPRI, 2026). SPAM 2020 is the most recent release available at the time of this study and was therefore chosen.

Each of the four variables is provided separately for irrigated and rainfed production systems, as well as for an all-technology layer that combines both. Environmental conditions and risks differ between irrigated and rainfed production, and the relevant system therefore varies across indicators. Which production system is used in each indicator calculation is determined by the nature of the indicator and documented under the relevant sections for both the environmental risk and environmental impact assessments. *Figure 5.2* shows an example of the SPAM 2020 output, displaying maize production volumes across Tanzania, which is later used as one of the demonstration countries in *Section 6.5*.

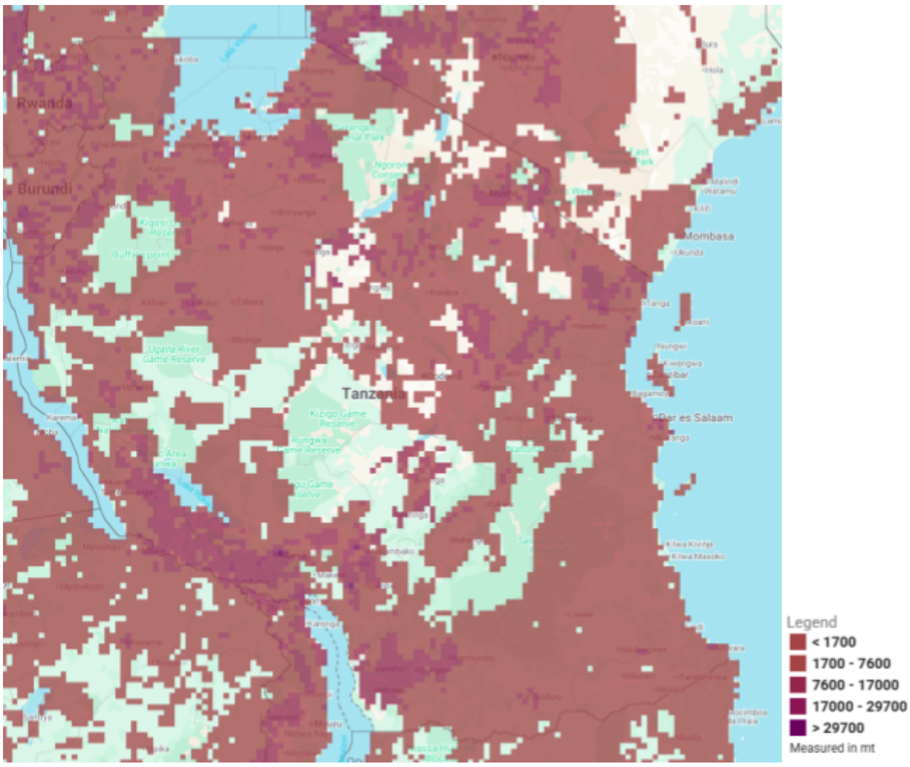

Figure 5.2: SPAM 2020 maize production estimates for Tanzania, expressed in metric tonnes per grid cell at approximately ten kilometre resolution (IFPRI, 2026).

The production statistics underlying SPAM 2020 are drawn primarily from FAOSTAT, which provides the national and sub-national totals that the model spatially distributes (IFPRI, 2026).

Summing SPAM production values across all pixels for a given crop and country therefore recovers the corresponding FAOSTAT national total.

5.1.3 Climatological Reference Period

All indicators that compute statistics over historical climate data require a defined analysis period. Without such a period, results are neither reproducible nor comparable across locations, as the value of any mean, frequency or variability measure depends directly on which years are included in its calculation. This section establishes the temporal reference adopted across all climatological indicators in the tool and justifies the choice.

The World Meteorological Organization (WMO) defines a climatological standard normal as the average of climate data over a 30-year period ending in a year divisible by ten, with the current standard being 1991 to 2020 (World Meteorological Organization, 2017). The 30-year window is widely regarded as the minimum period required for statistical robustness in climate analysis because it is long enough to characterise the underlying distribution of a climate variable and reduce the influence of anomalous years, while remaining short enough to be representative of current conditions rather than a historical past. This period is adopted as the temporal reference for all climatological indicators in this tool, covering 360 months of data.

The choice of 1991 to 2020 specifically, rather than the preceding standard period of 1961 to 1990, reflects the nature of the risk being assessed. The purpose of the tool is to characterise the climate conditions under which current crop systems are operating, as a basis for near-term sourcing decisions. A reference period anchored to the mid-twentieth century would reflect a cooler and less variable climate that no longer represents the conditions faced by producers across Sub-Saharan Africa today. The 1991 to 2020 period captures the climate experienced by the agricultural systems described by SPAM 2020, and thus supports internal temporal coherence across the tool. Where individual datasets do not permit the adoption of this period, the deviation is noted and justified at the indicator level.

5.1.4 Calculating African Reference Mean

To support interpretation of indicator outputs, each indicator value is presented alongside an African reference mean. For each indicator I and crop c, the reference mean is defined as the production-weighted mean of the indicator across all African countries that produce crop c:

$$\bar{I}_c = \frac{\sum_{k=1}^{N_c} I_{c,k} \cdot P_{c,k}}{\sum_{k=1}^{N_c} P_{c,k}} \tag{5.1}$$

where $I_{c,k}$ is the harvested-area-weighted indicator value for crop c and country k as defined in *Section 5.2*, $P_{c,k}$ is the national production volume of crop c in country k from FAOSTAT, and N_c is the number of countries that produce crop c. Weighting by production volume ensures that the reference mean reflects the environmental conditions under which the crop is actually produced across the region, rather than treating large and small producers as equally representative of typical conditions. The resulting normalised values feed directly into the radar visualisation described in *Section 4.4*, where each indicator corresponds to one sub-axis and the reference ring is drawn at 1.0.

5.2 Development of the Environmental Risk Assessment

Chapter 4 established that environmental sourcing risk in this study is understood through the potential for abiotic stressors to reduce crop yields in WFP sourcing regions. Translating this into measurable indicators requires connecting stressor data to where each crop is actually produced. As described in *Section 5.1.2*, no pre-built crop-specific risk indicators were found, meaning each indicator was constructed by combining a stressor-specific dataset with SPAM 2020 directly in Google Earth Engine.

The approach is consistent across all environmental risk dimensions and follows directly from how exposure was defined in *Section 4.1.2*. SPAM 2020 defines the spatial mask for a given crop and country, identifying which pixels are active production areas. A stressor dataset is then overlaid with that mask, and a production-weighted mean is computed across those pixels, producing a single indicator value that reflects environmental conditions within production areas rather than across an entire country.

Within the SPAM data, production volume is used as the weighting variable instead of harvested area. This approach gives greater weight to high-yielding pixels, as these contribute a larger share of national production. As a result, production located within hazard-prone areas has a greater influence on the indicator. This aligns with the indicator's intended purpose of characterising procurement risk, which follows tonnes of production rather than hectares of cultivated land.

This aggregation is expressed as:

$$I_{c,k} = \frac{\sum_{i \in M_{c,k}} w_i \cdot I_i}{\sum_{i \in M_{c,k}} w_i} \tag{5.2}$$

where $I_{c,k}$ is the final indicator score for crop c in country k, $M_{c,k}$ is the set of pixels in the SPAM 2020 mask for that crop and country, w_i is the production in tonnes at pixel i, and I_i is the pixel-level indicator value. This workflow is identical in structure across all indicators in the environmental risk framework, with only the stressor dataset and the pixel-level calculation varying by dimension. Which SPAM production systems are included in each calculation depends on the nature of the stressor and is specified under the relevant dimension section.

5.2.1 Dataset Selection Criteria

Selecting appropriate datasets for each indicator requires navigating a large and heterogeneous landscape of available geospatial products, which differ substantially in their resolution, temporal coverage, methodological foundations, and accessibility. To ensure that selection decisions are transparent and consistent across the full indicator set, an explicit two-tier framework was applied. This structure follows the variable selection principles outlined in *Section 2.4.3.1*, where selection should be guided first by a theoretical framework and then by data quality and usability (Freudenberg, 2003; European Commission et al., 2008). The first tier defines the minimum criteria that a dataset must satisfy to be considered at all. The second tier defines the criteria used to evaluate and compare datasets that meet the tier one requirements, guiding the final selection where multiple candidates are available.

A dataset was considered eligible only if it met three minimum conditions. It had to provide spatially continuous, raster-based data with coverage across Sub-Saharan Africa, as the entire analytical approach depends on pixel-level overlay with SPAM 2020, so point observations or country-level aggregates cannot serve this purpose. It had to be supported by a documented methodology and a citable source, whether a peer-reviewed publication or an authoritative institutional report, so that the indicator it underpins can be properly grounded in the academic literature. It also had to be freely and openly accessible without licensing restrictions that would limit reproducibility or future use by WFP or other humanitarian actors.[1]

Among datasets meeting these conditions, selection was guided by a further set of criteria weighted according to their relevance to the study context. Spatial resolution was considered relative to the ten kilometre resolution of SPAM 2020, as a substantially finer dataset adds no meaningful analytical gain when the underlying crop distribution is only known at that finer scale, while a substantially coarser dataset may obscure important spatial variation. The credibility and track record of the publishing institution was taken into account, with preference given to datasets produced by established research organisations or within frameworks that have been independently validated and widely cited. As noted in *Section 2.4.3.1*, the quality of the underlying data directly affects the quality of the final model (European Commission et al., 2008), making source credibility a meaningful selection criterion. Temporal alignment with the SPAM 2020 reference period around 2020 was considered, as datasets with outdated baselines or limited historical coverage reduce the internal consistency of the tool. Whether a dataset is actively maintained and will continue to be updated was also weighed, since a tool intended for repeated use by WFP should not depend on static products that cannot reflect changing conditions over time. Native availability within Google Earth Engine was treated as a meaningful advantage rather than a purely practical convenience, as it eliminates preprocessing steps, reduces the risk of data handling errors, and ensures that the full analytical pipeline remains reproducible within a single platform. Finally, where a dataset could plausibly serve more than one indicator dimension, this cross-indicator utility was considered a positive factor, as reducing the number of

[1] The managed water supply indicators are an exception, as water stress is physically determined at the catchment scale and is therefore assessed at sub-basin level rather than as a continuous raster. See *Section 5.2.2.2*.

distinct data sources improves the overall coherence of the tool.

The dataset selection criteria applied in the environmental risk assessment are summarised in Table 5.1. Not all criteria carried equal weight in every selection decision, and in some cases a clear advantage on one dimension was sufficient to outweigh limitations on others. This reflects the inherent trade-offs in indicator development described in *Section 2.4.3.4*, where conceptually stronger variables may be harder to measure consistently, and practically available ones may only partially capture the intended concept (Freudenberg, 2003; European Commission et al., 2008). Where trade-offs were made, these are documented in the relevant indicator sections that follow.

Table 5.1: Dataset selection criteria for the environmental risk assessment.

Tier	Criterion	Purpose
Minimum (Tier 1)	Spatial raster coverage across Sub-Saharan Africa	Enables pixel-level overlay analysis
	Documented methodology and source	Ensures transparency and traceability
	Open accessibility	Supports reproducibility and future use
Comparative (Tier 2)	Spatial resolution	Matches SPAM 2020 scale
	Publishing institution credibility	Ensures reliability
	Temporal alignment	Improves consistency with SPAM 2020
	Active maintenance	Supports long-term usability
	Availability in Google Earth Engine	Improves reproducibility and reduces pre-processing
	Cross-indicator utility	Improves coherence across indicators
Trade-offs	Context-dependent weighting	Different criteria prioritised depending on indicator needs

5.2.2 Environmental Risk Dimensions

This section documents the dataset selection and indicator construction for each environmental risk dimension. For each dimension, the candidate datasets identified were evaluated against the two-tier criteria established in *Section 5.2.1.* Table 5.2 provides a structured overview of all datasets considered, their status as chosen, rejected, or excluded, and their performance against both the minimum and comparative criteria. For each dimension, the subsequent subsections document the full indicator construction, including methodological decisions, formula derivation, and known limitations. Dimensions for which no eligible dataset could be identified are also discussed.

Table 5.2: Dataset selection summary for the environmental risk assessment.

Dimension	**Indicator**	**Dataset**	**Status**	**Tier 1**			**Tier 2**				
				Raster/ SSA	Documented	Open Access	GEE Native	Resolution	Temporal	Credibility	Maintained
Temperature	Heat stress	ERA5-Land (Muñoz Sabater, 2019)	**Chosen**	✓	✓	✓	✓	✓	✓	✓	✓
		GSHTD (Yao et al., 2023)	Rejected	✓	✓	✓	×	✓	×	—	×
Water	Flooding	JRC Flood Hazard v2.1 (Baugh et al., 2024)	**Chosen**	✓	✓	✓	✓	✓	✓	✓	—
		WRI Aqueduct Floods v2 (Ward et al., 2020)	Rejected	✓	✓	✓	✓	—	—	✓	—
	Drought	SPEIbase v2.10 (Beguería et al., 2024)	**Chosen**	✓	✓	✓	✓	—	✓	✓	✓
	Precip. variability	CHIRPS (Funk et al., 2015)	**Chosen**	✓	✓	✓	✓	✓	✓	✓	✓
		ERA5-Land (Muñoz Sabater, 2019)	Rejected	✓	✓	✓	✓	✓	✓	✓	✓
	Baseline water stress	Aqueduct 4.0 (Kuzma et al., 2023)	**Chosen**	✓	✓	✓	✓	—	—	✓	✓
	Interannual variability	Aqueduct 4.0 (Kuzma et al., 2023)	**Chosen**	✓	✓	✓	✓	—	—	✓	✓
Soil	Erosion	GloSEM 1.3 (Borrelli et al., 2021)	**Chosen**	✓	✓	✓	×	✓	✓	✓	—

Continued on next page

Table 5.2 continued from previous page

Dimension	**Indicator**	**Dataset**	**Status**	**Tier 1**			**Tier 2**				
				Raster/ SSA	Documented	Open Access	GEE Native	Resolution	Temporal	Credibility	Maintained
	Soil organic carbon	OpenLandMap SOC (Hengl et al., 2017)	**Chosen**	✓	✓	✓	✓	✓	—	✓	—
		iSDAsoil (Miller et al., 2021)	Rejected	✓	✓	✓	✓	✓	—	✓	—
Excluded	Chemical soil degradation	Hengl nutrient maps (Hengl et al., 2017)	Excluded	✓	✓	✓	—	—	—	—	—
		FAOSTAT (Ludemann et al., 2024)	Excluded	×	✓	✓	—	—	—	—	—
	Air quality	Sentinel-5P TROPOMI (ESA, n.d.)	Excluded	✓	✓	✓	✓	✓	—	✓	✓
	Light	ERA5-Land radiation (Muñoz Sabater, 2019)	Excluded	✓	✓	✓	✓	✓	✓	✓	✓
	Biotic stressors	No eligible dataset	Excluded	×	—	—	—	—	—	—	—

✓ = criterion met; × = not met; — = not applicable or partial. **Bold** = selected for final indicator set.

5.2.2.1 Temperature

Temperature affects nearly every stage of crop development and can expose crops to both heat and cold stress (FAO, n.d.). In Sub-Saharan Africa, however, elevated temperatures constitute the dominant temperature-related risk (Intergovernmental Panel On Climate Change, 2022). While cold stress exceptions exist in highland areas, these fall outside the core sourcing geography of this study. Including a cold stress indicator would therefore add limited analytical value relative to the other dimensions of the framework, and the decision was therefore made to focus the indicator on heat stress only.

The challenge of operationalising heat stress as an indicator lies in the complexity of how crops respond to temperature. Thresholds are not uniform across crops or growth stages, and the consequences of exceeding them differ substantially depending on when in the growing season heat events occur. Accurately capturing this stage-specific complexity would require integrating crop calendar data to identify the phenological windows during which heat events occur and weighting those events accordingly. While this approach would produce a more agronomically precise indicator, it was not implemented in the current version of the tool because it would substantially increase the methodological and implementation complexity of each indicator.

The decision was therefore made to use a simplified but transparent approach, defining the indicator as the proportion of days in a year on which daily maximum temperature exceeds a crop-specific heat stress threshold T_c. This annual fraction is then averaged across the 30 years of the WMO 1991–2020 reference period, as established in *Section 5.1.3*. Since air temperature at a given location does not differ between irrigated and rainfed fields, heat stress affects all crops regardless of production system. The indicator is therefore computed for the all-technology SPAM 2020 layer. For a single year within the reference period, the annual heat stress fraction at pixel i is expressed as:

$$f_{y,i,c,k} = \frac{1}{D_y} \sum_{d=1}^{D_y} \mathbf{1}(T_{\max,\,d,i} > T_c) \tag{5.3}$$

where $f_{y,i,c,k}$ is the fraction of heat stress days at pixel i in year y for crop c in country k. D_y is the number of days in year y (365 for regular years, 366 for leap years), $T_{\max,\,d,i}$ is the daily maximum temperature on day d, T_c is the crop-specific heat stress threshold in degrees Celsius for crop c, and $\mathbf{1}(\cdot)$ is an indicator function equal to 1 when the threshold is exceeded and 0 otherwise. The pixel-level indicator is then the mean of this fraction across all 30 years:

$$T_{i,c,k} = \frac{1}{Y} \sum_{y=1}^{Y} f_{y,i,c,k} \tag{5.4}$$

where $T_{i,c,k}$ is the heat stress score at pixel i for crop c in country k, and $Y = 30$ years. The final indicator $T_{c,k}$ for crop c in country k is obtained by aggregating pixel-level scores using the production-weighted mean described in Equation 5.2. This produces a value between zero and one that represents the proportion of the calendar year during which temperatures exceed the crop-specific heat tolerance threshold, and it is directly comparable across all country-crop combinations regardless of their differing absolute thresholds.

With this indicator defined, the selection of an appropriate dataset centred on the requirement for a global daily maximum air temperature product covering at minimum the full 1991–2020 reference period and available at a spatial resolution consistent with SPAM 2020.

The dataset selected is ERA5-Land Daily Aggregates, produced by the European Centre for Medium-Range Weather Forecasts. It satisfies all three tier 1 criteria, providing spatially continuous raster coverage across Sub-Saharan Africa, a thoroughly documented and extensively validated methodology, and free and open accessibility (Muñoz Sabater, 2019). ERA5-Land derives temperature through a physics-based atmospheric model, is continuously updated from 1950 to the present, and is available natively in Google Earth Engine. Its spatial resolution of approximately 11 km is effectively equivalent to the 10 km scale of SPAM 2020, meaning no resampling is required and a finer product would not improve the spatial accuracy of the analysis.

The main alternative considered was the Global Seamless High-resolution Temperature Dataset (GSHTD) developed by Yao et al. (2023). Despite its finer 1 km resolution, GSHTD is reconstructed through machine learning rather than physical modelling, and Sub-Saharan Africa's sparse station network limits the accuracy of that reconstruction regardless of the resolution (Gosset et al., 2023). The dataset's temporal coverage is limited to 2001–2020 and the dataset will not be updated, which prevents use of the full reference period. In addition, because it is a community-contributed asset rather than a native Google Earth Engine dataset, it requires additional processing steps for implementation.

A key limitation of the heat stress indicator is the use of a single temperature threshold per crop applied uniformly across the entire year. This ignores the fact that crop sensitivity to heat varies across growth stages, with flowering and grain filling being particularly vulnerable periods where even short heat exposure can cause major yield losses. This simplification can lead to bias in both directions. It may underestimate risk when heat events occur during sensitive reproductive stages, and overestimate risk when heat occurs outside the active growing period. This limitation is a direct consequence of excluding crop calendar data from the current implementation. Applying growing-season normalisation, potentially combined with stage-specific weighting of heat exposure, is identified as the most important improvement for future development of the temperature dimension of the tool.

5.2.2.2 Water

Water-related stressors are a major source of agricultural risk in Sub-Saharan Africa, but the mechanisms through which they affect production differ fundamentally between rainfed and irrigated systems. In rainfed systems, which account for the large majority of production across the region, risk arises from rainfall deficits, irregular seasonal distribution and year-to-year variability. In irrigated systems, risk is rooted in competition for and structural instability of managed water sources. Water can also threaten production through excess, where flooding constitutes a distinct hazard that operates independently of the production system.

The water risk dimension is therefore structured into three parts. Flooding is treated first as a physical inundation hazard that affects all production systems regardless of irrigation regime. The following two subsections then address rainfed and irrigated systems separately, each with indicators suited to the specific mechanisms through which water constrains production in those systems.

To support interpretation of the water risk indicators, the rainfed and irrigated shares of total harvested area are computed for each country-crop combination. Since the rainfall-driven and managed water supply indicators are designed for their respective production systems, knowing what proportion of production falls under each system allows the user to judge the relative weight of the two subsections when assessing overall water-related sourcing risk.

Flooding

River flooding poses a direct threat to crop production through inundation, soil compaction and damage to root systems. Flooding operates independently of how the crop is supplied with water, and both irrigated and rainfed fields are equally exposed when rivers rise above their banks. The flooding indicator is therefore computed for the all-technology SPAM 2020 layer.

River flooding is typically characterised in terms of return periods, which describe the average number of years between flood events of a given magnitude (Winsemius et al., 2013). A 1-in-10 year flood carries a 10 percent annual exceedance probability, while a 1-in-500 year flood carries a probability of 0.2 percent.

The methodological challenge was to translate information across multiple return periods into a single comparable measure of flood risk exposure. To address this, the logic of the expected annual damage approach commonly used in global flood risk assessment was adapted (Winsemius et al., 2013). All available return periods were integrated using probability weights based on their annual likelihood of occurrence. These probabilities are mutually exclusive and sum to the total annual flood probability across all return periods. The resulting measure represents the expected annual probability that a pixel falls within a flood inundation zone.

The dataset selected is the JRC Global River Flood Hazard Maps Version 2.1, produced by the European Commission Joint Research Centre as part of the Copernicus Emergency Management Service (Baugh et al., 2024). It satisfies all three tier 1 criteria: spatially continuous raster coverage across Sub-Saharan Africa, a thoroughly documented and peer-reviewed methodology and free accessibility without licensing restrictions. It is a native Google Earth Engine asset, provides water depth in metres for seven return periods at 90 metre resolution, and was published in 2024. The dataset has a native resolution of 90 metres, which is considerably finer than the approximately 10 km SPAM 2020 grid. Before overlaying it with the SPAM crop mask, the flood exposure values are aggregated to the SPAM scale by taking the mean of all 90 metre pixels within each SPAM cell.

The only alternative identified was the WRI Aqueduct Floods Hazard Maps Version 2. Both datasets provide flood inundation depth across multiple return periods and are available as native Google Earth Engine assets. JRC was preferred because it uses a more rigorous model to simulate how water moves across the landscape, which is expected to produce more reliable estimates of which areas are genuinely flood-prone. Aqueduct relies on a simplified approach that its producers acknowledge is not suitable for detailed flood inundation mapping (Ward et al., 2020). The main advantage of Aqueduct that JRC cannot offer is future flood projections under different climate scenarios up to 2080. This forward-looking dimension is not captured in the current version of the tool and is identified as a relevant direction for future development.

The indicator is constructed in two steps. Each return period depth band is first binarised to a flood exposure indicator:

$$F_{i,j} = \mathbf{1}\big(depth_{i,j} > 0\big) \tag{5.5}$$

where $F_{i,j}$ equals 1 if pixel i falls within the flood inundation extent for return period j and 0 otherwise. The pixel-level flood hazard score is then computed as:

$$F_{i,c,k} = \sum_{j=1}^{n} (p_j - p_{j+1}) \cdot F_{i,j} \tag{5.6}$$

where $F_{i,c,k}$ is the expected annual flood exposure score for pixel i, $n = 7$ is the number of return periods, $p_j = 1/T_j$ is the annual exceedance probability for return period T_j, $p_{n+1} = 0$ by convention, and $F_{i,j} \in \{0, 1\}$ is an indicator equal to 1 if pixel i falls within the flood inundation extent for return period j and 0 otherwise. The return periods used are $T = \{10, 20, 50, 75, 100, 200, 500\}$ years, corresponding to annual exceedance probabilities of 0.100, 0.050, 0.020, 0.013, 0.010, 0.005, and 0.002. The final indicator $F_{c,k}$ for crop c in country k is obtained by aggregating pixel-level scores using the production-weighted mean from Equation 5.2 for the all-technology SPAM 2020 layer.

The indicator has three main limitations. First, the JRC dataset only covers rivers draining catchments larger than 500 km^2, meaning smaller rivers and flash flooding are not captured. Second, aggregation to the 10 km SPAM grid smooths flood exposure within pixels, potentially underestimating risk for crops concentrated in low-lying areas. Third, all crops are treated as equally vulnerable despite evidence that flood sensitivity varies substantially across species. The literature shows that rice is uniquely tolerant, while most cereals and pulses are considerably more sensitive (Miro & Ismail, 2013). While globally consistent crop-specific tolerance data are not available, a simple three-level sensitivity classification, (low, moderate and high), would be a practical and meaningful improvement.

Rainfall-Driven Risks

For rainfed production systems, water availability is determined by precipitation rather than managed withdrawal. Risk therefore arises from rainfall deficits, irregular distribution and structural unreliability across seasons and years. Two indicators address these mechanisms. Drought captures cumulative moisture deficits relative to the local historical norm, while the precipitation coefficient of variation captures the structural reliability of rainfall as an agricultural input from year to year. Both indicators are restricted to the rainfed SPAM 2020 production system, consistent with their dependency on precipitation rather than managed withdrawal.

Drought

Several standardised drought indices exist in the literature and the first decision concerned which of these to adopt. The Standardised Precipitation Index (SPI) is widely applied but relies on precipitation data alone, meaning it cannot detect moisture stress driven by elevated evapotranspiration under warming conditions. The Standardised Precipitation-Evapotranspiration Index (SPEI), introduced by Vicente-Serrano et al. (2010), extends SPI by incorporating the climatic water balance as precipitation minus potential evapotranspiration, making it sensitive to both reduced rainfall and increased atmospheric demand. Given that Sub-Saharan Africa is projected to experience sustained temperature increases alongside variable precipitation, SPEI was selected as the more appropriate index for this application.

SPEI is a standardised variable with a mean of zero and a standard deviation of one (Vicente-Serrano et al., 2010). Positive values indicate wetter-than-average conditions, while negative values indicate drier-than-average conditions relative to the local historical average. Standard classification defines values between 0 and -0.99 as near normal, -1.0 to -1.49 as moderate drought, -1.5 to -1.99 as severe drought, and -2.0 and below as extreme drought. Because SPEI is calibrated against each location's historical climate distribution, values can be compared directly across different climate zones.

The second methodological decision concerned the choice of accumulation window. The SPEIbase dataset provides pre-calculated SPEI values for timescales ranging from 1 to 48 months. Longer accumulation windows capture multi-season hydrological drought but are less responsive to the shorter-term moisture deficits that directly affect rainfed crop growth. Shorter windows reflect sub-seasonal soil moisture conditions, but these can be highly variable and more difficult to interpret in agricultural terms. A three-month accumulation window (SPEI-3) was therefore selected because it is widely used to represent agricultural drought and captures seasonal moisture conditions relevant to crop development (Vicente-Serrano et al., 2010). Each monthly SPEI-3 value represents the standardised climatic water balance over the preceding three months, with one value calculated for each calendar month.

The third methodological decision concerned how to convert SPEI-3 into a single indicator score. The decision was made to use drought frequency, defined as the proportion of months during the reference period in which SPEI-3 falls below -1.0. The -1.0 threshold marks the standard classification boundary for moderate drought. The indicator captures how often a sourcing region experiences drought conditions and produces a comparable value between zero and one across all country-crop combinations. Mean SPEI was rejected because the index is standardised around a long-term mean of zero, which makes it unsuitable for distinguishing drought-prone from drought-resilient regions.

The analysis uses the WMO 1991–2020 climatological reference period established in *Section 5.1.3*, covering 360 months. This period aligns with the SPAM 2020 reference year, supporting temporal consistency across the framework. The indicator is therefore defined as:

$$DR_{i,c,k} = \frac{1}{M} \sum_{m=1}^{M} \mathbf{1}(SPEI3_{m,i} < -1) \tag{5.7}$$

where $DR_{i,c,k}$ is the drought indicator score at pixel i for crop c in country k, $M = 360$ is the total number of months in the reference period, m denotes an individual month, $SPEI3_{m,i}$ is the three-month SPEI value at pixel i in month m, and $\mathbf{1}(\cdot)$ is an indicator function equal to 1 when the condition is met and 0 otherwise. The equation is applied at pixel level across all rainfed pixels in the SPAM 2020 crop mask, and the final country-crop score is derived using the production-weighted mean from Equation 5.2.

The dataset used is the SPEIbase Version 2.10, which is the official global SPEI database produced and maintained by the Spanish National Research Council, the same institution that developed the index (Beguería et al., 2024). As the primary global source of pre-calculated SPEI data and the only SPEI product available natively in Google Earth Engine, it is the most practical dataset for this indicator. It meets all three tier 1 criteria, providing spatially continuous raster coverage across Sub-Saharan Africa, a thoroughly documented and peer-reviewed methodology, and free and open accessibility under a CC-BY 4.0 licence.

The indicator has three main limitations. First, the approximately 55 km spatial resolution does not capture sub-national variation in drought exposure. Second, the analysis is based on annual monthly drought frequency rather than crop-specific growing seasons. As a result, drought conditions outside periods of active crop growth still contribute to the indicator score. Third, the indicator does not incorporate crop-specific drought sensitivity thresholds. All rainfed crops are treated as equally exposed once the SPEI threshold of -1.0 is exceeded, despite substantial differences in drought tolerance across crops. Incorporating crop-specific sensitivity adjustments is therefore identified as a key area for future refinement.

Precipitation Variability

Precipitation variability is identified as one of the dominant threats to rainfed crop production (Intergovernmental Panel On Climate Change, 2022). Although the drought indicator captures moisture deficits relative to the local historical norm, it does not characterise whether precipitation is structurally reliable as an agricultural input from year to year. This is the analytical gap a dedicated precipitation indicator addresses.

The central methodological decision concerned how to measure rainfall reliability in a way that is comparable across regions with fundamentally different precipitation levels. The coefficient of variation (CV) of annual precipitation was selected, defined as the ratio of the standard deviation to the mean of annual totals over the reference period. By expressing variability relative to the mean, CV produces a dimensionless measure that is directly comparable across all country-crop combinations regardless of baseline rainfall levels. Higher CV values indicate less reliable rainfall as an agricultural input. This approach is consistent with the FAO ClimAfrica Climatic Stress Index, which identifies interannual rainfall variability as a primary indicator of climatic stress in African rainfed agriculture (FAO, 2017).

A dry spell frequency indicator, capturing the share of growing seasons containing a consecutive sequence of dry days exceeding a critical threshold, would more directly capture the intra-seasonal rainfall patterns most relevant to crop stress. However, it requires crop-specific growing season calendars to define the period during which dry spells actually threaten crop development. CV was therefore adopted as a practical and well-established alternative that captures the same underlying dimension of rainfall unreliability at the inter-annual rather than intra-seasonal scale.

The WMO 1991–2020 climatological reference period established in *Section 5.1.3* is adopted, covering 30 annual precipitation observations. For each pixel, daily precipitation values are first summed within each calendar year to produce one annual total per year, resulting in 30 annual values across the reference period. The indicator is then computed across these 30 values at pixel level:

$$PV_i = \frac{\sigma_i}{\mu_i} \tag{5.8}$$

where σ_i is the standard deviation and μ_i is the mean of the 30 annual precipitation totals at pixel i. The final indicator $PV_{c,k}$ for crop c in country k is obtained by aggregating pixel-level scores using the production-weighted mean from Equation 5.2, applied across the rainfed SPAM 2020 production system.

Operationalising this indicator requires a dataset providing daily precipitation at a spatial resolution covering the full 1991–2020 reference period. The dataset selected is the Climate Hazards Group InfraRed Precipitation with Station data (CHIRPS), available natively in Google Earth Engine. It meets all three tier 1 criteria, providing spatially continuous raster coverage across Sub-Saharan Africa, a thoroughly documented and peer-reviewed methodology and free and open accessibility (Funk et al., 2015). CHIRPS combines satellite-derived infrared estimates with ground station records at approximately 0.05 degree resolution, corresponding to roughly 5.5 km. As its resolution is finer than SPAM's approximately 10 km grid, resampling to the SPAM scale via mean aggregation is needed prior to indicator computation.

The ERA5-Land dataset was considered for cross-indicator consistency with the temperature indicator, but was set aside because reanalysis products derive precipitation through atmospheric modelling rather than direct observation. This is known to produce less accurate estimates for the short, intense convective rainfall events. The decision was therefore made to prioritise accuracy over cross-indicator consistency, and CHIRPS was selected.

The primary limitation of this indicator is that CV captures how much total annual rainfall varies from year to year but does not reflect how rainfall is distributed within a single growing season. As discussed in *Section 5.2.2.2*, rainfall timing and distribution within the growing season is of equal agronomic importance. Even in years with adequate total precipitation, crops may experience severe yield losses if rainfall does not align with critical growth stages. Incorporating an intra-seasonal dimension alongside the existing inter-annual indicator would therefore provide a more complete characterisation of precipitation risk for rainfed production, and operationalising this would require crop-specific growing season calendars. This is identified as the most important direction for future development of this indicator.

Managed Water Supply Risks

For irrigated production systems, water-related risk depends largely on the condition and reliability of the hydrological systems that serve as sources of irrigation water. Two indicators are operationalised to characterise these conditions across the irrigated SPAM 2020 production system. Baseline Water Stress captures the structural level of competition for available water resources, while Interannual Variability of Water Supply captures the year-to-year reliability of that supply. Together these describe both whether a sourcing region's water resources are already under pressure and whether that pressure is consistent or subject to large fluctuations between years.

Because both indicators are derived from Aqueduct 4.0, which operates at the level of hydrological sub-basins rather than as a continuous raster surface, the overlay procedure differs from all other indicators in this section. This is described in detail under each indicator below.

Baseline Water Stress

Baseline water stress measures the ratio of total water withdrawals to available renewable water within a hydrological sub-basin. It captures the degree to which water resources in a sourcing region are already committed to competing uses, leaving less available for agricultural withdrawal. For irrigated crop production, a high score indicates that production is drawing from a system under structural pressure, where any reduction in supply or increase in demand has limited capacity to be absorbed. The indicator is computed across the irrigated SPAM 2020 production system only.

Aqueduct 4.0 is the established global standard for sub-basin level water risk assessment, produced by the World Resources Institute in collaboration with Utrecht University (Kuzma et al., 2023). It is one of the most widely used and respected water risk frameworks in environmental and supply chain risk literature. The dataset is built on the PCR-GLOBWB 2 global hydrological model, freely accessible and available natively in Google Earth Engine. No alternative dataset of comparable methodological rigour and institutional credibility was identified.

The central methodological decision concerned which of Aqueduct's available expressions of water stress to adopt. The dataset provides both a raw stress ratio and a normalised score, which converts the raw ratio into a 0 to 5 scale using classification thresholds derived from the water stress literature (Kuzma et al., 2023). The normalised score was adopted because it maps directly onto the qualitative risk categories of low, low-medium, medium-high, high, and extremely high, making results interpretable for decision-makers without a hydrological background.

The baseline water stress score reflects Aqueduct 4.0's embedded 1979–2019 reference period, which is a fixed property of the published dataset and not modifiable. Although this does not align exactly with the WMO 1991–2020 baseline used for the other indicators, the discrepancy is considered acceptable, as the 40-year Aqueduct baseline exceeds the minimum 30-year robustness threshold established in *Section 5.1.3*.

The dataset operates at the level of hydrological sub-basin polygons rather than as a continuous raster, with a median sub-basin area of approximately 5,300 km^2. This is the appropriate spatial unit for water stress assessment, since water resources are shared and distributed across entire catchments rather than at individual pixel locations.

Each irrigated SPAM 2020 pixel is assigned the water stress score of the sub-basin it falls within, extracted from the bws_score field of the Aqueduct 4.0 baseline annual asset, after which the production-weighted mean from Equation 5.2 is applied to derive the final indicator $BWS_{c,k}$ for crop c in country k.

The indicator characterises water availability conditions at the hydrological source level rather than the crop level. Crops differ in their irrigation water requirements and sensitivity to supply shortfalls, meaning that the same stress level carries different implications depending on the crop. Incorporating crop-specific water demand data is identified as a direction for future refinement.

Interannual Variability of Water Supply

Interannual variability of water supply measures the year-to-year fluctuation in available renewable water within a hydrological sub-basin. Whereas Baseline Water Stress captures the structural level of competition for water resources, this indicator captures the reliability of water availability over time. A sourcing region may therefore exhibit moderate average water stress while still exposing irrigation-dependent production systems to substantial risk if water availability fluctuates strongly between years. Together, the two indicators provide a more complete characterisation of managed water supply risk than either alone. The indicator is operationalised across the irrigated SPAM 2020 production system only.

Aqueduct 4.0 provides a pre-calculated interannual variability indicator expressed as the coefficient of variation of available blue water, which directly operationalises this dimension without requiring additional data sources. The coefficient of variation was preferred over an absolute standard deviation because it expresses variability relative to the mean, making values comparable across sub-basins with fundamentally different absolute water volumes.

The normalised score is used rather than the raw value for the same reasons of interpretability and consistency established for baseline water stress. The same Aqueduct 4.0 asset is used, operating at HydroBASINS level 6 sub-basin resolution with the embedded 1979 to 2019 reference period.

Each irrigated SPAM 2020 pixel is assigned the interannual variability score of the sub-basin it falls within, extracted from the `iav_score` field of the same asset, after which the production-weighted mean from Equation 5.2 is applied to derive the final indicator $IAV_{c,k}$ for crop c in country k.

5.2.2.3 Soil

As established in *Section 2.5.3*, degradation is commonly expressed through physical, chemical and biological changes in soil properties (Weil & Brady, 2017). Physical degradation includes erosion and structural decline, chemical degradation includes salinity and nutrient depletion, and biological degradation is primarily characterised by declines in soil organic carbon (FAO, 2015).

Two indicators are operationalised here, one for physical degradation through erosion and one for biological degradation through soil organic carbon. Chemical degradation, particularly nutrient depletion, represents a major challenge for crop production in Sub-Saharan Africa.

Spatially explicit nutrient status data at sufficient resolution exists through the Hengl et al. (2017) soil nutrient maps, and country-level nutrient balance data is available through FAOSTAT (Ludemann et al., 2024).

However, static nutrient maps do not distinguish between soils that are inherently depleted and those maintained through fertiliser inputs, while country-level data masks important variation within countries. Chemical degradation is therefore not operationalised in the current version of the tool.

Erosion

Because erosion is a physical process driven by rainfall, slope, and land cover rather than by the crop's water supply regime, it affects all production systems. The indicator is therefore computed for the all-technology SPAM 2020 layer.

The established approach for quantifying water erosion at spatial scale is the Revised Universal Soil Loss Equation (RUSLE), which models mean annual soil loss as a function of rainfall erosivity, soil erodibility, slope, cover management and conservation practices. Identifying a dataset implementing RUSLE consistently across Sub-Saharan Africa and satisfying the tier 1 criteria therefore simultaneously determined both the modelling framework and the indicator.

GloSEM 1.3, developed by the Joint Research Centre under the Global Soil Erosion Modelling initiative, was selected as the most methodologically rigorous and widely cited global RUSLE implementation available (Borrelli et al., 2021). No alternative global product of comparable methodological rigour was identified. Unlike the climatological indicators in this chapter, soil erosion is represented as a static structural baseline rather than a multi-year average. No temporal reference period is therefore applied.

The dataset provides spatially continuous raster coverage across Sub-Saharan Africa at approximately 100 m resolution, a thoroughly documented and peer-reviewed methodology, and free accessibility upon registration without licensing restrictions (Borrelli et al., 2021). GloSEM 1.3 is not natively available in Google Earth Engine and is therefore uploaded as a user asset prior to analysis. Its 2019 baseline year is consistent with the SPAM 2020 reference frame, and the dataset is resampled to the SPAM 2020 grid via mean aggregation prior to overlay.

The mean annual soil loss rate is extracted directly from each pixel of the GloSEM 1.3 baseline 2019 raster, expressed in t / ha / yr. The final indicator $ERO_{c,k}$ for crop c and country k is obtained by aggregating pixel-level scores using the production-weighted mean from Equation 5.2. To support interpretation, the resulting indicator $ERO_{c,k}$ is read against the soil-loss tolerance threshold introduced in *Section 2.5.3.1.* Three tolerance bands are applied. Erosion rate below 5 t / ha / yr is considered low and fully tolerable, a rate between 5 and 12 t / ha / yr is considered medium, remaining tolerable for productivity but exceeding ecologically sustainable levels, and a rate above 12 t / ha / yr is considered high and places long-term productivity at clear risk. These bands provide a literature-based reference for judging whether a given country-crop result represents a material erosion concern, alongside the relative comparison against the African mean. It should be noted that soil-loss tolerance values were originally developed for temperate soils in the United States (Montgomery, 2007), and their applicability to the tropical soils of Sub-Saharan Africa is therefore an acknowledged limitation of this interpretation.

The primary limitations are that GloSEM 1.3 represents a static 2019 baseline and does not capture temporal trends in erosion intensity. In addition, the model represents water erosion only and does not capture other forms of physical degradation. These limitations are identified as priorities for future inclusion as appropriate spatial datasets become available.

Soil Organic Carbon

Soil organic carbon is a fundamental determinant of soil biological health. As with erosion, this is a static structural indicator and no temporal reference period is applied. The indicator is computed for the all-technology SPAM 2020 layer.

The central methodological decision concerned whether to measure SOC status or SOC change. A change indicator would more directly capture active degradation, which is ultimately what matters for long-term supply continuity. However, as established in *Section 2.5.3*, SOC stocks equilibrate over 20 years which limits the detection of change over short observation windows. SOC status over the standard 0 to 30 cm topsoil profile was therefore chosen, following the assessment depth established in *Section 2.5.3.*

The dataset selected is the OpenLandMap Soil Organic Carbon dataset, available natively in Google Earth Engine. It meets all three tier 1 criteria, providing spatially continuous raster coverage across Sub-Saharan Africa, a thoroughly documented and peer-reviewed methodology, and free and open accessibility (Hengl et al., 2017). It provides SOC content in g/kg at 250 m resolution across six standard depths from 0 to 200 cm. Pixel values are stored in units of 5 g/kg, such that each raw pixel value must be multiplied by five to obtain the actual SOC concentration in g/kg.

The dataset is compiled from global soil observations spanning 1950 to 2018. This creates a minor temporal gap relative to the SPAM 2020 reference frame but is considered acceptable given the slow dynamics of SOC change. The iSDAsoil dataset was considered as an Africa-specific alternative at 30 m resolution but was set aside in favour of methodological consistency with the global scope of the framework and confirmed native Google Earth Engine availability (Miller et al., 2021). Prior to overlay with the SPAM crop mask, the dataset is resampled to the SPAM 2020 grid via mean aggregation.

The indicator is expressed as a depth-weighted mean across the 0 to 30 cm profile:

$$SOC_i = 5 \cdot \frac{SOC_{0,i} \cdot 5 + SOC_{10,i} \cdot 10 + SOC_{30,i} \cdot 15}{30} \tag{5.9}$$

where $SOC_{0,i}$, $SOC_{10,i}$ and $SOC_{30,i}$ are the SOC values in units of 5 g/kg at depths 0, 10, and 30 cm at pixel i, and the coefficients 5, 10 and 15 represent the thickness in centimetres of the corresponding depth layers (0–5, 5–15 and 15–30 cm). The final indicator $SOC_{c,k}$ for crop c and country k is obtained by aggregating pixel-level scores using the production-weighted mean from Equation 5.2.

To support interpretation, the resulting indicator $SOC_{c,k}$ is read against the critical threshold introduced in *Section 2.5.3.1.* A widely applied reference level of 20 g/kg distinguishes soils that are functioning adequately from those entering a degradation risk zone (Loveland, 2003): values above this level indicate adequate soil function, whereas values below it place the soil in a risk zone. This provides a literature-based benchmark for judging soil health in absolute terms, complementing the relative comparison against the African mean. Because this is a single global value, and because critical SOC levels vary with soil texture and climate, its application to the contrasting soils of Sub-Saharan Africa is an acknowledged limitation.

Soil organic carbon also differs from every other environmental risk indicator in its direction of harm. For all other indicators a higher value reflects a more adverse condition, whereas for soil organic carbon a higher value reflects healthier soil and therefore lower risk. To preserve a consistent interpretation across the framework, in which a value above the reference benchmark always denotes worse-than-average conditions, the soil organic carbon ratio to the African reference mean defined in *Section 5.1.4* is inverted. After inversion, a normalised value above 1.0 indicates lower-than-average soil organic carbon, and therefore worse-than-average soil health, in line with all other indicators.

No crop-specific adjustment is incorporated, meaning all crops are treated as equally sensitive to SOC decline despite meaningful differences in dependence on soil organic matter across species. In addition, SOC levels are strongly influenced by soil texture, meaning absolute SOC values are not directly comparable across contrasting soil types.

5.2.2.4 Air and Light

Both air quality and light availability were evaluated for inclusion in the tool. For each dimension, datasets that would meet the tier 1 eligibility criteria set out in *Section 5.2.1* are technically accessible. The decision not to include either dimension therefore rests on considerations of regional relevance and indicator interpretability rather than data unavailability, and is documented below.

Regarding light, solar radiation products covering Sub-Saharan Africa are available within Google Earth Engine, including ERA5-Land derived radiation variables. However, as discussed in *Section 2.5.3.1*, light deficit is rarely a limiting factor for crop production in Sub-Saharan Africa given the region's high baseline solar radiation. Excessive radiation, in turn, causes significant crop damage primarily when it coincides with drought or cold stress rather than acting as an independent stressor. A standalone radiation indicator would therefore not reliably reflect light-driven crop risk in the regional context of this study. Since the conditions under which excessive light becomes damaging are already partly captured by the water and temperature dimensions, including a light indicator would risk overstating light as an independent hazard. Light was therefore excluded.

Regarding air quality, tropospheric ozone is the dominant crop-relevant pollutant and is accessible through Sentinel-5P TROPOMI, which is available natively in Google Earth Engine and maintained by the European Space Agency. Despite meeting the tier 1 criteria and several tier 2 criteria, two substantive issues argue against inclusion. First, tropospheric ozone concentrations in Sub-Saharan Africa's agricultural areas are comparatively low relative to South and East Asia, Europe and North America, limiting the practical risk signal the indicator would provide in the regional context. Second, as noted in *Section 2.5.3.1*, the effects of ozone on crops are not uniformly negative. At moderate exposure levels, ozone can activate cross-protection mechanisms that partially reduce damage. Without crop-specific and context-specific thresholds, the directional interpretation of an ozone-based indicator would be ambiguous. Air quality was therefore also excluded.

The exclusion of both dimensions does not imply that light and air are irrelevant to crop risk in the region. As discussed in *Section 2.5.3.3*, their effects are most consequential when they coincide with water deficit or heat stress, conditions that are captured through the existing dimensions of the tool. The combined risk profile produced by the tool therefore implicitly reflects the environmental conditions under which light and air stress are most likely to contribute to crop damage.

5.2.2.5 Biotic Stressors

The theoretical background establishes that biotic stressors include insects and pests, diseases and pathogens, and weeds. None of these dimensions were included in the final framework, as no identified dataset fulfilled the tier 1 requirements. More specifically, no openly accessible, spatially continuous raster dataset was found that covers Sub-Saharan Africa and represents biotic stress pressure in a way that is suitable for the framework. Their exclusion should not be understood as meaning that biotic stressors are not relevant. Including biotic stressors should be treated as a next development step if suitable crop-specific and spatially explicit datasets become available.

5.2.2.6 Synthesis of Limitations and Future Refinements

The limitations identified throughout *Section 5.2* are important not only for interpreting the results, but also for understanding how the framework can be improved in future work. The main limitations concern spatial resolution, crop-specific sensitivity, temporal alignment and data availability. First, spatial resolution is often coarser than the variation it is intended to capture, which can smooth exposure within the SPAM grid. Second, several indicators apply uniform crop sensitivity because crop-specific thresholds are not available in the underlying literature. Third, the climatological indicators are computed over the calendar year rather than the crop-specific growing season. Fourth, two dimensions, chemical soil degradation and biotic stressors, could not be operationalised because no openly accessible dataset met the tier-one requirements. To provide a clear overview, the limitations for each dimension and the corresponding opportunities for future refinement are summarised in Table 5.3.

Table 5.3: Limitations and future refinements of the environmental sourcing risk dimensions.

Dimension	**Indicator**	**Limitation**	**Future refinements**
Temperature	Heat stress	Crop-level threshold applied uniformly across the whole year, ignores stage-specific sensitivity. Can both under- and overestimate risk.	Apply growing-season normalisation, with stage-specific weighting of heat exposure.
Water	Flooding	Dataset only covers rivers draining catchments > 500 km^2, missing smaller rivers and flash flooding. Aggregation to the 10 km SPAM grid smooths exposure and may underestimate risk for crops in low-lying areas. All crops treated as equally vulnerable.	Crop sensitivity classification would be a practical improvement. Adding forward-looking flood projections under climate scenarios (e.g. WRI Aqueduct projections up to 2080)
	Drought	$\sim$55 km resolution misses sub-national variation. Annual monthly drought frequency rather than crop growing season. No crop-specific drought sensitivity thresholds, all rainfed crops treated as equally exposed once SPEI < -1.0.	Incorporating crop-specific sensitivity adjustments is identified as a key area for future refinement.
	Precipitation Variability	Captures inter-annual variation in total annual rainfall but not intra-seasonal distribution, crops can fail even in adequate-total years if rain misses critical growth stages.	Add an intra-seasonal dimension (e.g. dry-spell frequency) alongside the inter-annual indicator, requires crop-specific growing season calendars.

Continued on next page

Table 5.3 continued from previous page

Dimension	Indicator	Limitation	Future refinements
Water	Baseline Water Stress	Characterises water availability at hydrological catchment level rather than at crop level, the same stress level has different implications by crop. Aqueduct's 1979–2019 reference period also does not exactly align with the tool's WMO 1991–2020 baseline.	Incorporating crop-specific water demand data.
Soil	Chemical Soil Degradation	Not operationalised as static nutrient maps do not distinguish inherently depleted soils from fertiliser-maintained ones; country-level FAOSTAT masks within-country variation.	Include once spatially explicit data distinguishing depletion from fertilised maintenance becomes available.
	Erosion	Static 2019 baseline, no temporal trends. Captures only water erosion, not other forms of physical degradation.	These limitations are flagged as priorities for future inclusion as appropriate spatial datasets become available.
	Soil Organic Carbon	All crops treated equally sensitive. SOC is strongly influenced by soil texture, so absolute values are not directly comparable across contrasting soil types. Measures status rather than change.	Crop-specific sensitivity adjustment. SOC-change indicator if observation windows are long enough to overcome the ∼20-year equilibration.
Biotic stress		Excluded entirely as no openly accessible, spatially continuous raster dataset covering Sub-Saharan Africa met tier-1 requirements.	Include if suitable crop-specific, spatially explicit datasets become available.

5.3 Development of the Environmental Impact Assessment

Chapter 4 established that the environmental impact assessment should be structured around expressing each ecological consequence as an impact intensity per tonne of crop produced. The underlying logic follows a supply chain in reverse. WFP's procurement volume represents a share of a country's total harvested production of a given crop, and the environmental impact generated across that national production system is allocated to WFP's sourcing according to this share. Expressing impact per tonne is therefore not an arbitrary normalisation but a direct link between a procurement decision and the physical production system that generated the impact.

This structure produces a general scaling formula that applies across all environmental impact dimensions:

$$W_{c,k} = I_{c,k} \cdot Q_{c,k} \tag{5.10}$$

where $W_{c,k}$ is the total sourcing-attributed environmental impact for crop c in country k, $I_{c,k}$ is the impact intensity per tonne for that indicator, and $Q_{c,k}$ is WFP's intended procurement volume in tonnes.

Each indicator in the following sections defines its specific $I_{c,k}$. Where an underlying dataset already provides pre-calculated per-tonne intensities derived from its own SPAM-based production attribution, these are used directly as $I_{c,k}$, since they embed the exact spatial allocation logic of that dataset. Where a dataset provides total national impact only, $I_{c,k}$ is derived as:

$$I_{c,k} = \frac{M_{c,k}}{P_{c,k}} \tag{5.11}$$

where $M_{c,k}$ is the total national impact for crop c in country k expressed in the indicator-specific unit, and $P_{c,k}$ is the national crop production volume in tonnes from FAOSTAT, with the reference year matched to the SPAM version used by the underlying dataset. Since SPAM is calibrated to FAOSTAT national production statistics for its reference year, this ensures the denominator is consistent with the production concept embedded in each dataset's spatial attribution. Which approach applies to each indicator is documented in the relevant subsection below.

5.3.1 Dataset Selection Criteria

To ensure that selection decisions are transparent and consistent across the full indicator set, a two-tier framework similar to the one presented in *Section 5.2.1* is used here, with adaptations that reflect the structural requirements of the environmental impact assessment. The first tier defines the minimum criteria that a dataset must satisfy to be considered at all. The second tier defines the criteria used to evaluate and compare datasets that meet the tier one requirements, guiding the final selection where multiple candidates are available.

A dataset is considered eligible only if it meets four minimum criteria. First, it has to provide a conceptually valid and representative measure of the environmental impact dimension. Second, the environmental impact estimation must be able to support the country-crop level, either by providing country-crop impact data directly or by offering spatially continuous raster coverage impact data across Sub-Saharan Africa that could be combined with SPAM 2020. Consistent with *Section 5.2.1*, all datasets also had to be methodologically documented, citable and freely and openly accessible without licensing restrictions.

Among datasets meeting these conditions, selection was guided by a further set of comparative criteria. Preference was given to established datasets that already provide crop- and country-specific impact intensities, expressed as impact per tonne of production. Since WFP's sourcing impact is estimated by multiplying impact intensity by procurement volume, this format can be used directly in the assessment and requires the fewest additional assumptions. Where such datasets were not available, datasets providing total environmental impact by crop and country were also considered, provided that they could be converted into an impact intensity using consistent production data. If neither form was available, spatially explicit impact datasets were considered. In line with *Section 5.2.1*, these datasets were further evaluated based on temporal alignment with the SPAM 2020 reference period, spatial resolution relative to SPAM 2020 and native availability in Google Earth Engine.

Newer datasets were preferred over older ones, as more recent data better reflects current agricultural and environmental conditions. Consistently updated datasets were preferred over static products, since a tool intended for repeated use by WFP should be able to reflect changing conditions over time rather than depending on a fixed historical snapshot. The credibility and track record of the publishing institution was taken into account, with preference for datasets produced by established research organisations or within frameworks that have been independently validated and widely cited.

The dataset selection criteria applied in the environmental impact assessment are summarised in Table 5.4. The criteria were not weighted equally in every selection decision. In some cases, a strong advantage in one criterion outweighed limitations in another. Any such trade-offs are documented in the relevant indicator sections below.

Table 5.4: Dataset selection criteria for the environmental impact assessment.

Tier	Criterion	Purpose
Minimum (Tier 1)	Conceptually valid and representative measure of the environmental impact dimension	Ensures representative measurement of environmental impact
	Country-crop level impact data, or raster coverage across Sub-Saharan Africa compatible with SPAM 2020	Enables country-crop impact estimation
	Documented methodology and citable source	Ensures transparency and traceability
	Open accessibility	Supports reproducibility and future use
Comparative (Tier 2)	Direct impact-per-tonne format	Reduces additional assumptions and allows direct scaling by procurement volume
	Publishing institution credibility	Ensures reliability
	Recency and active maintenance	Supports accuracy and long-term usability
	Availability in Google Earth Engine	Improves reproducibility and reduces preprocessing
	Spatial resolution	Matches SPAM 2020 scale
	Temporal alignment	Improves consistency with SPAM 2020
Trade-offs	Context-dependent weighting	Different criteria prioritised depending on indicator needs

5.3.2 Environmental Impact Dimensions

This section documents the dataset selection and indicator construction for each environmental impact dimension. For each dimension, the candidate datasets identified were evaluated against the two-tier criteria established in *Section 5.3.1.* Table 5.5 provides a structured overview of all datasets considered, their status as chosen, rejected, or excluded, and their performance against both the minimum and comparative criteria. The subsections that follow document the full indicator construction for each dimension, including methodological decisions, derivation of impact intensities, and known limitations.

Table 5.5: Dataset selection summary for the environmental impact assessment.

Dimension	**Indicator**	**Dataset**	**Status**	**Tier 1**				**Tier 2**			
				Valid	Country-Crop	Open Access	Documented	Per Tonne	Credibility	Recency	Maintenance
GHG	GHG intensity	Cao et al. (2025)	**Chosen**	✓	✓	✓	✓	✓	✓	✓	×
		Carlson et al. (2017)	Rejected	✓	✓	✓	✓	×	✓	×	×
		FAO (2025)	Rejected	✓	×	✓	✓	×	✓	✓	✓
Deforestation	Agricultural forest loss	Hansen et al. (2013) + Sims et al. (2025)	**Chosen**	✓	✓	✓	✓	✓	✓	✓	—
		FAO Global Forest Resources Assessment	Rejected	×	×	✓	×	×	✓	✓	✓
Biodiversity	Biodiversity intactness loss	Nguyen et al. (2025)	**Chosen**	✓	✓	✓	✓	✓	✓	✓	×
		Beyer & Manica (2021)	Rejected	✓	✓	✓	✓	✓	✓	×	×
Water use	Absolute blue water footprint	Pfister & Bayer (2025)	**Chosen**	✓	✓	✓	✓	✓	✓	×	×
		Mekonnen & Hoekstra (2011)	Rejected	✓	✓	✓	✓	✓	✓	×	×

Continued on next page

Table 5.5 continued from previous page

Dimension	**Indicator**	**Dataset**	**Status**	**Tier 1**				**Tier 2**			
				Valid	Country-Crop	Open Access	Documented	Per Tonne	Credibility	Recency	Maintenance
	Scarcity-adjusted blue water footprint	Pfister (2021) + Boulay et al. (2019)	**Chosen**	✓	✓	✓	✓	✓	✓	×	×
Excluded	Water quality	Mekonnen & Hoekstra (2011)	Excluded	×	✓	✓	✓	✓	✓	×	×
	Pesticide use	FAO (n.d.)	Excluded	✓	×	✓	✓	×	✓	✓	✓

✓ = criterion met; × = not met; — = not applicable or partial. **Bold** = selected for final indicator set.

5.3.2.1 Greenhouse Gas Emissions

Greenhouse gas emissions from crop production are expressed in carbon dioxide equivalents, a standard metric that translates the warming effect of different gases into a common unit based on their 100-year global warming potential as defined by the IPCC (Intergovernmental Panel On Climate Change (Ipcc), 2023). This is the established basis for national emission inventories, international climate agreements and sector-level reporting, and it allows direct comparison of emission intensities across country-crop combinations and over time. Expressed per tonne of crop produced, it directly implements the impact intensity logic of *Section 4.2.1* and can be scaled by WFP's procurement volume to estimate the total climate cost of a specific sourcing decision.

The first decision addressed which dataset to use as the source of cropland GHG emission estimates. The selected dataset is the spatially explicit global cropland greenhouse gas emission dataset developed by Cao et al. (2026), published in Nature Climate Change and openly available through figshare. It provides emission estimates for 46 crop classes at five arc minute resolution for the reference year 2020, integrating synthetic fertiliser, manure, crop residues, rice cultivation, in-field burning, urea application and drained peatlands as emission sources (Cao et al., 2026). All gases are converted to CO_2 equivalents using IPCC AR6 global warming potential values. Against the tier one criteria of *Section 5.3.1*, the dataset satisfies all four minimum conditions. It provides a representative measure of the environmental impact dimension, supports country-crop level estimation, it is supported by a peer-reviewed article with methodology and it is freely and openly accessible, distributed under a CC BY 4.0 licence. Against the tier two criteria, its decisive strength is methodological alignment with the impact intensity logic. The dataset does not provide emission intensities in a direct per-tonne format as a primary output, but it does provide country-level and crop-specific summary tables containing both total emissions and production volumes derived from SPAM 2020, from which the per-tonne intensity can be derived by simple division. Institutional credibility is high, given the authors' affiliations with established institutions such as Cornell University, Colorado State University and the International Food Policy Research Institute.

Published in 2026 with a 2020 reference year, the dataset represents the most temporally current globally consistent cropland emission product identified in this study and provides an updated alternative to the earlier Carlson et al. (2017) dataset, which was based on data from around 2000. Given that cropland area in Sub-Saharan Africa expanded by 62 percent and global synthetic nitrogen fertiliser use increased by 37 percent between 2000 and 2020 (Cao et al., 2026), the older dataset no longer reflects current production conditions and was set aside based on the tier two criterion of temporal alignment. FAOSTAT greenhouse gas emission (FAO, 2025) data were also considered, but were excluded based on the tier one requirements because they do not disaggregate emissions by crop type at the country level and therefore cannot provide the crop-specific impact intensity required by the framework.

Greenhouse gas emissions are calculated using the Cao et al. (2026) dataset. The specific file used from this dataset is `Summary_cropland_emissions_country_crop_source_CO2e_kg_CO2e_20250825`, which provides country-crop level cropland emissions disaggregated by emission source. For each country-crop combination, total greenhouse gas emissions $E_{c,k}$ are calculated by summing all relevant emission-source columns in the file. The file provides both IPCC 2006 and IPCC 2019 estimates for several emission sources, but only the 2019 columns are used to avoid double-counting alternative methodological estimates. The summed emissions are divided by the total crop production volume $P_{c,k}$ in the column `crop_production_tons` from the same file, using the formula established in Equation 5.11. The indicator is defined as:

$$GHG_{c,k} = \frac{E_{c,k}}{P_{c,k}} \tag{5.12}$$

where $GHG_{c,k}$ is the greenhouse gas emission intensity in kg CO_2 equivalents per tonne for crop c in country k, $E_{c,k}$ is the total cropland emission summed across all sources from the Cao et al. (2026) summary table, and $P_{c,k}$ is the total production volume in tonnes drawn from the same dataset and consistent with FAOSTAT national totals.

The indicator has two main limitations. First, not all greenhouse gas emissions related to crop sourcing are currently included. The dataset is limited to field-level agricultural emissions directly linked to crop cultivation. It does not include emissions embedded in the production of inputs such as pesticides, fertilisers or machinery, nor does it include land-use change emissions. The results should therefore be interpreted as cultivation-level GHG emissions rather than a full life-cycle estimate. A further temporal limitation is that the dataset is centred on 2020. It aligns well with SPAM 2020, which supports consistency across the tool, but it remains a static snapshot. It does not capture trends over time or emission changes caused by management shifts after 2020. Future updates depend on whether Cao et al. (2026) release later versions of the dataset.

5.3.2.2 Deforestation and Land-use Change

Measuring a crop's contribution to deforestation requires both a spatial measure of where forest has been lost and an attribution of which human activities caused that loss. No single dataset that provides both was identified, so three datasets were combined to address this.

The first decision concerned how to measure forest loss. Total tree cover loss derived from the Global Forest Change product (Hansen et al., 2013) was the most straightforward candidate, providing annual detection of stand-replacement disturbance at thirty metre resolution. However, it registers all causes of disturbance together and cannot isolate agricultural clearing from fire, logging or disease. Country-level statistics from the FAO Global Forest Resources Assessment were also considered but set aside because they rely on national self-reporting with known cross-country inconsistencies and cannot be made spatially explicit. The GFC product was therefore retained solely as the loss detection layer, to be combined with a driver attribution layer.

The second decision concerned driver attribution. The WRI and Google DeepMind Global Drivers of Forest Loss dataset (Sims et al., 2025) is the only globally consistent, spatially explicit product that classifies the dominant driver of tree cover loss at one kilometre resolution. It covers the period 2001 to 2022 and distinguishes seven driver categories, of which permanent agriculture is the relevant one. Combining the GFC loss layer with this attribution layer isolates the area of forest lost specifically to permanent agricultural expansion. Both datasets satisfy all tier one criteria from *Section 5.3.1*, including being licensed under a CC BY 4.0 licence.

Making the indicator crop-specific requires a third layer. The SPAM 2020 crop mask, described in *Section 5.1.2*, restricts the analysis to the landscape where a specific crop is produced, following the same spatial overlay logic used in the environmental risk assessment. The SPAM mask is used here as a spatial filter only, not as a production weight, since the purpose is to measure the total area of deforestation associated with the crop's landscape rather than to attribute it to individual pixels proportionally.

An important conceptual trade-off follows from this combination. The Drivers dataset classifies the dominant driver per one kilometre cell over the full period, not per individual crop. A cell classified as permanent agriculture within the maize footprint may have been cleared for a different crop entirely. The indicator is therefore framed as a landscape intensity metric rather than a causal attribution, measuring how many hectares of permanent agricultural forest conversion are associated with producing one tonne of the crop in that landscape.

The indicator is expressed as impact intensity per tonne of production, consistent with the approach established in *Section 5.3*:

$$DF_{c,k} = \frac{A_{c,k}}{P_{c,k}} \tag{5.13}$$

where $DF_{c,k}$ is deforestation intensity in hectares of permanent agricultural forest loss per tonne of production, $A_{c,k}$ is the cumulative area of such loss within the SPAM footprint of crop c in country k over the 2001 to 2022 period, and $P_{c,k}$ is cumulative FAOSTAT production of crop c in country k over the same period. The GFC loss layer is resampled from thirty metres to one kilometre using a non-zero reducer before intersection with the Drivers layer and the SPAM crop mask.

Using cumulative production over the full 2001 to 2022 window as the denominator, rather than a single reference year, is essential for the intensity interpretation to be meaningful. The numerator $A_{c,k}$ accumulates deforestation over 22 years, so dividing it by a single year of production would produce an intensity value that is incomparable across countries with different production levels and trends, and would inflate the result by a factor of approximately 22. Matching the time window of numerator and denominator produces a stable, comparable intensity that reflects the average deforestation pressure associated with producing one tonne of the crop over the observed period.

The main limitations are that approximately 47% of GFC loss pixels lack driver classification and are excluded from the calculation, making $A_{c,k}$ a lower bound on agricultural deforestation within the crop footprint. The Drivers dataset represents the dominant driver as a static classification over the full period and does not capture changes in the primary cause of forest loss over time. The SPAM crop mask applied retrospectively assumes a broadly stable spatial distribution of production across the 2001 to 2022 window, which is an acknowledged simplification given the substantial agricultural expansion in Sub-Saharan Africa during this period. Overlapping crop footprints mean the same loss pixel may be attributed to more than one crop within a country.

5.3.2.3 Biodiversity Loss

There is no single universally adopted standard metric for biodiversity loss (United Nations Office for Disaster Risk Reduction, 2016). Several complementary indicators exist, such as species richness loss, threatened species richness, range rarity, and biodiversity intactness, each capturing different aspects of ecosystem degradation. The absence of a dominant standard therefore makes the metric choice inseparable from the dataset choice.

Quantifying biodiversity loss required identifying a dataset that could link biodiversity degradation to specific crops and countries. The selected dataset is the biodiversity intactness footprint dataset developed by Nguyen et al. (2025). It provides annual estimates of biodiversity loss footprints attributed to 154 crop items across 193 countries and territories, covering the period 2000 to 2020. The dataset was selected because it already provides a crop- and country-specific biodiversity loss footprint in km^2, making it directly usable in the tool. By dividing this footprint by the corresponding production volume, it can be converted into an impact intensity per tonne and scaled by procurement volume. The metric used in the dataset is the Biodiversity Intactness Index (BII), which estimates the average abundance of originally present species relative to an undisturbed reference baseline. A BII value of one represents fully intact biodiversity and values below one indicate a proportional reduction in species abundance. Biodiversity intactness loss is defined as one minus BII, and the corresponding footprint is expressed as the approximate area in square kilometres that experienced BII loss, calculated by multiplying the loss value by the pixel area. The indicator should be interpreted as an area-equivalent measure of biodiversity loss, rather than actual physical land conversion, allowing biodiversity pressure to be compared across country-crop combinations and over time.

Against the tier one criteria of *Section 5.3.1*, the dataset satisfies all four minimum conditions. It provides representative country-crop level impact estimates, supported by a peer-reviewed article with a fully documented methodology. It is openly accessible under the licence Creative Commons CC BY-NC-SA 4.0. Against the tier two criteria, a central methodological alignment advantage is that Nguyen et al. (2025) internally uses SPAM 2020 as the basis for crop distribution, meaning the crop allocation underpinning the footprint estimates is consistent with the production system reference used throughout this tool. The institutional basis is strong as the dataset is produced by researchers at Charles University's Environment Centre. Published in 2025 with a reference year of 2020, it represents the most temporally current globally consistent crop biodiversity footprint product identified in this study.

Another dataset was identified, evaluated and set aside. The biodiversity footprint dataset developed by Beyer & Manica (2021) provides country-crop estimates for 175 crops based on three biodiversity measures, species richness, threatened species richness, and range rarity. This dataset satisfies tier one on all four criteria, since it provides country-crop level data, has a documented and citable methodology, and is openly accessible under a CC BY 4.0 licence without restrictions. Against the tier two criteria, the main weakness is temporal alignment. The dataset is based on agricultural area distributions from 2000, making it poorly aligned with the SPAM 2020 reference year used in the tool. Given that Sub-Saharan African cropland expanded by 62% between 2000 and 2020 (Nguyen et al., 2025), the newer Nguyen et al. (2025) dataset was considered more likely to reflect current biodiversity pressures and the second dataset was therefore set aside.

The biodiversity loss intensity can therefore be calculated as:

$$BL_{c,k} = \frac{BF_{c,k}}{P_{c,k}} \tag{5.14}$$

where $BL_{c,k}$ is the biodiversity loss intensity in km^2 area-equivalents per tonne for crop c in country k, $BF_{c,k}$ is the total biodiversity loss in km^2 attributed to that country-crop combination for year 2020 in the Nguyen et al. (2025) dataset, and $P_{c,k}$ is the total production volume in tonnes for the same crop and country, drawn from FAOSTAT. The 2020 layer is used because it is the most recent year available in the dataset and aligns with the SPAM 2020 reference year used throughout this tool.

The selected indicator has two main limitations. First, BII is an aggregated metric and cannot capture all dimensions of biodiversity loss. It does not fully represent the loss of rare or threatened species, functional diversity, or ecosystem services beyond species abundance. The indicator should therefore be interpreted as a comparable measure of biodiversity intactness loss rather than a complete ecological assessment. Second, although the 2020 layer is the most recent available, it represents a static snapshot. In countries where agricultural expansion or land-use change has accelerated after 2020, the indicator may not reflect current biodiversity conditions.

5.3.2.4 Water Use and Quality

As established in *Section 2.5.4.4*, crop production affects water resources through both consumptive water use and water quality degradation. Further, the environmental pressure from water consumption is mainly associated with irrigated production, since irrigation withdraws blue water from rivers, lakes and aquifers and can reduce the volume available to other users and ecosystems. The blue water footprint, expressed in cubic metres of surface and groundwater consumed per tonne of crop produced, is a widely used metric for quantifying this form of consumptive irrigation water use in crop production (Mekonnen & Hoekstra, 2011). Rainfed water use is classified as green water, referring to precipitation consumed through evapotranspiration, and is not included because it does not represent a direct withdrawal from surface or groundwater resources. The water use impact indicators are therefore most relevant for country-crop combinations with a meaningful irrigated share of harvested area. The irrigated share variable computed for the water risk indicators is therefore used as a contextual reference for interpreting how relevant water use impact is for each country-crop combination. Because these per-tonne footprints are constructed over total production, their values are diluted across the full harvest as the irrigated share falls, in contrast to the managed water supply risk indicators, which are weighted over irrigated production only and therefore express a conditional source condition rather than a diluted intensity.

Two indicators are used: the absolute blue water footprint and the scarcity-adjusted blue water footprint. The absolute blue water footprint shows the volume of irrigation water consumed per tonne of crop. Since the environmental significance of this volume depends on local water availability, it should be interpreted together with the baseline water stress indicator. This is because the same volume of blue water consumption represents a greater concern where water resources are already under pressure. The absolute footprint is therefore most useful when assessing the physical water consumption of a specific country-crop combination. The scarcity-adjusted blue water footprint already incorporates local water scarcity by weighting blue water consumption according to the scarcity conditions where the water is used. It is used for comparing water consumption impacts across country-crop combinations, but should not be interpreted as an absolute volume of water consumed. Water quality degradation, through which agricultural inputs such as fertilisers and pesticides enter water bodies and alter their ecological condition, is conceptually relevant but is not operationalised in the current version of the tool for the reasons documented at the end of this section. It is identified as a next step for future refinement of the tool.

Absolute Blue Water Consumption

As established above, water consumption for irrigated crops is measured through blue water footprint, and the dataset selection therefore focused on identifying a source that provides blue water footprint estimates at country-crop level.

The selected dataset is the watershed-level crop water consumption dataset developed by Pfister & Bayer (2025). The dataset provides blue and green water consumption estimates for 160 crops across more than 12,000 watershed units with global coverage split by countries. The native spatial unit is the watershed, and the country-crop estimate is obtained by summing watershed contributions within each country. Against the tier one criteria, the dataset satisfies all four minimum criteria. It provides representative country-crop level impact estimates, the methodology is documented in a peer-reviewed article, and the data is openly accessible under a CC BY 4.0 licence.

Against the tier two criteria, its decisive strength is that it already provides blue water consumption in the direct m^3 per tonne for each crop as a direct output tab in the Excel file. This can be scaled by WFP's procurement volume without additional processing needed. Institutional credibility is supported by the affiliation of Pfister and Bayer with ETH Zurich. A limitation is that the estimates mainly represent crop production and irrigation conditions around the year 2000, making the dataset somewhat outdated relative to current agricultural conditions. Changes in irrigation practices, yields and cropping patterns since then may therefore not be fully reflected.

However, despite this limitation, the dataset was retained because it is still considered to provide a useful indication, provided that its temporal limitations are kept in mind when interpreting the results.

Another alternative dataset was evaluated and set aside. The global crop water footprint dataset developed by Mekonnen & Hoekstra (2011) provides green, blue and grey water footprints for 126 crops. The dataset satisfies all three tier one requirements but does not perform better than Pfister & Bayer (2025) in terms of temporal alignment. However, it was set aside in favour of Pfister & Bayer (2025) because the latter also provides a dataset for the scarcity-adjusted water footprint indicator used in the following section. Using Pfister & Bayer (2025) for both absolute and scarcity-adjusted water use therefore improves methodological consistency within the tool.

The indicator is defined as $BWF_{c,k}$, the blue water consumption in m^3 per tonne for crop c in country k, derived by summing the watershed-level blue water consumption estimates across all watersheds falling within country k for crop c. No additional derivation from FAOSTAT is required, as the per-tonne values are provided directly in the dataset.

Scarcity-Adjusted Blue Water Footprint

The absolute blue water footprint treats all water consumption as equivalent regardless of where it occurs. Using one cubic metre of water has a much greater impact in a water-scarce region than in a region where water is abundant, as established in *Section 2.5.4.4*. The scarcity-adjusted indicator addresses this by weighting consumption against local water availability conditions, producing a result that reflects not just how much water is used, but how much pressure that use places on the local water system relative to a global reference.

The Available Water Remaining (AWARE) methodology was developed under the UNEP-SETAC Life Cycle Initiative as the consensus characterisation model for water scarcity impact assessment in Life Cycle Assessment (LCA) (Boulay et al., 2018). The method quantifies the relative available water remaining per unit area once the demands of humans and aquatic ecosystems have been met, expressed as a characterisation factor (CF) in m^3 world-equivalents per m^3 consumed. A higher CF indicates that consumption occurs in a region where remaining available water is scarce relative to the world average, and thus carries a greater potential to deprive other users of water. Multiplying the blue water footprint by the AWARE characterisation factor for the corresponding country and crop produces a scarcity-weighted impact intensity in m^3 world-eq./ton.

AWARE factors were originally developed at watershed level and monthly scale. However, this level of detail is often difficult to use in practice because matching water consumption data are rarely available. Boulay et al. (2018) therefore also provide country-level factors, but these are less precise and are not recommended by the authors when more specific alternatives are available. For agriculture, the country-level agri factor is better than the generic country factor because it reflects where irrigation takes place. However, it is still a broad estimate and does not capture detailed crop or location-specific differences.

In 2019, Boulay et al. (2019) developed a set of 26 crop-specific AWARE factors for 224 countries by applying a consumption-weighted average approach: local annual AWARE agricultural characterisation factors at watershed scale are weighted by the blue water consumption required to grow each specific crop within each watershed, then aggregated to the country level. This produces a characterisation factor that reflects where a particular crop is actually grown within a country, not simply where water is consumed on average. The present study uses a dataset that implements the Boulay et al. (2019) methodology and provides both the absolute blue water footprint and the AWARE-adjusted value for each country-crop combination in a single product (Pfister, 2021). As the dataset is openly accessible under a CC BY 4.0 licence, it thereby fulfils all four tier one criteria.

The dataset used (Pfister, 2021) provides country-crop total AWARE-weighted water volumes rather than per-unit-of-production values. To derive the scarcity-adjusted blue water footprint in m^3 world-eq. per tonne of crop, the AWARE-weighted water total must be divided by production volume for the corresponding crop and country. Because the underlying model in the Boulay et al. (2019) methodology estimates crop water use based on cropping patterns, irrigation and climate data from 1998–2002, the resulting water consumption estimates reflect conditions from that period rather than today. To keep the calculation consistent, the AWARE-weighted water volumes are therefore matched with FAOSTAT production data averaged over the same period.

The scarcity-adjusted blue water footprint indicator is therefore defined as:

$$ABWF_{c,k} = \frac{AW_{c,k}}{P_{c,k}} \tag{5.15}$$

where $ABWF_{c,k}$ is the scarcity-adjusted blue water footprint in m^3 world-eq./tonne for crop c in country k, $AW_{c,k}$ is the total scarcity-adjusted blue water consumption for crop c in country k, and $P_{c,k}$ is the average total harvested production of crop c in country k in tonnes from FAOSTAT over the period 1998–2002.

Several limitations of the scarcity-adjusted indicator should be noted. First, the crop-specific factors are based on annual AWARE values rather than monthly values. This means that the indicator does not fully capture how water scarcity changes during the year. For example, a crop grown and irrigated during lower-stress months may appear more water-scarce than it actually is. Incorporating monthly water stress and crop-growing periods therefore represents an important next step for further developing the indicator and improving the accuracy of future versions of the tool.

A second limitation is that the underlying data are relatively old. The crop water consumption data used by Boulay et al. (2019) are based on cropping patterns and climate conditions from 1998–2002, while AWARE is based on hydrological data from 1960–2010. Since both crop production patterns and water availability have changed over time, the indicator should be understood as an estimate based on past conditions rather than a fully current representation.

Water Quality

Water quality degradation was identified as a relevant environmental impact pathway of crop production. It can arise from nutrient runoff and fertiliser leaching, particularly nitrogen and phosphorus, as well as from pesticide residues and other pollutants entering water bodies. One established way of representing this impact is the grey water footprint. The grey water footprint of a product refers to the volume of freshwater required to dilute pollutant loads to the point where water quality standards are met (Mekonnen & Hoekstra, 2011).

Among the datasets considered, the nitrogen-based grey water footprint developed by Mekonnen & Hoekstra (2011) was the option that fulfilled the greatest number of tier one criteria. However, it was still not included in the current version of the framework because it does not satisfy the tier one requirement of providing a sufficiently representative measure of the environmental impact dimension. It solely captures nitrogen-related water pollution and does not include phosphorus runoff, pesticide contamination, salinisation or broader aquatic toxicity pathways. As a result, it represents only one component of the broader water quality impact pathway identified in the theoretical background and is therefore not considered comprehensive enough to cover the water quality impact in a representative way. An indicator for water quality is therefore acknowledged as a gap in the current framework. If a dataset becomes available that meets all tier one requirements, it is the next step for expanding the tool's coverage of water quality impacts.

5.3.2.5 Pesticide Use

Pesticide use was not included as a dimension in the final tool because no identified dataset fulfilled the tier one requirements. The most relevant dataset identified was the FAOSTAT Pesticides Use domain (FAO, n.d.), which contains statistics on agricultural pesticide use by country, reported in active ingredients and by major pesticide category. The dataset is maintained by FAO, has global country coverage and is updated annually. However, it is reported at national level only and is not spatially explicit. It therefore does not show where within a country pesticides are used, nor does it attribute pesticide use to the production of specific crops. As stated in tier one requirements, a pesticide dataset would need to be spatially continuous and raster-based in order for it to be possible to combine it with SPAM and translate it into country-crop impact intensities per tonne. Pesticide use was therefore excluded, not because it is environmentally irrelevant, but because the available data did not meet the requirements of the framework. Once suitable country-crop specific use of pesticide data becomes available, pesticide use should be an additional dimension in the tool.

5.3.2.6 Synthesis of Limitations and Future Refinements

The limitations identified throughout *Section 5.3* are important for interpreting the results and for guiding future refinement of the framework. Across the environmental impact dimensions, the main limitations concern temporal alignment and data availability. Most underlying datasets are static products based on fixed reference periods rather than continuously updated data streams. Two dimensions, water quality and pesticide use, could not be operationalised because no dataset meeting the tier-one requirements in *Section 5.3.1* was available at country-crop resolution. To provide a structured overview, all limitations and the corresponding opportunities for future development are summarised in Table 5.6.

Table 5.6: Limitations and future refinements of the environmental impact indicators.

Indicator	Limitation	Future refinements
Greenhouse Gas Emissions	Limited to field-level cultivation emissions — excludes emissions from input production (pesticides, fertilisers, machinery) and land-use change. Static 2020 snapshot, does not capture trends over time or emission changes from management shifts after 2020.	Future updates depend on whether Cao et al. (2026) release later dataset versions.
Deforestation and Land-use Change	Landscape intensity rather than causal attribution. Approximately 47% of GFC loss pixels lack driver classification and are excluded, making $A_{c,k}$ a lower bound. Static dominant-driver classification,does not capture temporal change within the period. SPAM crop mask applied retrospectively assumes broadly stable spatial distribution. Overlapping crop footprints mean the same loss pixel may be attributed to more than one crop.	Finer-resolution driver attribution and crop-expansion-tracked SPAM versions would improve attribution.
Biodiversity Loss	BII is an aggregated abundance metric, does not capture rare or threatened species, functional diversity, or ecosystem services beyond species abundance. Static 2020 snapshot, may not reflect post-2020 changes	Complementary metrics for threatened species, range rarity, and functional diversity. Updated layers post-2020.

Continued on next page

Table 5.6 continued from previous page

Indicator	**Limitation**	**Future refinements**
Absolute Blue Water Consumption	Estimates mainly represent crop production and irrigation conditions around the year 2000. Changes in irrigation practices, yields and cropping patterns since then may not be fully reflected. Constructed over total production and the per-tonne value is therefore diluted by the rainfed share.	Updated water footprint datasets reflecting current irrigation practices, yields and cropping patterns. Report a per-irrigated-tonne value alongside the total-production value so irrigation exposure is expressed consistently across the risk and impact components.
Scarcity-Adjusted Blue Water Footprint	Crop-specific factors based on annual AWARE values rather than monthly values, does not fully capture how water scarcity changes during the year. Underlying data relatively old: crop water consumption based on 1998–2002 conditions; AWARE based on 1960–2010 hydrological data.	Incorporating monthly water stress and crop-growing periods for improving accuracy in future versions of the tool.
Water Quality	Not operationalised. Best candidate covers only nitrogen-related water pollution. Not representative enough to meet tier-1 requirements.	Include once a dataset meeting all tier-1 requirements becomes available.
Pesticide Use	Not operationalised. FAOSTAT Pesticides Use domain is reported at national level only, is not spatially explicit, nor does it attribute pesticide use to the production of specific crops. Not meeting tier-1 requirements.	Should be added as an additional dimension once suitable country-crop-specific spatially explicit pesticide data becomes available.

6 Final Decision Support Tool

This chapter presents the final structure of the decision support tool. It describes the overall framework, the environmental risk assessment component, and the environmental impact assessment component, before illustrating how the outputs are structured and interpreted through an applied example. The chapter concludes by verifying the plausibility of the computed results, evaluating the tool against the design objectives and decision support attributes and reflecting on the methodological trade-offs that shaped it.

Within the research design presented in *Section 3.5*, this chapter represents the fourth and final building component of the Design and Development phase, Output Formalisation (compare with *Figure 3.3*). It consolidates the indicators developed in *Chapter 5* into a coherent final structure and defines how the results are expressed and presented. The position of the chapter within the overall design and development phase is illustrated in *Figure 6.1*.

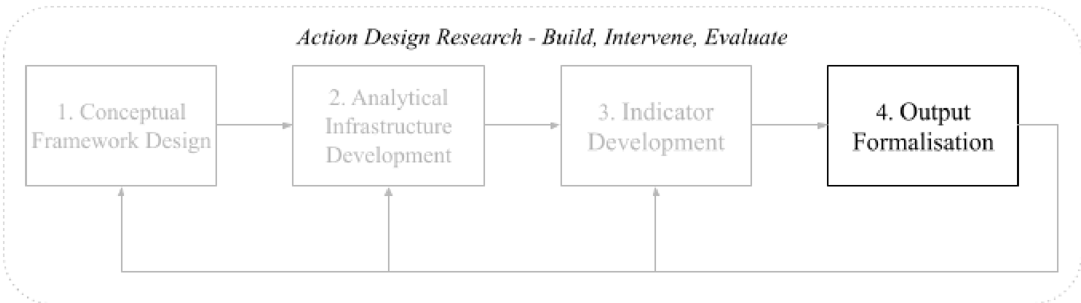

Figure 6.1: Position of *Chapter 6* within the Design and Development phase of the research design as the fourth building component, Output Formalisation.

The tool supports two main use cases. It enables comparative assessment when WFP is considering two or more sourcing options, allowing users to compare environmental sourcing risk and environmental impact across potential sourcing countries. It also supports sourcing profiling when a country-crop combination has already been selected, helping identify which environmental risk and environmental impact dimensions require attention, monitoring or further analysis. The tool should not be interpreted as producing a single recommendation, ranking or optimisation result. Instead, it provides a structured decision support tool that makes environmental trade-offs visible.

The chapter is structured as follows: *Section 6.1* presents the overall structure of the final framework and the complete indicator set. *Section 6.2* defines the general formulas and supporting variables that apply across the tool. *Section 6.3* documents the final environmental risk indicators and *Section 6.4* documents the final environmental impact intensity indicators. *Section 6.5* demonstrates the tool by applying it to maize sourced from Benin and Tanzania, two of WFP's largest current sourcing origins for maize in Sub-Saharan Africa.

6.1 Overview of the Final Framework

The tool is structured around two parallel but non-aggregated components. The environmental risk indicators provide visibility of environmental conditions that may constrain crop production and affect production stability, while the environmental impact indicators show how much environmental pressure is associated with sourcing a certain volume of crop from a specific country. Together they produce a side-by-side profile for each country-crop combination that makes environmental trade-offs visible without aggregating them into a single score.

Each indicator is presented in two forms. The absolute value retains the original unit and meaning of the indicator, allowing the result to be interpreted against any global or agronomic threshold established in the literature. The normalised value expresses the result as a ratio to the African production-weighted mean for the same crop and indicator, placing it in a regional context and showing whether a sourcing option performs above or below the conditions across Sub-Saharan Africa. A normalised value above 1.0 indicates that the sourcing option performs worse than the regional average and a value below 1.0 indicates better than average performance. Where established thresholds exist in the literature, these are applied as a complementary interpretive layer alongside the relative comparison. Table 6.1 presents all indicators included in the final tool across both components.

Table 6.1: Complete indicator set of the final decision support tool.

Component	Dimension	Indicator	Var.	Unit	System	Global threshold
Risk	Temperature	Heat stress	T	Proportion of days exceeding crop threshold $[0, 1]$	All	Crop-specific T_c
	Water	Flooding	F	Expected annual flood exposure $[0, 1]$	All	—
		Drought	DR	Share of months with SPEI-3 < -1.0 $[0, 1]$	Rainfed	SPEI < -1.0 (embedded)
		Precipitation variability	PV	Coefficient of variation of annual precipitation $[-]$	Rainfed	—
		Baseline water stress	BWS	Normalised water stress score $[0, 5]$	Irrigated	Aqueduct Low/Med/High
		Water supply reliability	IAV	Normalised interannual variability score $[0, 5]$	Irrigated	Aqueduct Low/Med/High
	Soil	Erosion	ERO	Mean annual soil loss rate [Mg/ha/yr]	All	5–12 Mg/ha/yr
		Soil organic carbon	SOC	Weighted mean topsoil SOC [g/kg]	All	20 g/kg
Impact	GHG emissions	Greenhouse gas intensity	GHG	kg CO_2e per tonne		
	Deforestation	Agricultural forest loss intensity	DF	Hectares per tonne		
	Biodiversity	Biodiversity intactness loss intensity	BL	km^2 area-equivalents per tonne		
	Water use	Absolute blue water footprint	BWF	m^3 per tonne		
		Scarcity-adjusted blue water footprint	$ABWF$	m^3 world-eq. per tonne		

6.2 General Formulas and Supporting Variables

Table 6.2 presents the general formulas and supporting variables that apply across the tool. Throughout the notation c denotes the crop and k denotes the country.

Table 6.2: General formulas and supporting variables.

Variable	Formula	Note
$I_{c,k}^{\text{risk}}$	$\frac{\sum_{i\in\Omega_{c,k}} w_i X_i}{\sum_{i\in\Omega_{c,k}} w_i}$	Production-weighted aggregation formula for all risk indicators. X_i is the pixel-level value of the stressor variable, w_i is the SPAM 2020 production weight at pixel i, and $\Omega_{c,k}$ is the relevant SPAM mask (all, rainfed or irrigated) for crop c in country k.
$I_{c,k}^{\text{impact}}$	$\frac{M_{c,k}}{P_{c,k}}$	General intensity formula for impact indicators following the production-normalisation approach. $M_{c,k}$ is the total national impact in indicator-specific units. $P_{c,k}$ is total national production.
$IRR_{c,k}$	SPAM 2020 (derived)	Contextual variable: irrigated share of harvested area. Not an indicator. Used to interpret $BWS_{c,k}$, $IAV_{c,k}$, $BWF_{c,k}$ and $ABWF_{c,k}$.
$RF_{c,k}$	$1 - IRR_{c,k}$	Contextual variable: rainfed share of harvested area. Used to interpret $DR_{c,k}$ and $PV_{c,k}$.
$W_{c,k}$	$I_{c,k} \cdot Q_{c,k}$	Total sourcing-attributed impact. $I_{c,k}$ refers to any impact intensity. $Q_{c,k}$ is WFP procurement volume in tonnes.
$\bar{I}_c$	$\frac{\sum_k I_{c,k} P_{c,k}}{\sum_k P_{c,k}}$	Production-weighted African reference mean for crop c. Computed separately for each indicator across all African countries that produce crop c. Presented as a reference column in all output tables to contextualise indicator values relative to the regional norm.

6.3 Environmental Risk Assessment Component

The final environmental risk dimensions included in the tool are summarised in Table 6.3. All environmental risk indicators follow the SPAM-overlay aggregation logic defined in *Section 6.2*, meaning that each environmental stressor is assessed only in the pixels where the crop is produced and weighted by the local production share. The irrigated and rainfed shares are displayed alongside the water-related indicators to support interpretation. $BWS_{c,k}$ and $IAV_{c,k}$ are calculated only over the irrigated production system and their decision relevance therefore scales with $IRR_{c,k}$. $DR_{c,k}$ and $PV_{c,k}$ are calculated only over the rainfed system and their relevance scales with $RF_{c,k}$. Flooding is assessed across both systems and is not interpreted through irrigation dependence.

Table 6.3: Risk indicator overview, including dataset references.

Dimension	Indicator	Variable	What it measures	Unit	Production system	Dataset
Temperature	Heat stress	$T_{c,k}$	Proportion of days per year on which daily maximum temperature exceeds the crop-specific heat stress threshold T_c, averaged over the 1991–2020 reference period.	Proportion of days exceeding T_c $[0, 1]$	Rainfed and irrigated SPAM 2020 systems	ERA5-Land Daily Aggregates (Muñoz Sabater, 2019)
Water	Flooding	$F_{c,k}$	Expected annual probability that a production pixel falls within a river flood inundation zone, integrated across seven return periods (10–500 years) using probability-weighted exceedance logic.	Expected annual flood exposure (prob. weighted) $[0, 1]$	Rainfed and irrigated SPAM 2020 systems	JRC Global River Flood Hazard Maps v2.1 (Baugh et al., 2024)
	Drought	$DR_{c,k}$	Share of months in the 1991–2020 reference period during which SPEI-3 falls below -1.0, the standard threshold for moderate drought. Captures how frequently a production area experiences cumulative moisture deficit relative to its local historical norm.	Share of months $[0, 1]$	Rainfed SPAM 2020 system	SPEIbase v2.10 (Beguería et al., 2024)
	Precipitation variability	$PV_{c,k}$	Coefficient of variation of annual precipitation totals over the 1991–2020 reference period, expressing year-to-year variability relative to the mean. Higher values indicate structurally less reliable rainfall as an agricultural input.	Coefficient of variation $[-]$	Rainfed SPAM 2020 system	CHIRPS (Funk et al., 2015)
	Baseline water stress	$BWS_{c,k}$	Ratio of total water withdrawals to available renewable water within the hydrological sub-basin, expressed as a normalised score on a 0–5 scale. Captures the degree to which water resources are already committed to competing uses.	Normalised score $[0, 5]$	Irrigated SPAM 2020 system only	WRI Aqueduct 4.0 (Kuzma et al., 2023)

Continued on next page

Table 6.3 continued from previous page

Dimension	Indicator	Variable	What it measures	Unit	Production system	Dataset
Water	Water supply reliability	$IAV_{c,k}$	Coefficient of variation of available renewable water supply within the hydrological sub-basin, expressed as a normalised score. Captures year-to-year fluctuation in irrigation water availability, complementing the structural level of stress captured by $BWS_{c,k}$.	Normalised score $[0, 5]$	Irrigated SPAM 2020 system only	WRI Aqueduct 4.0 (Kuzma et al., 2023)
Soil	Erosion	$ERO_{c,k}$	Mean annual soil loss rate within the crop's production footprint. Represents the physical degradation of soil structure through rainfall-driven erosion.	Mg/ha/yr	Rainfed and irrigated SPAM 2020 systems	GloSEM 1.3 (Borrelli et al., 2021)
	Soil organic carbon	$SOC_{c,k}$	Depth-weighted mean soil organic carbon content across the 0–30 cm topsoil profile. Captures the biological health of soils as a structural baseline condition for long-term agricultural productivity.	g/kg	Rainfed and irrigated SPAM 2020 systems	OpenLandMap SOC dataset (Hengl et al., 2017)

6.4 Environmental Impact Assessment Component

The final environmental impact dimensions included in the tool are summarised in Table 6.4. All environmental impact indicators follow the production-normalisation logic established in *Section 5.3*, expressing an environmental impact per tonne of crop produced. This structure allows any indicator to be scaled by WFP's procurement volume $Q_{c,k}$ to estimate the total sourcing-attributed impact $W_{c,k}$ for a specific procurement decision.

As noted in *Section 5.3.2.4* the blue water footprint and the scarcity-adjusted blue water footprint are most decision-relevant for country-crop combinations with a meaningful irrigated share. This follows directly from how the two indicators are constructed. Both express blue water consumption per tonne of total production $P_{c,k}$, yet blue water is consumed only by the irrigated portion of that production. The per-tonne value is therefore diluted across the entire harvest, so that the same physical irrigation intensity produces a lower indicator value as the irrigated share falls. The irrigated share variable $IRR_{c,k}$ is therefore displayed alongside these indicators in the tool output to allow users to contextualise near-zero results without misinterpreting them as indicating no water-related concern. The scarcity-adjusted footprint $ABWF_{c,k}$ is a comparative metric and is best interpreted when two or more sourcing options are assessed side by side. When a single country is profiled, the absolute blue water footprint together with the Baseline Water Stress score from the environmental risk component provides a more directly interpretable absolute result.

Table 6.4: Environmental impact indicator overview, including dataset references.

Dimension	Variable	What it measures	Unit	Dataset
GHG Emissions	$GHG_{c,k}$	Greenhouse gas intensity of producing one tonne of crop c in country k, covering field-level emissions with all gases expressed in CO_2 equivalents using IPCC AR6 GWP values.	kg CO_2e per tonne	(Cao et al., 2025) — Spatially explicit global assessment of cropland greenhouse gas emissions circa 2020
Deforestation	$DF_{c,k}$	Intensity of agriculturally driven forest loss associated with producing one tonne of crop c in country k, measured as cumulative permanent agricultural forest loss within the crop's landscape over 2001-2022 per tonne of cumulative production over the same period.	Hectares of agricultural forest loss per tonne	(Sims et al., 2025) — Global drivers of forest loss at 1km resolution + (Hansen et al., 2013) — WRI/Google DeepMind Global Drivers of Forest Loss dataset
Biodiversity Loss	$BL_{c,k}$	Biodiversity intactness loss footprint associated with producing one tonne of crop c in country k, expressed as an area-equivalent of habitat with reduced species abundance relative to an undisturbed baseline.	km^2 area-equivalents per tonne	(Nguyen et al., 2025) — Land Use, Biodiversity Intactness Index, and Biodiversity Intactness Footprint of Agricultural Production 2000–2020
Blue Water Footprint	$BWF_{c,k}$	Volume of surface and groundwater (blue water) consumed by crop c in country k per tonne of production.	m^3 per tonne	(Pfister & Bayer, 2025) — Water consumption of crop on watershed level
Scarcity-adjusted Blue Water Footprint	$ABWF_{c,k}$	Blue water consumption weighted by local water scarcity, expressing how much pressure water use places on the local water system relative to a global reference. A higher value indicates that consumption occurs where water is scarcer.	m^3 world-eq. per tonne	(Pfister, 2021) — Country-crop specific AWARE water scarcity factors for 160 crops and global coverage

6.5 Demonstration

To demonstrate the framework, it was applied to maize sourced from Benin and Tanzania. Maize is one of WFP's most procured commodities in Sub-Saharan Africa, and Benin and Tanzania represent two of the largest current sourcing origins for maize in the region. The combination allows the full indicator set to be illustrated across two contrasting country contexts, showing how the framework generates structured, interpretable and comparable outputs under realistic procurement conditions.

The results are presented as an environmental sourcing risk profile and an environmental impact profile. Each profile is reported in two complementary forms: a table presenting absolute values, the African production-weighted mean and normalised ratios, and a radar chart following the visualisation format specified in *Section 4.4*. In the radar charts, each axis represents an indicator normalised to the African production-weighted mean. A reference ring is drawn at 1.0, corresponding to the African production-weighted mean for each indicator as defined in *Section 6.2*. A normalised value above 1.0 indicates that the sourcing option performs worse than the regional average and a value below 1.0 indicates better than average performance. Where an established global threshold exists in the literature, values exceeding it are flagged with an asterisk (*).

6.5.1 Environmental Risk Profile

The environmental risk profile for maize sourced from Benin and Tanzania is presented in Table 6.5. The irrigated and rainfed shares are reported in the row block following the indicators to contextualise the water-related results. The results show that maize production in both countries is almost entirely rainfed, with Tanzania showing an irrigated share of 3.58 %, compared with essentially zero in Benin. Both values are well below the African mean for maize of 14.55 %.

Table 6.5: Environmental sourcing risk profile for maize sourced from Benin and Tanzania, with the African production-weighted mean and normalisation ratios.

Dimension	**Indicator**	**Variable**	**Unit**	**Benin**	**Tanzania**	**Africa mean**	**Benin / mean**	**Tanzania / mean**
Temperature	Heat stress	$T_{c,k}$	Proportion of days $[0,1]$	0.000	0.000	8.20×10^{-5}	n/a	n/a
Water	Flooding	$F_{c,k}$	Annual probability $[0,1]$	0.0225	0.0305	0.0399	0.56	0.76
	Drought	$DR_{c,k}$	Share of months$[0,1]$	0.194	0.228	0.206	0.94	1.11
	Precipitation var.	$PV_{c,k}$	—	0.116	0.173	0.138	0.84	1.25
	Baseline water stress	$BWS_{c,k}$	Score $[0,5]$	0.000	1.003	3.880	0.00	0.26
	Water supply reliab.	$IAV_{c,k}$	Score $[0,5]$	0.911	1.996	1.681	0.54	1.19
Soil	Erosion	$ERO_{c,k}$	Mg/ha/yr	12.1*	31.5*	23.4*	0.52	1.35
	Soil organic carbon	$SOC_{c,k}$	g/kg	8.78*	16.14*	13.60*	$1.538^{\dagger}$	$0.840^{\dagger}$
Contextual variables								
	Irrigated share	$IRR_{c,k}$	Proportion	0.00 %	3.58 %	14.55 %		
	Rainfed share	$RF_{c,k}$	Proportion	100.00 %	96.42 %	85.45 %		

Note. An asterisk (*) marks values that exceed (in the harmful direction) a global threshold established in the literature: for $SOC_{c,k}$, the threshold is 20 g/kg, below which soils are considered biologically degraded. For $ERO_{c,k}$ the threshold is 12 Mg/ha/yr, above which long-term productivity is at clear risk. Values marked with a dagger (†) are inverted to maintain a consistent interpretation, so that all values above 1.0 indicate worse-than-average conditions.

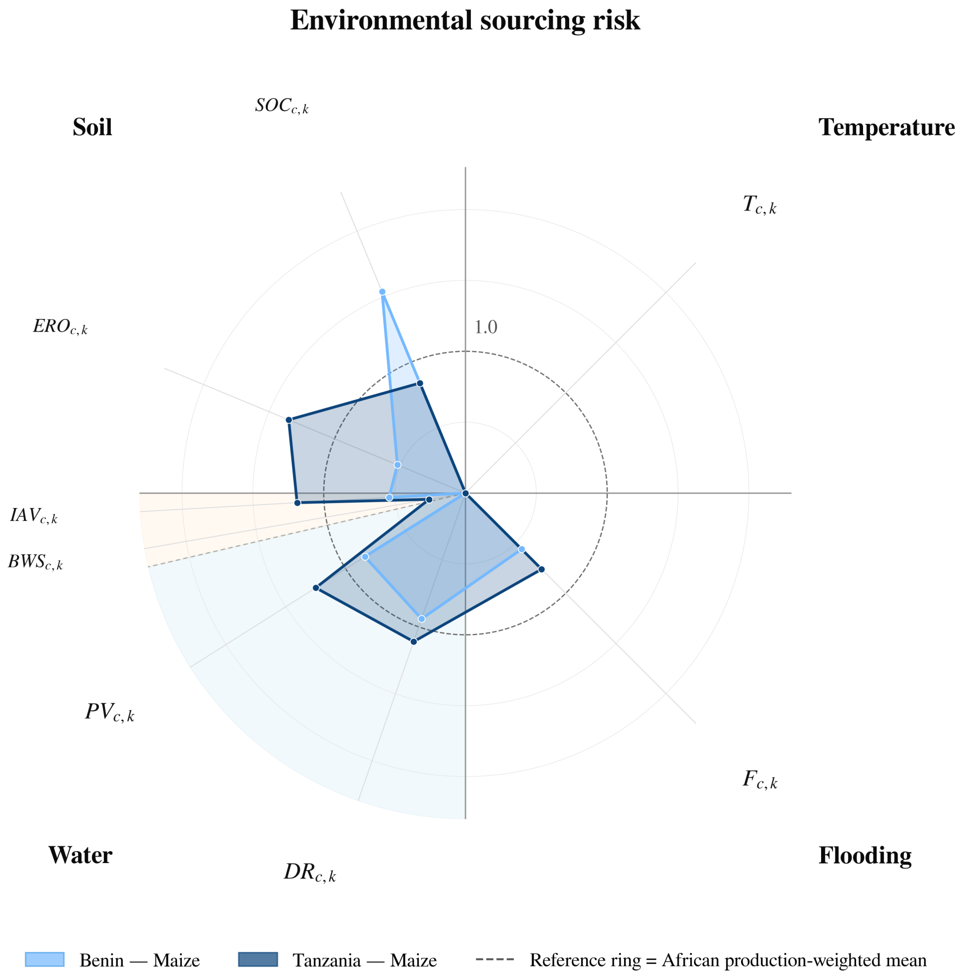

Figure 6.2: Environmental sourcing risk profile for maize sourced from Benin and Tanzania, normalised to the African production-weighted mean. Values outside the reference ring at 1.0 indicate worse-than-average conditions.

The full environmental risk profile is presented as *Figure 6.2* together with Table 6.5. Heat stress presents no measurable risk under current conditions in either country. The proportion of days exceeding the crop-specific threshold is zero in both Benin and Tanzania, against an African mean of essentially zero for maize. Heat stress is therefore not a differentiating dimension in this comparison. Flooding risk is low in absolute terms in both countries, and both sit well below the African mean of 0.040, with Tanzania (ratio 0.76) marginally more exposed than Benin (ratio 0.56).

The drought and precipitation variability indicators reveal a more pronounced contrast. Benin sits below the African mean on both ($DR_{c,k}$ ratio 0.94, $PV_{c,k}$ ratio 0.84), while Tanzania sits above on both (1.11 and 1.25). Because maize is mainly rainfed in both countries, the rainfall-related indicators carry full decision weight here, and Tanzanian maize is more exposed to year-to-year rainfall variability than maize sourced from Benin.

The managed water supply indicators, $BWS_{c,k}$ and $IAV_{c,k}$, are computed only over the irrigated production footprint. Because Benin's irrigated share is essentially zero, both indicators carry limited weight in this scenario. Tanzania, with a 3.58 % irrigated share, shows a $BWS_{c,k}$ score of 1.00 (Low to Medium on the Aqueduct scale) and an $IAV_{c,k}$ score of 2.00 (Medium to High on the Aqueduct scale). The $IAV_{c,k}$ ratio of 1.19 indicates that the limited irrigation that does take place in Tanzania is exposed to above-average interannual variability.

Turning to the soil dimension, both countries show erosion rates that exceed the 12 Mg/ha/yr threshold above which long-term soil productivity is considered at clear risk. Tanzania's rate of 31.5 Mg/ha/yr is particularly severe, placing it 35 % above the African mean of 23.4 Mg/ha/yr and more than two and a half times the tolerable threshold. Benin's rate of 12.1 Mg/ha/yr sits just at the threshold boundary and 48 % below the African mean, indicating meaningfully lower erosion pressure than the regional norm.

For soil organic carbon, the picture is reversed. Benin's value of 8.78 g/kg is well below the 20 g/kg threshold below which soils are considered biologically degraded, and 35 % below the African mean of 13.60 g/kg. Tanzania, at 16.14 g/kg, remains below the threshold but sits 19 % above the African mean. Taken together, the two soil indicators present contrasting risk profiles within the same dimension: Tanzania faces greater physical degradation pressure through erosion, while Benin's soils are more severely depleted in organic matter. In *Figure 6.2*, the $SOC_{c,k}$ axis is reversed relative to all other axes, so that a longer arm indicates lower soil carbon. Benin's arm extending outward therefore reflects worse-than-average soil carbon, while Tanzania's arm extending outward in the erosion axis reflects its higher erosion rate.

6.5.2 Environmental Impact Profile

The environmental impact profile for maize sourced from Benin and Tanzania is presented in Table 6.6.

Table 6.6: Environmental impact profile for maize sourced from Benin and Tanzania.

Dimension	**Variable**	**Unit**	**Benin**	**Tanzania**	**Africa mean**	**Benin / mean**	**Tanzania / mean**
GHG emissions	$GHG_{c,k}$	kg CO_2e per tonne	353.04	252.98	212.76	1.66	1.19
Deforestation	$DF_{c,k}$	ha per tonne	0.02633	0.03250	0.02342	1.12	1.39
Biodiversity loss	$BL_{c,k}$	km^2 area-eq. per tonne	3.81×10^{-4}	7.42×10^{-4}	5.04×10^{-4}	0.76	1.47
Blue water footprint	$BWF_{c,k}$	m^3 per tonne	56.05	70.09	257.84	0.22	0.27
Scarcity-adj. blue water	$ABWF_{c,k}$	m^3 world-eq. per tonne	164.65	827.99	20 522.85	0.01	0.04
Contextual variables							
Irrigated share	$IRR_{c,k}$		0.00 %	3.58 %	14.55 %		
Rainfed share	$RF_{c,k}$		100.00 %	96.42 %	85.45 %		

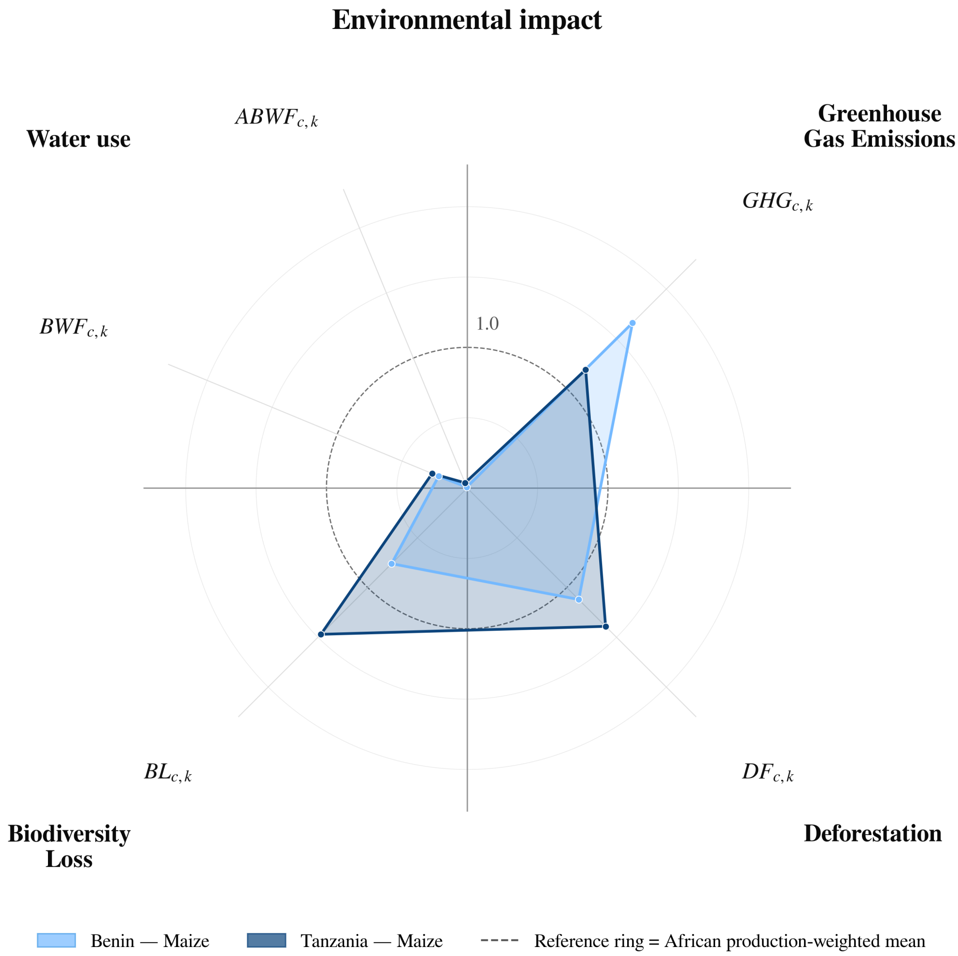

Figure 6.3: Environmental impact profile for maize sourced from Benin and Tanzania, normalised to the African production-weighted mean. Values outside the reference ring at 1.0 indicate worse-than-average impact intensity per tonne of crop produced.

The full environmental impact profile is presented as *Figure 6.3* together with Table 6.6. For greenhouse gas emissions, both countries are above the African production-weighted mean of 213 kg CO_2e per tonne. Benin's intensity of 353 kg CO_2e per tonne corresponds to a ratio of 1.66, placing it 66 % above the regional average, while Tanzania's intensity of 253 kg CO_2e per tonne corresponds to a ratio of 1.19, or 19 % above the mean. Benin's maize is therefore more emissions-intensive than Tanzania's in both absolute and relative terms.

For deforestation, both countries exceed the African production-weighted mean of 0.023 ha per tonne. Tanzania's intensity of 0.033 ha per tonne corresponds to a ratio of 1.39, placing it 39 % above the regional average. Benin's intensity of 0.026 ha per tonne corresponds to a ratio of 1.12, or 12 % above the mean. Both countries are therefore associated with above-average permanent agricultural forest loss per tonne procured, with Tanzania carrying the higher relative pressure on this dimension.

For biodiversity loss, the two countries fall on opposite sides of the African mean of $5.04{\times}10^{-4}$ km^2 area-equivalents per tonne. Benin's intensity of $3.81{\times}10^{-4}$ corresponds to a ratio of 0.76, placing it 24 % below the regional average, while Tanzania's intensity of 7.42×10^{-4} corresponds to a ratio of 1.47, placing it 47 % above the mean. Tanzanian maize is therefore associated with substantially higher biodiversity loss per tonne than the regional average, while Benin performs below average on this dimension.

Because both countries produce maize almost entirely under rainfed conditions, the blue water indicators carry limited weight in this specific comparison.

6.5.3 Combined Interpretation

Taken together, the environmental sourcing risk and environmental impact profiles (*Figure 6.4*) reveal a picture in which neither sourcing option dominates the other across all dimensions. The two profiles also differ in character. Tanzania's main disadvantages are short-horizon rainfall instability and biodiversity loss per-tonne impact intensity, whereas Benin's are concentrated in a long-horizon soil constraint and in emissions intensity. The country that looks worse therefore depends on both the time horizon and the dimension considered.

Figure 6.4 makes this visible. In the risk chart, Tanzania's polygon extends further into the rainfall and drought sector while Benin's extends further into the Soil sector. In the impact chart the positions partly reverse, with Benin reaching further on Greenhouse Gas Emissions and Tanzania further on Biodiversity Loss. Because both countries produce maize almost entirely under rainfed conditions, the blue water indicators carry limited weight in either chart. Neither polygon consistently encloses the other, which is the clearest visual confirmation that no single sourcing option is environmentally preferable in all aspects and that the weighting of dimensions remains a procurement judgement.

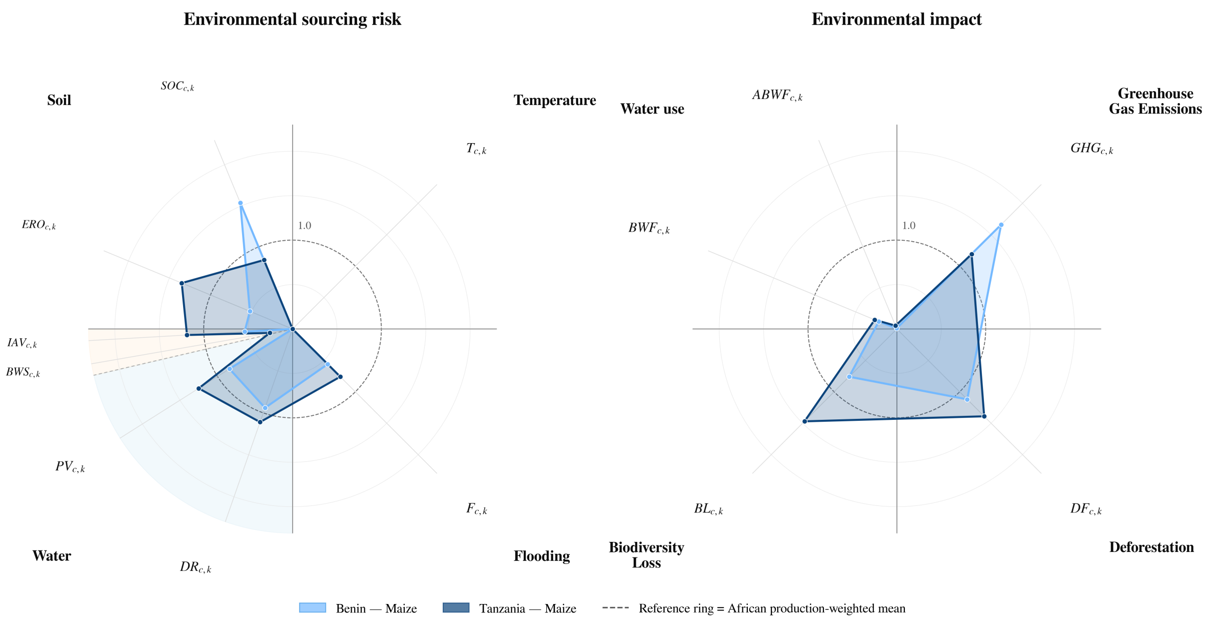

Figure 6.4: Integrated environmental sourcing risk profile (left) and environmental impact profile (right) for maize sourced from Benin and Tanzania, normalised to the African production-weighted mean.

6.6 Evaluation

This section evaluates the developed artifact in three steps. It first verifies that the computed indicator values are plausible, checking them against independent sources and known regional patterns. It then assesses the artifact against the design objectives and decision support attributes from *Section 1.3* and *Section 2.3.4*, before reflecting on the most significant methodological trade-offs that shaped the result.

6.6.1 Verification of Results

The following checks assess whether the computed indicator values are consistent with independent sources and known regional patterns. These are plausibility checks rather than formal statistical validation.

Temperature

The annual maximum temperature within the SPAM maize footprint was extracted for each year of the 1991–2020 reference period. It remained below the 45 °C threshold throughout in both countries, directly consistent with the indicator value of zero for both Benin and Tanzania.

Flooding

The JRC GloFAS RP10 layer was overlaid with the SPAM maize mask in GEE. In Benin, flood-exposed pixels were almost entirely absent from the maize production zones, with hazard concentrated in the southern coastal lowlands where maize production is negligible. In Tanzania, exposed pixels appeared along major river corridors and around Lake Victoria, while the highland production zones in Iringa and Mbeya remained largely unaffected. Both patterns are consistent with the computed values of 0.023 and 0.031 respectively, both below the African mean of 0.040.

Drought

The SPEI-3 drought share was visualised across the rainfed maize footprint. Benin showed spatially homogeneous moderate drought frequency, while Tanzania displayed higher values in the central and southern interior, consistent with published regional characterisations documenting greater drought frequency and intensity in Tanzania relative to West African maize zones (Haile et al., 2020). The values of 0.194 and 0.228, with Tanzania above and Benin below the African mean of 0.206, are consistent with these patterns.

Precipitation variability

The CV values of 0.116 for Benin and 0.173 for Tanzania place both countries in the less variable to moderately variable range, with Tanzania closer to the boundary. Benin's lower value is consistent with its location in the West African monsoon belt, where rainfall is relatively predictable from year to year. Tanzania's higher value reflects the fact that its main maize-producing highlands receive rainfall from two distinct seasonal systems that vary considerably in strength between years, making year-to-year rainfall less reliable as an agricultural input (Rowhani et al., 2011). Both values are consistent with the directional difference expected between the two regions, with Tanzania above and Benin below the African mean of 0.138.

Baseline water stress and interannual variability

The computed scores were cross-checked against the WRI Aqueduct Water Risk Atlas (Kuzma et al., 2023). All sampled basins in Benin returned Low water stress and Low to Low-Medium IAV, consistent with the near-zero computed values. In Tanzania, highland basins showed predominantly Low to Low-Medium stress with localised High to Extremely High stress in the Great Ruaha basin, and the production-weighted $IAV_{c,k}$ of 1.996 (Medium-High) is consistent with this mixed spatial pattern.

Erosion

The SPAM-derived production totals were verified against FAOSTAT 2020 reference values within the GEE script, and erosion raster coverage over the maize mask was confirmed at approximately 1.0. The African mean of 23.4 Mg/ha/yr is consistent with the continental cropland rate of 17.1 Mg/ha/yr reported by Borrelli et al. (2022), with the higher maize-specific value reflecting the concentration of production in sloped highland zones. Tanzania's value of 31.5 Mg/ha/yr is supported by field studies in Tanzanian highland maize zones where measured rates consistently exceed the tolerable threshold (Kimaro et al., 2008).

Soil organic carbon

The values of 8.78 g/kg for Benin and 16.14 g/kg for Tanzania are consistent with independent measurements. A national mapping study for Tanzania based on over 1 400 field samples reported a mean cropland topsoil SOC of approximately 13.3 g/kg (Winowiecki et al., 2016), with the somewhat higher SPAM-weighted value plausibly reflecting the concentration of production in more productive highland soils. Benin's below-mean value is consistent with documented long-term SOC depletion under continuous maize cultivation in West Africa (Bationo et al., 2007).

Deforestation

The FAOSTAT cumulative production denominators were confirmed against independently retrieved FAOSTAT statistics. The computed intensities were assessed against the Global Forest Watch tree cover loss layer (Hansen et al., 2013). Maize cultivation is documented as the primary driver of forest loss in Tanzania, identified in over half of all recorded deforestation events (Forest Trends, 2022), supporting the above-mean intensity of 0.033 ha/tonne. For Benin, despite a high national deforestation rate of 2.2 % annually (Sarraf & Ravina da Silva, 2020), loss within the northern maize production zones is spatially limited in the GFW layer, consistent with the lower intensity of 0.026 ha/tonne.

6.6.2 Evaluation Against the Design Objectives and DSS Design Attributes

This section is the formal evaluation step of the Design Science Research Methodology described in *Section 3.5.5* (Peffers et al., 2007). The tool is evaluated against two complementary sets of criteria, the design objectives established in *Section 1.3*, and the nine decision support system attributes synthesised in *Section 2.3.4*.

The design objectives established in *Section 1.3* framed the tool as a system that should support structured assessment and comparison of environmental impact and environmental sourcing risk across country-crop combinations. It should also be usable both for comparative assessment and for risk profiling, accept procurement volume as an input, be transparent as well as flexible and scalable.

The objective of structured assessment and comparison is met. The framework decomposes both environmental sourcing risk and environmental impact into well-defined dimensions, each operationalised by a documented indicator and reported results in a consistent format across country-crop combinations. The objective of supporting both comparative assessment and environmental risk profiling is met by the dual-output structure. The same indicator set serves both use cases. When two or more sourcing options are evaluated side by side, the normalised values support direct comparison and when a single country-crop combination is profiled, the absolute values, together with available thresholds, support standalone interpretation. The objective of procurement-volume scalability is met for the environmental impact component, where the per-tonne intensities can be multiplied by the intended procurement volume to produce a sourcing-attributed impact total. It does not apply to the environmental risk component, which describes structural environmental conditions in the sourcing region rather than impacts proportional to volume. The objectives of usability is not assessable but transparency are met. The tool is transparent at the level of the underlying logic, the formulas and the datasets used, all of which are documented in *Chapter 5* and *Chapter 6*. Usability in the sense of accessibility for non-technical personnel depends on the interface layer, which is outside the scope of this thesis. The objectives of flexibility and scalability are met at the framework level. The two-tier dataset selection criteria established in *Section 5.2.1* and *Section 5.3.1*, and the modular indicator structure allow new dimensions to be added or existing ones to be replaced when better datasets become available, without altering the overall framework.

The tool is also evaluated against the DSS design attributes. The synthesis in *Section 2.3.4* organises decision support design into the three subsystems, database, model base and user interface, each with three attributes.

For the database subsystem, scientific validity is met. Each indicator draws on a dataset that was selected through an explicit two-tier framework that required documented methodology and citable source. Beyond the credibility of the input datasets, the plausibility checks in *Section 6.6.1* provide output-level support for scientific validity, confirming that the computed indicator values are consistent with independent sources and known regional patterns for the demonstrated country-crop combinations. Traceability is met since every indicator can be traced back through its formula in *Section 6.2* to its dataset in *Section 6.3* or *Section 6.4* and through the Google Earth Engine script in Appendix B to the underlying raster cells. Parsimony is partially met. The indicator set is grounded directly in the theoretical dimensions identified in RQ1, and indicators that did not meet the tier-one criteria were excluded. However, the resulting set of thirteen indicators across both components is at the upper end of what a single procurement officer can be expected to interpret without summary aids.

For the model subsystem, robustness is partially met. The formulas are well defined and stable for the country-crop combinations tested, but the framework has not been stress-tested on edge cases such as countries where a metric is undefined and returns zero by construction. Intellectual accessibility is met as each formula is written in a form that follows directly from its definition, and the SPAM-overlay logic is consistent across all environmental risk indicators. Evolutionary capability is met. The two-tier dataset framework, combined with the modular indicator structure, allows the tool to grow as data availability and analytical capacity mature.

For the user interface subsystem, all three attributes, ease of communication, transparency and flexibility, are formally not met at the artifact level, because the interface itself is outside the scope of the thesis. However, the structural choices made in *Chapter 4* and *Chapter 5* were informed by the interface goals. The dual absolute and normalised output supports communication, the side-by-side environmental sourcing risk and environmental impact profiles support transparency and the dimension-level rather than composite output supports flexibility by allowing users to weight dimensions themselves. The full realisation of these attributes depends on interface development that is identified in *Section 7.3.2* as the highest-priority next step.

Overall, the evaluation shows that the tool fulfils the main objectives. At the same time, the evaluation highlights that the tool is not yet complete as an operational decision support system, since the user interface remains outside the scope of this thesis. The framework should therefore be understood as a validated analytical foundation that can support future implementation, rather than as a complete end-user decision support tool for procurement.

6.6.3 Reflections on Methodological Trade-offs

The development of the tool required a number of methodological trade-offs that shaped the form of the final result. This section reflects on the most consequential ones, beginning with the choices that defined the output structure of the tool and moving toward the spatial, normalisation and temporal foundations on which the indicators are built. The intention is not to repeat the indicator-level limitations already summarised in *Section 5.2.2.6* and *Section 5.3.2.6*, but to reflect on the higher-level design decisions that most directly affect how the results should be interpreted.

The most architectural choice was to retain the indicators as separate outputs rather than aggregate them, both within the dimensions and between the environmental risk and environmental impact components. This decision was made on theoretical grounds in *Section 4.1.5*, *Section 4.2.2* and *Section 4.3*. These sections show that aggregation would require expert-derived weights, which were outside the scope of this thesis. The decision therefore reflects a practical limitation, not a theoretical rejection of weighted aggregation. As discussed in *Section 2.4.3.3*, MCDM approaches such as AHP provide a recognised procedure for this kind of structured weighting. Producing a composite score would have made the tool more immediately rankable but would have implied a precision the underlying theory cannot justify at this stage. At the same time, the separate presentation of indicators should not be interpreted as meaning that the dimensions are independent. *Section 2.5.3.3* and *Section 2.5.5* establish that crop stressors can interact and that compound events may produce non-additive effects. The implication is that users should interpret the indicator profile as a structured overview of potential concern areas, rather than as a complete model of how environmental risks and environmental impacts interact. The cost of the choice is that the tool does not on its own answer the question of which sourcing option is preferable, and instead requires the user to weigh dimensions according to their own procurement context.

The final tool produces one value for each country-crop combination, rather than separate values for different production areas within a country. This means that sub-national variation is compressed into a single weighted average. In countries where the same crop is grown under very different environmental conditions, this average may not represent any specific growing region well, and the tool cannot show where environmental sourcing risk or environmental impact is higher or lower within the country. The indicators therefore reflect country-level production conditions and do not capture sub-national differences. Sub-national differentiation is identified as an important area for future refinement as more granular data become available for all dimensions.

The decision to base both the environmental sourcing risk and environmental impact assessments on SPAM 2020, introduced in *Section 5.1.2*, was one of the most important choices for how the tool works in practice. SPAM provides crop-specific spatial information, which makes it possible to calculate the same indicators consistently across all country-crop combinations. It also aligns the tool with the production statistics used by FAOSTAT and by several of the selected impact datasets. At the same time, this choice involves an important trade-off. SPAM is a modelled dataset rather than a directly observed crop map, and it represents crop production around 2020 rather than current real-time conditions. This means that the tool benefits from detailed crop-specific spatial data, but also inherits SPAM's modelling assumptions and local-level uncertainty. In practice, the tool's representation of where each crop is grown is therefore anchored to a static 2020 snapshot. For most country-crop combinations in Sub-Saharan Africa, this is unlikely to substantially distort the results in the near term, but the spatial allocation should be updated when new SPAM versions become available. More generally, both SPAM and other static datasets used in the tool reflect historical patterns rather than real-time production conditions.

Mean-referenced normalisation was adopted in *Section 4.3* to support comparison between sourcing options within the region by expressing each indicator value as a ratio to the African production-weighted mean for the same crop. This is appropriate for a tool designed for regional comparison, because it provides a common contextual reference. However, a known limitation of mean-based normalisation is that outliers can affect the reference point and thereby the interpretation of all normalised results (Freudenberg, 2003). The scarcity-adjusted blue water footprint indicator illustrates this trade-off. Across the African producer set, the median per-tonne intensity is approximately 1,140 m^3 world-equivalents per tonne, while the production-weighted mean is approximately 20,500 m^3 world-equivalents per tonne. This difference is driven largely by Egypt, where high production volume is combined with a high scarcity per-tonne intensity. As a result, the reference mean becomes much higher than what is typical for most African producers. If one producer performs extremely poorly, other producers may appear comparatively favourable even though their own environmental impact levels may still require attention. The normalised values are useful for comparing sourcing options, but they should be interpreted with awareness of this outlier sensitivity. Future refinements of the framework should strengthen the interpretation by adding literature-based thresholds where available, similar to the threshold logic used for soil organic carbon rate.

The conceptual framework in *Section 4.1* was structured around hazard, exposure and vulnerability, but in the operational tool crop-specific vulnerability is incorporated only where the literature provides clear thresholds, most directly in the heat-stress indicator. The drought, flood, precipitation-variability and soil indicators apply uniform crop sensitivity, with crop specificity entering only through the SPAM spatial mask that defines where the crop is grown. In addition, the climatological indicators are computed over the full calendar year rather than the crop-specific growing season. This means that off-season stressor conditions may be included in the indicator values, even when they have no direct biological effect on the crop. The implication is that the environmental risk indicators are closer to spatially attributed environmental-condition indicators than to crop-yield-loss estimates. Two crops grown in the same location will produce different absolute environmental risk values only where threshold-based vulnerability is encoded, in all other cases, the difference between crops reflects where they are grown rather than how they respond physiologically. Future refinements should therefore prioritise crop-specific vulnerability functions and growing-season-specific indicator calculations.

Finally, almost all underlying datasets are static products, based either on fixed reference periods or single-year snapshots, rather than continuously updated data streams. This reflects the available data landscape rather than a design preference. All published crop-attributed environmental datasets that meet the tier-one requirements established in *Section 5.3.1* are available as fixed or versioned datasets rather than continuously updated data sources. This limitation is important in relation to the monitoring role of SCRM discussed in *Section 2.2.2.4*. While risk monitoring involves continuously tracking how risks change over time, the tool developed in this thesis cannot provide continuous monitoring in that sense. The outputs should therefore be understood as snapshots based on the reference years and periods of the underlying datasets, rather than as representations of current real-time conditions. Future work should therefore ensure that the tool is periodically recomputed when updated dataset versions become available, and should explore whether more frequently updated datasets can be incorporated for dimensions where monitoring is especially important.

7 Conclusion and Discussion

This chapter brings the thesis to a close. It returns to the three research questions, positions the academic and practical contributions of the thesis and presents the limitations of the study and outlines a prioritised agenda for future research.

7.1 Answering the Research Questions

The purpose of this thesis was to develop, in collaboration with WFP, a decision support tool that informs sourcing decisions by presenting environmental impact and environmental sourcing risk indicators for country-crop combinations in Sub-Saharan Africa. Three research questions structured this work, and the following subsections summarise the answer to each.

7.1.1 Conclusions for RQ1

RQ1: *Which environmental impact and environmental sourcing risk dimensions are relevant for agricultural sourcing decisions in Sub-Saharan Africa?*

Environmental sourcing risk refers to the potential for environmental conditions in the production region to disrupt crop yield, and thereby procurement availability. Environmental impact refers to the ecological consequences generated by the production process itself.

For environmental sourcing risk, *Chapter 2* establishes that risk materialises through yield loss, and yield loss occurs when crop growth requirements deviate from their optimal range. The conditions that cause this deviation are referred to as stressors and constitute the hazard dimension of environmental sourcing risk. *Chapter 2* identifies two main categories. Abiotic stressors are non-living environmental factors and include temperature extremes, water-related conditions such as drought, flooding and water stress, soil degradation through erosion and declining organic matter, light availability and air quality. Biotic stressors arise from living organisms and include insects and pests, diseases and pathogens, and weeds. Both categories are relevant in Sub-Saharan Africa, where crops are simultaneously exposed to climatic pressures and biological threats that vary in intensity across regions and growing seasons. The relevance of any individual stressor for a given country-crop combination is determined by the physiological tolerances of the crop and the environmental conditions of the production region. For environmental impact, the literature search in *Chapter 2* identified five main impact dimensions through which crop production generates ecological harm. These are greenhouse gas emissions, deforestation and land use change, biodiversity loss, water use and quality, and pesticide use. Both dimensions are crop-specific and country-specific, meaning that the relevance of any individual indicator depends on the combination of crop physiology, production geography and regional environmental or agricultural conditions.

7.1.2 Conclusions for RQ2

RQ2: *How can these dimensions be quantified and compared across country-crop combinations?*

Quantification is achieved by translating each dimension identified in RQ1 into a measurable indicator with a defined formula and a documented dataset. *Chapter 5* establishes that this can be done in a structured and reproducible way by anchoring all indicators to a shared analytical foundation. The Spatial Production Allocation Model (SPAM 2020) provides the common spatial reference that disaggregates national crop production into crop-specific gridded estimates at approximately ten kilometre resolution. The 1991–2020 WMO climatological standard normal provides the temporal reference for all climate-based indicators and Google Earth Engine provides the computational environment in which the spatial overlays are executed. The two-tier dataset selection framework documented in *Section 5.2.1* and *Section 5.3.1* ensures that every dataset used in the tool is conceptually valid, methodologically documented, openly accessible and citable, before being compared against secondary criteria such as resolution, recency, native availability in Google Earth Engine and institutional credibility. Together, these elements make it clear how each indicator in the tool is calculated, from the raw raster data to the final value.

For the environmental risk component, the disaster risk framework introduced in *Section 4.1* provides the conceptual structure for quantification. Hazard is operationalised as stressor intensity in the production region, exposure as the spatial intersection between hazard conditions and the crop's SPAM footprint, and vulnerability as the crop-specific tolerance thresholds at which yield response is triggered. Each stressor dimension is then quantified as a production-weighted mean of pixel-level values across the crop's SPAM footprint in the sourcing country, as expressed by *Equation (5.2)*. The same aggregation logic applies to all eight risk indicators and varies only in the underlying stressor dataset, the pixel-level calculation, and whether the all-technology, rainfed or irrigated SPAM layer is used. Weighting by production rather than harvested area aligns the indicator with the procurement logic that risk materialises through tonnes of supply rather than hectares of land. Biotic stressors, although identified as relevant in RQ1, could not be quantified within this framework because no candidate dataset met the tier-one requirement of spatially continuous, crop-specific raster coverage.

For the environmental impact component, each ecological consequence is quantified as an impact intensity per tonne of crop produced. Where datasets already provide pre-calculated country-crop intensities derived from their own SPAM-based spatial attribution, these are used directly. Where only national totals are available, the intensity is derived through *Equation (5.11)* as the ratio between the total national impact and the corresponding national production from FAOSTAT. The per-tonne format allows each indicator to be scaled to a specific sourcing decision using the impact-scaling equation *Equation (5.10)*, thereby estimating the environmental impact associated with a given procurement volume. Four of the five impact dimensions identified in

RQ1 are operationalised in the final tool. Pesticide use, although conceptually relevant, was excluded because no spatially explicit, crop-attributable dataset met the tier-one requirements.

Comparison operates at the level of the individual indicators rather than through a single composite score. Each indicator is reported in two complementary forms. The absolute value preserves the original unit and meaning, enabling interpretation against any agronomic or environmental threshold established in the literature, such as the 20 g/kg agronomic floor for soil organic carbon. The normalised value expresses the result as a ratio to the African production-weighted reference mean for the same crop and indicator, calculated according to *Equation (5.1)*. A ratio above 1.0 indicates worse-than-average performance for that dimension while a ratio below 1.0 indicates better-than-average performance. Because the reference mean is computed separately for each crop, the normalisation enables direct comparison between sourcing-country options for a given crop, while the absolute value provides standalone interpretation when a country is profiled on its own.

7.1.3 Conclusions for RQ3

RQ3: *How can these indicators be structured into a decision support framework that informs WFP's sourcing decisions?*

The tool is structured as an integrated but non-aggregated framework that presents an environmental sourcing risk profile and an environmental impact profile side by side for each country-crop combination. This structure builds on the tool requirements established in *Section 1.3* and is consistent with the decision support attributes synthesised in *Section 2.3.4*. The indicators are deliberately kept as separate components rather than combined into a single composite score. This is because aggregation across dimensions would require additional assumptions about their relative importance. As discussed in *Section 2.4.3.3*, such assumptions would need to be made explicit, for example through stakeholder input or expert elicitation.

The result is shown in absolute values and relative to the African mean. To make the two profiles interpretable when several indicators are compared at once, the output is two side-by-side radar charts, developed and applied to real data in *Section 4.4* and visualised again here in *Figure 7.1*. Each indicator is shown relative to the African production-weighted mean, with a reference ring marking the regional benchmark, so that values outside the ring indicate worse-than-average conditions and overlaid polygons make the trade-offs between sourcing options directly visible. This profile-based output supports usability in a way that a single composite score would not. It allows procurement personnel to see which specific environmental dimensions drive a risk or impact result, identify mitigation or further-investigation actions accordingly, and apply judgement on which dimensions matter most for a given sourcing decision in line with WFP's strategic priorities at the time.

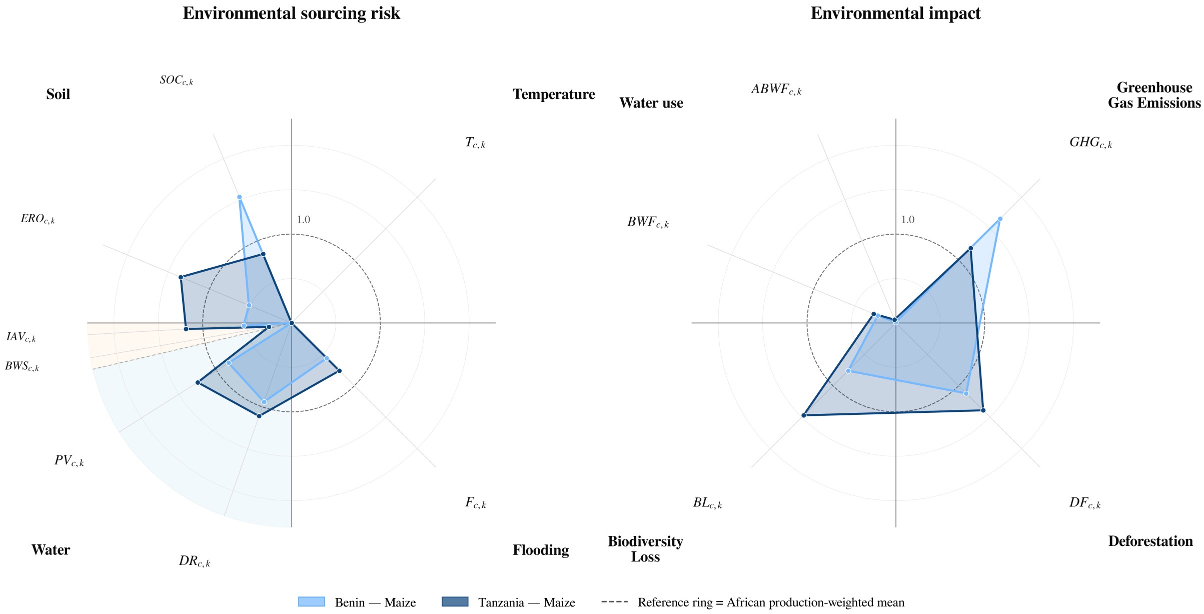

Figure 7.1: Integrated environmental sourcing risk profile (left) and environmental impact profile (right) for maize sourced from Benin and Tanzania, normalised to the African production-weighted mean.

The scope boundary of the tool delivered in this thesis is the data and model subsystems of the decision support system, as described in *Section 2.3*. The user interface subsystem, as defined in *Section 2.3.3*, is a design task identified for the next phase of development. This boundary is a deliberate scope decision rather than a failure to meet RQ3.

RQ3 asks how environmental risks and environmental impacts can be structured into a usable tool. The answer comprises the indicator set in *Chapter 6*, the formulas defined in *Section 6.2*, the dataset references in *Section 6.3* and *Section 6.4*, and the Google Earth Engine script in Appendix B. Together, these constitute the foundation on which a usable interface can be built, as illustrated in *Figure 7.2*.

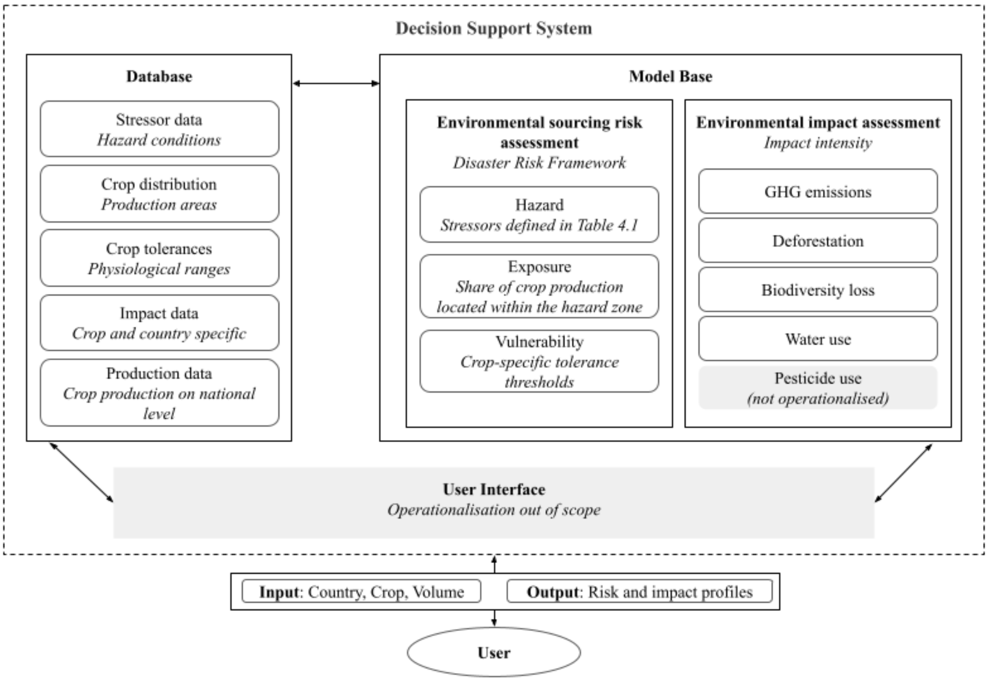

Figure 7.2: Detailed conceptual architecture of the decision support system, structured around a database subsystem, a model base subsystem and a user interface subsystem.

The demonstration in *Section 6.5* applying the framework to maize sourced from Benin and Tanzania, provides evidence that the structured artifact produces coherent, interpretable and comparable outputs under realistic WFP procurement scenarios. The indicator-level plausibility checks in *Section 6.6.1* further confirm that the computed values are consistent with independent sources and regional patterns, strengthening confidence in the analytical foundation of the tool. Benin's profile is primarily characterised by soil-related risks and higher greenhouse gas intensity per tonne, whereas Tanzania's profile is primarily characterised by rainfall-related risks and higher biodiversity pressure per tonne. Neither dominates the other, which is precisely the trade-off-visibility output that the framework is designed to support.

7.2 Contributions

This thesis contributes to both academic research and practical operations. The following sections discuss these contributions separately, first by positioning the thesis in relation to previous research and then by outlining its practical relevance for WFP and other potential users.

7.2.1 Academic Contribution

The academic contribution of this thesis lies primarily at the intersection of humanitarian logistics and sustainable supply chain risk management. It addresses the limited integration of environmental impact and environmental sourcing risk assessment in humanitarian procurement.

Humanitarian logistics has expanded from an early focus on the movement and storage of relief goods (Van Wassenhove, 2006; Tomasini & Van Wassenhove, 2009; Kovács & Spens, 2007) toward a broader supply chain perspective (Kembro et al., 2024), with increasing attention to environmental sustainability and life cycle impacts in humanitarian operations (Besiou & Van Wassenhove, 2020; Corbett et al., 2022). More recently, sustainability has also gained explicit attention in humanitarian procurement, calling for sourcing decisions that consider environmental consequences alongside cost, availability and operational feasibility (Thakur-Weigold et al., 2025; Tay et al., 2025). However, the literature has largely treated these issues in separate streams. Humanitarian logistics research has primarily addressed environmental impact through the ecological consequences of operations, such as emissions, waste, resource use and life cycle impacts (Van Wassenhove, 2006; Besiou & Van Wassenhove, 2020; Corbett et al., 2022; Kembro et al., 2024). In contrast, risk-oriented humanitarian procurement research has mainly focused on supply disruption, sourcing vulnerability and continuity of supply (Thakur-Weigold et al., 2025; Moshtari et al., 2021). Sustainable purchasing research, such as Pagell et al. (2010), has begun to incorporate environmental considerations into procurement portfolio logic, but limited attention has been given to integrated decision support tools that assess environmental impact and environmental sourcing risk together in humanitarian procurement. This thesis contributes to this gap by developing a framework that connects these previously separate perspectives and shows how environmental impact and environmental sourcing risk can be assessed in parallel within humanitarian procurement.

Within SSCRM, Hofmann et al. (2014) framed sustainability as an extension of SCRM rather than a replacement, while Giannakis & Papadopoulos (2016) provided a typology of sustainability-related supply chain risks. This literature shows that sustainability issues can become supply chain risks when they affect sourcing conditions, supplier performance or long-term supply stability, but it operates primarily at the level of frameworks and categorisations rather than measurable assessment. The conceptual integration of sustainability and risk in purchasing portfolios was advanced most directly by Pagell et al. (2010), whose Sustainable Purchasing Portfolio Model showed empirically that firms managing items with significant environmental or social implications often reclassified them as strategic, regardless of their position in the original Kraljic logic (Kraljic, 1983). However, Pagell et al. (2010) mainly described this empirical pattern. They did not provide a measurable, indicator-based method for systematically identifying items that should be treated as strategically important because of their environmental implications. This points to a need for approaches that move from recognising sustainability-related supply chain risk conceptually to assessing such risk in concrete sourcing decisions. This thesis provides such an operational layer with dimension-specific comparable indicators for environmental sourcing risk and environmental impact that allow a buyer to assess how a sourcing decision performs on each dimension. In this way, the thesis contributes to SSCRM by translating environmental sustainability-related supply chain risk from a conceptual category into a structured, indicator-based assessment approach for procurement decisions.

7.2.2 Practical Contribution

The practical contribution to WFP is the artifact itself and the documentation that allows it to be used, maintained and extended. In the immediate context of this thesis, the contribution is directed toward WFP's procurement activities in Sub-Saharan Africa, where the tool supports structured assessment of environmental impact and environmental sourcing risk across country-crop combinations.

What is directly usable from this research can be grouped into four components:

(i) The indicator formulas defined in *Section 6.2* and applied in *Section 6.3* and *Section 6.4*.

(ii) The documented dataset references and two-tier dataset selection framework presented in *Section 5.2.1* and *Section 5.3.1*, which enable indicators to be reproduced, audited, updated when source datasets are revised, and extended to future candidate datasets.

(iii) The Google Earth Engine script provided in Appendix B.

(iv) The demonstration in *Section 6.5*, which illustrates how the outputs should be interpreted in a realistic procurement scenario.

Beyond WFP's operations in Sub-Saharan Africa, the framework may also be useful for other WFP locations and UN organisations facing similar procurement decisions in environmentally sensitive or climate-exposed regions. Since the framework is based on openly available datasets, transparent indicator logic and reproducible computational steps, it can in principle be adapted to other geographic contexts where comparable crop, climate and environmental data are available. More broadly, the framework may also be relevant for other humanitarian organisations, public-sector buyers and large-scale food procurers that seek to integrate environmental impact and environmental sourcing risk into procurement decisions.

While the specific indicators developed in this thesis are tailored to agricultural sourcing, the underlying logic combines environmental impact assessment, environmental sourcing risk, transparent indicator selection and spatial data. This logic could also inspire similar assessment approaches in other sectors where procurement decisions are exposed to environmental risk and generate environmental impact. In this way, the thesis demonstrates that climate-smart and risk-informed procurement can be operationalised through an accessible and transparent methodology, potentially lowering the barriers for adoption beyond the specific WFP Sub-Saharan Africa case.

7.3 Limitations and Future Research

7.3.1 Limitations

The limitations of this thesis fall into three main categories. The first concerns the scope delimitations defined in *Section 1.6*. The tool is restricted to the sourcing stage, covering environmental conditions in the production region and their implications for procurement availability and impact. Post-procurement activities such as processing, in-country transport, warehousing and last-mile distribution are excluded, even though they generate their own environmental impacts and may be exposed to separate disruption risks. The framework is also restricted to environmental dimensions, meaning that social, economic, political and governance-related risks, including labour conditions, supplier ethics, corruption and broader market or policy risks, are excluded by design. In addition, the user interface subsystem is outside the scope of the thesis, meaning that the artifact should be understood as an analytical framework rather than a complete operational decision support system.

The second category concerns data limitations. These are addressed in detail in *Section 5.2.2.6* for the environmental sourcing risk component and *Section 5.3.2.6* for the environmental impact component. The main limitations relate to data availability, spatial resolution and temporal alignment. As a result, the indicators should be interpreted as indicative approximations rather than exact measurements of environmental sourcing risk or environmental impact.

The third category concerns methodological limitations. These are discussed in *Section 5.2.2.6* and mainly relate to aggregation, normalisation, spatial resolution and the static nature of the underlying data. Together, these limitations mean that the tool should be used to support structured comparison and interpretation, rather than to provide exact or exhaustive assessments of environmental sourcing risk and impact.

7.3.2 Future Refinements of the Tool

The future refinements identified throughout this thesis fall into three groups, presented here according to how directly they extend the current framework. Dimension-specific refinements are documented in Table 5.3 and Table 5.6 and this section summarises the main priorities for further development. Together, these refinements indicate where future development efforts should be directed if the tool is to become more operationally useful for WFP.

The first group concerns dataset operationalisation, updates and forward extension. Four dimensions identified as conceptually important in *Chapter 4*, could not be operationalised in this thesis because no openly accessible dataset met the tier-one requirements. These were chemical soil degradation, biotic stressors, water quality and pesticide use. The most direct refinement is to operationalise each of these as suitable datasets become available. Future development should also include regular updates of the underlying datasets as new versions become available, including future SPAM releases. The two-tier dataset selection criteria established in *Section 5.2.1* and *Section 5.3.1* provide the structured basis for evaluating both new indicators and future dataset updates consistently over time. As discussed in *Section 6.6.3*, the tool currently operates as a snapshot based on the reference years of its underlying datasets rather than as a real-time monitoring system. As more frequently updated datasets become available, the tool can gradually move closer to the continuous monitoring function emphasised in SCRM (*Section 2.2.2.4*). A complementary direction is the inclusion of forward-looking projections, illustrated in Table 5.3 by the WRI Aqueduct flood projections up to 2080, which would allow the tool to characterise not only current conditions but also how risks are likely to evolve under climate scenarios.

The second group concerns indicator refinements within existing dimensions. The most important refinement across several indicators is the introduction of crop-specific vulnerability in indicators where crop sensitivity is currently treated uniformly. As discussed in *Section 6.6.3*, vulnerability is included only in the heat-stress indicator, while the other indicators apply uniform crop sensitivity. Closely related is the shift from calendar-year calculations to growing-season-specific calculations of the climatological indicators, so that off-season conditions with no biological effect on the crop are excluded. Future refinements should also incorporate growth-stage-specific sensitivity thresholds.

The third group concerns refinements that build on or extend the existing framework. As more granular data become available for all dimensions, the tool should differentiate at sub-national level so that within-country variation in production conditions is no longer compressed into a single weighted average (*Section 6.6.3*). The dimension-specific profile could also be embedded within an MCDM framework, where procurement decision-makers define the relative importance of different risk and impact dimensions according to the decision context. As introduced in *Section 2.4.3.3* and acknowledged in *Chapter 4*, AHP provides a structured procedure for this kind of expert-elicited weighting, accommodating criteria that are qualitative, quantitative or measured on different scales. An MCDM layer would sit on top of the current output rather than replace it, preserving dimension-level visibility while enabling aggregated comparison where the weighting can be justified by the decision context. This would allow agreed priorities to be applied consistently across sourcing options, making comparisons faster and less dependent on individual procurement-level interpretation. Finally, integration of the tool as a standalone module within ECODASH, including a full user interface, was identified at the outset as the long-term goal for WFP (*Section 1.3*). The development of a fully integrated technical application was beyond the scope of this thesis, but the framework, indicator formulas and Google Earth Engine script provided here are designed to support that integration as a natural next step.

7.3.3 Future Research

Beyond the refinements of the artifact discussed in *Section 7.3.2*, this section identifies broader research directions that the thesis opens up. These are framed below as open questions in those fields rather than as direct extensions of the present tool.

The first research direction concerns the integration of sustainability into humanitarian logistics. As discussed in *Section 2.1*, humanitarian supply chains have historically been shaped by urgency, cost constraints and beneficiary access, with environmental sustainability only recently becoming an operational consideration. Integrating sustainability into this context raises questions that this thesis only begins to address. Under what conditions do environmental sourcing decisions support humanitarian priorities such as timeliness and cost, and under what conditions do they create trade-offs that must be addressed explicitly? How should sustainability principles developed in commercial logistics be adapted to the specific characteristics of humanitarian contexts (*Section 2.1.2*)? A further open question is how environmental risk and impact assessment should be extended across the rest of the humanitarian supply chain, since post-procurement stages such as in-country transport, storage and last-mile distribution are exposed to their own disruption risks and generate their own impacts. Future research should therefore explore how sustainability can be integrated without weakening the core humanitarian priorities of speed, cost and access.

The second research direction addresses how the relationship between environmental sourcing risk and environmental impact can be represented and eventually quantified within SCRM. As discussed in *Section 2.5.3.3*, crop stressors do not act independently, but can interact in ways that amplify or reduce their effects on production. *Section 2.5.5* further shows that environmental impacts from crop production can become drivers or amplifiers of future crop stressors. The present thesis treats environmental sourcing risk and environmental impact as separate analytical outputs, because the available literature does not yet provide a defensible way to quantify these relationships. Future research should therefore examine how impact-to-risk feedbacks can be measured and how the most consequential links between risk and impact dimensions can be qualitatively mapped. Such work would allow the two components to be connected in a way that is conceptually supported by the literature, but not yet operationalised in the current framework.

Bibliography

Altenbach, T. J., (1995). A comparison of risk assessment techniques from qualitative to quantitative. Technical Report UCRL-JC-119106, Lawrence Livermore National Laboratory, California, USA. URL https://digital.library.unt.edu/ark:/67531/metadc706979/.

Aven, T., (2010). On how to define, understand and describe risk. *Reliability Engineering & System Safety*, 95(6):623–631. ISSN 09518320. doi: 10.1016/j.ress.2010.01.011. URL https://linkinghub.elsevier.com/retrieve/pii/S095183201000027X.

Aven, T., (2012). The risk concept—historical and recent development trends. *Reliability Engineering & System Safety*, 99:33–44. ISSN 09518320. doi: 10.1016/j.ress.2011.11.006. URL https://linkinghub.elsevier.com/retrieve/pii/S0951832011002584.

Aven, T., (2016). Risk assessment and risk management: Review of recent advances on their foundation. *European Journal of Operational Research*, 253(1):1–13. ISSN 03772217. doi: 10.1016/j.ejor.2015.12.023. URL https://linkinghub.elsevier.com/retrieve/pii/S0377221715011479.

Aven, T., (2019). The Call for a Shift from Risk to Resilience: What Does it Mean? *Risk Analysis*, 39(6):1196–1203. ISSN 0272-4332, 1539-6924. doi: 10.1111/risa.13247. URL https://onlinelibrary.wiley.com/doi/10.1111/risa.13247.

Bandaly, D., Satir, A., Kahyaoglu, Y., and Shanker, L., (2012). Supply chain risk management – I: Conceptualization, framework and planning process. *Risk Management*, 14(4):249–271. ISSN 1460-3799, 1743-4637. doi: 10.1057/rm.2012.7. URL http://link.springer.com/10.1057/rm.2012.7.

Bationo, A., Kihara, J., Vanlauwe, B., Waswa, B., and Kimetu, J., (2007). Soil organic carbon dynamics, functions and management in West African agro-ecosystems. *Making Carbon Sequestration Work for Africa's Rural Poor*, 94(1):13–25. ISSN 0308-521X. doi: 10.1016/j.agsy.2005.08.011. URL https://www.sciencedirect.com/science/article/pii/S0308521X06001065.

Baugh, C., Colonese, J., D'Angelo, C., Dottori, F., Neal, J., Prudhomme, C., and Salamon, P., (2024). Global River Flood Hazard Maps. URL http://data.europa.eu/89h/jrc-floods-floodmapgl_rp50y-tif.

Bedeke, S. B., (2023). Climate change vulnerability and adaptation of crop producers in sub-Saharan Africa: a review on concepts, approaches and methods. *Environment, Development and Sustainability*, 25(2):1017–1051. ISSN 1387-585X, 1573-2975. doi: 10.1007/s10668-022-02118-8. URL https://link.springer.com/10.1007/s10668-022-02118-8.

Beguería, S., Vicente Serrano, S. M., Reig-Gracia, F., and Latorre Garcés, B., (2024). SPEIbase v.2.10 [Dataset]. URL https://digital.csic.es/handle/10261/364137 [Accessed 2026-05-17].

Besiou, M. and Van Wassenhove, L. N., (2020). Humanitarian Operations: A World of Opportunity for Relevant and Impactful Research. *Manufacturing & Service Operations Management*, 22(1):135–145. ISSN 1523-4614, 1526-5498. doi: 10.1287/msom.2019.0799. URL https://pubsonline.informs.org/doi/10.1287/msom.2019.0799.

Beyer, R. and Manica, A., (2021). Global and country-level data of the biodiversity footprints of 175 crops and pasture. *Data in Brief*, 36:106982. ISSN 23523409. doi: 10.1016/j.dib.2021.106982. URL https://linkinghub.elsevier.com/retrieve/pii/S2352340921002663.

Binswanger, H. P. and Landell-Mills, P., (1995). The World Bank's strategy for reducing poverty and hunger: A report to the development community. Technical Report Environmentally Sustainable Development Studies and Monographs Series No. 4, World Bank, Washington D.C. URL http://hdl.handle.net/10919/65983.

Birkmann, J., (2007). Risk and vulnerability indicators at different scales:Applicability, usefulness and policy implications. *Environmental Hazards*, 7(1):20–31. ISSN 17477891. doi: 10.1016/j.envhaz.2007.04.002. URL http://www.tandfonline.com/doi/abs/10.1016/j.envhaz.2007.04.002.

Birkmann, J., editor, (2006). *Measuring vulnerability to natural hazards: towards disaster resilient societies*. United Nations University, Tokyo ; New York. ISBN 978-92-808-1135-3.

Birkmann, J. and UNU-EHS Expert Working Group on Measuring Vulnerability, editors, (2013). *Measuring vulnerability to natural hazards: towards disaster resilient societies*. United Nations University Press, Tokyo ; New York, second edition edition. ISBN 978-92-808-1202-2.

Blessing, L. T. and Chakrabarti, A., (2009). *DRM, a Design Research Methodology*. Springer London, London. ISBN 978-1-84882-586-4 978-1-84882-587-1. doi: 10.1007/978-1-84882-587-1. URL http://link.springer.com/10.1007/978-1-84882-587-1.

Borrelli, P., Alewell, C., Alvarez, P., Anache, J. A. A., Baartman, J., Ballabio, C., Bezak, N., Biddoccu, M., Cerdà, A., Chalise, D., Chen, S., Chen, W., De Girolamo, A. M., Gessesse, G. D., Deumlich, D., Diodato, N., Efthimiou, N., Erpul, G., Fiener, P., Freppaz, M., Gentile, F., Gericke, A., Haregeweyn, N., Hu, B., Jeanneau, A., Kaffas, K., Kiani-Harchegani, M., Villuendas, I. L., Li, C., Lombardo, L., López-Vicente, M., Lucas-Borja, M. E., Märker, M., Matthews, F., Miao, C., Mikoš, M., Modugno, S., Möller, M., Naipal, V., Nearing, M., Owusu, S., Panday, D., Patault, E., Patriche, C. V., Poggio, L., Portes, R., Quijano, L., Rahdari, M. R., Renima, M., Ricci, G. F., Rodrigo-Comino, J., Saia, S., Samani, A. N., Schillaci, C., Syrris, V., Kim, H. S., Spinola, D. N., Oliveira, P. T., Teng, H., Thapa, R., Vantas, K., Vieira, D., Yang, J. E., Yin, S., Zema, D. A., Zhao, G., and Panagos, P., (2021). Soil erosion modelling: A global review and statistical analysis. *Science of The Total Environment*, 780:146494. ISSN 00489697. doi: 10.1016/j.scitotenv.2021.146494. URL https://linkinghub.elsevier.com/retrieve/pii/S004896972101562X.

Borrelli, P., Ballabio, C., Yang, J., Robinson, D., and Panagos, P., (2022). GloSEM: High-resolution global estimates of present and future soil displacement in croplands by water erosion. *Scientific Data*, 9:406. doi: 10.1038/s41597-022-01489-x.

Boulay, A.-M., Bare, J., Benini, L., Berger, M., Lathuillière, M. J., Manzardo, A., Margni, M., Motoshita, M., Núñez, M., Pastor, A. V., Ridoutt, B., Oki, T., Worbe, S., and Pfister, S., (2018). The WULCA consensus characterization model for water scarcity footprints: assessing impacts of water consumption based on available water remaining (AWARE). *The International Journal of Life Cycle Assessment*, 23(2):368–378. ISSN 0948-3349, 1614-7502. doi: 10.1007/s11367-017-1333-8. URL http://link.springer.com/10.1007/s11367-017-1333-8.

Boulay, A.-M., Lenoir, L., and Manzardo, A., (2019). Bridging the Data Gap in the Water Scarcity Footprint by Using Crop-Specific AWARE Factors. *Water*, 11(12):2634. ISSN 2073-4441. doi: 10.3390/w11122634. URL https://www.mdpi.com/2073-4441/11/12/2634.

Cao, P., Bilotto, F., Gonzalez Fischer, C., Mueller, N. D., Driscoll, A. W., Carlson, K. M., Gerber, J. S., Smith, P., Tubiello, F. N., West, P. C., You, L., and Herrero, M., (2025). Data and code for Spatially explicit global assessment of cropland greenhouse gas emissions circa 2020. URL https://figshare.com/articles/dataset/Data_and_code_for_Mapping_greenhouse_gas_emissions_from_global_cropland_circa_2020/29089973 [Accessed 2026-06-01]. https://creativecommons.org/licenses/by/4.0/.

Cao, P., Bilotto, F., Gonzalez Fischer, C., Mueller, N. D., Carlson, K. M., Driscoll, A. W., Gerber, J. S., Smith, P., Tubiello, F. N., West, P. C., You, L., and Herrero, M., (2026). Spatially explicit global assessment of cropland greenhouse gas emissions circa 2020. *Nature Climate Change*, 16(3):354–363. ISSN 1758-678X, 1758-6798. doi: 10.1038/s41558-026-02558-4. URL https://www.nature.com/articles/s41558-026-02558-4.

Cardona, O. D., Aalst, M. K.van , Birkmann, J., Fordham, M., McGregor, G., Perez, R., Pulwarty, R. S., Schipper, E. L. F., and Sinh, B. T., (2012). Determinants of risk: exposure and vulnerability. In Field, C. B., Barros, V., Stocker, T. F., Qin, D., Dokken, D. J., Ebi, K. L., Mastrandrea, M. D., Mach, K. J., Plattner, G.-K., Allen, S. K., Tignor, M., and Midgley, P. M., editors, *Managing the Risks of Extreme Events and Disasters to Advance Climate Change Adaptation*, pages 65–108. Cambridge University Press, Cambridge, UK, and New York, NY, USA. doi: 10.1017/CBO9781139177245.004.

Cardona, O. D., Inter American Development Bank, and Universidad Nacional de Colombia, (2005). Indicators of Disaster Risk and Risk Management. Technical report, Inter-American Development Bank. URL https://publications.iadb.org/en/indicators-disaster-risk-and-risk-management.

Carlson, K. M., Gerber, J. S., Mueller, N. D., Herrero, M., MacDonald, G. K., Brauman, K. A., Havlik, P., O'Connell, C. S., Johnson, J. A., Saatchi, S., and West, P. C., (2017). Greenhouse gas emissions intensity of global croplands. *Nature Climate Change*, 7(1):63–68. ISSN 1758-678X, 1758-6798. doi: 10.1038/nclimate3158. URL https://www.nature.com/articles/nclimate3158.

Corbett, C. J., Pedraza-Martinez, A. J., and Van Wassenhove, L. N., (2022). Sustainable humanitarian operations: An integrated perspective. *Production and Operations Man-*

agement, 31(12):4393–4406. ISSN 1059-1478, 1937-5956. doi: 10.1111/poms.13848. URL https://journals.sagepub.com/doi/10.1111/poms.13848.

Cox, L. A., (2008). What's Wrong with Risk Matrices? *Risk Analysis*, 28(2):497–512. ISSN 0272-4332, 1539-6924. doi: 10.1111/j.1539-6924.2008.01030.x. URL https://onlinelibrary.wiley.com/doi/10.1111/j.1539-6924.2008.01030.x.

Cramer, G. R., Urano, K., Delrot, S., Pezzotti, M., and Shinozaki, K., (2011). Effects of abiotic stress on plants: a systems biology perspective. *BMC Plant Biology*, 11(1):163. ISSN 1471-2229. doi: 10.1186/1471-2229-11-163. URL http://bmcplantbiol.biomedcentral.com/articles/10.1186/1471-2229-11-163.

Cutter, S. L., (1996). Vulnerability to environmental hazards. *Progress in Human Geography*, 20(4):529–539. ISSN 0309-1325, 1477-0288. doi: 10.1177/030913259602000407. URL https://journals.sagepub.com/doi/10.1177/030913259602000407.

Dasgupta, S. and Robinson, E. J. Z., (2022). Attributing changes in food insecurity to a changing climate. *Scientific Reports*, 12(1):4709. ISSN 2045-2322. doi: 10.1038/s41598-022-08696-x. URL https://www.nature.com/articles/s41598-022-08696-x.

Denscombe, M., (2010). *The good research guide: for small-scale social research projects*. McGraw-Hill/Open University Press, Maidenhead, England, 4th ed edition. ISBN 978-0-335-22968-0. OCLC: 702134616.

Deutsch, C. A., Tewksbury, J. J., Tigchelaar, M., Battisti, D. S., Merrill, S. C., Huey, R. B., and Naylor, R. L., (2018). Increase in crop losses to insect pests in a warming climate. *Science*, 361(6405):916–919. ISSN 0036-8075, 1095-9203. doi: 10.1126/science.aat3466. URL https://www.science.org/doi/10.1126/science.aat3466.

Duijm, N. J., (2015). Recommendations on the use and design of risk matrices. *Safety Science*, 76:21–31. ISSN 09257535. doi: 10.1016/j.ssci.2015.02.014. URL https://linkinghub.elsevier.com/retrieve/pii/S0925753515000429.

Er, M. C., (1988). Decision Support Systems: A summary, problems, and future trends. *Decision Support Systems*, 4(3):355–363. ISSN 0167-9236. doi: 10.1016/0167-9236(88)90022-X. URL https://www.sciencedirect.com/science/article/pii/016792368890022X.

ESA, (n.d.). Sentinel-5P Datasets in Earth Engine | Earth Engine Data Catalog. URL https://developers.google.com/earth-engine/datasets/catalog/sentinel-5p [Accessed 2026-06-01].

European Commission, Organisation for Economic Co-operation and Development, and SourceOECD (Online service), editors, (2008). *Handbook on constructing composite indicators: methodology and user guide*. OECD, Paris. ISBN 978-92-64-04345-9.

Falasca, M. and Zobel, C. W., (2011). A two-stage procurement model for humanitarian relief supply chains. *Journal of Humanitarian Logistics and Supply Chain Management*, 1(2):151–169. ISSN 2042-6747. doi: 10.1108/20426741111188329. URL http://www.emerald.com/jhlscm/article/1/2/151-169/214465.

Fan, Y. and Stevenson, M., (2018). A review of supply chain risk management: definition, theory, and research agenda. *International Journal of Physical Distribution & Logistics Management*, 48 (3):205–230. ISSN 0960-0035. doi: 10.1108/IJPDLM-01-2017-0043. URL http://www.emerald.com/ijpdlm/article/48/3/205-230/389713.

FAO, (n.d.). Crop Information. URL https://www.fao.org/land-water/databases-and-software/crop-information/en/ [Accessed 2026-06-01].

FAO, (n.d.). FAOSTAT. URL https://www.fao.org/faostat/en/#data/RP [Accessed 2026-06-01].

FAO, (1996). Rome Declaration on World Food Security and World Food Summit Plan of Action: World Food Summit, 13-17 November 1996, Rome, Italy. Official Declaration FAO(063)/F688, Food and Agriculture Organization of the United Nations, Rome. FAO.

FAO, (2015). *Status of the world's soil resources: main report*. Food and Agriculture Organization of the United Nations, Rome. ISBN 978-92-5-109004-6. FAO.

FAO, (2017). *ClimAfrica: Climate change predictions in Sub-Saharan Africa : impacts and adaptations*. Food and Agriculture Organization of the United Nations, Rome. ISBN 978-92-5-109706-9. OCLC: 1082354922.

FAO, (2025). Greenhouse gas emissions from agrifood systems. Technical report, Food and Agriculture Organization. URL https://openknowledge.fao.org/handle/20.500.14283/cd7300en.

FAO and WMO, (2026). *Extreme heat and agriculture*. Food and Agriculture Organization of the United Nations; World Meteorological Organization. ISBN 978-92-5-140656-4. doi: 10.4060/cd9394en. URL https://openknowledge.fao.org/handle/20.500.14283/cd9394en.

FAO, IFAD, UNICEF, WFP, and WHO, (2020). *The State of Food Security and Nutrition in the World 2020: Transforming food systems for affordable healthy diets*. Food and Agriculture Organization of the United Nations; International Fund for Agricultural Development; World Food Programme; The World Health Organization, Rome. ISBN 978-92-5-132901-6. doi: 10.4060/ca9692en. FAO et al.

FAO, IFAD, UNICEF, WFP, and WHO, (2025). *The State of Food Security and Nutrition in the World 2025: Addressing high food price inflation for food security and nutrition*. Food and Agriculture Organization of the United Nations; International Fund for Agricultural Development; World Food Programme; The World Health Organization, Rome. ISBN 978-92-5-139937-8. doi: 10.4060/cd6008en.

Faruquee, M., Saqib, S., Akman, A. N., and Alam, M. D. S., (2026). Understanding the Humanitarian Supply Chain. In *Resilience Lessons from Humanitarian Supply Chains*, pages 19–35. Springer Nature Switzerland, Cham. ISBN 978-3-032-08471-2 978-3-032-08472-9. doi: 10.1007/978-3-032-08472-9_2. URL https://link.springer.com/10.1007/978-3-032-08472-9_2.

Felzer, B. S., Cronin, T., Reilly, J. M., Melillo, J. M., and Wang, X., (2007). Impacts of ozone on trees and crops. *Comptes Rendus. Géoscience*, 339(11-12):784–798. ISSN 1631-0713, 1778-7025. doi: 10.1016/j.crte.2007.08.008. URL https://comptes-rendus.academie-sciences.fr/geoscience/articles/10.1016/j.crte.2007.08.008/.

Forest Trends, (2022). Illegal Deforestation for Forest Risk Commodities Dashboard: Tanzania. Technical report, Forest Trends. URL https://www.forest-trends.org/publications/illegal-deforestation-for-forest-risk-commodities-dashboard-tanzania/.

Freudenberg, M., (2003). Composite Indicators of Country Performance: A Critical Assessment. OECD Science, Technology and Industry Working Papers 2003/16, OECD. URL https://www.oecd.org/en/publications/composite-indicators-of-country-performance_405566708255.html.

Funk, C., Peterson, P., Landsfeld, M., Pedreros, D., Verdin, J., Shukla, S., Husak, G., Rowland, J., Harrison, L., Hoell, A., and Michaelsen, J., (2015). The climate hazards infrared precipitation with stations—a new environmental record for monitoring extremes. *Scientific Data*, 2(1):150066. ISSN 2052-4463. doi: 10.1038/sdata.2015.66. URL https://www.nature.com/articles/sdata201566.

Gallardo, R. K., (2024). The Environmental Impacts of Agriculture: A Review. *International Review of Environmental and Resource Economics*, 18(1-2):165–235. ISSN 1932-1465, 1932-1473. doi: 10.1561/101.00000166. URL https://www.emerald.com/irere/article/18/1-2/165/1334039/The-Environmental-Impacts-of-Agriculture-A-Review.

Giannakis, M. and Papadopoulos, T., (2016). Supply chain sustainability: A risk management approach. *International Journal of Production Economics*, 171:455–470. ISSN 09255273. doi: 10.1016/j.ijpe.2015.06.032. URL https://linkinghub.elsevier.com/retrieve/pii/S0925527315002704.

Gorelick, N., Hancher, M., Dixon, M., Ilyushchenko, S., Thau, D., and Moore, R., (2017). Google Earth Engine: Planetary-scale geospatial analysis for everyone. *Remote Sensing of Environment*, 202:18–27. ISSN 00344257. doi: 10.1016/j.rse.2017.06.031. URL https://linkinghub.elsevier.com/retrieve/pii/S0034425717302900.

Gosset, M., Dibi-Anoh, P. A., Schumann, G., Hostache, R., Paris, A., Zahiri, E.-P., Kacou, M., and Gal, L., (2023). Hydrometeorological Extreme Events in Africa: The Role of Satellite Observations for Monitoring Pluvial and Fluvial Flood Risk. *Surveys in Geophysics*, 44(1):197–223. ISSN 0169-3298, 1573-0956. doi: 10.1007/s10712-022-09749-6. URL https://link.springer.com/10.1007/s10712-022-09749-6.

Haile, G. G., Tang, Q., Hosseini-Moghari, S.-M., Liu, X., Gebremicael, T. G., Leng, G., Kebede, A., Xu, X., and Yun, X., (2020). Projected Impacts of Climate Change on Drought Patterns Over East Africa. *Earth's Future*, 8(7):e2020EF001502. doi: 10.1029/2020EF001502. URL https://doi.org/10.1029/2020EF001502.

Handfield, R., Walton, S. V., Sroufe, R., and Melnyk, S. A., (2002). Applying environmental criteria to supplier assessment: A study in the application of the Analytical Hierarchy Process. *European Journal of Operational Research*, 141(1):70–87. ISSN 0377-2217. doi: 10.1016/S0377-2217(01)00261-2. URL https://www.sciencedirect.com/science/article/pii/S0377221701002612.

Hansen, M. C., Potapov, P. V., Moore, R., Hancher, M., Turubanova, S. A., Tyukavina, A., Thau, D., Stehman, S. V., Goetz, S. J., Loveland, T. R., Kommareddy, A., Egorov, A., Chini, L., Justice, C. O., and Townshend, J. R. G., (2013). High-Resolution Global Maps of 21st-Century Forest Cover Change. *Science*, 342(6160):850–853. ISSN 0036-8075, 1095-9203. doi: 10.1126/science.1244693. URL https://www.science.org/doi/10.1126/science.1244693. https://creativecommons.org/licenses/by/4.0/.

Hatfield, J. L., Boote, K. J., Kimball, B. A., Ziska, L. H., Izaurralde, R. C., Ort, D., Thomson, A. M., and Wolfe, D., (2011). Climate Impacts on Agriculture: Implications for Crop Production. *Agronomy Journal*, 103(2):351–370. ISSN 0002-1962, 1435-0645. doi: 10.2134/agronj2010.0303. URL https://acsess.onlinelibrary.wiley.com/doi/10.2134/agronj2010.0303.

Hengl, T., Mendes De Jesus, J., Heuvelink, G. B. M., Ruiperez Gonzalez, M., Kilibarda, M., Blagotić, A., Shangguan, W., Wright, M. N., Geng, X., Bauer-Marschallinger, B., Guevara, M. A., Vargas, R., MacMillan, R. A., Batjes, N. H., Leenaars, J. G. B., Ribeiro, E., Wheeler, I., Mantel, S., and Kempen, B., (2017). SoilGrids250m: Global gridded soil information based on machine learning. *PLOS ONE*, 12(2):e0169748. ISSN 1932-6203. doi: 10.1371/journal.pone.0169748. URL https://dx.plos.org/10.1371/journal.pone.0169748.

Hevner, A. R., March, S. T., Park, J., and Ram, S., (2004). Design Science in Information Systems Research1. *MIS Quarterly*, 28(1):75–106. ISSN 0276-7783, 2162-9730. doi: 10.2307/25148625. URL https://misq.umn.edu/misq/article/28/1/75/261/Design-Science-in-Information-Systems-Research1.

Ho, W., Zheng, T., Yildiz, H., and Talluri, S., (2015). Supply chain risk management: a literature review. *International Journal of Production Research*, 53(16):5031–5069. ISSN 0020-7543, 1366-588X. doi: 10.1080/00207543.2015.1030467. URL http://www.tandfonline.com/doi/full/10.1080/00207543.2015.1030467.

Hoekstra, A. Y., Chapagain, A. K., Aldaya, M. M., and Mekonnen, M. M., (2011). *The water footprint assessment manual: setting the global standard*. Earthscan from Routledge, London Washington, D.C. ISBN 9781849712798 9781849775526 9781136538476 9781136538513 9781136538520.

Hofmann, H., Busse, C., Bode, C., and Henke, M., (2014). Sustainability-Related Supply Chain Risks: Conceptualization and Management. *Business Strategy and the Environment*, 23(3):160–172. ISSN 0964-4733, 1099-0836. doi: 10.1002/bse.1778. URL https://onlinelibrary.wiley.com/doi/10.1002/bse.1778.

Holsapple, C. W., (2008). DSS Architecture and Types. In *Handbook on Decision Support Systems 1*, pages 163–189. Springer Berlin Heidelberg, Berlin, Heidelberg. ISBN 978-3-540-48712-

8 978-3-540-48713-5. doi: 10.1007/978-3-540-48713-5_9. URL http://link.springer.com/10.1007/978-3-540-48713-5_9.

IFPRI, (2026). Global Spatially-Disaggregated Crop Production Statistics Data for 2020 Version 2.0 Release 2. URL https://mapspam.info/. https://creativecommons.org/licenses/by/4.0/.

Intergovernmental Panel On Climate Change, (2022). *Climate Change and Land: IPCC Special Report on Climate Change, Desertification, Land Degradation, Sustainable Land Management, Food Security, and Greenhouse Gas Fluxes in Terrestrial Ecosystems*. Cambridge University Press, 1 edition. ISBN 978-1-009-15798-8 978-1-009-15801-5. doi: 10.1017/9781009157988. URL https://www.cambridge.org/core/product/identifier/9781009157988/type/book.

Intergovernmental Panel On Climate Change (Ipcc), (2023). *Climate Change 2022 – Impacts, Adaptation and Vulnerability: Working Group II Contribution to the Sixth Assessment Report of the Intergovernmental Panel on Climate Change*. Cambridge University Press, 1 edition. ISBN 978-1-009-32584-4. doi: 10.1017/9781009325844. URL https://www.cambridge.org/core/product/identifier/9781009325844/type/book.

ISO, (2018). ISO 31000:2018 Risk management – Guidelines. Standard ISO 31000:2018, International Organization for Standardization, Geneva, Switzerland. URL https://www.iso.org/standard/65694.html.

Jahre, M. and Heigh, I., (2008). Does the Current Constraints in Funding Promote Failure in Humanitarian Supply Chains? *Supply Chain Forum: An International Journal*, 9(2):44–54. ISSN 1625-8312, 1624-6039. doi: 10.1080/16258312.2008.11517198. URL https://www.tandfonline.com/doi/full/10.1080/16258312.2008.11517198.

Jahre, M. and Jensen, L., (2010). Coordination in humanitarian logistics through clusters. *International Journal of Physical Distribution & Logistics Management*, 40(8/9):657–674. ISSN 0960-0035. doi: 10.1108/09600031011079319. URL http://www.emerald.com/ijpdlm/article/40/8-9/657-674/161755.

Jahre, M., Pazirandeh, A., and Van Wassenhove, L., (2016). Defining logistics preparedness: a framework and research agenda. *Journal of Humanitarian Logistics and Supply Chain Management*, 6(3):372–398. ISSN 2042-6747. doi: 10.1108/JHLSCM-04-2016-0012. URL http://www.emerald.com/jhlscm/article/6/3/372-398/213544.

Jwaideh, M. A. A. and Dalin, C., (2025). The multi-dimensional environmental impact of global crop commodities. *Nature Sustainability*, 8(4):396–410. ISSN 2398-9629. doi: 10.1038/s41893-025-01528-6. URL https://www.nature.com/articles/s41893-025-01528-6.

Kaplan, S. and Garrick, B. J., (1981). On The Quantitative Definition of Risk. *Risk Analysis*, 1(1):11–27. ISSN 0272-4332, 1539-6924. doi: 10.1111/j.1539-6924.1981.tb01350.x. URL https://onlinelibrary.wiley.com/doi/10.1111/j.1539-6924.1981.tb01350.x.

Kembro, J., Kunz, N., Frennesson, L., and Vega, D., (2024). Revisiting the definition of humanitarian logistics. *Journal of Business Logistics*, 45(2):e12376. ISSN 0735-3766, 2158-1592. doi: 10.1111/jbl.12376. URL https://onlinelibrary.wiley.com/doi/10.1111/jbl.12376.

Kern, D., Moser, R., Hartmann, E., and Moder, M., (2012). Supply risk management: model development and empirical analysis. *International Journal of Physical Distribution & Logistics Management*, 42(1):60–82. ISSN 0960-0035. doi: 10.1108/09600031211202472. URL http://www.emerald.com/ijpdlm/article/42/1/60-82/162688.

Khan, I., Sohail, Zaman, S., Li, G., and Fu, M., (2025). Adaptive responses of plants to light stress: mechanisms of photoprotection and acclimation. A review. *Frontiers in Plant Science*, 16:1550125. ISSN 1664-462X. doi: 10.3389/fpls.2025.1550125. URL https://www.frontiersin.org/articles/10.3389/fpls.2025.1550125/full.

Kimaro, D., Poesen, J., Msanya, B., and Deckers, J., (2008). Magnitude of soil erosion on the northern slope of the Uluguru Mountains, Tanzania: Interrill and rill erosion. *Catena*, 75(1): 38–44. doi: 10.1016/j.catena.2008.04.007.

Kovács, G. and Spens, K. M., (2007). Humanitarian logistics in disaster relief operations. *International Journal of Physical Distribution & Logistics Management*, 37(2):99–114. ISSN 0960-0035. doi: 10.1108/09600030710734820. URL http://www.emerald.com/ijpdlm/article/37/2/99-114/162643.

Kraljic, P., (1983). Purchasing Must Become Supply Management. *Harvard Business Review*, 61 (5):109–117. URL https://hbr.org/1983/09/purchasing-must-become-supply-management.

Kuzma, S., Bierkens, M. F., Lakshman, S., Luo, T., Saccoccia, L., Sutanudjaja, E. H., and Van Beek, R., (2023). Aqueduct 4.0: Updated Decision-Relevant Global Water Risk Indicators. *World Resources Institute*. doi: 10.46830/writn.23.00061. URL https://www.wri.org/research/aqueduct-40-updated-decision-relevant-global-water-risk-indicators?auHash=74cRjEQPsHONDpgT1NqIfNpqV-QpYNR4oiPo1HRhpGs.

Lal, R., (2004). Soil Carbon Sequestration Impacts on Global Climate Change and Food Security. *Science*, 304(5677):1623–1627. ISSN 0036-8075, 1095-9203. doi: 10.1126/science.1097396. URL https://www.science.org/doi/10.1126/science.1097396.

Lesk, C., Rowhani, P., and Ramankutty, N., (2016). Influence of extreme weather disasters on global crop production. *Nature*, 529(7584):84–87. ISSN 0028-0836, 1476-4687. doi: 10.1038/nature16467. URL https://www.nature.com/articles/nature16467.

Little, J. D. C., (1970). Models and Managers: The Concept of a Decision Calculus. *Management Science*, 16(8):B–466–B–485. ISSN 0025-1909, 1526-5501. doi: 10.1287/mnsc.16.8.B466. URL https://pubsonline.informs.org/doi/10.1287/mnsc.16.8.B466.

Loveland, P., (2003). Is there a critical level of organic matter in the agricultural soils of temperate regions: a review. *Soil and Tillage Research*, 70(1):1–18. ISSN 01671987. doi: 10.1016/S0167-1987(02)00139-3. URL https://linkinghub.elsevier.com/retrieve/pii/S0167198702001393.

Ludemann, C. I., Wanner, N., Chivenge, P., Dobermann, A., Einarsson, R., Grassini, P., Gruere, A., Jackson, K., Lassaletta, L., Maggi, F., Obli-Laryea, G., Van Ittersum, M. K., Vishwakarma, S., Zhang, X., and Tubiello, F. N., (2024). A global FAOSTAT reference database of cropland nutrient budgets and nutrient use efficiency (1961–2020): nitrogen, phosphorus and potassium. *Earth System Science Data*, 16(1):525–541. ISSN 1866-3516. doi: 10.5194/essd-16-525-2024. URL https://essd.copernicus.org/articles/16/525/2024/.

Marhavilas, P., Koulouriotis, D., and Gemeni, V., (2011). Risk analysis and assessment methodologies in the work sites: On a review, classification and comparative study of the scientific literature of the period 2000–2009. *Journal of Loss Prevention in the Process Industries*, 24(5): 477–523. ISSN 09504230. doi: 10.1016/j.jlp.2011.03.004. URL https://linkinghub.elsevier.com/retrieve/pii/S0950423011000325.

Meier, U., editor, (2001). *Growth stages of mono-and dicotyledonous plants: BBCH Monograph*. Federal Biological Research Centre for Agriculture and Forestry, Braunschweig, Germany, 2 edition.

Mekonnen, M. M. and Hoekstra, A. Y., (2011). The green, blue and grey water footprint of crops and derived crop products. *Hydrology and Earth System Sciences*, 15(5):1577–1600. ISSN 1607-7938. doi: 10.5194/hess-15-1577-2011. URL https://hess.copernicus.org/articles/15/1577/2011/.

Miller, M. A. E., Shepherd, K. D., Kisitu, B., and Collinson, J., (2021). iSDAsoil: The first continent-scale soil property map at 30 m resolution provides a soil information revolution for Africa. *PLOS Biology*, 19(11):e3001441. ISSN 1545-7885. doi: 10.1371/journal.pbio.3001441. URL https://dx.plos.org/10.1371/journal.pbio.3001441.

Mir, S. A. and Quadri, S. M. K., (2009). Decision Support Systems: Concepts, Progress and Issues – A Review. In Lichtfouse, E., editor, *Climate Change, Intercropping, Pest Control and Beneficial Microorganisms*, pages 373–399. Springer Netherlands, Dordrecht. ISBN 978-90-481-2715-3 978-90-481-2716-0. doi: 10.1007/978-90-481-2716-0_13. URL http://link.springer.com/10.1007/978-90-481-2716-0_13.

Miro, B. and Ismail, A. M., (2013). Tolerance of anaerobic conditions caused by flooding during germination and early growth in rice (Oryza sativa L.). *Frontiers in Plant Science*, 4. ISSN 1664-462X. doi: 10.3389/fpls.2013.00269. URL http://journal.frontiersin.org/article/10.3389/fpls.2013.00269/abstract.

Mittler, R., (2006). Abiotic stress, the field environment and stress combination. *Trends in Plant Science*, 11(1):15–19. ISSN 13601385. doi: 10.1016/j.tplants.2005.11.002. URL https://linkinghub.elsevier.com/retrieve/pii/S1360138505002918.

Montgomery, D. R., (2007). Soil erosion and agricultural sustainability. *Proceedings of the National Academy of Sciences*, 104(33):13268–13272. ISSN 0027-8424, 1091-6490. doi: 10.1073/pnas.0611508104. URL https://pnas.org/doi/full/10.1073/pnas.0611508104.

Moshtari, M., Altay, N., Heikkilä, J., and Gonçalves, P., (2021). Procurement in humanitarian organizations: Body of knowledge and practitioner's challenges. *International Journal* *of Production Economics*, 233:108017. ISSN 09255273. doi: 10.1016/j.ijpe.2020.108017. URL https://linkinghub.elsevier.com/retrieve/pii/S0925527320303662.

Muñoz Sabater, J., (2019). ERA5-Land monthly averaged data from 1950 to present.

Ngoune Tandzi, L. and Mutengwa, C. S., (2020). Factors Affecting Yield of Crops. In Amanullah, editor, *Agronomy - Climate Change and Food Security*. IntechOpen. ISBN 978-1-83881-222-5 978-1-83881-223-2. doi: 10.5772/intechopen.90672. URL https://www.intechopen.com/books/agronomy-climate-change-food-security/factors-affecting-yield-of-crops.

Nguyen, C. T., Vačkářová, D., and Weinzettel, J., (2025). Consistent global dataset on biodiversity intactness footprint of agricultural production from 2000 to 2020. *Scientific Data*, 12 (1):1613. ISSN 2052-4463. doi: 10.1038/s41597-025-05901-0. URL https://www.nature.com/articles/s41597-025-05901-0.

Näslund, D., Kale, R., and Paulraj, A., (2010). ACTION RESEARCH IN SUPPLY CHAIN MANAGEMENT—A FRAMEWORK FOR RELEVANT AND RIGOROUS RESEARCH. *Journal of Business Logistics*, 31(2):331–355. ISSN 0735-3766, 2158-1592. doi: 10.1002/j.2158-1592.2010.tb00155.x. URL https://onlinelibrary.wiley.com/doi/10.1002/j.2158-1592.2010.tb00155.x.

Oliveira, F. N. D., Leiras, A., and Ceryno, P., (2019). Environmental risk management in supply chains: A taxonomy, a framework and future research avenues. *Journal of Cleaner Production*, 232:1257–1271. ISSN 09596526. doi: 10.1016/j.jclepro.2019.06.032. URL https://linkinghub.elsevier.com/retrieve/pii/S0959652619319857.

Olsson, L., Barbosa, H., Bhadwal, S., Cowie, A., Delusca, K., and others, (2019). Land Degradation. In Shukla, P. R., Skea, J., Calvo Buendia, E., and others, editors, *Climate Change and Land: IPCC Special Report on Climate Change, Desertification, Land Degradation, Sustainable Land Management, Food Security, and Greenhouse Gas Fluxes in Terrestrial Ecosystems*, pages 345–436. Cambridge University Press, Cambridge, UK and New York, NY, USA. doi: 10.1017/9781009157988.006.

Omokpariola, D. O., Agbanu-Kumordzi, C., Samuel, T., Kiswii, L., Moses, G. S., and Adelegan, A. M., (2025). Climate change, crop yield, and food security in Sub-Saharan Africa. *Discover Sustainability*, 6(1):678. ISSN 2662-9984. doi: 10.1007/s43621-025-01580-4. URL https://link.springer.com/10.1007/s43621-025-01580-4.

Pagell, M., Wu, Z., and Wasserman, M. E., (2010). THINKING DIFFERENTLY ABOUT PURCHASING PORTFOLIOS: AN ASSESSMENT OF SUSTAINABLE SOURCING: Thinking Differently about Purchasing Portfolios. *Journal of Supply Chain Management*, 46(1): 57–73. ISSN 15232409, 1745493X. doi: 10.1111/j.1745-493X.2009.03186.x. URL https://onlinelibrary.wiley.com/doi/10.1111/j.1745-493X.2009.03186.x.

Pan, T., Wang, Y., Wang, L., Ding, J., Cao, Y., Qin, G., Yan, L., Xi, L., Zhang, J., and Zou, Z., (2020). Increased CO_2 and light intensity regulate growth and leaf gas exchange in tomato.

Physiologia Plantarum, 168(3):694–708. ISSN 0031-9317, 1399-3054. doi: 10.1111/ppl.13015. URL https://onlinelibrary.wiley.com/doi/10.1111/ppl.13015.

Peffers, K., Tuunanen, T., Rothenberger, M. A., and Chatterjee, S., (2007). A Design Science Research Methodology for Information Systems Research. *Journal of Management Information Systems*, 24(3):45–77. ISSN 0742-1222, 1557-928X. doi: 10.2753/MIS0742-1222240302. URL https://www.tandfonline.com/doi/full/10.2753/MIS0742-1222240302.

Pereira, P., Inacio, M., Barcelo, D., and Zhao, W., (2025). Impacts of agriculture intensification on biodiversity loss, climate change and ecosystem services. *Current Opinion in Environmental Science & Health*, 46:100637. ISSN 24685844. doi: 10.1016/j.coesh.2025.100637. URL https://linkinghub.elsevier.com/retrieve/pii/S2468584425000467.

Pfister, S., (2021). Crop-country specific AWARE water scarcity factors for 160 crops and global coverage. URL https://data.mendeley.com/datasets/2x8z6sw249/1 [Accessed 2026-05-26]. https://creativecommons.org/licenses/by/4.0/.

Pfister, S. and Bayer, P., (2025). Water consumption of crop on watershed level (blue and green water, uncertainty, incl. shapefile) and monthly irrigation water consumption. URL https://data.mendeley.com/datasets/brn4xm47jk/4 [Accessed 2026-05-17]. https://creativecommons.org/licenses/by/4.0/.

Polyviou, M., Ramos, G., and Schneller, E., (2022). Supply Chain Risk Management: An Enterprise View and a Survey of Methods. In Khojasteh, Y., Xu, H., and Zolfaghari, S., editors, *Supply Chain Risk Mitigation*, volume 332, pages 27–58. Springer International Publishing, Cham. ISBN 978-3-031-09182-7 978-3-031-09183-4. doi: 10.1007/978-3-031-09183-4_2. URL https://link.springer.com/10.1007/978-3-031-09183-4_2. Series Title: International Series in Operations Research & Management Science.

Pontré, J., Welter, V., Veiga Malta, J. N., Faria, I., and Chernyshova, A., (2011). Risk management in humanitarian procurement and supply chain. *Journal of Public Procurement*, 11(3): 301–322. ISSN 1535-0118. doi: 10.1108/JOPP-11-03-2011-B001. URL http://www.emerald.com/jopp/article/11/3/301-322/233054.

Power, D. J., (2002). *Decision support systems: concepts and resources for managers*. Quorum Books, Westport, Conn., 1. publ edition. ISBN 978-1-56720-497-1 978-0-387-23174-7.

Reynolds, T. W., Waddington, S. R., Anderson, C. L., Chew, A., True, Z., and Cullen, A., (2015). Environmental impacts and constraints associated with the production of major food crops in Sub-Saharan Africa and South Asia. *Food Security*, 7(4):795–822. ISSN 1876-4517, 1876-4525. doi: 10.1007/s12571-015-0478-1. URL http://link.springer.com/10.1007/s12571-015-0478-1.

Rowhani, P., Lobell, D. B., Linderman, M., and Ramankutty, N., (2011). Climate variability and crop production in Tanzania. *Agricultural and Forest Meteorology*, 151(4):449–460. ISSN 01681923. doi: 10.1016/j.agrformet.2010.12.002. URL https://linkinghub.elsevier.com/retrieve/pii/S0168192310003357.

Saaty, T. L., (1990). How to make a decision: The analytic hierarchy process. *European Journal of Operational Research*, 48(1):9–26. ISSN 03772217. doi: 10.1016/0377-2217(90)90057-I. URL https://linkinghub.elsevier.com/retrieve/pii/037722179090057I.

Sadras, V. O., Villalobos, F. J., and Fereres, E., (2016). Crop Development and Growth. In Villalobos, F. J. and Fereres, E., editors, *Principles of Agronomy for Sustainable Agriculture*, pages 141–158. Springer International Publishing, Cham. ISBN 978-3-319-46115-1 978-3-319-46116-8. doi: 10.1007/978-3-319-46116-8_11. URL http://link.springer.com/10.1007/978-3-319-46116-8_11.

Saisana, M. and Tarantola, S., (2016). State-of-the-art report on current methodologies and practices for composite indicator development. URL https://www.researchgate.net/doi/10.13140/RG.2.1.1505.1762 [Accessed 2026-05-17].

Salehi Heidari, S., Khanbabaei, M., and Sabzehparvar, M., (2018). A model for supply chain risk management in the automotive industry using fuzzy analytic hierarchy process and fuzzy TOPSIS. *Benchmarking: An International Journal*, 25(9):3831–3857. ISSN 1463-5771. doi: 10.1108/BIJ-11-2016-0167. URL https://doi.org/10.1108/BIJ-11-2016-0167.

Saltelli, A., (2007). Composite Indicators between Analysis and Advocacy. *Social Indicators Research*, 81(1):65–77. ISSN 0303-8300, 1573-0921. doi: 10.1007/s11205-006-0024-9. URL http://link.springer.com/10.1007/s11205-006-0024-9.

Samani, Z., (2014). Evaluating and Managing Crops Water Requirement. In Pessarakli, M., editor, *Handbook of Plant and Crop Physiology*, pages 209–222. CRC Press, 0 edition. ISBN 978-0-429-09788-1. doi: 10.1201/b16675-13. URL https://www.taylorfrancis.com/books/9781466553293/chapters/10.1201/b16675-13.

Sarraf, M. and Silva, M.Ravina da , (2020). The hidden value of Benin's forests. URL https://blogs.worldbank.org/en/nasikiliza/hidden-value-benins-forests [Accessed 2026-06-03].

Saunders, M., Thornhill, A., and Lewis, P., (2019). *Research methods for business students*. Pearson, Harlow, United Kingdom, eigth edition edition. ISBN 978-1-292-20878-7 978-1-292-20879-4.

Sein, M. K., Henfridsson, O., Purao, S., Rossi, M., and Lindgren, R., (2011). Action Design Research1. *MIS Quarterly*, 35(1):37–56. ISSN 0276-7783, 2162-9730. doi: 10.2307/23043488. URL https://misq.umn.edu/misq/article/35/1/37/1434/Action-Design-Research1.

Shim, J., Warkentin, M., Courtney, J. F., Power, D. J., Sharda, R., and Carlsson, C., (2002). Past, present, and future of decision support technology. *Decision Support Systems*, 33(2):111–126. ISSN 01679236. doi: 10.1016/S0167-9236(01)00139-7. URL https://linkinghub.elsevier.com/retrieve/pii/S0167923601001397.

Sims, M. J., Stanimirova, R., Raichuk, A., Neumann, M., Richter, J., Follett, F., MacCarthy, J., Lister, K., Randle, C., Sloat, L., Esipova, E., Jupiter, J., Stanton, C., Morris, D., Melhart Slay, C., Purves, D., and Harris, N., (2025). Global drivers of forest loss at 1 km resolution. *Environmental Research Letters*, 20(7):074027. ISSN 1748-9326. doi: 10.1088/1748-9326/add606. URL https://iopscience.iop.org/article/10.1088/1748-9326/add606. https://creativecommons.org/licenses/by/4.0/.

Singh, B., (2023). Managing Biotic Stress in Agriculture Strategies, Solutions, and Emerging Technologies. In *Modern Agriculture: Exploring Current Trends*. BS Global Publication House. ISBN 978-81-964973-5-4.

Slovic, P., Finucane, M. L., Peters, E., and MacGregor, D. G., (2004). Risk as Analysis and Risk as Feelings: Some Thoughts about Affect, Reason, Risk, and Rationality. *Risk Analysis*, 24(2):311–322. ISSN 0272-4332, 1539-6924. doi: 10.1111/j.0272-4332.2004.00433.x. URL https://onlinelibrary.wiley.com/doi/10.1111/j.0272-4332.2004.00433.x.

Sprague, R. and Carlson, E., (1982). *Building Effective Decision Support Systems*. Grolier computer sciences library. Prentice-Hall. ISBN 978-0-13-086215-0. URL https://books.google.se/books?id=89_sPTAmkVsC.

Swann, A. L. S., Hoffman, F. M., Koven, C. D., and Randerson, J. T., (2016). Plant responses to increasing CO_2 reduce estimates of climate impacts on drought severity. *Proceedings of the National Academy of Sciences*, 113(36):10019–10024. ISSN 0027-8424, 1091-6490. doi: 10.1073/pnas.1604581113. URL https://pnas.org/doi/full/10.1073/pnas.1604581113.

Tang, C. S., (2006). Perspectives in supply chain risk management. *International Journal of Production Economics*, 103(2):451–488. ISSN 09255273. doi: 10.1016/j.ijpe.2005.12.006. URL https://linkinghub.elsevier.com/retrieve/pii/S0925527306000405.

Tay, H. L., Loh, H. S., and Chen, H. S., (2025). Exploring humanitarian procurement: a systematic review. *Cogent Business & Management*, 12(1):2445182. ISSN 2331-1975. doi: 10.1080/23311975.2024.2445182. URL https://www.tandfonline.com/doi/full/10.1080/23311975.2024.2445182.

Tchonkouang, R. D., Onyeaka, H., and Nkoutchou, H., (2024). Assessing the vulnerability of food supply chains to climate change-induced disruptions. *Science of The Total Environment*, 920:171047. ISSN 00489697. doi: 10.1016/j.scitotenv.2024.171047. URL https://linkinghub.elsevier.com/retrieve/pii/S0048969724011860.

Thakur-Weigold, B., Parsa, I., Balcik, B., and Van Wassenhove, L. N., (2025). Purchasing and supply management in humanitarian settings. *Journal of Purchasing and Supply Management*, 31(3):100975. ISSN 14784092. doi: 10.1016/j.pursup.2024.100975. URL https://linkinghub.elsevier.com/retrieve/pii/S1478409224000840.

Tomasini, R. M. and Van Wassenhove, L. N., (2009). From preparedness to partnerships: case study research on humanitarian logistics. *International Transactions in Operational Research*, 16(5):549–559. ISSN 0969-6016, 1475-3995. doi: 10.1111/j.1475-3995.2009.00697.x. URL https://onlinelibrary.wiley.com/doi/10.1111/j.1475-3995.2009.00697.x.

Tummala, R. and Schoenherr, T., (2011). Assessing and managing risks using the Supply Chain Risk Management Process (SCRMP). *Supply Chain Management: An International Journal*, 16(6):474–483. ISSN 1359-8546. doi: 10.1108/13598541111171165. URL http://www.emerald.com/scm/article/16/6/474-483/446818.

United Nations Office for Disaster Risk Reduction, (2016). Report of the open-ended intergovernmental expert working group on indicators and terminology relating to disaster risk reduction. Technical Report A/71/644, United Nations General Assembly, Geneva, Switzerland. URL https://www.undrr.org/publication/report-open-ended-intergovernmental-expert-working-group-indicators-and-terminology.

Van Wassenhove, L. N., (2006). Humanitarian aid logistics: supply chain management in high gear. *Journal of the Operational Research Society*, 57(5):475–489. ISSN 0160-5682, 1476-9360. doi: 10.1057/palgrave.jors.2602125. URL https://www.tandfonline.com/doi/full/10.1057/palgrave.jors.2602125.

Vicente-Serrano, S. M., Beguería, S., and López-Moreno, J. I., (2010). A Multiscalar Drought Index Sensitive to Global Warming: The Standardized Precipitation Evapotranspiration Index. *Journal of Climate*, 23(7):1696–1718. ISSN 1520-0442, 0894-8755. doi: 10.1175/2009JCLI2909.1. URL http://journals.ametsoc.org/doi/10.1175/2009JCLI2909.1.

Vinnem, J.-E., (2014). *Offshore Risk Assessment vol 1.* Springer Series in Reliability Engineering. Springer London, London. ISBN 978-1-4471-5206-4 978-1-4471-5207-1. doi: 10.1007/978-1-4471-5207-1. URL http://link.springer.com/10.1007/978-1-4471-5207-1.

Wang, L., Cheng, Y., and Wang, Z., (2022). Risk management in sustainable supply chain: a knowledge map towards intellectual structure, logic diagram, and conceptual model. *Environmental Science and Pollution Research*, 29(44):66041–66067. ISSN 0944-1344, 1614-7499. doi: 10.1007/s11356-022-22255-x. URL https://link.springer.com/10.1007/s11356-022-22255-x.

Ward, P. J., Winsemius, H. C., Kuzma, S., Bierkens, M. F. P., Bouwman, A., Moel, H.de , Díaz Loaiza, A., Eilander, D., Englhardt, J., Erkens, G., Gebremedhin, E. T., Iceland, C., Kooi, H., Ligtvoet, W., Muis, S., Scussolini, P., Sutanudjaja, E. H., Beek, R.van , Bemmel, B.van , Huijstee, J.van , Rijn, F.van , Wesenbeeck, B.van , Vatvani, D., Verlaan, M., Tiggeloven, T., and Luo, T., (2020). Aqueduct Floods Methodology. Technical Note, World Resources Institute, Washington, D.C. URL https://www.wri.org/publication/aqueduct-floods-methodology.

Weele, A. J. v. and Rozemeijer, F., (2022). *Procurement and supply chain management*. Cengage, Andover, UK, eighth edition edition. ISBN 978-1-4737-7911-2.

Weil, R. and Brady, N., (2017). *The Nature and Properties of Soils. 15th edition.* Pearson Education. ISBN 978-0-13-325448-8.

WFP, (2021). Strategic plan 2022 - 2025: Executive summary. Technical Report WFP/EB.2/2021/4-A/1/Rev.2, World Food Programme, Rome.

WFP, (2024). WFP's Updated Climate Change Policy - 2024. Technical Report WFP/EB.1/2024/4, World Food Programme, Rome. URL https://www.wfp.org/publications/wfps-updated-climate-change-policy-2024.

WFP, (2026a). Eco-DASH: Giving our supply chain a greener future. Technical report, World Food Programme Innovation Accelerator, Munich, Germany. URL https://innovation.wfp.org/project/ecodash. WFP.

WFP, (2026b). Ending hunger. URL https://www.wfp.org/ending-hunger [Accessed 2026-05-17]. WFP.

Wheeler, T. and Von Braun, J., (2013). Climate Change Impacts on Global Food Security. *Science*, 341(6145):508–513. ISSN 0036-8075, 1095-9203. doi: 10.1126/science.1239402. URL https://www.science.org/doi/10.1126/science.1239402.

Winowiecki, L., Vågen, T.-G., and Huising, J., (2016). Effects of land cover on ecosystem services in Tanzania: A spatial assessment of soil organic carbon. *Geoderma*, 263:274–283. ISSN 00167061. doi: 10.1016/j.geoderma.2015.03.010. URL https://linkinghub.elsevier.com/retrieve/pii/S0016706115000816.

Winsemius, H. C., Van Beek, L. P. H., Jongman, B., Ward, P. J., and Bouwman, A., (2013). A framework for global river flood risk assessments. *Hydrology and Earth System Sciences*, 17(5): 1871–1892. ISSN 1607-7938. doi: 10.5194/hess-17-1871-2013. URL https://hess.copernicus.org/articles/17/1871/2013/.

World Meteorological Organization, (2017). *WMO Guidelines on the Calculation of Climate Normals*. World Meteorological Organization, Geneva, Switzerland, 2017 edition edition. ISBN 978-92-63-11203-3. URL https://public.wmo.int/en/resources/meteoterm.

Xu, M., Cui, Y., Hu, M., Xu, X., Zhang, Z., Liang, S., and Qu, S., (2019). Supply chain sustainability risk and assessment. *Journal of Cleaner Production*, 225:857–867. ISSN 09596526. doi: 10.1016/j.jclepro.2019.03.307. URL https://linkinghub.elsevier.com/retrieve/pii/S0959652619310236.

Yali, W. and Begna, T., (2022). Crops Production and Factors Limiting the Yield. doi: 10.4172/2329-8863.1000537.

Yao, R., Wang, L., Huang, X., Cao, Q., Wei, J., He, P., Wang, S., and Wang, L., (2023). Global seamless and high-resolution temperature dataset (GSHTD), 2001–2020. *Remote Sensing of Environment*, 286:113422. ISSN 00344257. doi: 10.1016/j.rse.2022.113422. URL https://linkinghub.elsevier.com/retrieve/pii/S0034425722005284.

Yin, R. K., (2014). *Case study research: design and methods*. SAGE, Los Angeles, fifth edition edition. ISBN 978-1-4522-4256-9.

You, L., Wood, S., Wood-Sichra, U., and Wu, W., (2014). Generating global crop distribution maps: From census to grid. *Agricultural Systems*, 127:53–60. ISSN 0308521X. doi: 10.1016/j.agsy.2014.01.002. URL https://linkinghub.elsevier.com/retrieve/pii/S0308521X14000110.

Zhang, H., Zhu, J., Gong, Z., and Zhu, J.-K., (2022). Abiotic stress responses in plants. *Nature Reviews Genetics*, 23(2):104–119. ISSN 1471-0056, 1471-0064. doi: 10.1038/s41576-021-00413-0. URL https://www.nature.com/articles/s41576-021-00413-0.

A SPAM 2020 Crop Coverage

Table A.1 lists all 46 crops included in the Spatial Production Allocation Model (SPAM 2020, Version 2.0), together with their internal crop codes used throughout the scripts in *Chapter B*.

ID	Code	Crop	ID	Code	Crop
1	whea	Wheat	24	sunf	Sunflower
2	rice	Rice	25	rape	Rapeseed
3	maiz	Maize	26	sesa	Sesame seed
4	barl	Barley	27	ooil	Other oil crops
5	mill	Small millet	28	sugc	Sugarcane
6	pmil	Pearl millet	29	sugb	Sugar beet
7	sorg	Sorghum	30	cott	Cotton
8	ocer	Other cereals	31	ofib	Other fibre crops
9	pota	Potato	32	coff	Arabica coffee
10	swpo	Sweet potato	33	rcof	Robusta coffee
11	yams	Yams	34	coco	Cocoa
12	cass	Cassava	35	teas	Tea
13	orts	Other roots	36	toba	Tobacco
14	bean	Bean	37	bana	Banana
15	chic	Chickpea	38	plnt	Plantain
16	cowp	Cowpea	39	citr	Citrus
17	pige	Pigeon pea	40	trof	Other tropical fruit
18	lent	Lentil	41	temf	Temperate fruit
19	opul	Other pulses	42	toma	Tomato
20	soyb	Soybean	43	onio	Onion
21	grou	Groundnut	44	vege	Other vegetables
22	cnut	Coconut	45	rubb	Rubber
23	oilp	Oil palm	46	rest	Rest of crops

Table A.1: All 46 crops included in SPAM 2020 Version 2.0, with their internal crop codes.

B Google Earth Engine Scripts

The following scripts were used to compute the environmental sourcing risk indicators in Google Earth Engine. All scripts use SPAM 2020 production volume as spatial weight and the WMO 1991–2020 climatological reference period where applicable.

B.1 Temperature

```
// ============================================================
// TEMPERATURE INDICATOR - Maize (Tc = 45 degrees C)
// Tanzania (TZA) and Benin (BEN)
// WMO reference period: 1991-2020
// Weight: SPAM 2020 production volume (P_MAIZ_A)
// ============================================================
var countries = ee.FeatureCollection('USDOS/LSIB_SIMPLE/2017');
var tanzania  = countries.filter(ee.Filter.eq('country_na', 'Tanzania'));
var benin     = countries.filter(ee.Filter.eq('country_na', 'Benin'));

var maiz_A     = ee.Image('projects/exjobb-490711/assets/spam2020_V2r2_global_P_MAIZ_A');
var maiz_A_TZA = maiz_A.clip(tanzania);
var maiz_A_BEN = maiz_A.clip(benin);
var mask_TZA   = maiz_A_TZA.gt(0);
var mask_BEN   = maiz_A_BEN.gt(0);

var Tc = 45 + 273.15; // Kelvin

// --- Pixel-level heat stress fraction (mean across 1991-2020) ---
var T_pixel = ee.ImageCollection('ECMWF/ERA5_LAND/DAILY_AGGR')
  .select('temperature_2m_max')
  .filter(ee.Filter.date('1991-01-01', '2020-12-31'))
  .map(function(img) { return img.gt(Tc).rename('heat_stress'); })
  .mean().rename('T_pixel');

var T_pixel_TZA = T_pixel.updateMask(mask_TZA);
var T_pixel_BEN = T_pixel.updateMask(mask_BEN);

// --- Production-weighted mean ---
var T_ck_TZA = T_pixel_TZA.multiply(maiz_A_TZA)
  .reduceRegion({reducer: ee.Reducer.sum(), geometry: tanzania, scale: 9280, maxPixels: 1e9})
  .getNumber('T_pixel')
  .divide(maiz_A_TZA.updateMask(mask_TZA)
    .reduceRegion({reducer: ee.Reducer.sum(), geometry: tanzania, scale: 9280, maxPixels: 1e9}).getNumber('b1'));

var T_ck_BEN = T_pixel_BEN.multiply(maiz_A_BEN)
  .reduceRegion({reducer: ee.Reducer.sum(), geometry: benin, scale: 9280, maxPixels: 1e9})
  .getNumber('T_pixel')
  .divide(maiz_A_BEN.updateMask(mask_BEN)
    .reduceRegion({reducer: ee.Reducer.sum(), geometry: benin, scale: 9280, maxPixels: 1e9}).getNumber('b1'));

// --- Annual max temp validation ---
var years = ee.List.sequence(1991, 2020);
var annualRows = years.map(function(y) {
  y = ee.Number(y);
  var col = ee.ImageCollection('ECMWF/ERA5_LAND/DAILY_AGGR')
    .select('temperature_2m_max').filter(ee.Filter.calendarRange(y, y, 'year'));
  var maxTZA = col.max().updateMask(mask_TZA)
    .reduceRegion({reducer: ee.Reducer.max(), geometry: tanzania, scale: 9280, maxPixels: 1e9})
    .getNumber('temperature_2m_max');
  var maxBEN = col.max().updateMask(mask_BEN)
    .reduceRegion({reducer: ee.Reducer.max(), geometry: benin, scale: 9280, maxPixels: 1e9})
    .getNumber('temperature_2m_max');
  return ee.Feature(null, {
    'type': 'annual_max', 'year': y,
    'max_temp_C_TZA': maxTZA.subtract(273.15),
    'max_temp_C_BEN': maxBEN.subtract(273.15),
    'T_ck_TZA': -9999, 'T_ck_BEN': -9999
  });
});

var summaryTZA = ee.Feature(null, {
```

```
  'type': 'T_ck', 'year': -9999,
  'max_temp_C_TZA': -9999, 'max_temp_C_BEN': -9999,
  'T_ck_TZA': T_ck_TZA, 'T_ck_BEN': -9999
});
var summaryBEN = ee.Feature(null, {
  'type': 'T_ck', 'year': -9999,
  'max_temp_C_TZA': -9999, 'max_temp_C_BEN': -9999,
  'T_ck_TZA': -9999, 'T_ck_BEN': T_ck_BEN
});

var allRows = ee.FeatureCollection(annualRows)
  .merge(ee.FeatureCollection([summaryTZA, summaryBEN]));
Export.table.toDrive({
  collection: allRows, description: 'temperature_indicator_maize_TZA_BEN', fileFormat: 'CSV'
});
```

B.2 Flooding

```
// ============================================================
// FLOODING INDICATOR - Maize
// Africa (continental), Tanzania (TZA), and Benin (BEN)
// Source: JRC GloFAS Flood Hazard v2.1
// Return periods: 10, 20, 50, 75, 100, 200, 500 years
// Weight: SPAM 2020 production volume (P_MAIZ_A)
// ============================================================
var countries = ee.FeatureCollection('USDOS/LSIB_SIMPLE/2017');
var tanzania = countries.filter(ee.Filter.eq('country_na', 'Tanzania'));
var benin    = countries.filter(ee.Filter.eq('country_na', 'Benin'));
var africa   = countries.filter(ee.Filter.eq('wld_rgn', 'Africa'));

var maiz_A     = ee.Image('projects/exjobb-490711/assets/spam2020_V2r2_global_P_MAIZ_A');
var maiz_A_TZA = maiz_A.clip(tanzania);
var maiz_A_BEN = maiz_A.clip(benin);
var maiz_A_AFR = maiz_A.clip(africa);
var mask_TZA = maiz_A_TZA.gt(0);
var mask_BEN = maiz_A_BEN.gt(0);
var mask_AFR = maiz_A_AFR.gt(0);

var glofas = ee.ImageCollection('JRC/CEMS_GLOFAS/FloodHazard/v2_1').mosaic();

var returnPeriods = [
  {band: 'RP10_depth',  p: 1/10},  {band: 'RP20_depth',  p: 1/20},
  {band: 'RP50_depth',  p: 1/50},  {band: 'RP75_depth',  p: 1/75},
  {band: 'RP100_depth', p: 1/100}, {band: 'RP200_depth', p: 1/200},
  {band: 'RP500_depth', p: 1/500}
];

// --- Pixel-level flood hazard score ---
var F_pixel = ee.Image(0).rename('flood_score');
for (var j = 0; j < returnPeriods.length; j++) {
  var pj   = returnPeriods[j].p;
  var pj1  = j + 1 < returnPeriods.length ? returnPeriods[j + 1].p : 0;
  var F_ij = glofas.select(returnPeriods[j].band).gt(0);
  F_pixel  = F_pixel.add(F_ij.multiply(pj - pj1));
}
F_pixel = F_pixel.rename('flood_score');

var F_pixel_TZA = F_pixel.updateMask(mask_TZA);
var F_pixel_BEN = F_pixel.updateMask(mask_BEN);
var F_pixel_AFR = F_pixel.updateMask(mask_AFR);

var F_ck_TZA = F_pixel_TZA.multiply(maiz_A_TZA)
  .reduceRegion({reducer: ee.Reducer.sum(), geometry: tanzania, scale: 9280, maxPixels: 1e10})
  .getNumber('flood_score')
  .divide(maiz_A_TZA.updateMask(mask_TZA)
    .reduceRegion({reducer: ee.Reducer.sum(), geometry: tanzania, scale: 9280, maxPixels: 1e10}).getNumber('b1'));

var F_ck_BEN = F_pixel_BEN.multiply(maiz_A_BEN)
  .reduceRegion({reducer: ee.Reducer.sum(), geometry: benin, scale: 9280, maxPixels: 1e10})
  .getNumber('flood_score')
  .divide(maiz_A_BEN.updateMask(mask_BEN)
    .reduceRegion({reducer: ee.Reducer.sum(), geometry: benin, scale: 9280, maxPixels: 1e10}).getNumber('b1'));

var F_ck_AFR = F_pixel_AFR.multiply(maiz_A_AFR)
  .reduceRegion({reducer: ee.Reducer.sum(), geometry: africa, scale: 9280, maxPixels: 1e13})
  .getNumber('flood_score')
  .divide(maiz_A_AFR.updateMask(mask_AFR)
    .reduceRegion({reducer: ee.Reducer.sum(), geometry: africa, scale: 9280, maxPixels: 1e13}).getNumber('b1'));

print('F_c,k Maize - Tanzania:', F_ck_TZA);
```

```
print('F_c,k Maize - Benin:',    F_ck_BEN);
print('F_c,k Maize - Africa:',   F_ck_AFR);

var results = ee.FeatureCollection([
  ee.Feature(null, {'indicator': 'F_ck', 'country': 'Tanzania', 'value': F_ck_TZA}),
  ee.Feature(null, {'indicator': 'F_ck', 'country': 'Benin',    'value': F_ck_BEN}),
  ee.Feature(null, {'indicator': 'F_ck', 'country': 'Africa',   'value': F_ck_AFR})
]);
Export.table.toDrive({
  collection: results, description: 'flooding_indicator_maize_TZA_BEN_AFR', fileFormat: 'CSV'
});
```

B.3 Drought

```
// ============================================================
// DROUGHT INDICATOR - Maize (SPEI-3 < -1.0)
// Africa (continental), Tanzania (TZA), and Benin (BEN)
// WMO reference period: 1991-2020 (360 months)
// Rainfed only: SPAM _R layer as weights
// Source: CSIC SPEIbase v2.10, band: SPEI_03_month
// Weight: SPAM 2020 production volume (P_MAIZ_R)
// ============================================================
var countries = ee.FeatureCollection('USDOS/LSIB_SIMPLE/2017');
var tanzania = countries.filter(ee.Filter.eq('country_na', 'Tanzania'));
var benin    = countries.filter(ee.Filter.eq('country_na', 'Benin'));
var africa   = countries.filter(ee.Filter.eq('wld_rgn', 'Africa'));

var maiz_R     = ee.Image('projects/exjobb-490711/assets/spam2020_V2r2_global_P_MAIZ_R');
var maiz_A     = ee.Image('projects/exjobb-490711/assets/spam2020_V2r2_global_P_MAIZ_A');
var maiz_R_TZA = maiz_R.clip(tanzania);  var maiz_A_TZA = maiz_A.clip(tanzania);
var maiz_R_BEN = maiz_R.clip(benin);     var maiz_A_BEN = maiz_A.clip(benin);
var maiz_R_AFR = maiz_R.clip(africa);    var maiz_A_AFR = maiz_A.clip(africa);
var mask_R_TZA = maiz_R_TZA.gt(0);
var mask_R_BEN = maiz_R_BEN.gt(0);
var mask_R_AFR = maiz_R_AFR.gt(0);

// --- Rainfed share (R/A) ---
var IRR_TZA = maiz_R_TZA.reduceRegion({reducer: ee.Reducer.sum(), geometry: tanzania, scale: 9280, maxPixels: 1e9})
  .getNumber('b1').divide(maiz_A_TZA.reduceRegion({reducer: ee.Reducer.sum(), geometry: tanzania, scale: 9280, maxPixels:
   1e9}).getNumber('b1'));
var IRR_BEN = maiz_R_BEN.reduceRegion({reducer: ee.Reducer.sum(), geometry: benin, scale: 9280, maxPixels: 1e9})
  .getNumber('b1').divide(maiz_A_BEN.reduceRegion({reducer: ee.Reducer.sum(), geometry: benin, scale: 9280, maxPixels: 1e9
   }).getNumber('b1'));
var IRR_AFR = maiz_R_AFR.reduceRegion({reducer: ee.Reducer.sum(), geometry: africa, scale: 9280, maxPixels: 1e13})
  .getNumber('b1').divide(maiz_A_AFR.reduceRegion({reducer: ee.Reducer.sum(), geometry: africa, scale: 9280, maxPixels: 1
   e13}).getNumber('b1'));

// --- SPEI-3: binary drought months ---
var DR_pixel = ee.ImageCollection('CSIC/SPEI/2_10')
  .select('SPEI_03_month')
  .filter(ee.Filter.date('1991-01-01', '2020-12-31'))
  .map(function(img) { return img.lt(-1.0).rename('drought'); })
  .mean().rename('DR_pixel');

var DR_pixel_TZA = DR_pixel.updateMask(mask_R_TZA);
var DR_pixel_BEN = DR_pixel.updateMask(mask_R_BEN);
var DR_pixel_AFR = DR_pixel.updateMask(mask_R_AFR);

var DR_ck_TZA = DR_pixel_TZA.multiply(maiz_R_TZA)
  .reduceRegion({reducer: ee.Reducer.sum(), geometry: tanzania, scale: 9280, maxPixels: 1e9})
  .getNumber('DR_pixel')
  .divide(maiz_R_TZA.updateMask(mask_R_TZA)
    .reduceRegion({reducer: ee.Reducer.sum(), geometry: tanzania, scale: 9280, maxPixels: 1e9}).getNumber('b1'));

var DR_ck_BEN = DR_pixel_BEN.multiply(maiz_R_BEN)
  .reduceRegion({reducer: ee.Reducer.sum(), geometry: benin, scale: 9280, maxPixels: 1e9})
  .getNumber('DR_pixel')
  .divide(maiz_R_BEN.updateMask(mask_R_BEN)
    .reduceRegion({reducer: ee.Reducer.sum(), geometry: benin, scale: 9280, maxPixels: 1e9}).getNumber('b1'));

var DR_ck_AFR = DR_pixel_AFR.multiply(maiz_R_AFR)
  .reduceRegion({reducer: ee.Reducer.sum(), geometry: africa, scale: 9280, maxPixels: 1e13})
  .getNumber('DR_pixel')
  .divide(maiz_R_AFR.updateMask(mask_R_AFR)
    .reduceRegion({reducer: ee.Reducer.sum(), geometry: africa, scale: 9280, maxPixels: 1e13}).getNumber('b1'));

print('DR_c,k Maize - Tanzania:', DR_ck_TZA);
print('DR_c,k Maize - Benin:',    DR_ck_BEN);
print('DR_c,k Maize - Africa:',   DR_ck_AFR);
```

```
var results = ee.FeatureCollection([
  ee.Feature(null, {'indicator': 'DR_ck', 'country': 'Tanzania', 'value': DR_ck_TZA, 'rainfed_share': IRR_TZA}),
  ee.Feature(null, {'indicator': 'DR_ck', 'country': 'Benin',    'value': DR_ck_BEN, 'rainfed_share': IRR_BEN}),
  ee.Feature(null, {'indicator': 'DR_ck', 'country': 'Africa',   'value': DR_ck_AFR, 'rainfed_share': IRR_AFR})
]);
Export.table.toDrive({
  collection: results, description: 'drought_indicator_maize_TZA_BEN_AFR', fileFormat: 'CSV'
});
```

B.4 Precipitation Variability

```
// ============================================================
// PRECIPITATION VARIABILITY INDICATOR - Maize
// Africa (continental), Tanzania (TZA), and Benin (BEN)
// WMO reference period: 1991-2020 (30 annual totals)
// PV_i = stdDev_i / mean_i (coefficient of variation)
// Rainfed only: SPAM _R layer as weights
// Source: CHIRPS Daily, band: precipitation
// Weight: SPAM 2020 production volume (P_MAIZ_R)
// ============================================================
var countries = ee.FeatureCollection('USDOS/LSIB_SIMPLE/2017');
var tanzania = countries.filter(ee.Filter.eq('country_na', 'Tanzania'));
var benin    = countries.filter(ee.Filter.eq('country_na', 'Benin'));
var africa   = countries.filter(ee.Filter.eq('wld_rgn', 'Africa'));

var maiz_R     = ee.Image('projects/exjobb-490711/assets/spam2020_V2r2_global_P_MAIZ_R');
var maiz_R_TZA = maiz_R.clip(tanzania);
var maiz_R_BEN = maiz_R.clip(benin);
var maiz_R_AFR = maiz_R.clip(africa);
var mask_R_TZA = maiz_R_TZA.gt(0);
var mask_R_BEN = maiz_R_BEN.gt(0);
var mask_R_AFR = maiz_R_AFR.gt(0);

// --- Stack 30 annual precipitation totals ---
var years = ee.List.sequence(1991, 2020);
var annualStack = ee.ImageCollection(
  years.map(function(y) {
    y = ee.Number(y);
    return ee.ImageCollection('UCSB-CHG/CHIRPS/DAILY')
      .select('precipitation')
      .filter(ee.Filter.calendarRange(y, y, 'year'))
      .sum()
      .rename(ee.String('y').cat(ee.Number(y).int().format()));
  })
).toBands();

// --- Pixel-level CV = stdDev / mean across 30 bands ---
var PV_pixel = annualStack.reduce(ee.Reducer.stdDev())
  .divide(annualStack.reduce(ee.Reducer.mean()))
  .rename('PV_pixel');

var PV_pixel_TZA = PV_pixel.updateMask(mask_R_TZA);
var PV_pixel_BEN = PV_pixel.updateMask(mask_R_BEN);
var PV_pixel_AFR = PV_pixel.updateMask(mask_R_AFR);

var PV_ck_TZA = PV_pixel_TZA.multiply(maiz_R_TZA)
  .reduceRegion({reducer: ee.Reducer.sum(), geometry: tanzania, scale: 9280, maxPixels: 1e9})
  .getNumber('PV_pixel')
  .divide(maiz_R_TZA.updateMask(mask_R_TZA)
    .reduceRegion({reducer: ee.Reducer.sum(), geometry: tanzania, scale: 9280, maxPixels: 1e9}).getNumber('b1'));

var PV_ck_BEN = PV_pixel_BEN.multiply(maiz_R_BEN)
  .reduceRegion({reducer: ee.Reducer.sum(), geometry: benin, scale: 9280, maxPixels: 1e9})
  .getNumber('PV_pixel')
  .divide(maiz_R_BEN.updateMask(mask_R_BEN)
    .reduceRegion({reducer: ee.Reducer.sum(), geometry: benin, scale: 9280, maxPixels: 1e9}).getNumber('b1'));

var PV_ck_AFR = PV_pixel_AFR.multiply(maiz_R_AFR)
  .reduceRegion({reducer: ee.Reducer.sum(), geometry: africa, scale: 9280, maxPixels: 1e13})
  .getNumber('PV_pixel')
  .divide(maiz_R_AFR.updateMask(mask_R_AFR)
    .reduceRegion({reducer: ee.Reducer.sum(), geometry: africa, scale: 9280, maxPixels: 1e13}).getNumber('b1'));

print('PV_c,k Maize - Tanzania:', PV_ck_TZA);
print('PV_c,k Maize - Benin:',    PV_ck_BEN);
print('PV_c,k Maize - Africa:',   PV_ck_AFR);
```

B.5 Baseline Water Stress and Interannual Variability

```
// ============================================================
// BASELINE WATER STRESS (BWS) + INTERANNUAL VARIABILITY (IAV)
// Maize - Africa (continental), Tanzania (TZA), and Benin (BEN)
// Irrigated only: SPAM _I layer as weights
// Source: WRI Aqueduct 4.0 baseline annual (FeatureCollection)
// Weight: SPAM 2020 production volume (P_MAIZ_I)
// ============================================================
var countries = ee.FeatureCollection('USDOS/LSIB_SIMPLE/2017');
var tanzania = countries.filter(ee.Filter.eq('country_na', 'Tanzania'));
var benin    = countries.filter(ee.Filter.eq('country_na', 'Benin'));
var africa   = countries.filter(ee.Filter.eq('wld_rgn', 'Africa'));

var maiz_I     = ee.Image('projects/exjobb-490711/assets/spam2020_V2r2_global_P_MAIZ_I');
var maiz_A     = ee.Image('projects/exjobb-490711/assets/spam2020_V2r2_global_P_MAIZ_A');
var maiz_I_TZA = maiz_I.clip(tanzania);  var maiz_A_TZA = maiz_A.clip(tanzania);
var maiz_I_BEN = maiz_I.clip(benin);     var maiz_A_BEN = maiz_A.clip(benin);
var maiz_I_AFR = maiz_I.clip(africa);    var maiz_A_AFR = maiz_A.clip(africa);
var mask_I_TZA = maiz_I_TZA.gt(0);
var mask_I_BEN = maiz_I_BEN.gt(0);
var mask_I_AFR = maiz_I_AFR.gt(0);

// --- Irrigated share (I/A) ---
var share_I_TZA = maiz_I_TZA.reduceRegion({reducer: ee.Reducer.sum(), geometry: tanzania, scale: 9280, maxPixels: 1e9})
  .getNumber('b1').divide(maiz_A_TZA.reduceRegion({reducer: ee.Reducer.sum(), geometry: tanzania, scale: 9280, maxPixels:
   1e9}).getNumber('b1'));
var share_I_BEN = maiz_I_BEN.reduceRegion({reducer: ee.Reducer.sum(), geometry: benin, scale: 9280, maxPixels: 1e9})
  .getNumber('b1').divide(maiz_A_BEN.reduceRegion({reducer: ee.Reducer.sum(), geometry: benin, scale: 9280, maxPixels: 1e9
   }).getNumber('b1'));
var share_I_AFR = maiz_I_AFR.reduceRegion({reducer: ee.Reducer.sum(), geometry: africa, scale: 9280, maxPixels: 1e13})
  .getNumber('b1').divide(maiz_A_AFR.reduceRegion({reducer: ee.Reducer.sum(), geometry: africa, scale: 9280, maxPixels: 1
   e13}).getNumber('b1'));

// --- Load Aqueduct and rasterize ---
var aqueduct = ee.FeatureCollection('WRI/Aqueduct_Water_Risk/V4/baseline_annual');
var bws_raster = aqueduct
  .filter(ee.Filter.notNull(['bws_score'])).filter(ee.Filter.gte('bws_score', 0))
  .reduceToImage({properties: ['bws_score'], reducer: ee.Reducer.first()}).rename('bws_score');
var iav_raster = aqueduct
  .filter(ee.Filter.notNull(['iav_score'])).filter(ee.Filter.gte('iav_score', 0))
  .reduceToImage({properties: ['iav_score'], reducer: ee.Reducer.first()}).rename('iav_score');

var bws_TZA = bws_raster.updateMask(mask_I_TZA);
var bws_BEN = bws_raster.updateMask(mask_I_BEN);
var bws_AFR = bws_raster.updateMask(mask_I_AFR);
var iav_TZA = iav_raster.updateMask(mask_I_TZA);
var iav_BEN = iav_raster.updateMask(mask_I_BEN);
var iav_AFR = iav_raster.updateMask(mask_I_AFR);

// --- Production-weighted mean: BWS ---
var BWS_ck_TZA = bws_TZA.multiply(maiz_I_TZA)
  .reduceRegion({reducer: ee.Reducer.sum(), geometry: tanzania, scale: 9280, maxPixels: 1e9}).getNumber('bws_score')
  .divide(maiz_I_TZA.updateMask(mask_I_TZA).reduceRegion({reducer: ee.Reducer.sum(), geometry: tanzania, scale: 9280,
   maxPixels: 1e9}).getNumber('b1'));
var BWS_ck_BEN = bws_BEN.multiply(maiz_I_BEN)
  .reduceRegion({reducer: ee.Reducer.sum(), geometry: benin, scale: 9280, maxPixels: 1e9}).getNumber('bws_score')
  .divide(maiz_I_BEN.updateMask(mask_I_BEN).reduceRegion({reducer: ee.Reducer.sum(), geometry: benin, scale: 9280,
   maxPixels: 1e9}).getNumber('b1'));
var BWS_ck_AFR = bws_AFR.multiply(maiz_I_AFR)
  .reduceRegion({reducer: ee.Reducer.sum(), geometry: africa, scale: 9280, maxPixels: 1e13}).getNumber('bws_score')
  .divide(maiz_I_AFR.updateMask(mask_I_AFR).reduceRegion({reducer: ee.Reducer.sum(), geometry: africa, scale: 9280,
   maxPixels: 1e13}).getNumber('b1'));

// --- Production-weighted mean: IAV ---
var IAV_ck_TZA = iav_TZA.multiply(maiz_I_TZA)
  .reduceRegion({reducer: ee.Reducer.sum(), geometry: tanzania, scale: 9280, maxPixels: 1e9}).getNumber('iav_score')
  .divide(maiz_I_TZA.updateMask(mask_I_TZA).reduceRegion({reducer: ee.Reducer.sum(), geometry: tanzania, scale: 9280,
   maxPixels: 1e9}).getNumber('b1'));
var IAV_ck_BEN = iav_BEN.multiply(maiz_I_BEN)
  .reduceRegion({reducer: ee.Reducer.sum(), geometry: benin, scale: 9280, maxPixels: 1e9}).getNumber('iav_score')
  .divide(maiz_I_BEN.updateMask(mask_I_BEN).reduceRegion({reducer: ee.Reducer.sum(), geometry: benin, scale: 9280,
   maxPixels: 1e9}).getNumber('b1'));
var IAV_ck_AFR = iav_AFR.multiply(maiz_I_AFR)
  .reduceRegion({reducer: ee.Reducer.sum(), geometry: africa, scale: 9280, maxPixels: 1e13}).getNumber('iav_score')
  .divide(maiz_I_AFR.updateMask(mask_I_AFR).reduceRegion({reducer: ee.Reducer.sum(), geometry: africa, scale: 9280,
   maxPixels: 1e13}).getNumber('b1'));

print('BWS_c,k Maize - Tanzania:', BWS_ck_TZA);
print('BWS_c,k Maize - Benin:',    BWS_ck_BEN);
print('BWS_c,k Maize - Africa:',   BWS_ck_AFR);
print('IAV_c,k Maize - Tanzania:', IAV_ck_TZA);
print('IAV_c,k Maize - Benin:',    IAV_ck_BEN);
print('IAV_c,k Maize - Africa:',   IAV_ck_AFR);
```

```
var bws_rows = ee.FeatureCollection([
  ee.Feature(null, {'indicator': 'BWS_ck', 'country': 'Tanzania', 'value': BWS_ck_TZA, 'irrigated_share': share_I_TZA}),
  ee.Feature(null, {'indicator': 'BWS_ck', 'country': 'Benin',    'value': BWS_ck_BEN, 'irrigated_share': share_I_BEN}),
  ee.Feature(null, {'indicator': 'BWS_ck', 'country': 'Africa',   'value': BWS_ck_AFR, 'irrigated_share': share_I_AFR})
]);
Export.table.toDrive({collection: bws_rows, description: 'BWS_indicator_maize_TZA_BEN_AFR', fileFormat: 'CSV'});

var iav_rows = ee.FeatureCollection([
  ee.Feature(null, {'indicator': 'IAV_ck', 'country': 'Tanzania', 'value': IAV_ck_TZA, 'irrigated_share': share_I_TZA}),
  ee.Feature(null, {'indicator': 'IAV_ck', 'country': 'Benin',    'value': IAV_ck_BEN, 'irrigated_share': share_I_BEN}),
  ee.Feature(null, {'indicator': 'IAV_ck', 'country': 'Africa',   'value': IAV_ck_AFR, 'irrigated_share': share_I_AFR})
]);
Export.table.toDrive({collection: iav_rows, description: 'IAV_indicator_maize_TZA_BEN_AFR', fileFormat: 'CSV'});
```

B.6 Erosion

```
// ============================================================
// EROSION INDICATOR - Maize (GloSEM 1.3, t/ha/yr)
// Uses the NEW re-uploaded asset (glosem_africa).
// Benin -> Tanzania -> African mean, production-weighted by SPAM P_MAIZ_A.
// ============================================================

// >>> EDIT THIS to the exact ID from the Assets tab if different <<<
var ASSET = 'projects/exjobb-490711/assets/glosem_africa_10km';

var countries = ee.FeatureCollection('USDOS/LSIB_SIMPLE/2017');
var benin     = countries.filter(ee.Filter.eq('country_na', 'Benin'));
var tanzania  = countries.filter(ee.Filter.eq('country_na', 'Tanzania'));
var africa    = countries.filter(ee.Filter.eq('wld_rgn', 'Africa'));

var maiz_A  = ee.Image('projects/exjobb-490711/assets/spam2020_V2r2_global_P_MAIZ_A'); // band 'b1'
var erosion = ee.Image(ASSET).select(0).rename('ero');
erosion     = erosion.updateMask(erosion.gte(0).and(erosion.lt(1e4)));  // drop nodata/fill

// ---------- STEP 0: DATA SANITY CHECK (run this first!) -------------
// If B0_count is > 0 and the min/max look like real erosion numbers
// (roughly 0 up to a few hundred t/ha/yr), the new asset is good.
print('SANITY raw over Benin @ 1km:', ee.Image(ASSET).select(0).reduceRegion({
  reducer: ee.Reducer.minMax().combine(ee.Reducer.count(), '', true),
  geometry: benin, scale: 1000, maxPixels: 1e12, bestEffort: true
}));

// ---------- Production-weighted erosion (direct overlay @ 9280 m) ---
// Same pattern as the other risk indicators in the appendix.
function ERO(region, maxPx) {
  var maiz     = maiz_A.clip(region);
  var maizMask = maiz.gt(0);
  // pixels usable for the weighted mean: maize present AND erosion valid
  var both = maizMask.updateMask(erosion.mask());

  var num = erosion.updateMask(both).multiply(maiz)
    .reduceRegion({reducer: ee.Reducer.sum(), geometry: region, scale: 9280, maxPixels: maxPx})
    .getNumber('ero');
  var denMatched = maiz.updateMask(both)
    .reduceRegion({reducer: ee.Reducer.sum(), geometry: region, scale: 9280, maxPixels: maxPx})
    .getNumber('b1');
  var denFull = maiz.updateMask(maizMask)
    .reduceRegion({reducer: ee.Reducer.sum(), geometry: region, scale: 9280, maxPixels: maxPx})
    .getNumber('b1');

  return ee.Dictionary({
    ERO_t_ha_yr:                    num.divide(denMatched),
    production_full_t:              denFull,             // FAOSTAT check
    production_on_erosion_pixels_t: denMatched,
    erosion_coverage_frac:          denMatched.divide(denFull)  // ~1.0 = good data
  });
}

print('ERO Maize - Benin:',    ERO(benin,    1e10));   // small -> start here
print('ERO Maize - Tanzania:', ERO(tanzania, 1e10));
print('ERO Maize - Africa:',   ERO(africa,   1e13));   // = Eq. african-mean

// ---------- Verification ------------------------------------------
// production_t should match FAOSTAT 2020 maize (~1.60 Mt BEN, ~6.45 Mt TZA).
// Plausibility: erosion stats over maize pixels vs the 5 / 12 t/ha/yr bands.
function eroRange(region) {
  var mask = maiz_A.clip(region).gt(0);
  return erosion.updateMask(mask).reduceRegion({
    reducer: ee.Reducer.minMax().combine(ee.Reducer.mean(), '', true),
```

```
    geometry: region, scale: 9280, maxPixels: 1e10
  });
}
print('Erosion range over maize (Benin):',    eroRange(benin));
print('Erosion range over maize (Tanzania):', eroRange(tanzania));

// ---------- Map (eyeball Benin first) -------------------------------
Map.centerObject(benin, 7);
Map.addLayer(erosion.updateMask(maiz_A.gt(0)),
  {min: 0, max: 20, palette: ['ffffcc','fd8d3c','bd0026']}, 'Erosion on maize (t/ha/yr)');
```

B.7 Soil Organic Carbon

```
// ============================================================
// SOIL ORGANIC CARBON (SOC) INDICATOR - Maize
// Africa (continental), Tanzania (TZA), and Benin (BEN)
// Depth-weighted mean: 0-30 cm profile
// Source: OpenLandMap SOC v02
// Weight: SPAM 2020 production volume (P_MAIZ_A)
// ============================================================
var countries = ee.FeatureCollection('USDOS/LSIB_SIMPLE/2017');
var tanzania = countries.filter(ee.Filter.eq('country_na', 'Tanzania'));
var benin    = countries.filter(ee.Filter.eq('country_na', 'Benin'));
var africa   = countries.filter(ee.Filter.eq('wld_rgn', 'Africa'));

var maiz_A     = ee.Image('projects/exjobb-490711/assets/spam2020_V2r2_global_P_MAIZ_A');
var maiz_A_TZA = maiz_A.clip(tanzania);
var maiz_A_BEN = maiz_A.clip(benin);
var maiz_A_AFR = maiz_A.clip(africa);
var mask_TZA = maiz_A_TZA.gt(0);
var mask_BEN = maiz_A_BEN.gt(0);
var mask_AFR = maiz_A_AFR.gt(0);

// --- Load SOC image (raw values = g/kg x 5) ---
var soc   = ee.Image('OpenLandMap/SOL/SOL_ORGANIC-CARBON_USDA-6A1C_M/v02');
var SOC0  = soc.select('b0').multiply(5);
var SOC10 = soc.select('b10').multiply(5);
var SOC30 = soc.select('b30').multiply(5);

// --- Depth-weighted mean: SOC_i = (5*SOC0 + 10*SOC10 + 15*SOC30) / 30 ---
var SOC_pixel = SOC0.multiply(5).add(SOC10.multiply(10)).add(SOC30.multiply(15))
  .divide(30).rename('SOC_pixel');

var SOC_TZA = SOC_pixel.updateMask(mask_TZA);
var SOC_BEN = SOC_pixel.updateMask(mask_BEN);
var SOC_AFR = SOC_pixel.updateMask(mask_AFR);

var SOC_ck_TZA = SOC_TZA.multiply(maiz_A_TZA)
  .reduceRegion({reducer: ee.Reducer.sum(), geometry: tanzania, scale: 9280, maxPixels: 1e9}).getNumber('SOC_pixel')
  .divide(maiz_A_TZA.updateMask(mask_TZA).reduceRegion({reducer: ee.Reducer.sum(), geometry: tanzania, scale: 9280,
   maxPixels: 1e9}).getNumber('b1'));

var SOC_ck_BEN = SOC_BEN.multiply(maiz_A_BEN)
  .reduceRegion({reducer: ee.Reducer.sum(), geometry: benin, scale: 9280, maxPixels: 1e9}).getNumber('SOC_pixel')
  .divide(maiz_A_BEN.updateMask(mask_BEN).reduceRegion({reducer: ee.Reducer.sum(), geometry: benin, scale: 9280, maxPixels
   : 1e9}).getNumber('b1'));

var SOC_ck_AFR = SOC_AFR.multiply(maiz_A_AFR)
  .reduceRegion({reducer: ee.Reducer.sum(), geometry: africa, scale: 9280, maxPixels: 1e13}).getNumber('SOC_pixel')
  .divide(maiz_A_AFR.updateMask(mask_AFR).reduceRegion({reducer: ee.Reducer.sum(), geometry: africa, scale: 9280,
   maxPixels: 1e13}).getNumber('b1'));

print('SOC_c,k Maize - Tanzania:', SOC_ck_TZA);
print('SOC_c,k Maize - Benin:',    SOC_ck_BEN);
print('SOC_c,k Maize - Africa:',   SOC_ck_AFR);

var results = ee.FeatureCollection([
  ee.Feature(null, {'indicator': 'SOC_ck', 'country': 'Tanzania', 'value': SOC_ck_TZA}),
  ee.Feature(null, {'indicator': 'SOC_ck', 'country': 'Benin',    'value': SOC_ck_BEN}),
  ee.Feature(null, {'indicator': 'SOC_ck', 'country': 'Africa',   'value': SOC_ck_AFR})
]);
Export.table.toDrive({
  collection: results, description: 'SOC_indicator_maize_TZA_BEN_AFR', fileFormat: 'CSV'
});
```

B.8 Deforestation

```
// ============================================================
// DEFORESTATION INDICATOR - Maize
// DF_c,k = A_c,k (ha permanent ag forest loss 2001-2022
//          within maize footprint) / P_c,k (FAO cumulative
//          production 2001-2022, tonnes)
// Datasets: Hansen v1.13 + WRI/DeepMind drivers + SPAM 2020
// NOTE: SPAM layer used as spatial mask only, not as weight.
// ============================================================
var countries = ee.FeatureCollection('USDOS/LSIB_SIMPLE/2017');
var tanzania = countries.filter(ee.Filter.eq('country_na', 'Tanzania'));
var benin    = countries.filter(ee.Filter.eq('country_na', 'Benin'));
var africa   = countries.filter(ee.Filter.eq('wld_rgn', 'Africa'));

var maiz_A     = ee.Image('projects/exjobb-490711/assets/spam2020_V2r2_global_P_MAIZ_A');
var maiz_A_TZA = maiz_A.clip(tanzania);
var maiz_A_BEN = maiz_A.clip(benin);
var maiz_A_AFR = maiz_A.clip(africa);
var mask_TZA = maiz_A_TZA.gt(0);
var mask_BEN = maiz_A_BEN.gt(0);
var mask_AFR = maiz_A_AFR.gt(0);

// --- Hansen forest loss 2001-2022 ---
var hansen     = ee.Image('UMD/hansen/global_forest_change_2025_v1_13');
var lossyear   = hansen.select('lossyear');
var loss_01_22 = lossyear.gte(1).and(lossyear.lte(22));

// --- WRI/DeepMind permanent agriculture driver ---
var drivers     = ee.Image('projects/landandcarbon/assets/wri_gdm_drivers_forest_loss_1km/v1_2001_2022')
  .select('classification');
var perm_ag     = drivers.eq(1);
var perm_ag_30m = perm_ag.reproject({crs: loss_01_22.projection(), scale: 30});
var ag_defor    = loss_01_22.and(perm_ag_30m).rename('ag_defor');

// --- Apply SPAM maize mask at 30m ---
var mask_TZA_30m = mask_TZA.reproject({crs: loss_01_22.projection(), scale: 30});
var mask_BEN_30m = mask_BEN.reproject({crs: loss_01_22.projection(), scale: 30});
var mask_AFR_30m = mask_AFR.reproject({crs: loss_01_22.projection(), scale: 30});
var ag_defor_TZA = ag_defor.updateMask(mask_TZA_30m);
var ag_defor_BEN = ag_defor.updateMask(mask_BEN_30m);
var ag_defor_AFR = ag_defor.updateMask(mask_AFR_30m);

// --- A_c,k: total hectares of agricultural deforestation ---
var pixelArea = ee.Image.pixelArea().divide(10000);
var A_ck_TZA = ag_defor_TZA.multiply(pixelArea)
  .reduceRegion({reducer: ee.Reducer.sum(), geometry: tanzania, scale: 30, maxPixels: 1e13}).getNumber('ag_defor');
var A_ck_BEN = ag_defor_BEN.multiply(pixelArea)
  .reduceRegion({reducer: ee.Reducer.sum(), geometry: benin, scale: 30, maxPixels: 1e13}).getNumber('ag_defor');
var A_ck_AFR = ag_defor_AFR.multiply(pixelArea)
  .reduceRegion({reducer: ee.Reducer.sum(), geometry: africa, scale: 30, maxPixels: 1e13}).getNumber('ag_defor');

// --- P_c,k: FAO cumulative maize production 2001-2022 (tonnes) ---
var P_ck_TZA = ee.Number(110523488);
var P_ck_BEN = ee.Number(11717405);
var P_ck_AFR = ee.Number(1503666262);

// --- DF_c,k = A_c,k / P_c,k ---
var DF_ck_TZA = A_ck_TZA.divide(P_ck_TZA);
var DF_ck_BEN = A_ck_BEN.divide(P_ck_BEN);
var DF_ck_AFR = A_ck_AFR.divide(P_ck_AFR);

print('DF_c,k (ha/tonne) - Tanzania:', DF_ck_TZA);
print('DF_c,k (ha/tonne) - Benin:',    DF_ck_BEN);
print('DF_c,k (ha/tonne) - Africa:',   DF_ck_AFR);

var results = ee.FeatureCollection([
  ee.Feature(null, {'indicator': 'DF_ck', 'country': 'Tanzania',
    'A_ck_ha': A_ck_TZA, 'P_ck_tonnes': P_ck_TZA, 'value_ha_per_tonne': DF_ck_TZA}),
  ee.Feature(null, {'indicator': 'DF_ck', 'country': 'Benin',
    'A_ck_ha': A_ck_BEN, 'P_ck_tonnes': P_ck_BEN, 'value_ha_per_tonne': DF_ck_BEN}),
  ee.Feature(null, {'indicator': 'DF_ck', 'country': 'Africa',
    'A_ck_ha': A_ck_AFR, 'P_ck_tonnes': P_ck_AFR, 'value_ha_per_tonne': DF_ck_AFR})
]);
Export.table.toDrive({
  collection: results, description: 'deforestation_indicator_maize_TZA_BEN_AFR', fileFormat: 'CSV'
});
```

C Dataset Licenses

Table C.1: Datasets used in Chapter 5 and their licences.

Dataset	Used for	Licence
Spatial Production Allocation Model 2020, Version 2.0 (SPAM 2020) (IFPRI, 2026)	Spatial crop mask (both assessments)	CC0
FAOSTAT crop production statistics (FAO, n.d.)	Production volumes (both assessments)	CC BY 4.0
ERA5-Land Daily Aggregates (ECMWF / Copernicus Climate Change Service) (Muñoz Sabater, 2019)	Heat stress indicator	CC BY 4.0
JRC Global River Flood Hazard Maps, Version 2.1 (Baugh et al., 2024)	Flood hazard indicator	No restriction (JRC open data)
SPEIbase Version 2.10 (Beguería et al., 2024)	Drought indicator	CC BY 4.0
Climate Hazards Group InfraRed Precipitation with Station data (CHIRPS) (Funk et al., 2015)	Precipitation variability indicator	Public domain
WRI Aqueduct 4.0 (Kuzma et al., 2023)	Baseline water stress and interannual variability indicators	CC BY 4.0
Global Soil Erosion Modelling platform, Version 1.3 (GloSEM 1.3) (Borrelli et al., 2021)	Erosion indicator	CC BY 4.0
OpenLandMap Soil Organic Carbon Content (Hengl et al., 2017)	Soil organic carbon indicator	CC BY 4.0
Spatially explicit global cropland GHG emission dataset (Cao et al., 2026)	GHG intensity indicator	CC BY 4.0
Global Forest Change, University of Maryland (Hansen et al., 2013)	Deforestation indicator (forest loss layer)	CC BY 4.0
WRI/Google DeepMind Global Drivers of Forest Loss (Sims et al., 2025)	Deforestation indicator (driver attribution)	CC BY 4.0
Biodiversity intactness footprint of agricultural production, 2000–2020 (Nguyen et al., 2025)	Biodiversity loss indicator	CC BY-NC-SA 4.0
Watershed-level crop water consumption dataset (Pfister & Bayer, 2025)	Absolute blue water footprint indicator	CC BY 4.0
Crop-country specific AWARE water scarcity characterisation factors (Pfister, 2021)	Scarcity-adjusted blue water footprint indicator	CC BY 4.0